

**Strigolactone hormonal actions in plant tolerance to
heat and chilling stress, adventitious root development,
and seedling de-etiolation**

By

Luke Odianose Omoarelojie

Submitted in fulfillment of the academic requirements for the degree of
Doctor of Philosophy

in the

Research Centre for Plant Growth and Development,
School of Life Sciences,
University of KwaZulu-Natal,
Pietermaritzburg,
South Africa.

December 2020

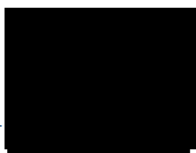
College of Agriculture, Engineering and Science

Declaration 1 – Plagiarism

I, **Luke Odianose Omoarelojie (217080288)**, declare that:

1. The research reported in this thesis, except where otherwise indicated, is my original work.
2. This thesis has not been submitted for any degree or examination at any other university.
3. This thesis does not contain other persons' data, pictures, graphs, or other information unless specifically acknowledged as being sourced from other persons.
4. This thesis does not contain other persons' writing unless specifically acknowledged as being sourced from other researchers. Where other written sources have been quoted, then:
 - a. their words have been re-written, but the general information attributed to them has been referenced, and
 - b. where their exact words have been used, then their writing has been placed in italics and inside quotation marks and referenced.
5. This thesis does not contain text, graphics, or tables copied and pasted from the Internet, unless specifically acknowledged, and the source being detailed in the thesis and in the References sections.

Signed at on the day of December 2020

A solid black rectangular box redacting the signature of the author.

SIGNATURE

Student Declaration

Strigolactone hormonal actions in plant tolerance to heat and chilling stress, adventitious root development, and seedling de-etiolation

I, **Luke Odianose Omoarelojie**, with student number: **217080288**, declare that:

- i. the research reported in this dissertation, except where otherwise indicated, is the result of my own endeavors in the Research Centre for Plant Growth and Development, School of Life Sciences, University of KwaZulu-Natal, Pietermaritzburg, South Africa;
- ii. this dissertation has not been submitted for any degrees or examination at any other University;
- iii. this thesis does not contain data, figures or writing, unless specifically acknowledged, copied from other researchers; and
- iv. where I have reproduced a publication of which I am an author or co-author, I have indicated which part of the publication was contributed by me.

Signed at on the day of December 2020

A solid black rectangular box redacting the signature of the student.

SIGNATURE

Declaration by Supervisors

We hereby declare that we acted as Supervisors for this Ph.D. student:

Students Full Name: **Luke Odianose Omoarelojie**

Student Number: **217080288**

Thesis Title: **Strigolactone hormonal actions in plant tolerance to heat and chilling stress, adventitious root development, and seedling de-etiolation**

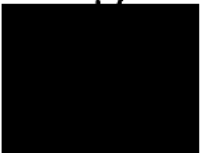
Regular consultations took place between the student and ourselves throughout the investigation. We advised the student to the best of our ability and approved the final document for submission to the College of Agriculture, Engineering and Science, Higher Degrees Office for examination by the University appointed Examiners.

SUPERVISOR:



Professor J. F. Finnie

CO-SUPERVISORS:



Professor J. F. Finnie



Dr. M. G. Kulkarni

Publications from this Thesis

Omoarelojie, L.O., Kulkarni, M.G., Finnie, J.F., Van Staden, J. 2019. Strigolactones and their crosstalk with other phytohormones. *Annals of Botany* 124, 749-767.

Omoarelojie, L.O., Kulkarni, M.G., Finnie, J.F., Pospíšil, T., Strnad, M., Van Staden, J. 2020. Synthetic strigolactone (*rac*-GR24) alleviates the adverse effects of heat stress on seed germination and photosystem II function in lupine seedlings. *Plant Physiology and Biochemistry* 155, 965-979.

Omoarelojie, L.O., Kulkarni, M.G., Finnie, J.F., Van Staden, J. 2020. Strigolactone inhibits hydrogen peroxide and plasma membrane H⁺-ATPase activities to downregulate adventitious root formation in mung bean hypocotyls. Submitted

Omoarelojie, L.O., Kulkarni, M.G., Finnie, J.F., Van Staden, J. 2020. Strigolactone analog (*rac*-GR24) enhances chilling tolerance in mungbean seedlings. Submitted

College of Agriculture, Engineering and Science

Declaration 2 – Publications

Details of contribution to publications that form part and/or include research presented in this thesis (including publications in preparation, submitted, in press and published and give details of the contributions of each author to the experimental work and writing of each publication)

Publication 1 Contributions: LOO wrote the manuscript. MGK, JFF, and JVS contributed to designing and editing the final manuscript.

Publication 2 Contributions: LOO performed the experiment and wrote the manuscript. TP and MS synthesized strigolactone (*racemic* GR24) for the study. MGK, JFF, and JVS supervised the whole study and edited the final manuscript.

Publication 3 Contributions: LOO performed the experiment and wrote the manuscript. MGK, JFF, and JVS supervised the study, read, and edited the final manuscript before submission.

Publication 4 Contributions: LOO performed the experiment and prepared the manuscript. MGK, JFF, and JVS supervised the study and revised the manuscript for submission.

Author's abbreviation

LOO	Luke O. Omoarelojie
MGK	Manoj G. Kulkarni
JFF	Jeffrey F. Finnie
TP	Tomáš Pospíšil
MS	Miroslav Strnad
JVS	Johannes van Staden

Signed aton the day of December 2020



SIGNATURE

Conference Contributions from this Thesis

Omoarelojie, L.O., Kulkarni, M.G., Finnie, J.F., Strnad, M., van Staden, J. 2020. Strigolactone (*rac*-GR24) confers photosystem II resilience under heat and chilling stress. The 46th Annual Conference of the South African Association of Botanists (SAAB). 7 – 10 January 2020, University of the Free State, Qwaqwa, South Africa. Oral presentation.

Acknowledgments

My profound gratitude goes to my supervisors Prof van Staden, Prof Finnie, and Dr. Kulkarni, for the opportunity to pursue my research interests in strigolactones, the advice, encouragements, and guidance throughout this academic pursuit, and for constructive criticism of my manuscripts.

I would also like to thank Prof Miroslav Strnad and Dr. Tomáš Pospíšil for providing the synthetic strigolactone analog (*rac*-GR24) used in this study. Your generosity made this research endeavor achievable. Thank you!

To Mrs. Lee Warren, Dr. Wendy Stirk, Mrs. Celeste Clark, Dr. Shubhpriya Gupta, and Mrs. Allison Young, I am very grateful for the support and guidance. You were always available for me to reach out to whenever I needed anything for my work.

A heart of gratitude to friends and colleagues at the Centre for the experiences.

Table of Contents

College of Agriculture, Engineering and Science Declaration 1 – Plagiarism	ii
Student Declaration	iii
Declaration by Supervisors	iv
Publications from this Thesis	v
College of Agriculture, Engineering and Science Declaration 2 – Publications	vi
Conference Contributions from this Thesis	vii
Acknowledgments	viii
Table of Contents	ix
List of Abbreviations	xiv
List of Figures	xviii
List of Tables	xxv
Abstract	xxvi
Chapter 1: General introduction	1
1.1. Introduction	1
1.2. Aims and objectives of the study	2
1.3. Overview of chapters in this thesis	3
Chapter 2: Literature Review	4
2.1. Introduction	4
2.2. Chemical nature of strigolactones	4
2.3. Biosynthesis of strigolactones	7
2.4. Strigolactone transport	8
2.5. Strigolactone perception and signal transduction	9
2.6. Strigolactone-mediated responses in plants	12
2.6.1. Germination stimulants for seeds of root-parasitic plants	12
2.6.2. Strigolactones as chemical cues for plant-microbe symbiotic interactions	12
2.6.3. Regulation of photomorphogenesis	14
2.6.4. Regulation of shoot branching and plant architecture	14

2.6.5. Mediation of plant tolerance to nutrient deficiency	16
2.6.6. Mediation of plant responses to abiotic and biotic stressors	16
2.7. Strigolactone interactions with other phytohormones	17
2.7.1. Strigolactone crosstalk with auxin signaling	17
2.7.2. Strigolactone crosstalk with cytokinin signaling	21
2.7.3. Strigolactone crosstalk with abscisic acid signaling	23
2.7.4. Strigolactone crosstalk with gibberellin signaling	24
2.7.5. Strigolactone crosstalk with ethylene signaling	25
2.7.6. Strigolactone crosstalk with jasmonate signaling	27
2.7.7. Strigolactone crosstalk with salicylic acid signaling	28
2.8. Pigment accumulation during de-etiolation	28
2.8.1. Phytohormones in the regulation of chlorophyll biosynthesis	29
2.8.2. Phytohormones in the regulation of carotenogenesis	29
Chapter 3: Strigolactone in the mediation of tolerance to heat stress	31
3.1. Introduction	31
3.2. Materials and methods	32
3.2.1. Plant materials	32
3.2.2. Experiment I: Seed germination	32
3.2.2.1. Germination conditions, chemical treatments, and experimental design	32
3.2.2.2. Germination indices	33
3.2.2.3. Determination of antioxidant enzyme activities	33
3.2.2.4. Estimation of lipid peroxidation	35
3.2.2.5. Determination of total antioxidant capacity	35
3.2.2.6. Determination of total phenolic content	35
3.2.2.7. Estimation of proline content	36
3.2.3. Experiment II: OJIP analysis, biochemical and physiological responses of seedlings	36
3.2.3.1. Growth conditions	36
3.2.3.2. Chemical and heat stress treatments	36
3.2.3.3. Chlorophyll a fluorescence transient and OJIP analysis	37
3.2.3.4. Physiological and biochemical responses of seedlings	37
3.2.3.5. Determination of glyoxalase I and II activities	37

3.2.4. Statistical analysis	39
3.3. Results	39
3.3.1. Experiment I: Seed germination	39
3.3.1.1. GR24 enhances seed germination under HS	39
3.3.1.2. GR24 enhanced superoxide radical scavenging while inhibiting peroxidase activity	42
3.3.1.3. GR24 inhibits HS-induced peroxidation of lipids and increase proline content	42
3.3.1.4. Total antioxidant capacity and phenolic content	42
3.3.2. Experiment II: Chlorophyll a fluorescence, biochemical and physiological responses of lupine seedlings under HS	45
3.3.2.1. Effects of GR24 and strigolactone inhibitors on PSII and PSI activity in lupine seedlings under HS	45
3.3.2.2. Antioxidant enzyme activities are enhanced in GR24-treated lupine seedlings under HS	54
3.3.2.3. GR24 stimulates glyoxalase I and II activity in lupine seedlings under HS	54
3.3.2.4. Lipid peroxidation and proline accumulation in seedlings	54
3.3.2.5. Total antioxidant capacity and phenolic content	54
3.4. Discussion	58
Chapter 4: Strigolactone in the mediation of tolerance to chilling stress	63
4.1. Introduction	63
4.2. Materials and methods	65
4.2.1. Plant material and seedling growth conditions	65
4.2.2. Strigolactone and chilling treatments	65
4.2.3. Chlorophyll fluorescence index	66
4.2.4. Physiological and biochemical assessment of seedlings	66
4.2.4.1. Estimation of leaf relative water content	66
4.2.4.2. Histochemical detection and quantification of reactive oxygen species	66
4.2.4.2.1. Superoxide radical	66
4.2.4.2.2. Hydrogen peroxide	67
4.2.4.3. Quantification of total soluble sugars	68
4.2.4.4. Estimation of lipid peroxidation	68
4.2.4.5. Estimation of radical scavenging activity	68
4.2.4.6. Total antioxidant capacity and total phenolic content	69
4.2.4.7. Estimation of proline content	69

4.2.4.8. Enzyme activity assays	69
4.2.5. Statistical analysis	71
4.3. Results	71
4.3.1. GR24 limits chilling-induced inhibition of PSII function	71
4.3.2. GR24 inhibits O_2^- and H_2O_2 accumulation in chilling-stressed mung bean seedlings	72
4.3.3. Phenolic content and radical scavenging activities are diminished in GR24-treated mung bean seedlings under chilling stress	72
4.3.4. GR24 counteracts chilling stress-induced disruption of leaf water status and augment osmolyte accumulation	76
4.3.5. SOD, LOX, PAL, and TAL activities are stimulated in GR24-treated mung bean seedlings under chilling stress	76
4.4. Discussion	79
Chapter 5: Strigolactone targets in the regulation of adventitious root formation	82
5.1. Introduction	82
5.2. Materials and methods	84
5.2.1. Plant material and explant treatment	84
5.2.2. Explant treatments	84
5.2.3. Visualization of H_2O_2 by diaminobenzidine staining	84
5.2.5. Estimation of plasma membrane H^+ -ATPase activity	85
5.2.6. Statistical analysis	86
5.3. Results	86
5.3.1. GR24 inhibits adventitious rooting in mung bean hypocotyls	86
5.3.2. GR24 counteracts the stimulatory effects of H_2O_2 on adventitious rooting	86
5.3.3. GR24 diminishes H_2O_2 levels in mung bean hypocotyls	86
5.3.4. Plasma membrane H^+ -ATPase serves as a downstream regulatory component in GR24-mediated control of ARF in mung bean.	87
5.4. Discussion	93
Chapter 6: Strigolactone interactions with ethylene and sucrose in the regulation of pigment accumulation during de-etiolation	96
6.1. Introduction	96
6.2. Materials and methods	98
6.2.1. Plant materials	98

6.2.2. Chemical treatments	98
6.2.3. Chlorophyll and total carotenoid quantification	98
6.2.4. Estimation of total soluble sugar content	99
6.2.5. Statistical analyses	99
6.3. Results	100
6.3.1. GR24 and ethylene precursor (ACC) repress pigment accumulation in de-etiolating mung bean seedlings	100
6.3.2. D14 inhibitor (TL) masks the effects of GR24 on pigment accumulation	100
6.3.3. Sucrose-induced pigment accumulation is antagonized by GR24	100
6.3.4. Sucrose reverses ACC-induced repression of pigment accumulation	101
6.4. Discussion	106
Chapter 7: General conclusions	108
References	111

List of Abbreviations

°C	degree Celsius
ABA	abscisic acid
ABS/RC	Absorption flux per reaction centre
AR	adventitious rooting
ARF	adventitious root formation
PstHS	after heat stress treatment
ACC	1-aminocyclopropane-1-carboxylic acid
AVG	aminoethoxyvinyl glycine
ANOVA	analysis of variance
AMF	arbuscular mycorrhizal fungi
APX	ascorbate peroxidase
AXR1	AUXIN RESISTANCE1
PreHS	before heat stress treatment
BES	BRI1-EMS-SUPPRESSOR1
BSA	bovine serum albumin
BRC1	BRANCHED1
CCD	carotenoid cleavage dioxygenase
C_a	chlorophyll a
ChlF	Chlorophyll a fluorescence
C_b	chlorophyll b
C_{a+b}	total chlorophyll
C_{x+c}	total carotenoid
CS	Chilling stress treatment
CVG	coefficient of velocity of germination
COPI	CONSTITUTIVE PHOTOMORPHOGENESIS 1
CTL	Control seedlings
CLIM	covalently linked intermediate molecule
d	day(s)
DAB	3,3'-diaminobenzidine
DTT	dithiothreitol
DW	dry weight
D3	DWARF3

D10	DWARF10
D14	DWARF14
D27	DWARF27
D53	DWARF53
HY5	ELONGATED HYPOCOTYL 5
EDTA	ethylenediaminetetraacetic acid
EAR	Ethylene-responsive element-binding factor-associated Amphiphilic Repression
F_o	Fluorescence intensity at $\sim 20 \mu\text{s}$ (minimal)
F_k	Fluorescence intensity at $\sim 0.3 \text{ ms}$
F_j	Fluorescence intensity at 2 ms
F_i	Fluorescence intensity at 30 ms
F_m	Maximal fluorescence intensity
M_o	Approximated initial slope (in ms^{-1}) of the fluorescence transient
φ_{Po}	The maximum quantum yield of primary photochemistry
φ_{Do}	Quantum yield of energy dissipation
ψ_{Eo}	The probability that a trapped exciton is used for electron transport beyond Q_A
φ_{Eo}	Quantum yield of electron transport beyond Q_A
δ_{Ro}	The efficiency with which an electron reduces PSI end electron acceptors
φ_{Ro}	The quantum yield of reduction of PSI end acceptors
PI	Performance index
Q_A	Primary quinone electron acceptor of PSII
Q_B	Secondary quinone electron acceptor of PSII
FGP	final germination percentage
FC1	FINE CULM1
FW	fresh weight
FUL	FRUITFUL
FC	fusicoccin
GI	germination index
GSTI	germination stress tolerance index
GAI	GIBBERELLIC ACID INSENSITIVE
GID1	GIBBERELLIN INSENSITIVE DWARF1
GID2	GIBBERELLIN INSENSITIVE DWARF2
GR24	<i>racemic</i> GR24

HS	heat stress
h	hour(s)
IPA1	IDEAL PLANT ARCHITECTURE1
JA	jasmonic acid
LBO	LATERAL BRANCHING OXIDOREDUCTASE
LR	lateral root
LRR	leucine-rich repeat
LEDs	light emitting diodes
LOX	lipoxygenase
MDA	malondialdehyde
MG	methylglyoxal
min	minute(s)
MAX1	MORE AXILLARY GROWTH 1
MES	2-(N-morpholino)ethanesulfonic acid
NBT	nitroblue tetrazolium
Nod	nodulation factors
<i>oreo9</i>	<i>oresara9</i>
OSHI	ORYZA SATIVA HOMEobox 1
OEC	oxygen evolving complex
POX	peroxidase
PAL	phenylalanine ammonia-lyase
PMSF	phenylmethylsulfonyl fluoride
PIN	PIN-FORMED
PM	plasma membrane
PDR1	PLEIOTROPIC DRUG RESISTANCE 1
PAT	polar auxin transport
PreCS	pre-chilling stress treatment
PI	promptness index
RC	reaction centre
ROS	reactive oxygen species
RIN	RIPENING INHIBITOR
RSL4	ROOT HAIR DEFECTIVE 6-LIKE 4
SA	salicylic acid
SE	standard error
SHY2	SHORT HYPOCOTYL 2

STS	silver thiosulfate
SCF	Skp1-Cullin-F-box
SLG	S-lactoylglutathione
SLY1	SLEEPY1
SLR1	SLENDER RICE1
SNE	SNEEZY
VA	sodium orthovanadate
SPL3/17	SQUAMOSA PROMOTER BINDING PROTEIN-LIKE3/17
SUC	sucrose
SOD	superoxide dismutase
SMXL6-8	SUPPRESSOR OF MAX2-LIKE6-8
SMAX1	SUPPRESSOR OF MAX2 1
TB	tebuconazole
TB1	TEOSINTE BRANCHED1
TL	tolfenamic acid
TT	tolfenamic acid + tebuconazole
TAG	TOMATO AGAMOUS
TPR	TOPLESS (TPL)/TPL-RELATED
TFs	transcription factors
TCA	trichloroacetic acid
Tris	Tris(hydroxymethyl)aminomethane
TAL	tyrosine ammonia-lyase
WTs	wild types

List of Figures

- Figure 2.1. Chemical structures of canonical strigolactones, GR24, and karrikin. 5
- Figure 2.2. Chemical structures of non-canonical strigolactones. 3
- Figure 3.1. The effects of GR24, tolfenamic acid, and tebuconazole treatments on germination of *Lupinus angustifolius* L. seeds under normal (NS) and elevated temperature (HS). Final germination percentage (**A**); coefficient of velocity of germination (**B**); germination index (**C**); and germination stress tolerance index (**D**). Treatments: control, CTL; strigolactone, GR24; tolfenamic acid, TL; tebuconazole, TB; tolfenamic acid + tebuconazole, TT. NS: seeds germinated under non-stress/ambient condition; HS: seeds germinated under heat stress. Different letters indicate statistically significant differences ($p < 0.05$) between the treatment group means. Values represent mean \pm standard error ($n = 2$ and 3 seed lots with 10 seeds each for non-stress and stress germination, respectively). 41
- Figure 3.2. Antioxidant enzyme activities, viz. superoxide dismutase (**A**), ascorbate peroxidase (**B**), and peroxidase (**C**) in germinating *Lupinus angustifolius* L. seeds treated with GR24, tolfenamic acid, and tebuconazole germinated under high temperature. Treatments: control, CTL; strigolactone, GR24; tolfenamic acid, TL; tebuconazole, TB; tolfenamic acid + tebuconazole, TT. Different letters indicate statistically significant differences ($p < 0.05$) between the treatment group means. Data represent mean \pm standard error ($n = 4$). 43
- Figure 3.3. Malondialdehyde content (**A**), proline content (**B**), total antioxidant capacity (**C**), and phenolic content (**D**) of *Lupinus angustifolius* L. seeds treated with GR24, tolfenamic acid, and tebuconazole and germinated under high temperature. Treatments: control, CTL; strigolactone, GR24; tolfenamic acid, TL; tebuconazole, TB; tolfenamic acid + tebuconazole, TT. Different letters indicate 44

statistically significant differences ($p < 0.05$) between the treatment group means. Values represent mean \pm standard error ($n = 4$).

- Figure 3.4. The influence of GR24, tolfenamic acid, and tebuconazole treatments on the changes in average foliar fluorescence intensities in *Lupinus angustifolius* L. seedlings after three consecutive days under heat stress (compared to preheat stress values). Percentage change in the minimal fluorescence intensity (F_o) when all PSII reaction centers are open, the O-step (**A**); the fluorescence intensity at the K-step at $\sim 300 \mu\text{s}$, F_k (**B**); the fluorescence intensity at the J-step at 2 ms, F_j (**C**); the fluorescence intensity at the I-step at 30 ms, F_i (**D**); the maximal fluorescence intensity at the P-step when all PSII reaction centers are closed, F_m (**E**); and the approximated initial slope (in ms^{-1}) of the fluorescence transient, M_o (**F**). Positive values indicate a percentage increase, while negative values indicate a percentage decrease. Treatments: control, CTL; strigolactone, GR24; tolfenamic acid, TL; tebuconazole, TB; tolfenamic acid + tebuconazole, TT. Asterisks show significant difference (** at $p < 0.01$ and * for $p < 0.05$) compared to the initial (PreHS) values before heat stress. 49
- Figure 3.5. The effects of GR24, tolfenamic acid, and tebuconazole on foliar relative variable fluorescence (**A–C**) and the approximated initial slope of the fluorescence transient (**D**) of *Lupinus angustifolius* L. seedlings before heat treatment (PreHS), after heat stress (HS), and after 3-day recovery (PstHS). Treatments: control, CTL; strigolactone, GR24; tolfenamic acid, TL; tebuconazole, TB; tolfenamic acid + tebuconazole, TT. Data are means \pm standard error ($n = 5$). 50
- Figure 3.6. Effect of GR24, tolfenamic acid, and tebuconazole treatments on the quantum yields and efficiencies/probabilities of *Lupinus angustifolius* L. seedlings before heat stress (PreHS), after heat stress (HS), and after recovery (PstHS). φ_{Po} , the maximum quantum yield of PSII photochemistry (**A**); φ_{Do} , the quantum yield of energy (heat) dissipation (**B**); ψ_{Eo} , the fraction of electrons transported beyond Q_A^- 51

per exciton trapped by the open reaction centers of PSII (**C**); φ_{Eo} , the quantum yield of electron transport beyond Q_A (**D**); δ_{Ro} , the efficiency with which an electron can move from the reduced intersystem electron acceptors to the PSI end acceptors (**E**); and φ_{Ro} , the quantum yield of reduction of PSI end acceptors (**F**). Treatments: control, CTL; strigolactone, GR24; tolfenamic acid, TL; tebuconazole, TB; tolfenamic acid + tebuconazole, TT. Data represents mean \pm standard error ($n = 5$).

- Figure 3.7. Effect of GR24, tolfenamic acid, and tebuconazole treatments on the specific energy fluxes per Q_A reducing PSII reaction center (RC) of *Lupinus angustifolius* L. seedlings before heat stress (PreHS), after heat stress (HS), and after recovery (PstHS). ABS/RC, absorption flux per RC (**A**); and TR_o/RC , trapped energy flux per RC (**B**). Treatments: control, CTL; strigolactone, GR24; tolfenamic acid, TL; tebuconazole, TB; tolfenamic acid + tebuconazole, TT. Data represents mean \pm standard error ($n = 5$). 52
- Figure 3.8. The effect of GR24, tolfenamic acid, and tebuconazole treatments on the performance indices of *Lupinus angustifolius* L. seedlings before heat stress (PreHS), after heat stress (HS), and after recovery (PstHS). PI_{abs} , performance index on absorption basis, i.e., energy conservation from photons absorbed by PSII to the reduction of intersystem electron acceptors (**A**) and PI_{total} , the total performance index for energy conservation from photons absorbed by PSII to the reduction of PSI end acceptors (**B**). Treatments: control, CTL; strigolactone, GR24; tolfenamic acid, TL; tebuconazole, TB; tolfenamic acid + tebuconazole, TT. Data represents mean \pm standard error ($n = 5$). 53
- Figure 3.9. The effect of GR24, tolfenamic acid, and tebuconazole on antioxidant enzymes, viz. superoxide dismutase (**A**), ascorbate peroxidase (**B**), and peroxidase (**C**) in *Lupinus angustifolius* L. seedlings under heat stress. Treatments: control, CTL; strigolactone, GR24; tolfenamic acid, TL; tebuconazole, TB; tolfenamic acid + tebuconazole, TT. Different letters indicate statistically significant differences ($p < 0.05$) between 55

the treatment group means. Data represent mean \pm standard error ($n = 4$).

- Figure 3.10. Effect of GR24, tolfenamic acid, and tebuconazole treatments on glyoxalase I (A) and glyoxalase II (B) activities in *Lupinus angustifolius* L. seedlings under heat stress. Treatments: control, CTL; strigolactone, GR24; tolfenamic acid, TL; tebuconazole, TB; tolfenamic acid + tebuconazole, TT. Different letters indicate statistically significant differences ($p < 0.05$) between the treatment group means. Data represent mean \pm standard error ($n = 4$). 56
- Figure 3.11. Lipid peroxidation levels (A), proline content (B), total antioxidant capacity (C), and phenolic content (D) of heat-stressed *Lupinus angustifolius* L. seedlings treated with GR24, tolfenamic acid, and tebuconazole. Treatments: control, CTL; strigolactone, GR24; tolfenamic acid, TL; tebuconazole, TB; tolfenamic acid + tebuconazole, TT. Different letters indicate statistically significant differences ($p < 0.05$) between the treatment group means. Data represent mean \pm standard error ($n = 4$). 57
- Figure 4.1. Photosystem II quantum yields and efficiencies in GR24-treated mung bean [*Vigna radiata* (L.) R. Wilczek] seedlings before chilling stress (PreCS) and after chilling stress (CS). φ_{Po} , the maximum quantum yield of PSII photochemistry (A); ψ_{Eo} , the efficiency of electron transport beyond Q_A^- per trapped exciton (B); φ_{Eo} , the quantum yield of electron transport beyond Q_A (C); φ_{Do} , the quantum yield of energy (heat) dissipation (D). Data represent means, and the bars depict standard error ($n = 10$) for each treatment. 73
- Figure 4.2. Accumulation of superoxide anion (O_2^-) and hydrogen peroxide (H_2O_2) in mung bean [*Vigna radiata* (L.) R. Wilczek] seedlings under chilling conditions and GR24 treatments. (A) Nitroblue tetrazolium (NBT) staining for O_2^- and diaminobenzidine (DAB) staining for H_2O_2 in mung bean leaves. Effect of GR24 treatments on formazan formation in NBT-stained leaves (B) and H_2O_2 content (C) of chilling-stressed 74

mung bean seedlings. Data shown are the means \pm standard error (SE), $n = 4$. Different letters indicate significant differences among treatments according to Duncan's Multiple Range Test with confidence level set at $p < 0.01$.

- Figure 4.3. The total phenolic contents (**A**), antioxidant capacities (**B**), radical (DPPH) scavenging activities (**C**), and lipid peroxidation levels (**D**) in mung bean [*Vigna radiata* (L.) R. Wilczek] seedlings treated with different doses of GR24 and subjected to chilling stress. Data represent means and standard error of $n = 5$, and significant differences among treatment group means at $p < 0.01$ according to Duncan's Multiple Range Test are indicated by different letters. 75
- Figure 4.4. Effects of GR24 treatments on relative water content (**A**), proline (**B**), and soluble sugar accumulation (**C**) in mung bean [*Vigna radiata* (L.) R. Wilczek] seedlings exposed to chilling stress. Data are means \pm standard error, $n = 5$. Different letters indicate significant differences among treatments according to Duncan's Multiple Range Test with confidence level set at $p < 0.01$. 77
- Figure 4.5. The effect of GR24 application on superoxide dismutase (**A**), lipoxygenase (**B**), phenylalanine ammonia-lyase (**C**), and tyrosine ammonia-lyase (**D**) activities in mung bean [*Vigna radiata* (L.) R. Wilczek] seedlings exposed to chilling stress. Data are presented as means and standard error ($n = 4$), and significant differences among the treatment group mean at $p < 0.01$, according to Duncan's Multiple Range Test, are indicated by different letters. 78
- Figure 5.1. Effects of treatments (as outlined below) on adventitious root formation in mung bean hypocotyls. (a) H₂O (control); (b) GR24 1 μ M; (c) GR24 5 μ M; (d) GR24 10 μ M; (e) 30 mM H₂O₂; (f) 50 mM H₂O₂; (g) 70 mM H₂O₂; (h) GR24 1 μ M + 30 mM H₂O₂; (i) GR24 5 μ M + 30 mM H₂O₂; (j) GR24 10 μ M + 30 mM H₂O₂; (k) fusicoccin (FC) 0.5 μ M; (l) FC 1 μ M; (m) Na₃VO₄ (VA) 100 mM; (n) VA 300 mM; (o) VA 500 mM; (p) 30 mM H₂O₂ + VA 300 mM; (q) 50 mM 89

H₂O₂ + VA 300 mM; (r) 70 mM H₂O₂ + VA 300 mM; (s) GR24 5 μM + FC 1 μM; (t) GR24 10 μM + FC 1 μM. Bar = 1 cm.

- Figure 5.2. Quantitative changes in the number of adventitious roots formed in mung bean hypocotyls in response to (A) GR24; (B) H₂O₂; and (C) combination of GR24 and H₂O₂; and (D) the impact of GR24 on endogenous H₂O₂ during adventitious root formation in mung bean (mean ± SE of *n* = 3). HP, hydrogen peroxide (H₂O₂). Different letters above error bars indicate statistically significant differences among treatments at *p* < 0.05. The expressed number of adventitious roots per explants are means from three independent experiments with 12 explants per treatment. 90
- Figure 5.3. *In situ* visualization of H₂O₂ in mung bean hypocotyl sections by 3,3-diaminobenzidine (DAB) staining. The effect of strigolactone (GR24) treatments on the generation of H₂O₂ in explants during cutting-induced adventitious root formation. Treatments: (a) distilled water (control); (b) 1 μM GR24; (c) 5 μM GR24; and (d) 10 μM GR24. Bar = 1 mm. 91
- Figure 5.4. The effects of (A) fusicoccin, (B) sodium orthovanadate (Na₃VO₄), and (C) combined GR24-fusicoccin treatments on adventitious root formation; and (D) PM H⁺-ATPase activities in response to GR24 and H₂O₂ treatments (mean ± SE of *n* = 3). GR24 concentrations: 0, 1, 5, 10 μM. HP: 30 mM H₂O₂, SL+HP: 5 μM GR24 + 30 mM H₂O₂. Different letters above the error bars indicate statistically significant differences among treatments at *p* < 0.05. The expressed number of adventitious roots per explants are means from three independent experiments with 12 explants per treatment. 92
- Figure 6.1. The influence of GR24 on pigment accumulation during de-etiolation of dark-grown mung bean seedlings. Total chlorophyll (A) and carotenoid (B) contents in GR24-treated mung bean seedlings after exposure to 16 h of light. Effects of GR24, ethylene precursor (ACC) and inhibitors (AVG & STS) on total chlorophyll (C) and carotenoid 102

(D) contents in de-etiolating mung bean seedlings. Data are presented as means and standard error ($n = 4$), and significant differences among treatment mean at $p < 0.05$, according to Duncan's Multiple Range Test, are indicated by different letters.

- Fig. 6.2. Tolfenamic acid-induced reversal of GR24 influence on pigment accumulation during de-etiolation of dark-grown mung bean seedlings. Total chlorophyll (A) and carotenoid (B) contents of mung bean seedlings treated as indicated and exposed to 16 h of light. TL, tolfenamic acid; GR24, racemic GR24; Suc, sucrose. Data are means \pm standard error ($n = 4$), and significant differences among treatment mean at $p < 0.05$ are indicated by different letters. 103
- Figure 6.3. Sucrose-GR24 interactions in the regulation of chlorophyll (A) and carotenoid (B) accumulation during the de-etiolation of dark-grown mung bean seedlings. Total soluble sugar (C) content of de-etiolating mung bean seedlings after treatments. TL, tolfenamic acid. Data represent means \pm standard error ($n = 4$), and significant differences among treatment mean at $p < 0.05$ are indicated by different letters. 104
- Figure 6.4. Sucrose, ethylene, and GR24 interactions in the regulation of chlorophyll (A) and carotenoid (B) accumulation during the de-etiolation of dark-grown mung bean seedlings. ACC, 1-aminocyclopropane-1-carboxylic acid, AVG, aminoethoxyvinyl glycine; GR24, racemic GR24; Suc, sucrose; STS, silver thiosulfate. Data represent means \pm standard error ($n = 4$), and significant differences among treatment mean at $p < 0.05$ are indicated by different letters. 105

List of Tables

Table 3.1.	Seed germination index and their formula, parameters, and description (Kader, 2005; Partheeban <i>et al.</i> , 2017).	34
Table 3.2.	Description of JIP-test parameters adapted from Strasser <i>et al.</i> (2010) and Jedmowski and Brüggemann (2015).	38

Abstract

Strigolactones are apocarotenoid, sesquiterpenoid hormones with a butenolide functional group that serves as the essential bioactiphore for their hormonal activities. The hormonal actions of this class of phytohormone in the mediation of plant tolerance to abiotic stress are still emerging. This study was therefore carried out using a synthetic strigolactone analog, *racemic* GR24 (GR24), to evaluate strigolactone hormonal actions in enabling plants to tolerate heat and chilling stress, adventitious root formation as an adaptive response to cutting, and pigment accumulation during the seedling transition from growth in the dark to development in light.

To determine if strigolactones could ameliorate thermoinhibition of seed germination and seedling development, the effects of GR24, strigolactone biosynthesis and signal receptor inhibitors [tebuconazole (TB) and tolfenamic acid (TL) respectively], on the physiological and biochemical responses associated with thermotolerance during seed germination and seedling growth in *Lupinus angustifolius* under heat stress (HS) were examined. Seed germination indices were significantly enhanced by GR24 treatments with 90% final germination and a stress tolerance index of ~78.5%. Similarly, enzymatic scavenging of O₂⁻ was enhanced by GR24 with an attendant decrease in lipid peroxidation while proline content was also enhanced, thereby improving osmotic balance to enhance seed germination under HS. However, observations with TL-treated seeds suggest that strigolactone-D14 signals play a limited role in seed germination while blocking strigolactone biosynthesis had no effect on germination under normal and HS conditions, thus implying that strigolactone biosynthesis is not required for lupine seed germination.

Chlorophyll a transient analysis was employed to assess photosystem functions in lupine seedlings treated with GR24, TB, and TL and subjected to HS. This revealed that GR24-induced OECs resistance to HS and ensured PSII thermostability while also alleviating the limiting effects of heat stress on the quantum yields, efficiencies, and performance indexes of PSII. The accumulation of phenolics and induction of antioxidant and glyoxalase enzymes in GR24-treated seedlings alludes to the mitigation of HS-induced oxidative injury by strengthening ROS homeostasis. However, since TL treatments did not limit PSII thermotolerance, GR24-mediated thermotolerance may not be attributed to D14-dependent signaling, but KAI2 signals since GR24 also elicits the karrikin signal pathway.

In order to determine if strigolactones can also induce tolerance to cold stress, mung bean seedlings were treated with different concentrations of GR24 and subjected to chilling stress (CS) treatment. Chilling-induced inhibition of PSII activities and ROS imbalance was limited by GR24 via improved ROS scavenging. There was a GR24-mediated increase in osmolyte (soluble sugars and proline) accumulation with an attendant improvement in leaf tissue water status, thus indicating that GR24 may broker the mitigation of abiotic stress via osmotic adjustment. GR24-treated seedlings showed induced PAL, TAL, and LOX activities, thus suggesting that the phenylpropanoid pathway and oxylipin-dependent stress coping mechanisms may be involved in strigolactone-mediated abiotic stress tolerance.

Adventitious root formation in excised mung bean hypocotyl was evaluated after treatment with GR24. The number of adventitious roots formed on hypocotyl cuttings was decreased in GR24 treated explants. H₂O₂ content of cut hypocotyls was diminished by GR24 treatments, which also counteracted H₂O₂-induced adventitious rooting in hypocotyl cuttings. The results from physiological tests employing fusicoccin and vanadate showed that plasma membrane H⁺-ATPase is involved in the regulation of cutting-induced adventitious rooting and was negatively influenced by GR24 treatments. These suggest that H₂O₂ and PM H⁺-ATPase are hormonal targets of strigolactones in the regulation of adventitious rooting.

To evaluate the impacts of strigolactone hormonal actions and the interactions with ethylene and sucrose on chlorophyll and carotenoid accumulation during de-etiolation, dark-grown and etiolated mung bean seedlings were treated with test solutions and exposed to light after 24 h. Pigment accumulation was inhibited by GR24 and ethylene precursor (ACC), while sucrose and ethylene inhibitors (AVG and STS) enhanced pigment content. The inhibitory effect of GR24 was masked by ethylene inhibitors, thus suggesting GR24 requires ethylene-dependent signals to elicit their control on pigment accumulation. The results from TL treatments show that the strigolactone-D14 signal pathway is involved in GR24-mediated effects on pigment accumulation during de-etiolation. On the other hand, sucrose and strigolactone signals acted antagonistically, with sucrose overriding the repressive impact of GR24. The observed GR24-induced repression of pigment accumulation was not achieved via limitations on sugar content since GR24 treatment did not significantly affect the soluble sugar content of de-etiolating seedlings.

Chapter 1

General Introduction

1.1. Introduction

Strigolactones are sesquiterpenoid hormones with a butenolide functional group and are derived from dioxygenase-mediated oxidative cleavage of carotenoids. They have been implicated in the regulation of diverse aspects of plant growth, development, plant-environment, and plant-microbe interactions. Initially identified for their roles in the stimulation of seed germination in root-parasitic plants (Cook *et al.*, 1972; Hauck *et al.*, 1992; Müller *et al.*, 1992; Brun *et al.*, 2018), and symbiotic plant-microbe interactions within the rhizosphere (Akiyama *et al.*, 2005; Akiyama *et al.*, 2010; Genre *et al.*, 2013; Torres-Vera *et al.*, 2014; Mori *et al.*, 2016; Cheng *et al.*, 2017), they mediate other aspects of plant growth and development such as root and shoot architecture patterning (Marzec and Melzer, 2018), responses to nutrient (nitrogen and phosphate) deficiencies (Ito *et al.*, 2016), leaf senescence (Tian *et al.*, 2018) and tolerance to abiotic and biotic stressors (Cheng *et al.*, 2017; Saeed *et al.*, 2017; Mostofa *et al.*, 2018).

The roles of strigolactones in mediating plant responses and tolerance to abiotic stress are still emerging (Mostofa *et al.*, 2018). Strigolactone hormonal actions are implicated in the enhancement of innate response and tolerance mechanisms in plants under limiting ambient conditions such as drought and salt stress (Ha *et al.*, 2014; Ma *et al.*, 2017b; Lv *et al.*, 2018). However, investigations into the roles of strigolactones in plants subjected to suboptimal or supra-optimal ambient temperatures are scarce. Similarly, reports on downstream strigolactone hormonal signal targets during adventitious root formation, a coping strategy for ensuring species survival via enhanced nutrient and water uptake as well as vegetative propagation, are mostly unavailable. Even though several studies have reported the regulatory roles of strigolactones in adventitious root formation (Kapulnik *et al.*, 2011a; Kapulnik *et al.*, 2011b; Rasmussen *et al.*, 2012a; Sun *et al.*, 2014; Sun *et al.*, 2015; Sun *et al.*, 2016a; Rasmussen *et al.*, 2017; Marzec and Melzer, 2018).

Chlorophyll biosynthesis and carotenoid accumulation are central developmental processes that accompany seedling de-etiolation and photomorphogenic development. In etiolated seedlings, the chlorophyll precursor, protochlorophyllide, is accumulated and closely associated with a paracrystalline lipid-pigment-protein tubular structure called the prolamellar body, a defining ultrastructural component of etioplasts (Armarego-Marriott *et al.*, 2019; Kowalewska *et al.*, 2019). The low carotenoid content associated with etiolated seedlings (compared to light-grown seedlings) is partly attributed to repressed phytoene synthase (PSY) activity. This is due to limited expression of PSY genes, which is a crucial enzyme in carotenogenesis (Nisar *et al.*, 2015) that requires light cues mediated via phytochrome for transcriptional activation, and the absence of a requisite competent membrane for PSY function as a membrane-bound protein. Prolamellar bodies, in which most PSY proteins are localized, lack well-developed membranes (Yuan *et al.*, 2015). Although strigolactones regulate photomorphogenic processes like hypocotyl elongation (Jia *et al.*, 2014; Thussagunpanit *et al.*, 2017), their role(s), if any, in pigment (chlorophyll and carotenoid) accumulation during seedling de-etiolation are yet to be reported. Furthermore, whether any interaction exists between strigolactones, ethylene (a phytohormone with enormous influence on photomorphogenesis), and sugar signals in the regulation of pigment accumulation during seedling de-etiolation is yet to be determined.

1.2. **Aims and objectives of the study**

This study was focused on evaluating the impact(s) of strigolactone signaling on:

- i. seed resilience and germination under heat stress;
- ii. plant innate responses and coping mechanisms such as the enzymatic and non-enzymatic antioxidant systems, osmolyte accumulation, and glyoxalase system in seedlings subjected to heat-induced oxidative stress;
- iii. tolerance strategies such as the regulation of reactive oxygen species accumulation and scavenging, non-enzymatic antioxidant systems, osmolyte accumulation, the activities of lipoxygenases and phenylpropanoid pathway enzymes under chilling stress;
- iv. downstream strigolactone hormonal targets involved in cutting-induced adventitious root formation and their actions; and

- v. pigment accumulation as well as strigolactone, ethylene, and sugar interactions in the regulation of chlorophyll and carotenoid contents during de-etiolation.

1.3. Overview of chapters in this thesis

Chapter Two provides a comprehensive review of strigolactones, their chemical nature and classifications, the current understanding of strigolactone biosynthesis, transport, signal perception, and transduction. It also covers a concise overview of several reported strigolactone-mediated responses and bioactivities, as well as a detailed presentation of strigolactone interaction with other phytohormones.

Chapter Three investigates the role of strigolactones in the mediation of tolerance to heat stress during seed germination and seedling development in blue lupine via photosystem resilience, antioxidant system function, osmolyte accumulation, and glyoxalase enzyme responses.

Chapter Four reports the impacts of strigolactone treatments on photosynthetic activities, reactive species accumulation and scavenging, phenolic accumulation, water, and osmolyte status, the activity of lipoxygenase, and phenylpropanoid pathway enzymes in mung bean subjected to chilling stress.

Chapter Five investigates and identifies hydrogen peroxide and plasma membrane H⁺-ATPase as downstream signal targets of strigolactone hormonal signal in the regulation of cutting-induced adventitious root formation in mung bean hypocotyls.

Chapter Six reports the impacts of strigolactones on photosynthetic pigment accumulation as well as strigolactone-ethylene-sugar interactions in the regulation of chlorophyll and carotenoid content during photomorphogenesis in etiolated mung bean seedlings.

Chapter Seven provides a summary of the major findings of these studies.

References provide an outline of the literature and materials cited in this thesis.

Chapter 2

Literature Review

2.1. Introduction

Naturally occurring biomolecules with butenolide moieties elicit a plethora of biological activities in plants. Their bioactivities range from serving as chemical cues or signal molecules for host-parasite/symbiont interactions (Akiyama *et al.*, 2005; Akiyama *et al.*, 2010; Foo and Davies, 2011; De Cuyper *et al.*, 2015), stimulation and/or inhibition of germination in seeds (van Staden *et al.*, 2004; Daws *et al.*, 2007; Soós *et al.*, 2012), mediation of abiotic and biotic stress responses (Soós *et al.*, 2009; Cheng *et al.*, 2017; Haider *et al.*, 2018) to increasing seedling establishment, growth and vigor in plants (Light *et al.*, 2010). Karrikins and strigolactones are two classes of butenolides with significant influences on plant growth and development and with ecologically relevant functions. While strigolactones are endogenous phytohormones that are synthesized mainly in root tissues and transported to other parts of the plant or exuded into the rhizosphere in root exudates, karrikins are components of smoke that are derived from the combustion of plant materials (van Staden *et al.*, 1995; Flematti *et al.*, 2004; Kulkarni *et al.*, 2010; Flematti *et al.*, 2013). Despite the marked similarities in the bioactivities and signal pathways of karrikins and strigolactones (Nelson *et al.*, 2011; Waters *et al.*, 2012c), the discovery of *kai2* mutants which are defective in karrikin perception but still retain their strigolactone sensitivity, and *d14* mutants lacking response to strigolactones but still retain their sensitivity to karrikins confirm that plants can distinguish between these two molecular cues (Waters *et al.*, 2012b; Waters *et al.*, 2012c; Flematti *et al.*, 2013). In the light of extant and emerging experimental data, karrikins and strigolactones are distinct chemical cues with distinct roles in the regulation of plant growth and development, although empirical data exist that shows the sharing of functions and signal pathways by both signal molecules (Li *et al.*, 2017; Yao and Waters, 2019).

2.2. Chemical nature of strigolactones

Strigolactones are grouped into two classes, canonical and non-canonical strigolactones, based on the presence or absence of a tricyclic lactone ring. Canonical strigolactones consist of a four-ring system designated A, B, C, and D (Fig. 2.1). The tricyclic lactone is linked to a butenolide moiety,

the D ring, via an *enol-ether* bridge. As a result of functional group variability, A and B rings show maximum divergence, whereas C and D are highly conserved (Fig. 2.1).

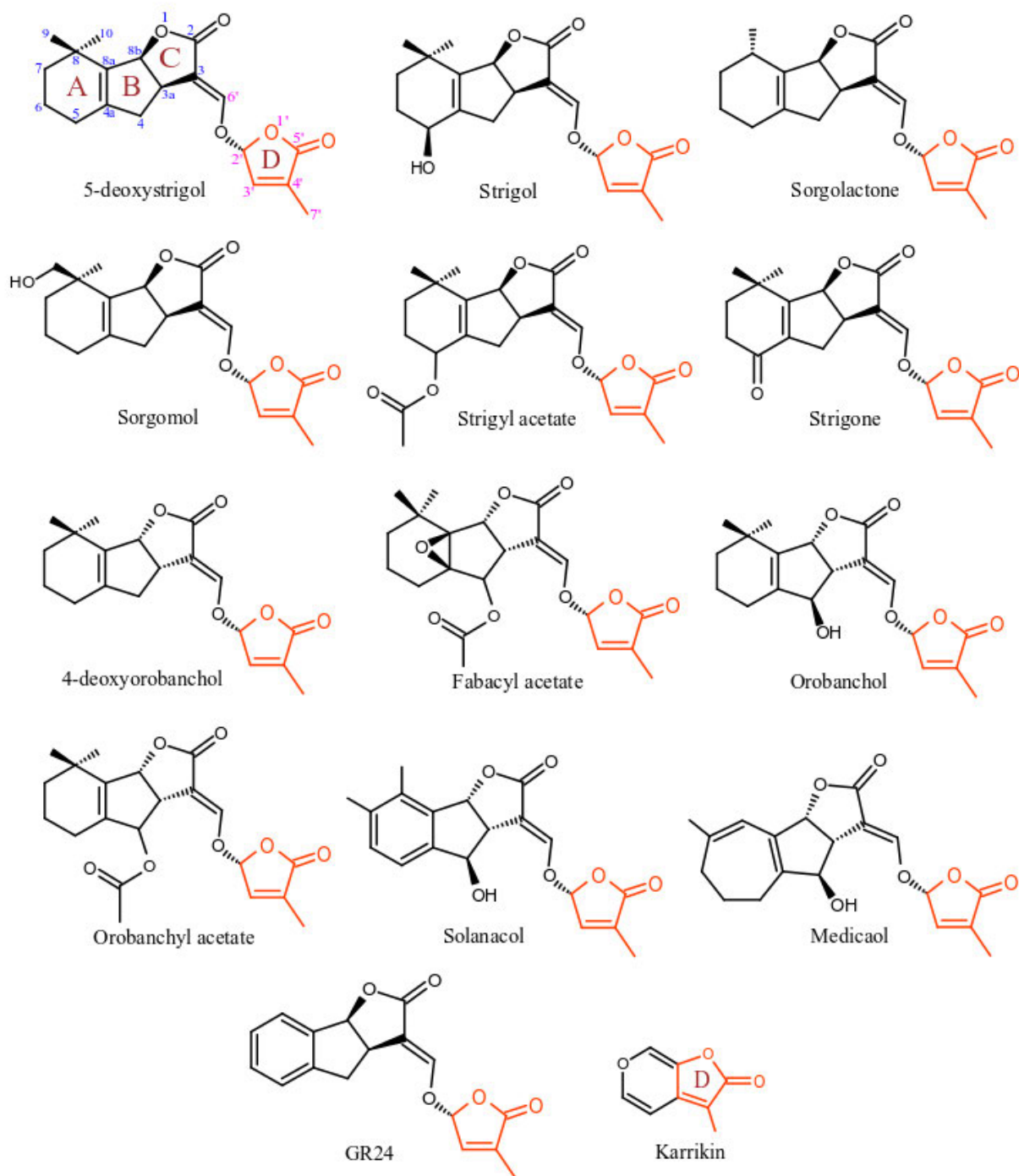


Figure 2.1. Chemical structures of canonical strigolactones, GR24, and karrikin.

On the other hand, non-canonical strigolactones (Fig. 2.2) are very diverse in the structure of their ABC ring. Carlactone-type strigolactones possess the A and D rings as well as the *enol-ether* bridge but lack the B and C rings (i.e., having unclosed ring) (Fig. 2.2). Among others in this group, we find carlactone and its derivatives such as carlactonoic acid, 3-hydroxycarlactone, methyl

carlactonoate (Alder *et al.*, 2012; Abe *et al.*, 2014; Seto *et al.*, 2014; Baz *et al.*, 2018), avenaol (Kim *et al.*, 2014) and zealactones (Charnikhova *et al.*, 2017; Xie *et al.*, 2017). Reports of non-canonical strigolactones which differ structurally from carlactone-type strigolactones such as heliolactone (Ueno *et al.*, 2014), zeapyranolactone—with 4,4-dimethyltetrahydropyran-2-one as its A ring (Charnikhova *et al.*, 2018) and lotuslactone (Xie *et al.*, 2019), among others, suggest that biomolecules with strigolactone activity accommodate a high level of structural plasticity in their ABC rings.

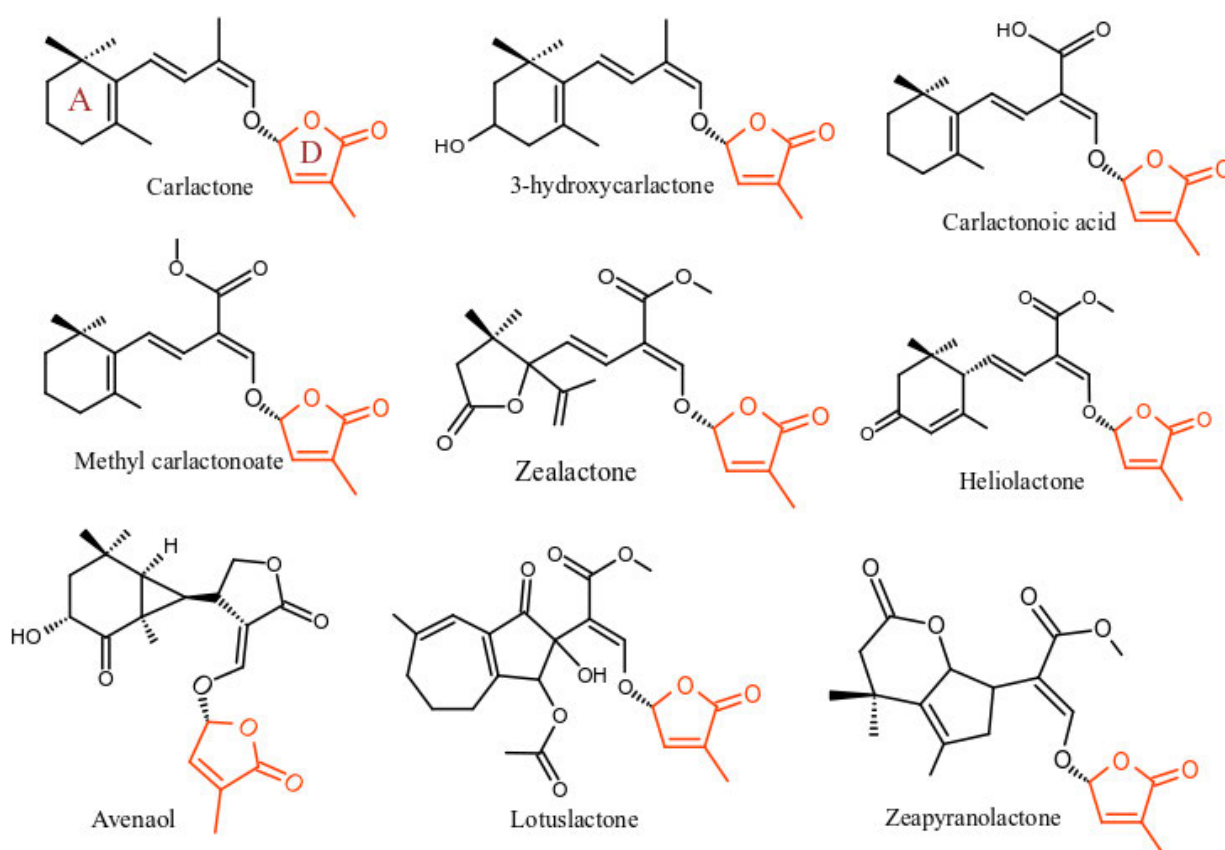


Figure 2.2. Chemical structures of non-canonical strigolactones.

With respect to the steric orientation of the BC ring junction, canonical strigolactones are categorized into either strigol or orobanchol classes. This stereochemistry contributes and determines the functional specificity of strigolactones (Akiyama *et al.*, 2010; Nomura *et al.*, 2013; Scaffidi *et al.*, 2014). The C-ring in strigol type strigolactones is in the β -orientation but in an α -orientation in orobanchol type strigolactones. Plants usually produce and transport one of either class of strigolactones; however, both have been observed in some species (Xie *et al.*, 2013; Xie *et al.*, 2016). Several studies, including those on structure-activity relationships of strigolactones in

stimulating germination in parasitic plants and hyphal branching in arbuscular mycorrhizal fungi (AMF), have established the butenolide moiety as the essential ‘*bioactiphore*’ for strigolactone activity (Akiyama *et al.*, 2010; Kim *et al.*, 2010; Zwanenburg and Pospíšil, 2013).

2.3. Biosynthesis of strigolactones

Strigolactones are downstream products of carotenoid catabolism, with the root tissues being the primary site of biosynthesis. Shoot tissues produce strigolactones in lower quantities compared to the root, and this is sufficient for shoot function in the absence of root-derived strigolactones (Domagalska and Leyser, 2011). For the purpose of clarity, rice and *Arabidopsis* gene nomenclatures are employed in describing the strigolactone biosynthetic pathway. The early dedicated steps in the biosynthesis of strigolactones lead to the production of carlactone, the primary precursor of endogenous strigolactones (Seto *et al.*, 2014; Iseki *et al.*, 2018). Carlactone is derived from a series of reactions, which includes: the isomerization of *all-trans* β -carotene C9–C10 double bond by DWARF27 (D27) (Alder *et al.*, 2012; Waters *et al.*, 2012a; Bruno and Al-Babili, 2016) to form 9-*cis*- β -carotene; the stereospecific cleavage of 9-*cis*- β -carotene to yield 9-*cis*- β -*apo*-10'-carotenal and β -ionone catalyzed by carotenoid cleavage dioxygenase 7 (CCD7) (Booker *et al.*, 2004; Bruno *et al.*, 2014); and the conversion of 9-*cis*- β -*apo*-10'-carotenal to carlactone by CCD8 via oxygenation and functional group rearrangements (Alder *et al.*, 2012; Waters *et al.*, 2012a). The resulting carlactone is exported into the cytoplasm where it undergoes oxidation, ring closures, and functional group modifications in a series of reactions catalyzed by MORE AXILLARY GROWTH 1 (MAX1), a class of cytochrome P450 monooxygenases (Seto *et al.*, 2014; Zhang *et al.*, 2014). Carlactone is first converted into carlactonoic acid by MAX1 and then used to synthesize other strigolactones (Yoneyama *et al.*, 2018). This MAX1-dependent reaction is conserved among plants. In rice, OsMAX1 (Os900) serves as a carlactone oxidase which converts carlactone via carlactonoic acid into 4-deoxyorobanchol, the precursor for the orobanchol class of strigolactones (Zhang *et al.*, 2014; Yoneyama *et al.*, 2018). Just like Os900, *Selaginella moellendorffii* MAX1 homologs, *Sm*-MAX1a, and *Sm*-MAX1b catalyze the conversion of carlactone to 4-deoxyorobanchol (Yoneyama *et al.*, 2018). On the other hand, MAX1 homologs of maize and rice, *Zm*-MAX1b, and Os1400, respectively, also oxidize carlactone into carlactonoic acid and synthesize orobanchol via the hydroxylation of 4-deoxyorobanchol (Cardoso *et al.*, 2014;

Zhang *et al.*, 2014; Yoneyama *et al.*, 2018). However, *At*-MAX1 only produces carlactonoic acid and its methyl ester from carlactone (Abe *et al.*, 2014; Yoneyama *et al.*, 2018). Brewer *et al.* (2016) identified *LATERAL BRANCHING OXIDOREDUCTASE (LBO)*, a branching gene in *Arabidopsis* that encodes an oxidoreductase-like enzyme of the 2-oxoglutarate and iron (II)-dependent dioxygenase superfamily. LBO acts downstream of MAX1 to produce a strigolactone-active compound, which is yet to be chemically described.

Recent data show that MAX1 can catalyze the biosynthesis of both canonical and non-canonical strigolactones from carlactone (Yoneyama *et al.*, 2018); and both carlactone and carlactonoic acid served as precursors for the biosynthesis of orobanchol and strigol type strigolactones (Iseki *et al.*, 2018; Yoneyama *et al.*, 2018). Furthermore, the inability of cowpea to convert 4-deoxyorobanchol despite converting carlactone and carlactonoic acid into orobanchol and alectrol; and the fact that 5-deoxystrigol was not converted to strigol in moonseed (*Menispermum dauricum*) are clear indications that the biosynthesis of hydroxylated strigolactones does not always require a deoxy-strigolactone precursor (Iseki *et al.*, 2018).

2.4. Strigolactone transport

Aside from those delegated to eliciting local actions within root tissues, there are two major destinations for root-derived strigolactones—the rhizosphere and the shoot. Strigolactones released into the rhizosphere as part of root exudate serve as cues to initiate mycorrhizae or nodule formation. They also induce the germination of seeds of root-parasitic plants, thus mediating such interactions. On the other hand, root-to-shoot transport of strigolactones serves as a significant source of strigolactones in shoot tissues where they modulate diverse aspects of shoot growth and development. Shoot-ward directional transport of strigolactones and localized exudation into the rhizosphere is mediated by an ABC subtype G (ABCG) class of transporters, PLEIOTROPIC DRUG RESISTANCE 1 (PDR1) (Kretzschmar *et al.*, 2012; Sasse *et al.*, 2015). Thus far, the only identified strigolactone transporter is PDR1 from *Petunia axillaris* and *P. hybrida*. Overexpression of PDR1 in *P. hybrida* upregulates strigolactone biosynthesis while also influencing strigolactone-related responses such as an increase in root biomass, auxin distribution, and mycorrhization (Liu *et al.*, 2018). *Petunia axillaris* PDR1 (*Pa*-PDR1) exhibits a cell-type-specific polar and

asymmetrical localization as it is localized on the apical membrane of hypodermal cells in the root apex while laterally localized on the outer membrane of hypodermal passage cells that occur above the root tip and also serve as an entry point for AMF during mycorrhization (Sasse *et al.*, 2015). In stem tissues, *Ph-PDR1* expression occurs in the vasculature and nodal tissues in close proximity with the lateral axils but is absent in dormant buds (Kretschmar *et al.*, 2012). The expression of these transporters is upregulated by endogenous and exogenous cues that are known to elicit strigolactone production and signals, such as auxin signals, limited inorganic phosphate (P_i), and AMF colonization (Kretschmar *et al.*, 2012). Furthermore, interference with the *Pa-PDR1* function results in phenotypes that are associated with flawed strigolactone production and signaling (Sasse *et al.*, 2015). The aforementioned observations from localization studies, in addition to impaired strigolactone transport towards the shoot and exudation into the rhizosphere in *Pa-pdr1* mutants (Sasse *et al.*, 2015), as well as reduced strigolactone levels in root exudates of *Ph-pdr1* mutants (Kretschmar *et al.*, 2012) together, establish the roles of PDR1 in strigolactone transport.

In a screen of xylem saps from different plant species to determine the root-to-shoot path of strigolactone transport, strigolactones were not detected in xylem saps, although exogenous strigolactones applied to roots were detected in shoot tissues after 20 hours of treatment (Xie *et al.*, 2015b). These suggest a cell-to-cell movement of strigolactones from the root to the shoot that is independent of the xylem stream. Strigolactone transport was further demonstrated to be structure- and stereo-specific (Xie *et al.*, 2016).

2.5. Strigolactone perception and signal transduction

Strigolactone signaling is a hormone-activated cascade of events that culminate in the poly-ubiquitination and proteolysis of specific target proteins as well as the hydrolytic inactivation of the hormone. This process is mediated by three main components: DWARF14 (D14), D3, and an Skp1-Cullin-F-box (SCF) E3 ubiquitin ligase complex (Stirnberg *et al.*, 2007; Hamiaux *et al.*, 2012; Shabek *et al.*, 2018; Seto *et al.*, 2019). The prevailing strigolactone signaling model posits that D14—the strigolactone receptor/perception protein—is activated by strigolactone binding, the ligand-bound D14 forms a signaling complex with other signaling partners leading to the

transduction of the hormonal signal and finally the hydrolysis of the bound strigolactone at the *enol-ether* bridge to deactivate the hormone (Hamiaux *et al.*, 2012; Waters *et al.*, 2012b; Marzec *et al.*, 2016; Seto *et al.*, 2019).

Strigolactone signal perception involves ligand docking in the catalytic cleft of D14, which results in conformational changes (open-to-closed state transition) in D14 (Yao *et al.*, 2016; Yao *et al.*, 2018; Seto *et al.*, 2019). D14 belongs to the α/β serine hydrolase superfamily (Hamiaux *et al.*, 2012; Nakamura *et al.*, 2013; Tsuchiya *et al.*, 2015; Seto *et al.*, 2019), and its hydrolytic activity is mediated by a serine-histidine-aspartate catalytic triad located within its active site (Hamiaux *et al.*, 2012; Zhao *et al.*, 2013). Ligand-induced conformational changes in D14 is characteristic of a catalytically inactive state that results from the rearrangement of four top helices that constitute a V-shaped lid domain and an alteration in the shape of the catalytic triad due to a shift by the loop bearing the catalytic Asp residue (Zhao *et al.*, 2013; Yao *et al.*, 2016; Seto *et al.*, 2019).

Interactions/complex formation involving strigolactone-bound D14, F-box protein, and target proteins leading to the polyubiquitination and proteasomal degradation of target proteins are believed to underpin strigolactone signal transduction. In its active state, D14 associates with D3—the F-box protein component of SCF E3 ubiquitin ligase complex (Stirnberg *et al.*, 2007; Zhao *et al.*, 2013; Zhao *et al.*, 2015)—and then a specific protein substrate is recruited for polyubiquitination and 26S proteasome-mediated degradation (Jiang *et al.*, 2013; Zhao *et al.*, 2015). The lid domain of D14 interacts with D3 (Zhao *et al.*, 2013) via a C-terminal α -helix of a leucine-rich repeat (LRR) domain on D3, with D14 catalytic cavity facing the LRR domain of D3 (Yao *et al.*, 2016; Shabek *et al.*, 2018). Strigolactone-induced D14-D3 interaction further destabilizes D14 (Zhao *et al.*, 2015), albeit how this specifically bears on strigolactone signal transduction is yet to be described in detail. The signaling complex, SCF^{D3-D14}, forms a stable ternary complex with a target protein (e.g., D53) via an ATPase domain on D53 (Shabek *et al.*, 2018). The target protein undergoes proteasome-mediated degradation after polyubiquitination (Jiang *et al.*, 2013; Soundappan *et al.*, 2015; Wang *et al.*, 2015).

After strigolactone signal transduction, D14 hydrolyses the bound strigolactone molecule, thus inactivating it. The hydrolysis of strigolactone is induced in order to restore the catalytic triad to its open state conformation (Seto *et al.*, 2019). A nucleophilic attack on the *enol-ether* bridge of the docked strigolactone molecule separates the ABC ring from its D ring. The propositions that D14 is a single-turnover enzyme and that strigolactone hydrolysis and a strigolactone-derived covalently linked intermediate molecule (CLIM) were central or necessary for strigolactone signal transduction (de Saint Germain *et al.*, 2016; Yao *et al.*, 2016; Saeed *et al.*, 2017; Yao *et al.*, 2018) have been subjects of serious debate. These views have been shown to be inconsistent with recent experimental observations. First, Carlsson *et al.* (2018)—after reanalyzing structural data including the electron density maps calculated from co-ordinates of the crystallized strigolactone-induced *At*-D14-D3-ASK1 complex reported by Yao *et al.* (2016)—concluded that what was previously thought to be bound to the active cleft of D14 was not CLIM but probably a component of the crystallization reagent. By monitoring the timing of *At*-D14 activation relative to strigolactone hydrolysis, Seto *et al.* (2019) demonstrated that the intact strigolactone molecule, not CLIM nor the hydrolysis products, triggers the conformational changes in *At*-D14 and strigolactone signal transduction. Similarly, functional analysis of *At*-D14 catalytic triad mutants with reduced hydrolase activity showed that these mutants were still capable of strigolactone signal transduction and complementation of the *At-d14* mutant phenotype despite lacking their hydrolase activity (Seto *et al.*, 2019). In the same study, the missense mutation of a highly conserved amino acid in *At*-D14 and *Os*-D14 significantly influenced strigolactone signal transduction without affecting the hydrolytic function of D14. Together these are clear indications that strigolactone hydrolysis during strigolactone signaling is not required for signal transduction but serves to deactivate the hormone.

Proteins targeted by SCF^{D3-D14} such as SUPPRESSOR OF MAX2 1 (SMAX1) (Stanga *et al.*, 2013), D53 (Jiang *et al.*, 2013; Zhou *et al.*, 2013) and SUPPRESSOR OF MAX2-LIKE6–8 (SMXL6, SMXL7, and SMXL8) are known repressors of downstream strigolactone responses (Soundappan *et al.*, 2015; Wang *et al.*, 2015). Strigolactone-D14-D3 facilitated the proteasomal degradation of these repressors paves the way for the activation of the hitherto repressed transcription factors (TFs), which leads to the transcriptional activation of associated genes. Examples of such TFs suppressed by D53/SMXLs are BRANCHED1 (BRC1) (Soundappan *et al.*, 2015), TEOSINTE

BRANCHED1 (TB1) (Liu *et al.*, 2017a), IDEAL PLANT ARCHITECTURE1 (IPA1) (Song *et al.*, 2017), and *SQUAMOSA PROMOTER BINDING PROTEIN-LIKE3/17* (*SPL3/17*) (Liu *et al.*, 2017a). BRI1-EMS-SUPPRESSOR1 (BES1), a positive regulator in brassinosteroid signaling, was suggested to be targeted for degradation via SCF^{MAX2} (Wang *et al.*, 2013), although a contrasting observation was recently reported by Bennett *et al.* (2016). Also, D53/SMXL interaction with TOPLESS (TPL)/TPL-RELATED (TPR) family of transcriptional repressors via Ethylene-responsive element-binding factor-associated Amphiphilic Repression (EAR) motifs suggests a putative role for strigolactone signaling in TPL/TPR mediated regulation of gene expression (Jiang *et al.*, 2013; Soundappan *et al.*, 2015; Wang *et al.*, 2015; Ma *et al.*, 2017a).

2.6. Strigolactone-mediated responses in plants

Strigolactones regulate a broad group of developmental processes in plants. A number of these major responses in plants that are elicited by strigolactones are highlighted below.

2.6.1. Germination stimulants for seeds of root-parasitic plants

The first strigolactone bioactivity to be demonstrated was the induction of seed germination in root-parasitic plants. Strigol, strigyl acetate, and sorgolactone act as germination stimulants for *Striga* species. These compounds are secreted in root exudates of cotton, maize, and rice, among others (Cook *et al.*, 1972; Hauck *et al.*, 1992). Alectrol and orobanchol were identified as germination stimulants for *Alectra vogelii* (Müller *et al.*, 1992) and *Orobanche* species, respectively, both of which parasitize some temperate crops (Yokota *et al.*, 1998). Brun *et al.* (2018) provide an extensive review of this aspect of strigolactone bioactivity.

2.6.2. Strigolactones as chemical cues for plant-microbe symbiotic interactions

Another early discovery is strigolactone-induced hyphal branching in AMF. Akiyama *et al.* (2005) identified 5-deoxystrigol in root exudates of *Lotus japonicus* as a cue that triggered hyphal branching. Other strigolactones like sorgolactone, strigol, orobanchol (Akiyama *et al.*, 2010), as well as carlactone and its derivatives (Mori *et al.*, 2016), also induced hyphal branching. In addition to the induction of hyphal branching, the roles of strigolactones in AM symbiosis are evident from the following observations. First, the production of short-chain chitin oligomers, a group of mycorrhizal factors that are believed to elicit the symbiotic signals necessary for fungal root

colonization in plants, is enhanced in AMF by racemic GR24 (GR24), a synthetic strigolactone analog (Fig. 2.1) (Genre *et al.*, 2013). Second, fungal metabolism—evident as increased ATP production/respiration and mitochondrial division, up-regulation of the expression of mitochondrial genes as well as proteins associated with other cell components—is also induced by strigolactones [reviewed in Lanfranco *et al.* (2017)]. Finally, in addition to serving as molecular cues and their effects on the mycosymbiont in the stages just before fungal colonization of the root, strigolactones also perform endogenous roles within the root during mycorrhizal development. This is evident from the fact that strigolactone-signaling mutants show defective mycorrhizal phenotypes. For instance, *rms4* mutants (defective in strigolactone perception but having relatively normal strigolactone content) have significantly reduced mycorrhizal colonisation compared to wild-type (WT) plants (Foo *et al.*, 2013). In a similar manner, *Sl-IAA27*-silenced tomato lines with undetectable strigolactone content showed mycorrhizal defects characterized by a decrease in infection frequency and arbuscule abundance (Guillotin *et al.*, 2017). Furthermore, AMF-inoculated *d3-1* rice mutants showed defects in the early stages of AM symbiosis and an almost abolished expression of AM-inducible genes (Yoshida *et al.*, 2012). Despite these observations, the endogenous roles of strigolactones in mycorrhizal development remain largely elusive. It is worthy of note that strigolactone production/exudation does not translate into an ability to form AM associations as non-AM host plants also produce strigolactones that induce AM activities, and exogenous supply of strigolactones does not result in AM formation in non-host plants (Mori *et al.*, 2016).

The early stages of root nodule organogenesis are characterized by an exchange of chemical signals between the bacterial symbiont and the host plant. Chemical cues exuded into the rhizosphere by host plants trigger the expression of bacterial nodulation genes which direct the production of signal molecules such as nodulation (Nod) factors which when perceived by the host plant elicit nodule organogenesis such as root hair curling, infection thread formation, and the attendant division of inner cortical and pericycle cells to form nodule meristem. Strigolactone-deficient mutants form fewer nodules, and treatment with GR24 increased the nodule number in both mutants and WT plants (Foo and Davies, 2011; Foo *et al.*, 2013; De Cuyper *et al.*, 2015). Unlike in AM symbiosis, strigolactone response mutants displayed enhanced nodulation with increased nodule number (Foo

et al., 2013). Attempts at establishing how strigolactones feature in nodulation revealed that Nod factors induce rapid expression of strigolactone biosynthesis genes (Liu *et al.*, 2011; van Zeijl *et al.*, 2015) and strigolactone actions are limited to the formation of infection threads and the expression of some genes that are induced by the Nod factor signal cascade (McAdam *et al.*, 2017).

2.6.3. Regulation of photomorphogenesis

How strigolactones feature in photomorphogenesis is still emerging, with reports of strigolactones influences in this aspect of plant development largely conflicting. Shen *et al.* (2012) showed that MAX2 interacts with gibberellin and abscisic acid (ABA) signaling to mediate light-induced seed germination and CONSTITUTIVE PHOTOMORPHOGENESIS 1 (COP1) to regulate photomorphogenesis, but strigolactones were not involved. Similarly, photomorphogenic seedling responses were not affected by strigolactone deficiency in *Arabidopsis* (Nelson *et al.*, 2011) and in pea (Urquhart *et al.*, 2015). Despite these, recent studies indicate strigolactones are active in photomorphogenesis. For instance, strigolactones regulate hypocotyl elongation via a number of processes that require the actions of cryptochrome, phytochrome (Jia *et al.*, 2014), and STH7/BBX20, a member of the B-box zinc-finger protein family which are known downstream effectors of photomorphogenesis (Thussagunpanit *et al.*, 2017).

2.6.4. Regulation of shoot branching and plant architecture

In shaping the plant's overall structure, strigolactones control bud activation/branching, secondary growth, and root morphology. Strigolactone-deficient and signaling mutants exhibit excessive shoot branching, and a direct application of strigolactone to axillary buds fully inhibits bud development/branching (Braun *et al.*, 2012; Dun *et al.*, 2013). The influence of strigolactones on bud development is predominantly mediated via either or both of these two mechanisms [reviewed in Waters *et al.* (2017)]. One involves strigolactone-induced direct up-regulation of a broad group of conserved negative regulators of shoot branching such as *BRC1* (Dun *et al.*, 2013), its ortholog in rice, *FINE CULM1* (FC1) (Xu *et al.*, 2015), and *IPAI* (Song *et al.*, 2017). Also, *BES1* (a gene that encodes a positive regulator of shoot branching) undergoes strigolactone-SCF^{MAX2}-induced proteasomal degradation (Wang *et al.*, 2013). The other mechanism is auxin-dependent, and it involves strigolactone-induced modulation of PIN-FORMED (PIN) activities and polar auxin transport (PAT)/canalisation (Bennett *et al.*, 2006; Crawford *et al.*, 2010; Shinohara *et al.*, 2013).

In rice, *FCI* acts downstream of strigolactones to suppress tillering since *fc1* mutants are insensitive to high doses of GR24 when compared to WTs with respect to bud growth and tillering. However, unlike *BRC1*, *FCI* expression is not induced by GR24 treatment (Minakuchi *et al.*, 2010) rather *FCI* (reported as *Os-TB1*) perturbs the suppression of *D14* transcription by *Os-MADS57*, a TF of the MADS-domain family, by binding to *Os-MADS57* (Guo *et al.*, 2013). These show that the interactions between strigolactone signal elements and the *BRC1* family of TFs are complex and require further investigations to develop a lucid picture of how they function to regulate shoot branching.

To promote internode/stem elongation and secondary growth, strigolactones stimulate cell division/increase in cell number (de Saint Germain *et al.*, 2013) and cambial activity within the stem (Agusti *et al.*, 2011). In addition to shoot elongation, leaf margin serration in *Medicago truncatula* is also controlled by strigolactones in a process that appeared to be dependent on auxin transport (Lauressergues *et al.*, 2015). Leaf senescence, which marks the last stage of leaf development, is also regulated by strigolactones (Yamada *et al.*, 2014). Leaves of the *oresara9* (*ore9*) mutant of *Arabidopsis* exhibit the delayed onset of senescence. *At-ORE9* is identical to *At-MAX2* (Woo *et al.*, 2001; Stirnberg *et al.*, 2007). Leaf senescence is accelerated under phosphate limiting conditions and in the presence of exogenous strigolactone (Yamada *et al.*, 2014; Ueda and Kusaba, 2015; Tian *et al.*, 2018).

Strigolactones mediate the tuning of crucial aspects of root architecture. This is evident in the restoration of normal primary root length in strigolactone mutants of *Arabidopsis* by GR24 (Ruyter-Spira *et al.*, 2011); GR24-induced suppression of adventitious root (AR) formation in *Arabidopsis* and pea (Rasmussen *et al.*, 2012b) while promoting crown root growth and AR elongation in rice (Arite *et al.*, 2012; Sun *et al.*, 2014); the repression of lateral root (LR) formation (Kapulnik *et al.*, 2011a; Kapulnik *et al.*, 2011b; Ruyter-Spira *et al.*, 2011; De Cuyper *et al.*, 2015); and the regulation of root hair elongation (Kapulnik *et al.*, 2011a; Kapulnik *et al.*, 2011b). Sun *et al.* (2016a) and Marzec and Melzer (2018) provide a detailed review of strigolactones as regulators of root development.

2.6.5. Mediation of plant tolerance to nutrient deficiency

Under limited nutrient conditions, especially in phosphate and nitrogen-deficient soils, plants increase strigolactone biosynthesis, which becomes evident as an increase in the strigolactone content of root exudates (Yoneyama *et al.*, 2007; Yoneyama *et al.*, 2012; Koltai, 2013, 2015). This is significant since high levels of strigolactones facilitate root branching (Ruyter-Spira *et al.*, 2011) while also increasing the molecular signal content of root exudates for the establishment of symbiotic associations with AMF. Under limiting P_i conditions, Mayzlish-Gati *et al.* (2012) found both strigolactone-deficient (*max4-1*) and insensitive (*max2-1*) mutants had reduced root hair densities. Treatment with GR24 increased root hair density in *max4-1* to similar levels as in the WTs but didn't significantly alter root hair densities in *max2-1*. These processes promote efficient mobilization of limited nutrients in soils (Akiyama *et al.*, 2010; Kapulnik *et al.*, 2011a; Kapulnik *et al.*, 2011b; Liu *et al.*, 2018). Strigolactones may also modulate P_i utilization in addition to P_i acquisition in plants under limited P_i . Czarnecki *et al.* (2013) suggested that strigolactone-induced suppression of shoot branching in *Arabidopsis* in response to P_i deficiency may be a means to reduce P_i utilization. Strigolactones also regulate plant responses to nitrogen supply. Both strigolactone-deficient (*d10* and *d27*) and strigolactone-insensitive (*d3*) mutants of rice lack the root responses to low P_i and nitrogen concentrations observed in the WTs (Sun *et al.*, 2014). And GR24 treatments compensate for the reduced responses in strigolactone-deficient mutants but not in the strigolactone-insensitive mutants. Genetic evidence for strigolactones' role in plant responses to nitrogen deficiency was also provided by Ito *et al.* (2016). They reported an alteration in the expression of *MAX3* and *MAX4* under nitrogen-deficient conditions.

2.6.6. Mediation of plant responses to abiotic and biotic stressors

Strigolactone hormonal actions in plant responses to abiotic stress cues still require more research attention. However, available data portray strigolactones as positive regulators of abiotic stress responses. Stomatal closure, a process that fosters drought tolerance by reducing water loss via transpiration, is induced by strigolactones (Lv *et al.*, 2018; Zhang *et al.*, 2018b). Similarly, strigolactone-deficient and strigolactone-response mutants exhibited hypersensitivity to drought (Bu *et al.*, 2014; Ha *et al.*, 2014; Li *et al.*, 2016), with shoots receiving few strigolactones from the

root behaving as if they were under mild drought stress even when supplied with enough water (Visentin *et al.*, 2016). Furthermore, treatment with exogenous strigolactones rescued drought-sensitivity in strigolactone-deficient mutants but not in signaling mutants (Ha *et al.*, 2014) while also enhancing drought tolerance in WTs. Under salinity stress, ABA actions in ameliorating the deleterious effects of salinity were seen to be dependent on strigolactone biosynthesis and signaling (Ren *et al.*, 2018).

In establishing the roles of strigolactones in the regulation of plant responses to biotic stressors, Cheng *et al.* (2017) showed that strigolactone-deficient tomato plants displayed increased susceptibility to *Phelipanche ramosa* infection and rapid development of the parasite. A report by Torres-Vera *et al.* (2014) also indicated that strigolactone-deficient tomato mutants, *Sl-ccd8*, were susceptible to foliar fungal pathogens, *Botrytis cinerea*, and *Alternaria alternata*, and this was found to be coupled to a reduction in the concentrations of defense-related hormones such as jasmonates, salicylic acid, and ABA.

2.7. Strigolactone interactions with other phytohormones

2.7.1. Strigolactone crosstalk with auxin signaling

Auxins interact synergistically or antagonistically with other phytohormones hormones to regulate biological processes in plants (Naseem *et al.*, 2015; Liu *et al.*, 2017b; Leyser, 2018). Studies on strigolactone and auxin interactions have revealed links between strigolactone and auxin signaling. Auxins exert their influence on strigolactone signaling mainly by modulating strigolactone biosynthesis, which in turn may act as a second messenger in eliciting or regulating some auxin-dependent responses. The expression of *CCD7* and *CCD8* encoding genes are upregulated by auxin to regulate shoot branching (Zou *et al.*, 2006; Arite *et al.*, 2007). Hayward *et al.* (2009) found these to be an *AUXIN RESISTANCE1* (*AXR1*)-dependent process. Experimental data is still lacking on the role(s) of auxin in strigolactone flux and transport.

In regulating shoot branching, strigolactones interfere with PAT/distribution and, in effect, auxin canalization (Bennett *et al.*, 2006; Ruyter-Spira *et al.*, 2011; Sun *et al.*, 2014). Auxin flux/canalization is a significant factor in bud activation and outgrowth (Prusinkiewicz *et al.*, 2009;

Balla *et al.*, 2011; Balla *et al.*, 2016). Strigolactones downregulate PIN protein expression, a family of transporters that control auxin influx and efflux from cells, and the polarised localization of PINs on plasma membrane (Crawford *et al.*, 2010; Shinohara *et al.*, 2013; Hu *et al.*, 2018). This dampens auxin sinking strength of the PAT stream, thus hampering auxin export from buds and canalization that ultimately results in the repression of bud development. However, diminished auxin transport in pea shows little inhibitory effects on bud outgrowth in strigolactone-deficient mutants as well as strigolactones' ability to inhibit bud outgrowth in pea plants with impaired auxin transport (Brewer *et al.*, 2015), thus indicating that though PAT/canalization may feature in strigolactone-mediated modulation of branching, strigolactones can act independently of this mechanism.

Experimental observations show inconsistencies in the two models of strigolactone action in bud activation. These include the uncoupling of *TBI* sub-network from strigolactone signaling in maize (Guan *et al.*, 2012); the insensitivity of *FCI* expression to GR24 (Minakuchi *et al.*, 2010); buds lacking *BRC1* expression remaining inhibited and being sensitive to inhibition by strigolactones, buds with high *BRC1* transcripts being active (Seale *et al.*, 2017); and the conflicting reports of strigolactone influence on auxin transport and canalization. All these calls for a rethink of these models with a view to developing new ones that consider these limitations. The solutions may lie in the events that occur upstream, in parallel with and/or downstream of *BRC1/FC1/TB1* activities. Auxin canalization and the repression of branching factors may be necessary for bud activation/development, but some other mechanisms which may or may not be under the influence of these two hormones may determine whether or not an activated bud proceeds to develop into a branch.

The regulation of secondary growth by strigolactones occurs by promoting interfascicular cambial activities (Agusti *et al.*, 2011). The slight induction of cambium-like cell division in *max2* plants by GR24 treatment, which contrasts the complete insensitivity observed in other processes, suggests other factors act in parallel with MAX2-dependent strigolactone signaling to affect secondary growth (Agusti *et al.*, 2011). In addition, observations in *max* and auxin response mutants suggest strigolactones affect secondary growth directly, independent of auxin accumulation, and they act downstream of auxin. These highlights the question of how

strigolactones elicit cambial activity and secondary growth independent of auxin-induced cambial activity.

As with shoot branching, strigolactones interacts with auxin to control root development by modulating auxin sensitivity (Mayzlish-Gati *et al.*, 2012), PAT from shoot to root (Sun *et al.*, 2014), and auxin flux within root tissues (Koren *et al.*, 2013; Kumar *et al.*, 2015). Here, auxin signal modules act downstream of strigolactones. The early steps in lateral root formation—which includes the priming of pericycle cells in the basal meristem to specify them for lateral root initiation; the transition from founder cells to LR initiation and primordium formation; and the development of LR primordium until LR emergence—are all driven by local auxin gradients and response maxima [reviewed in Olatunji *et al.* (2017)]. Since GR24 has been shown to affect the polarisation and localization of PIN proteins as well as lateral root-forming potential (Ruyter-Spira *et al.*, 2011; Pandya-Kumar *et al.*, 2014; Kumar *et al.*, 2015), strigolactones most likely influence these processes by modulating local auxin flux and homeostasis that is required to establish the auxin response maxima.

Similarly, strigolactones inhibitory effects on auxin efflux via its modulation of PIN activities also result in the accumulation of auxin within primary root meristem cells. This promotes cell division and number, expansion of meristem and transition zone sizes, and, consequently, primary root length (Ruyter-Spira *et al.*, 2011). Similar crosstalk between strigolactones and auxin occurs in the regulation of root hair development where strigolactones induce an increase in auxin accumulation/levels within epidermal cells by modulating auxin efflux (Koltai *et al.*, 2010) to promote root hair elongation. ROOT HAIR DEFECTIVE 6-LIKE 4 (RSL4) is an auxin-responsive TF that positively regulates root hair formation by controlling genes associated with root hair morphogenesis and is suggested to be an integrator of internal and external cues (Yi *et al.*, 2010). P_i deficiency significantly enhances RSL4 synthesis and half-life (Datta *et al.*, 2015). With these, RSL4 might serve as a nexus for strigolactone-auxin crosstalk in modulating root hair development. Experimental data suggest ethylene features prominently in strigolactone-auxin crosstalk in the regulation of root hair growth (Kapulnik *et al.*, 2011b).

In regulating AR formation, strigolactones and auxin elicit opposing effects. The role of auxin in promoting AR formation and the inhibition of it by strigolactones are well documented. Unraveling the nature of strigolactone-auxin crosstalk in AR development, Rasmussen *et al.* (2012b) discovered that GR24 partially revert the stimulatory effects of auxin on AR formation while auxin increased the number of ARs in *max* mutants of *Arabidopsis* and pea. Of note is the fact that strigolactones inhibitory effects occurred even in the presence of high auxin content. These suggest both hormones act independently, and strigolactones suppression of AR formation is not mediated by limiting local auxin accumulation. In contrast, rice mutants defective in strigolactone biosynthesis and signaling exhibited reduced AR formation, and GR24 treatment ameliorated AR number in strigolactone deficient mutants but not in signaling mutants (Sun *et al.*, 2015). Modulation of PAT also seemed to be employed to regulate AR formation in rice. Taken together, strigolactone-auxin crosstalk in this process appears to be complicated, and strigolactone actions in regulating AR formation might be species dependent. Further investigations of this process in other species and the effects of strigolactone signals on the expression and stability of downstream targets of auxin signals involved in AR development such as ADVENTITIOUS ROOTLESS 1 [an auxin-responsive factor involved in auxin-mediated cell dedifferentiation and AR formation; Liu *et al.* (2005)] may be required to make valid conclusions on strigolactone-auxin interactions in AR development.

Plant P_i status is critical in strigolactones' influence on root development and architecture. Under normal/high P_i levels, LR development is inhibited but stimulated in P_i -limiting conditions (Ruyter-Spira *et al.*, 2011; Mayzlish-Gati *et al.*, 2012; Jiang *et al.*, 2016). Though it is clear that strigolactones serve to translate ambient signals into growth cues in the root, the precise mechanism that enables strigolactones to delineate their influence under normal P_i levels from those under P_i limiting conditions is not fully described. A possible avenue to explore for answers is how strigolactones influence ethylene signaling under P_i status since ethylene stalls auxin-driven lateral root development (Lewis *et al.*, 2011).

Models of auxin-strigolactone interactions in AM and rhizobial symbiosis are quite sketchy. Observations by Foo (2013) suggest that auxin regulates the early stages of AM symbiosis by

modulating strigolactone levels. Recently, the expression of *Sl-IAA27*—a downstream component/repressor of auxin signaling—was shown to be upregulated by AM colonization and *Sl-IAA27*-silencing adversely affected AM colonization (Guillotin *et al.*, 2017). Interestingly, aside from the down-regulation of genes involved in strigolactone biosynthesis in *Sl-IAA27*-silenced plants, treatment with GR24 complemented the mycorrhizal defect by increasing infection frequency and arbuscule abundance. These show the existence of a yet-to-be-identified hormonal signal link between auxin and strigolactones in mycorrhizal development. In addition, the signal channel(s) by which *Sl-IAA27*-induced strigolactones production and signaling influence arbuscule development remains unexplained. Computer modelling and experimental data have established the crucial role of auxin accumulation in nodule organogenesis [reviewed in Kohlen *et al.* (2017)]. Since strigolactones regulate auxin transport and flux, strigolactones might elicit some influence on nodule development via this channel.

2.7.2. Strigolactone crosstalk with cytokinin signaling

The interactions between cytokinin and strigolactones seem to vary with physiological processes. They act independently of each other in adventitious rooting (Rasmussen *et al.*, 2012b), antagonistically in bud activation and shoot branching (Dun *et al.*, 2012; Xu *et al.*, 2015; Manandhar *et al.*, 2018) but act synergistically in the regulation of LR development (Jiang *et al.*, 2016). Both hormones regulate the expression of the other's biosynthesis genes (Zhang *et al.*, 2010; Dun *et al.*, 2012). While strigolactones associated genes have been shown to mediate cytokinin biosynthesis and export from the root (Beveridge, 2000; Dun *et al.*, 2012), reports on cytokinin influence on strigolactone transport are lacking.

In mediating bud activation/shoot branching, strigolactones and cytokinin interact directly in buds with their actions converging at the transcriptional regulation of *BRC1* in *Arabidopsis* and pea (Aguilar-Martínez *et al.*, 2007; Braun *et al.*, 2012; Dun *et al.*, 2012) and *FC1* in rice (Xu *et al.*, 2015). Given the above, any factor that influences strigolactones and cytokinin homeostasis in the bud will determine bud development. This is where auxin features, its induction of strigolactone biosynthesis, but inhibition of cytokinin biosynthesis in the root ensures more strigolactones get to the shoot and repress branching. To shed more light on cytokinin-strigolactone crosstalk in

regulating bud development, the influence(s), if any, of strigolactones or their signals on downstream cytokinin signal components/pathways involved in bud activation must be elucidated. In resolving the role of sucrose mentioned above, other crucial questions to be investigated include: does sucrose supply affect strigolactones and/or cytokinin homeostasis in the bud? If yes, what are the molecular mechanisms that drive this process, and at what point in this cascade of events is the sucrose signal integrated?

Cytokinin signaling components are required in GR24-induced suppression of LR development (Jiang *et al.*, 2016). The repression of LR development by GR24 under sufficient P_i , via the downregulation of PIN genes expression, is mediated by AHK3, ARR1, and ARR12 via *SHORT HYPOCOTYL2* (*SHY2*). And since auxin transport is required to develop an auxin gradient, which is vital for the induction of LR initiation from pericycle founder cells, *SHY2* repression of PIN activity stalls LR formation (Goh *et al.*, 2012). Loss-of-function mutation in *SHY2* results in an insensitivity to GR24 with respect to LR development (Koren *et al.*, 2013). *SHY2* is also central to the balancing of auxin and cytokinin signaling, with cytokinin promoting its expression while auxin promotes its degradation (Ioio *et al.*, 2008; Moubayidin *et al.*, 2010). It is clear that *SHY2* acts as a nexus for the integration of auxin, cytokinin, and strigolactones signaling to regulate LR development in P_i -sufficient conditions. Whether strigolactones employ this same channel and crosstalk to promote LR development under P_i -limiting conditions is yet to be determined.

The relative rate of cell division to cell differentiation is a crucial driver of growth in the root meristem. Growth, fostered by cell division, is repressed when the rates of cell division and differentiation reach a balance after the final meristem size is attained. Cytokinin promotes cell differentiation and hence reduced meristem size (Ioio *et al.*, 2007; Ioio *et al.*, 2008), while GR24 promotes an increase in meristem cell number and size (Ruyter-Spira *et al.*, 2011; Koren *et al.*, 2013). As with LR development, *SHY2* could be a converging point for the antagonistic crosstalk between cytokinin and strigolactones in the regulation of primary root growth. This is supported by observations like the insensitivity of loss-of-function mutant, *shy2-31*, to GR24 with respect to meristem cell number/size (Koren *et al.*, 2013); the induction of *SHY2* transcript expression by

cytokinin (Ioio *et al.*, 2008; Moubayidin *et al.*, 2010); and the reduced sensitivity of *shy2-31* and *max2* to cytokinin (Koren *et al.*, 2013).

2.7.3. Strigolactone crosstalk with abscisic acid signaling

With more data supporting an active role for strigolactones in the mediation of plant responses and resilience to abiotic and biotic stressors, it is expected that strigolactones might interact, either directly or indirectly, with ABA in the regulation of adaptive stress responses in plants. So far, three highlights can be inferred from available data concerning ABA–strigolactone interactions. First, ABA acts upstream of strigolactones, and strigolactone production/signaling is required and modulated to elicit ABA-mediated responses. In support of this view are the observations that—the expression of strigolactone biosynthesis genes and strigolactone content are significantly lowered in ABA-deficient plants (López-Ráez *et al.*, 2010; Wang *et al.*, 2018); strigolactone-deficient and signaling mutants are hypersensitive to drought stress, less sensitive to exogenous ABA (Ha *et al.*, 2014; Visentin *et al.*, 2016) and exhibit reduced stomatal sensitivity to ABA (Bu *et al.*, 2014; Liu *et al.*, 2015; Lv *et al.*, 2018); an increase in stomatal aperture and water loss caused by an infection-induced rise in ABA levels were not seen in strigolactone-deficient lines (Cheng *et al.*, 2017); and finally, ABA upregulated the expression of strigolactone production and signaling genes to mediate tolerance to salt stress in *Sesbania cannabina* but was only able to induce partial and transient increases in salt tolerance of plants treated with an inhibitor of strigolactone synthesis (Ren *et al.*, 2018). Second, strigolactone and ABA interactions are antagonistic in regulating certain aspects such as shoot architecture and fruit ripening. ABA suppresses the expression of strigolactone biosynthesis and signaling genes to enhance tiller formation (Wang *et al.*, 2018). On the other hand, rather than promote ABA action, exogenous application of GR24 markedly inhibited ABA-induced accumulation of sugars and anthocyanins in grape berries (Ferrero *et al.*, 2018). Finally, in addition to being a requirement for ABA-mediated responses, strigolactones may also serve as a feedback channel in modulating ABA signaling. This is evident from the following reports that treatment with GR24 resulted in the reduction of endogenous ABA concentrations. GR24 inhibited the stress-induced increase in ABA levels, transcriptional activation of ABA biosynthetic gene in *Lotus japonicas* root (Liu *et al.*, 2015), and upregulated the expression of ABA catabolic genes but not biosynthetic genes (Ferrero *et al.*, 2018). Also supporting this view is the

observed high ABA content in strigolactone-deficient and insensitive mutant rice plants with greater tolerance to drought (Haider *et al.*, 2018).

Despite all the above, some experimental observations suggest some inconsistencies. For instance, strigolactone-deficient mutants did not display the rapid water loss and hypersensitivity to ABA and drought observed in strigolactone-signaling mutant, thus suggesting MAX2 signaling, but not strigolactones, is involved in drought responses (Bu *et al.*, 2014). These allude to the existence of a complex interaction between strigolactones, ABA, and their downstream signaling components that only further extensive investigations would unravel. Since the expression and accumulation of ELONGATED HYPOCOTYL 5 (HY5), a negative transcriptional regulator and integrator of light and ABA responses (Chen *et al.*, 2008a), is under the control of strigolactones (Jia *et al.*, 2014; Tsuchiya *et al.*, 2015), it is possible that HY5 might be one of the missing links in ABA-strigolactone crosstalk.

2.7.4. Strigolactone crosstalk with gibberellin signaling

Though still largely unclear, strigolactone-gibberellin crosstalk is implied by some experimental observations. For instance, Lantzouni *et al.* (2017) reported an additive transcriptional change in an overlapping set of genes in response to gibberellin and GR24. Their data also suggest an antagonistic effect by gibberellin on strigolactone-induced upregulation of some ABC-type transporters. Furthermore, *in silico* analysis show that the biosynthesis of strigolactones is under gibberellin regulation (Marzec and Muszynska, 2015). This was subsequently demonstrated to be achieved via a GID1-DELLA signal pathway (Ito *et al.*, 2017). In the control of branching/tillering, the observed upregulation of *ORYZA SATIVA HOMEBOX 1 (OSH1)* expression in highly branched gibberellin-deficient mutants (Lo *et al.*, 2008) and strigolactone-signaling mutants (Gao *et al.*, 2009) alludes to the sharing of a similar molecular mechanism by strigolactones and gibberellin although this is yet to be demonstrated experimentally.

Attempts have been made to find a direct molecular link between downstream components of gibberellin signaling and those of strigolactones. For instance, D14 interacts with SLENDER RICE1 (SLR1)—a DELLA protein, which is a downstream signal component and repressor of

gibberellin signaling—in a strigolactone-dependent manner (Nakamura *et al.*, 2013). Despite this, strigolactone-induced degradation of SLR1 is yet to be demonstrated experimentally, and the functional relevance/downstream effect(s) of this interaction is still largely unknown. Recent attempts at finding a molecular nexus between strigolactone and gibberellin signaling have yielded data that support functional independence between both hormones. For instance, the stability (Bennett *et al.*, 2016) and accumulation (Lantzouni *et al.*, 2017) of DELLA proteins were not affected by strigolactone signaling. Experimental data are lacking on the influence of strigolactone signals on the stability and transcriptional regulation of vital components of gibberellin signaling such as GIBBERELLIN INSENSITIVE DWARF1 and 2 (GID1 & GID2), GIBBERELIC ACID INSENSITIVE (GAI), SLEEPY1 (SLY1), and SNEEZY (SNE) (Nelson and Steber, 2016). Further supporting a functional diversification for both hormone is the report that strigolactones stimulate the elongation of internodes independent of gibberellin by increasing cell number and not cell length (de Saint Germain *et al.*, 2013). Against the backdrop of the above, it is likely that strigolactone and gibberellin crosstalk is limited; or might not be mediated by direct interactions between their signaling components; and inhibition of strigolactone synthesis by gibberellin serves only to modulate strigolactone content. Whatever the case may be, further investigations are required to evince the true nature of strigolactone-gibberellin crosstalk.

2.7.5. Strigolactone crosstalk with ethylene signaling

Ethylene signals are involved in the control of some growth and developmental processes that are also regulated by strigolactones. Among these are hypocotyl growth, root hair elongation, seed germination, and leaf senescence. During hypocotyl development, the COP1-HY5 complex acts as an integrator of light and hormonal signaling in regulating hypocotyl growth. In light, strigolactones inhibit hypocotyl elongation by upregulating HY5 expression in a MAX2 dependent process (Jia *et al.*, 2014) while ethylene enhances COP1-mediated degradation of HY5 to promote hypocotyl elongation (Yu *et al.*, 2013). Together, these observations suggest that an antagonistic interaction between strigolactones and ethylene signaling might exist in regulating hypocotyl growth. Since hypocotyl growth is rapidly arrested in light, an important question begging for answer is how strigolactones override the promoting effects of ethylene on hypocotyl growth in light.

Strigolactone control of root hair elongation is also dependent on ethylene signaling. This is evident as ethylene signaling mutants, *At-ein* and *At-etr*, displayed reduced sensitivity to GR24 treatment, and blockage of ethylene production completely eliminated strigolactone effects on root hair elongation (Kapulnik *et al.*, 2011b). Furthermore, GR24 treatment enhanced *At-ACS2* transcription, a gene involved in ethylene biosynthesis (Kapulnik *et al.*, 2011b). Observations from the same study also suggest strigolactones employ ethylene, which may, in turn, recruit auxin signaling, thus implying the existence of a three-way hormonal crosstalk in the control of root hair development. Nonetheless, the report that a transcriptional complex—consisting of an ethylene-activated factor and a positive regulator of hair cells—coactivates hair length-determining gene (ROOT HAIR DEFECTIVE 6-LIKE) and other root hair genes (Feng *et al.*, 2017) shows that ethylene can act independently and does not always require auxin signaling to influence root hair development.

Further demonstrating crosstalk between strigolactones and ethylene, an early report indicated that strigolactones induced the biosynthesis of ethylene in the seeds of *Striga* prior to germination (Sugimoto *et al.*, 2003). And in promoting leaf senescence, strigolactones also acted by activating ethylene-mediated senescence signals, although ethylene-independent pathways may be employed (Ueda and Kusaba, 2015). Taken together, in addition to suggesting that ethylene acts downstream of strigolactones, these show that strigolactone-mediated responses that require ethylene signaling are elicited by modulating ethylene content in tissues. Also supporting the view that ethylene may act downstream of strigolactones is ethylene control over adventitious root initiation sites in *Arabidopsis* hypocotyl independent of strigolactones (Rasmussen *et al.*, 2017). Regardless of these, the precise molecular channels employed by strigolactones to elicit the transcriptional control of ethylene production remains undescribed. Since light is a potent regulator of ethylene biosynthesis—via processes that are mediated by phytochrome/phytochrome interacting factors [reviewed in Zdarska *et al.* (2015)]—and given that some strigolactone responses are elicited via cryptochrome and phytochrome (Jia *et al.*, 2014), the idea that strigolactones might modulate ethylene signalling in a phytochrome-dependent manner is worth investigating.

Again, as with gibberellins, describing a lucid and complete strigolactone-ethylene crosstalk model in regulating developmental processes in plants is still beyond reach with extant experimental data. Providing answers on how D14/MAX2 signaling and D53/SMXL activity affects essential ethylene signaling components and ethylene-responsive TFs and vice-versa will be invaluable in understanding the role of strigolactone-ethylene hormonal and signaling crosstalk(s) in processes like root development, fruit ripening, and senescence.

2.7.6. Strigolactone crosstalk with jasmonate signaling

Jasmonates, a group of plant oxylipins, mediate a range of physiological processes during vegetative growth, secondary metabolism, plant-insect, and plant-pathogen interactions, wounding, etc. The nature of strigolactones-jasmonate crosstalk cannot be clearly described at this point due to limited experimental data. However, the report that jasmonic acid (JA) content, and the expression of a jasmonate-dependent gene PINII (a gene responsible for tomato resistance to *Botrytis cinerea*), was reduced in a strigolactone-deficient tomato mutant (*Sl-ccd8*) (Torres-Vera *et al.*, 2014) points to a connection between strigolactones and jasmonates in disease tolerance. Further alluding to this link is that methyl jasmonate, a plant defense signaling molecule, exerts some influences on *Nicotiana tabacum PDR6* (*Nt-PDR6*), which is an ortholog of the strigolactone transporter gene, *Ph-PDR1* (Xie *et al.*, 2015a). Though strongly induced by phosphate starvation and also involved in the regulation of shoot branching (Xie *et al.*, 2015a), *Nt-PDR6* has not been reported to be involved in strigolactone transport. A somewhat inconsistent observation was reported recently in which GR24 supply did not affect JA accumulation in WTs, *At-max1*, and *At-max2*, and neither did inoculation with *Mucor* sp. (Rozpádek *et al.*, 2018). Altogether these observations are not sufficient to draw valid conclusions on the nature of strigolactone-jasmonate crosstalk, the fact that both hormones elicit responses in similar developmental processes—like mesocotyl elongation, senescence, plant-microbe interactions, etc.—offer some indications that strigolactone-jasmonate crosstalks are likely to feature actively in these processes and cannot be completely ruled out.

2.7.7. Strigolactone crosstalk with salicylic acid signaling

Salicylic acid (SA) features prominently in plant perception and defense against pathogens as well as tolerance to abiotic stressors (Herrera-Vásquez *et al.*, 2015; Khan *et al.*, 2015; Prodhan *et al.*, 2018). Its control in this aspect is largely because of its influence on the reactive oxygen species (ROS) status of plants (Herrera-Vásquez *et al.*, 2015). Salicylic acid controls drought tolerance (Askari and Ehsanzadeh, 2015), senescence (Ji *et al.*, 2016), and stomatal closure/conductance (Prodhan *et al.*, 2018), all of which are under strigolactone regulation. Thus far, SA-SLs interactions have only been demonstrated in plant-endophytic fungus interactions where GR24 induced the accumulation of SA while strigolactone signaling mutant, *max2*, had decreased SA concentrations (Rozpádek *et al.*, 2018). This is an indication that strigolactones may influence plant defense responses to infection by inducing SA signaling. Whether strigolactones elicit SA accumulation by direct transcriptional control of SA biosynthetic genes or by inducing oxidative outburst/ROS which are known to induce SA production remains to be determined. Given the recent reports of strigolactone actions in ABA-induced stomatal closure under drought conditions (Ha *et al.*, 2014; Visentin *et al.*, 2016) and senescence (Yamada *et al.*, 2014; Ueda and Kusaba, 2015; Tian *et al.*, 2018), exploring strigolactones-SA crosstalk in these aspects may provide invaluable tools for breeding programs aimed at developing drought tolerant crops with increased fruit shelf life.

2.8. Pigment accumulation during de-etiolation

The early stages of embryo development just before exposure to light and transformation into a competent photosynthesizing seedling during germination and seedling development are characterized by heterotrophic growth. Prior to emergence from the soil, a seedling lacks the capacity to photosynthesize due to the absence of functional chloroplasts since it follows a skotomorphogenic growth pattern due to insufficient or absence of light beneath the soil (Josse and Halliday, 2008). Rapid hypocotyl or epicotyl elongation, accumulation of protochlorophyllide and chlorophyllide, development of etioplasts, the presence of an apical hook, and repressed cotyledon expansion and root development are characteristic of skotomorphogenic development (Guo dong *et al.*, 2016; Kobayashi, 2016; Armarego-Marriott *et al.*, 2019; Pipitone *et al.*, 2020).

2.8.1. Phytohormones in the regulation of chlorophyll biosynthesis

Due to the critical role of chlorophyll biosynthesis in ensuring seedling adaptation to autotrophic growth and development, this process is tightly regulated by several hormonal signals. Gibberellins are negative regulators of photomorphogenesis in the absence of light and repressing signals while gibberellin-regulated DELLAs, via PHYTOCHROME INTERACTING FACTORS (PIFs)-dependent signaling, positively modulate chlorophyll biosynthesis by enhancing the expression of genes involved in chlorophyll biosynthesis such as the light-dependent enzyme NADPH:protochlorophyllide oxidoreductase (POR) and chlorophyll a oxygenase genes (Cheminant *et al.*, 2011). Cytokinins enhance HY5 protein levels, thus fostering photomorphogenic development while cytokinin-responsive TFs (ARRs) upregulate the expression of chlorophyll biosynthetic genes [reviewed in Cortleven and Schmölling (2015)]. Ethylene and its downstream signal components repress protochlorophyllide accumulation, activate POR gene expression, and downregulate photomorphogenic development by cooperating with COP1 and PIFs (Alscher and Castelfranco, 1972; Yu *et al.*, 2013; Zhong *et al.*, 2014; Melo *et al.*, 2016; Shi *et al.*, 2016; Xu *et al.*, 2016; Liu *et al.*, 2017c). Chlorophyll content was reduced in ethylene-treated tomato seedlings undergoing de-etiolation (Melo *et al.*, 2016). Abscisic acid and strigolactones influence photomorphogenic development via their effects on COP1 activities, with abscisic acid mediating the repression of seedling de-etiolation (Shen *et al.*, 2012; Jia *et al.*, 2014; Xu *et al.*, 2016). Although strigolactones have been shown to feature in photomorphogenic development, their influences and how their crosstalk with other vital regulators affect pigment accumulation during light-driven de-etiolation remains to be determined.

2.8.2. Phytohormones in the regulation of carotenogenesis

Several phytohormones feature actively in the control of carotenoid biosynthesis, accumulation, and homeostasis in plants. Ethylene is a central hormonal cue in carotenogenesis, and its roles in carotenoid accumulation, especially during fruit ripening, have been extensively investigated (Liu *et al.*, 2014c). Ethylene, and ethylene-dependent/responsive hormonal factors, are influenced, or they interact with several critical transcriptional factors that are considered significant regulators of carotenogenesis such as MADS-box transcription factors like RIPENING INHIBITOR (RIN), TOMATO AGAMOUS (TAG), FRUITFUL (FUL) (Liu *et al.*, 2014c; Stanley and Yuan, 2019).

On the other hand, auxin generally acts antagonistically to ethylene, thereby inhibiting carotenogenesis (Su *et al.*, 2015). Abscisic acid, a downstream derivative of carotenoid oxidation with diverse stress signaling roles, plays complicated roles in carotenogenesis. Experimental data support both stimulatory and inhibitory functions of ABA in carotenoid biosynthesis and accumulation (Liu *et al.*, 2014c; Stanley and Yuan, 2019). However, an established concept common to majority is that ABA-dependent carotenoid regulation involves ethylene signalling. Other phytohormones implicated in carotenogenesis include cytokinins, gibberellins, jasmonates and brassinosteroids (Liu *et al.*, 2012; Liu *et al.*, 2014b; Zhang *et al.*, 2018a). The role(s) of strigolactones in carotenogenesis/carotenoid accumulation during seedling de-etiolation remain mostly unexplored even though strigolactones are downstream derivatives of carotenoid oxidation products just like ABA.

Chapter 3

Strigolactone in the mediation of tolerance to heat stress

3.1. Introduction

Global warming, a phenomenon which is evident as a rise in global average surface temperature (Pachauri *et al.*, 2014), significantly impacts plant growth, biomass production, and crop productivity (Asseng *et al.*, 2015; Narayanan *et al.*, 2015; Bergkamp *et al.*, 2018). High temperatures pose devastating effects on plants via heat stress (HS), which can cause severe damage to physiological and morphological processes in plants within a very short period if ambient temperatures reach extreme levels. During the early stages of plant development, the impact of HS is evident as decreased seed germination potential, poor germination, reduced seedling vigor, and, in extreme cases, complete loss of viability (Egli *et al.*, 2005; Essemine *et al.*, 2007; Iloh *et al.*, 2014).

The photosynthetic machinery is among the most susceptible to HS of all plant biochemical systems, with PSI, PSII, and the carbon assimilation pathway (Calvin Cycle) being the most affected (Berry and Bjorkman, 1980; Essemine *et al.*, 2011). Though PSII was previously thought to be the most heat-labile, some findings suggest that carbon assimilation is impaired due to thermal inactivation of Rubisco activase, long before the effects of HS is evident in PSII (Salvucci *et al.*, 2001; Rashid *et al.*, 2018). Heat stress particularly affects PSII by inhibiting the oxygen-evolving complexes (OECs) (Havaux, 1993) and inactivating PSII reaction centers (RCs) (Sun *et al.*, 2017). On the other hand, PSI appears to be somewhat resistant to thermal stress since HS induces PSI activity and cyclic electron flow around PSI (Havaux *et al.*, 1991; Sun *et al.*, 2017). Chlorophyll a fluorescence transient (OJIP) analysis provides an efficient, fast, and non-invasive method of probing photosynthetic processes in plants. Indices derived from the polyphasic rise in chlorophyll a fluorescence, which reflects the events that characterize the light-dependent reactions of photosynthesis, can be used to draw real-time inferences on the photosynthesis-associated biochemical and physiological status of the leaf (Strasser *et al.*, 1995; Strasser *et al.*, 2000; Kalaji *et al.*, 2016). These have served as tools for evaluating plants under limiting conditions including drought (Zivcak *et al.*, 2008; Urban *et al.*, 2017), nutrient status (Kalaji *et al.*, 2014; Kalaji *et al.*, 2018), salinity (Zushi and Matsuzoe, 2017) and thermal stress (Oukarroum *et al.*, 2016).

Plants have evolved several biochemical strategies for coping with HS. These include the biosynthesis of heat shock factors and heat shock proteins (Park and Seo, 2015; Guo *et al.*, 2016);

the induction of hormone-mediated thermotolerance (Ahammed *et al.*, 2016); induction of enzymatic and non-enzymatic antioxidant systems (Caverzan *et al.*, 2016; Ergin *et al.*, 2016); and the accumulation of osmolytes such as proline and betaine. The glyoxalase system is an enzymatic system that has also been linked to stress tolerance in plants. Glyoxalase I (GlyI; lactoylglutathione lyase; EC 4.4.1.5) and glyoxalase II (GlyII; hydroxyacylglutathione hydrolase; EC 3.1.2.6), which make up this pathway, prevent the accumulation of methylglyoxal (MG), a highly cytotoxic by-product of glucose metabolism produced under normal conditions, to toxic levels within tissues. Under stress conditions, MG production increases and manipulating the glyoxalase pathway has been shown to enhance plant tolerance to abiotic stress, for example salinity stress (Singla-Pareek *et al.*, 2003; Yadav *et al.*, 2005).

Limited data are available on the nature of strigolactone actions in plants under HS. This chapter investigates the impact of treatments with GR24, tolfenamic acid (a strigolactone signal pathway inhibitor), and tebuconazole (a strigolactone biosynthesis inhibitor) (Ito *et al.*, 2013; Hamiaux *et al.*, 2018) on seed germination, antioxidant enzymes, and biochemical responses of narrow-leafed lupine (*Lupinus angustifolius* L.) seeds germinated under high temperature. We also evaluated, using chlorophyll a fluorescence transient analysis, PSII function, and glyoxalase enzyme activities in narrow-leafed lupine seedlings subjected to HS treatments.

3.2. Materials and methods

3.2.1. Plant materials

Seeds of narrow-leafed lupine (*Lupinus angustifolius* L.) were sorted and selected based on uniformity in size and health. The seeds were divided into two groups and used for each experiment.

3.2.2. Experiment I: Seed germination

3.2.2.1. Germination conditions, chemical treatments, and experimental design

Two-hundred and fifty seeds were taken from one set of the selected seeds, rinsed several times with distilled water, and placed in five beakers with 50 seeds in each. Each set of 50 seeds were primed as follows: the beaker with seeds which served as control (CTL) received 100 mL of distilled water (containing 500 μ L acetone in 1 L distilled water); for strigolactone (GR24) treatment, 100 mL of 3 μ M GR24 solution (prepared from a 10 μ M stock: 3 mg GR24 dissolved in 500 μ L acetone and diluted in 1 L of distilled water); for tolfenamic acid (TL), 100 mL of 50 μ M tolfenamic acid solution; tebuconazole (TB), 100 mL of 20 μ M tebuconazole solution; and a combination of tolfenamic acid and tebuconazole (TT), 100 mL solution containing 50 μ M tolfenamic acid and 20 μ M tebuconazole. The seeds were allowed to imbibe for 20 h in the dark

under room temperature (~23 °C). Seeds from each beaker were then transferred into five Petri dishes (lined with filter paper) with 10 seeds in each. Three Petri dishes from each treatment were transferred to a growth chamber set at 30 ± 1 °C and allowed to germinate. The remaining two Petri dishes from each treatment were placed in a growth room with ambient temperature set at 23 °C. All the Petri dishes were kept moist with their respective treatment solutions to prevent drying out. Seeds were considered germinated when the radicle punctured the seed coat and became visible.

3.2.2.2. Germination indices

A daily count of germinated seeds was carried out for four days. These were used to compute germination attributes, which include final germination percentage (GP), coefficient of velocity of germination (CVG), germination index (GI) (Kader, 2005), promptness index (PI), and germination stress tolerance index (GSTI) (Partheeban *et al.*, 2017) using the formula in Table 3.1.

3.2.2.3. Determination of antioxidant enzyme activities

The ruptured testa of each germinated seed was removed, the cotyledons were weighed, and homogenized using a bead beater in an extraction solution containing 0.1 M phosphate buffer (pH 7.0) and 0.1 mM EDTA. The homogenate was centrifuged at 15000 *g* for 20 min at 4 °C. The supernatant was used to evaluate the activity of superoxide dismutase (SOD), ascorbate peroxidase (APX), and peroxidase (POX) spectrophotometrically. Protein concentration was determined following the method of Bradford (1976).

Superoxide dismutase activity was estimated by the nitroblue tetrazolium (NBT) method as described by Beauchamp and Fridovich (1971), with slight modifications. Briefly, the 3 mL assay reaction mixture contained 100 μ L of 200 mM methionine, 100 μ L of 2.25 mM NBT, 100 μ L of 3 mM EDTA, 1500 μ L of 100 mM potassium phosphate buffer, 1000 μ L of distilled water, and 100 μ L of enzyme extract. The reaction was initiated by adding 100 μ L of 1 mM riboflavin, and the samples were illuminated under white light (LED) for 15 min. Duplicate tubes with the same reaction mixture but without enzyme extract, which developed maximum color, were used as a background control. Absorbance was read at 560 nm immediately after the reaction was stopped. A non-irradiated tube containing the reaction mixture, which did not develop color, was used as a blank. One unit of SOD activity was defined as the enzyme quantity that inhibited the photo-reduction of NBT by 50 % compared to tubes lacking enzymes and expressed as SOD units per gram FW ($U\ g^{-1}\ FW$).

Table 3.1. Seed germination index and their formula, parameters, and description (Kader, 2005; Partheeban *et al.*, 2017).

<i>Germination Index</i>	<i>Formula and Description</i>
Final germination percentage (FGP)	<p>It is estimated as:</p> $FGP = \frac{N_g}{N_t} \cdot 100$ <p>Where, N_g is the total number of seeds that germinated after 4 days and N_t is the total number of seeds in each seed lot.</p>
Coefficient of velocity of germination (CVG)	<p>It is estimated as:</p> $CVG = \frac{\sum N_i}{\sum (N_i \cdot T_i)} \cdot 100$ <p>Where, N_i is the number of seeds germinated on the i^{th} day and T_i is the time (in days) from the start of the experiment.</p>
Germination index (GI)	<p>It is estimated as:</p> $GI = (10 \cdot N_1) + (9 \cdot N_2) + (8 \cdot N_3) + (7 \cdot N_4)$ <p>Where, N_1, N_2, N_3, N_4 are the number of seeds germinated on the first, second, third, and fourth day, respectively; 10, 9... are weights given to the number of germinated seeds on the first, second, and subsequent days, respectively.</p>
Promptness index (PI)	<p>It is estimated as:</p> $PI = (N_1 \cdot 1.0) + (N_2 \cdot 0.75) + (N_3 \cdot 0.50) + (N_4 \cdot 0.25)$ <p>Where, N_1, N_2, N_3, N_4 are the number of seeds germinated on the first, second, third, and fourth day, respectively.</p>
Germination stress tolerance index (GSTI)	<p>It is estimated as:</p> $GSTI = \frac{PI_s}{PI_n} \cdot 100$ <p>Where, PI_s is the promptness index of stressed seed lots and PI_n is the promptness index of unstressed seed lots.</p>

Ascorbate peroxidase activity was assayed, according to Nakano and Asada (1981). The 1 mL assay reaction mixture contained 50 mM phosphate buffer (pH 7.0), 0.1 μ M EDTA, 0.5 mM ascorbate, 0.5 mM H₂O₂ and 50 μ L enzyme extract. The reaction was initiated by adding H₂O₂, and the decrease in absorbance due to ascorbate oxidation read at 290 nm for 3 min. Enzyme activity was calculated using the molar extinction coefficient (ϵ) for reduced ascorbate (2.8 mM⁻¹ cm⁻¹) and the specific activity of APX expressed in units per gram FW (U g⁻¹ FW).

Peroxidase activity was estimated by following the oxidation of *o*-dianisidine (3,3'-dimethoxybenzidine) at 460 nm (Ranieri *et al.*, 2000). The assay mixture contained 900 μ L of potassium phosphate buffer (100 mM, pH 6.0) with 1 % *o*-dianisidine (in methanol), 50 μ L of enzyme extract, and 50 μ L H₂O₂ (10 mM). The specific activity was calculated using the extinction coefficient of *o*-dianisidine ($\epsilon = 11.3$ mM⁻¹ cm⁻¹) and expressed as units per gram FW (U g⁻¹ FW).

3.2.2.4. Estimation of lipid peroxidation

The accumulation of malondialdehyde (MDA) due to lipid peroxidation was determined according to Heath and Packer (1968). Weighed samples were homogenized in 3 mL of 0.1 % trichloroacetic acid (TCA) and centrifuged at 10000 *g* for 20 min. One milliliter of supernatant was mixed with 2 mL of 20 % TCA and 2 mL of 0.5 % thiobarbituric acid, and the mixture incubated at 95 °C for 30 min and cooled on ice thereafter. Absorbance was read at 532 nm and 600 nm against a reagent blank, and MDA content calculated using the extinction coefficient of MDA ($\epsilon = 155$ mM⁻¹ cm⁻¹).

3.2.2.5. Determination of total antioxidant capacity

Samples were weighed and homogenized with 3 mL of distilled water, centrifuged at 15000 *g* at 4 °C for 30 min. The total antioxidant capacity of the supernatants was determined, as described by Prieto *et al.* (1999). Briefly, 1.5 mL of reagent solution (0.6 M H₂SO₄, 28 mM sodium phosphate, 4 mM ammonium molybdate mixture) was mixed with 100 μ L of aqueous extract in a tube and incubated at 95 °C for 90 min. The tubes were cooled on ice, and the absorbance read at 695 nm. An incubated tube containing the reagent solution without extract was used as the blank. Total antioxidant capacity was determined from a standard prepared using ascorbic acid and expressed as milligram ascorbic acid equivalent per gram FW (mg AAE g⁻¹ FW).

3.2.2.6. Determination of total phenolic content

Total phenolic content was determined by the Folin–Ciocalteu reagent-based method, as described by Panuccio *et al.* (2014) with slight modifications. To 2.5 mL of Folin–Ciocalteu reagent (1:10 diluted with distilled water), 100 μ L of aqueous extract was added and followed by 2 mL of

saturated sodium carbonate solution ($\sim 75 \text{ g L}^{-1}$). The tubes were shaken to mix the reaction mixture properly and allowed to stand for 2 h at room temperature before taking the absorbance at 760 nm. Gallic acid was used as a reference standard, and the results expressed as milligram gallic acid equivalents per gram FW ($\text{mg GAE g}^{-1} \text{ FW}$).

3.2.2.7. Estimation of proline content

Proline content was estimated according to the protocol in *Ábrahám et al.* (2010). Weighed samples were homogenized in 1 mL of 3 % sulfosalicylic acid and centrifuged at 10000 *g* for 10 min. To 100 μL of the supernatant in a tube, 100 μL of 3 % sulfosalicylic acid, 200 μL glacial acetic acid, and 200 μL acidic ninhydrin were added and incubated at 95 °C for 60 min. The reaction was terminated on ice, and the mixtures were extracted with 1 mL toluene, vortexed, and the organic phase was allowed to separate for 5 min. The absorbance of the chromophore containing the toluene phase was read at 520 nm using toluene as reference. Proline concentration was determined using a standard concentration curve and expressed in milligram per gram FW ($\text{mg g}^{-1} \text{ FW}$).

3.2.3. Experiment II: OJIP analysis, biochemical and physiological responses of seedlings

Seeds were surface sterilized using 25 % (v/v) sodium hypochlorite solution for 5 min and rinsed several times with distilled water. The sterilized seeds were then soaked in distilled water for 20 h, rinsed, and sown in Petri dishes lined with filter paper. The setup was irrigated with distilled water and incubated in a growth chamber at 23 °C to germinate.

3.2.3.1. Growth conditions

After two days, germinated seeds were transferred into 75 mm x 100 mm plastic pots (2 seeds per pot) with vermiculite as a potting medium. Each pot was irrigated every three days with nutrient medium containing 5 mM KNO_3 , 3 mM $\text{Ca}(\text{NO}_3)_2$, 0.75 mM KH_2PO_4 , 3 mM MgSO_4 , 0.5 mM KCl , 0.1 mM CaCl_2 , 1 mM NaCl , 50 μM $\text{NaFe}(\text{III})\text{EDTA}$, 50 μM H_3BO_3 , 5 μM MnCl_2 , 10 μM ZnSO_4 , 0.5 μM CuSO_4 and 0.1 μM Na_2MoO_3 adjusted to pH 5.0 using concentrated NaOH solution. Growth room temperature was set at 22 ± 2 °C, 70 % relative humidity with white light (LED, PAR $\sim 120 \mu\text{mol m}^{-2} \text{ s}^{-1}$) in a 16/8-h light/dark period, respectively.

3.2.3.2. Chemical and heat stress treatments

After 14 days, seedlings were assigned and treated as follows: control (CTL) was watered with the nutrient solution alone; strigolactone (GR24) received nutrient solution containing 10 μM GR24; tolfenamic acid (TL) supplied with the nutrient solution with 100 μM tolfenamic acid; tebuconazole (TB) received nutrient solution containing 20 μM tebuconazole; tolfenamic acid and

tebuconazole (TT) received nutrient solution with 100 μM tolfenamic acid and 20 μM tebuconazole.

Twenty-four hours after treatment initiation, the growth room temperature was gradually increased from 22 °C to 40 °C over 2 h, maintained at 40 °C for an hour, and then gradually decreased to 22 °C over 2 h. After that, seedlings were dark-adapted for at least 1 h before fluorescence data were taken. Similar heat treatment was repeated for Day 2 and Day 3.

3.2.3.3. *Chlorophyll a fluorescence transient and OJIP analysis*

Chlorophyll a fluorescence (ChlF) measurements commenced 24 h after treatment initiation. Data were collected before (PreHS) heat treatment, on the third day after three consecutive days of heat treatment (HS), and 3 days after returning the plants to normal growth conditions (PstHS). After at least 1 h of dark-adaptation following heat treatment, ChlF measurements were carried out in the dark on the adaxial lamina of a leaflet on the youngest but mature leaf using a portable chlorophyll fluorometer (OS-30p; Opti-Sciences, Inc., NH, USA). The instrument was set at maximum saturating flash (actinic light intensity; 3500 $\mu\text{mol photons m}^{-2} \text{s}^{-1}$), and ChlF emission induced by the strong pulse was recorded for 1 s. All measured, derived JIP-test parameters and their respective definitions are provided in Table 3.2.

3.2.3.4. *Physiological and biochemical responses of seedlings*

After three consecutive days of heat treatment, leaflets were harvested and assessed for antioxidant enzyme activities, lipid peroxidation, total antioxidant capacity, and the accumulation of phenolic and proline as described above.

3.2.3.5. *Determination of glyoxalase I and II activities*

Glyoxalase enzyme activities were determined according to the method described by Mustafiz *et al.* (2010). Weighed leaflets were homogenised and extracted in an extraction buffer containing 100 mM sodium phosphate buffer (pH 7.0), 50 % glycerol, 16 mM MgSO_4 , 0.2 mM PMSF, and 0.2 % PVPP. The extract was centrifuged at 12000 g for 30 min at 4 °C, and the supernatant was collected and placed on ice. Glyoxalase I assay mixture, which contained 100 mM sodium phosphate buffer (pH 7.5), 3.5 mM MG, 1.7 mM GSH, and 16 mM MgSO_4 , was prepared and incubated in the dark for a minimum of 10 min to allow for the formation of the substrate hemiacetal. The supernatant was added in a final volume of 1 mL, and the change in absorbance due to *S*-lactoylglyutathione (SLG) formation was read at 240 nm. The molar absorption coefficient

Table 3.2: Description of JIP-test parameters adapted from Strasser *et al.* (2010) and Jedmowski and Brüggemann (2015).

Extracted and derived fluorescence parameters.	
F_o	Minimum fluorescence at the O–step ($\approx 20 \mu\text{s}$) when all PSII reaction centers are open.
F_k	Fluorescence intensity at the K–step ($\sim 300 \mu\text{s}$).
F_j	Fluorescence intensity at the J–step (2 ms).
F_i	Fluorescence intensity at the I–step (30 ms).
F_m	Maximum fluorescence at the P–step, when all PSII reaction centers are closed.
$V_k = \frac{F_k - F_o}{F_m - F_o}$	Relative variable fluorescence at K–step.
$V_j = \frac{F_j - F_o}{F_m - F_o}$	Relative variable fluorescence at J–step.
$V_i = \frac{F_i - F_o}{F_m - F_o}$	Relative variable fluorescence at I–step.
$M_o = 4 \cdot \left(\frac{F_k - F_o}{F_m - F_o} \right)$	Approximated initial slope (in ms^{-1}) of the fluorescence transient normalized on the maximal variable fluorescence.
Quantum yields and efficiencies/probabilities.	
$\varphi_{Po} = 1 - \frac{F_o}{F_m}$	The maximum quantum yield of PSII photochemistry (Q_A reduction).
$\varphi_{Do} = 1 - \varphi_{Po}$	Quantum yield of energy dissipation.
$\psi_{Eo} = 1 - V_j$	Efficiency/probability that a trapped exciton is used to move an electron further than Q_A .
$\varphi_{Eo} = \varphi_{Po} \cdot (1 - V_j)$	Quantum yield of the electron transport beyond Q_A .
$\varphi_{Ro} = \varphi_{Po} \cdot (1 - V_i)$	Quantum yield for reduction of end electron acceptors at the PSI acceptor side.
$\delta_{Ro} = \frac{1 - V_i}{1 - V_j}$	The efficiency of electron transfer from the reduced intersystem electron acceptors to the final electron acceptors of PSI.
Specific energy fluxes per Q_A reducing the PSII reaction center	
$ABS/RC = M_o \cdot \frac{1}{V_j} \cdot \frac{1}{\varphi_{Po}}$	Absorption flux per RC (also a measure of PSII apparent antenna size/the ratio between antenna light-harvesting complex (ABS) and active PSII per RC).
$TR_o/RC = M_o \cdot \frac{1}{V_j}$	Trapping flux (leading to Q_A reduction) per RC.
Performance indices	
$PI_{abs} = \left(\frac{\varphi_{Po} \cdot V_j}{M_o} \right) \cdot \left(\frac{\varphi_{Po}}{1 - \varphi_{Po}} \right) \cdot \left(\frac{\psi_{Eo}}{1 - \psi_{Eo}} \right)$	The performance index for energy conservation from photons absorbed by PSII to the reduction of intersystem electron acceptor.
$PI_{total} = PI_{abs} \cdot \left(\frac{\delta_{Ro}}{1 - \delta_{Ro}} \right)$	The performance index for energy conservation from photons absorbed by PSII to the reduction of PSI end acceptors.

of SLG at 240 nm ($3.37 \text{ mM}^{-1}\text{cm}^{-1}$) was used to calculate the specific activity of glyoxalase I and expressed in units per gram FW ($\text{U g}^{-1} \text{FW}$).

Glyoxalase II activity was determined by adding supernatant to an assay mixture containing 50 mM Tris-HCl (pH 7.2) and 300 μM SLG in a total volume of 1 mL, and the rate of SLG hydrolysis followed at 240 nm. The molar absorption coefficient of SLG at 240 nm ($3.370 \text{ mM}^{-1}\text{cm}^{-1}$) was used to calculate the specific activity of glyoxalase II and expressed in units per gram FW ($\text{U g}^{-1} \text{FW}$).

3.2.4. Statistical analysis

All data were subjected to analysis of variance (ANOVA) with the chemical treatments as the grouping factor and *post hoc* analysis carried out with the Duncan's Multiple Range Test to compare all pairs of means of the response variables. The confidence level was set at $p \leq 0.05$, except otherwise stated. All statistical analyses were performed using SPSS for Windows v25.0 (IBM Corp., Armonk, NY, USA).

3.3. Results

3.3.1. Experiment I: Seed germination

3.3.1.1. GR24 enhances seed germination under HS

As can be inferred from Fig. 3.1, treatment-mediated tolerance to the deleterious effects of high temperature on seed germination occurred in the following order: $\text{TT} < \text{TL} < \text{CTL} < \text{TB} < \text{GR24}$. Under ambient conditions, all the treatment solutions did not affect the final percentage of seeds that germinated, as shown in Fig. 3.1A. However, under heat stress, the least final germination percentage was observed in TT (23%), while the highest was recorded in GR24 (90%) (Fig. 3.1A). Compared to the control, treatment with TL did not significantly affect seed tolerance to HS during germination (27%). Though TB had a significantly lower ameliorating effect on seed germination (53%) when compared to GR24 (90%), it appeared to stimulate seed germination when compared to CTL though this was not statistically significant. The rapidity of seed germination, here represented as the coefficient of velocity of germination (CVG: Fig. 3.1B), was affected by the treatment solutions under the ambient condition with TL lowering CVG significantly. This did not have a detrimental effect on seed germination since all treatments showed 100 % germination (Fig. 3.1A). Under heat stress, CVG was not significantly different between CTL and the treatment groups (Fig. 3.1B). However, between GR24 ($\sim 68\% \text{ day}^{-1}$) and TT ($\sim 31\% \text{ day}^{-1}$), there was a significant difference in CVG, indicating an inhibitory effect by TT on the rate of seed germination. As with CVG, the germination index, which combines germination percentage and germination

speed (GI: Fig. 3.1C), was also significantly decreased by TL under ambient conditions. On the other hand, in seeds germinated under heat stress, GI was significantly higher in GR24-treated seeds (85 a.u.) compared to CTL (34 a.u.). In TB, TL, and TT-treated seeds, GI was not significantly different from CTL. Similarly, the germination stress tolerance index (Fig. 3.1D) was not significantly different in all treatment groups compared to CTL, with the exception of GR24 (78.48%), where it was over twice that of CTL (~31%). These observed significant positive relationships between GR24 and seed germination indices indicate that GR24 confers some degree of thermotolerance on lupine seeds during germination under HS.

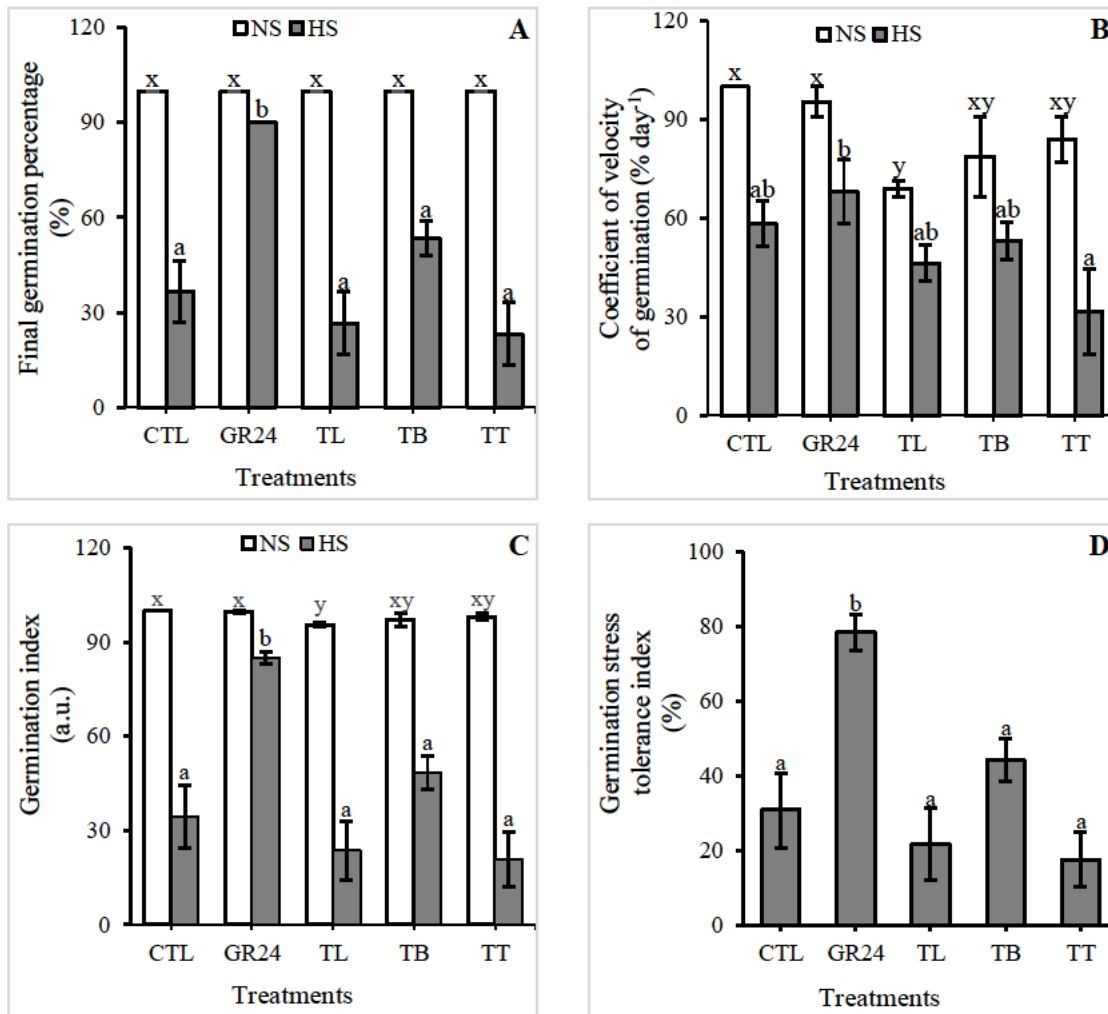


Figure 3.1. The effects of GR24, tolfenamic acid, and tebuconazole treatments on germination of *Lupinus angustifolius* L. seeds under normal (NS) and elevated temperature (HS). Final germination percentage (A); coefficient of velocity of germination (B); germination index (C); and germination stress tolerance index (D). Treatments: control, CTL; strigolactone, GR24; tolfenamic acid, TL; tebuconazole, TB; tolfenamic acid + tebuconazole, TT. NS: seeds germinated under non-stress/ambient condition; HS: seeds germinated under heat stress. Different letters indicate statistically significant differences ($p < 0.05$) between the treatment group means. Values represent mean \pm standard error ($n = 2$ and 3 seed lots with 10 seeds each for non-stress and stress germination, respectively).

3.3.1.2. *GR24 enhanced superoxide radical scavenging while inhibiting peroxidase activity*

As shown in Fig. 3.2A, GR24 induced a significant increase in superoxide anion (O_2^-) scavenging as SOD activity in GR24-treated seeds was ~53% significantly higher than that of the control. Contrary to the observation with GR24, strigolactone inhibitors, TB and TL, as well as the combined treatment (TT), had no significant effect on O_2^- scavenging capacity of germinating seeds as SOD activities in TB-, TL- and TT-treated seeds were not significantly different from the control. In comparison to CTL, APX (Fig. 3.2B), as well as POX (Fig. 3.2C), activities were significantly reduced in all the treatments. While GR24 induced approximately 47% and 42% decreases in APX and POX activities, respectively, TL treatment, similarly, resulted in ~64% and ~29% reduction in APX and POX activities. Tebuconazole showed a very strong inhibitory effect on seed peroxidase activity as it induced a 92% and 94% reduction in APX and POX activities, respectively.

3.3.1.3. *GR24 inhibits HS-induced peroxidation of lipids and increase proline content*

As depicted in Fig. 3.3A, peroxidation of lipids, estimated as MDA content, was significantly lowered in GR24-treated seeds (approximately 51% lower with respect to the control). Though TB induced a significant reduction (~20% decrease) in the MDA content of germinating seeds, the lipid peroxidation level in TL and TT-treated seeds was not significantly different from that of the control. Proline content in all treatments was significantly higher than that of CTL (Fig. 3.3B). GR24 induced a 3% increase in proline content of germinating seeds compared with the control while TL and TB induced a 2% and 2.3% increase, respectively.

3.3.1.4. *Total antioxidant capacity and phenolic content*

Total antioxidant capacities of germinating seeds, expressed as ascorbic acid equivalent, were not significantly different in GR24, TL, and TT except in TB-treated seeds where there was a significant ($p < 0.05$) increase of ~34% with respect to the control (Fig. 3.3C). In all the treatments, total phenolic content, expressed as gallic acid equivalents (Fig. 3.3D), was not significantly different from that of the control.

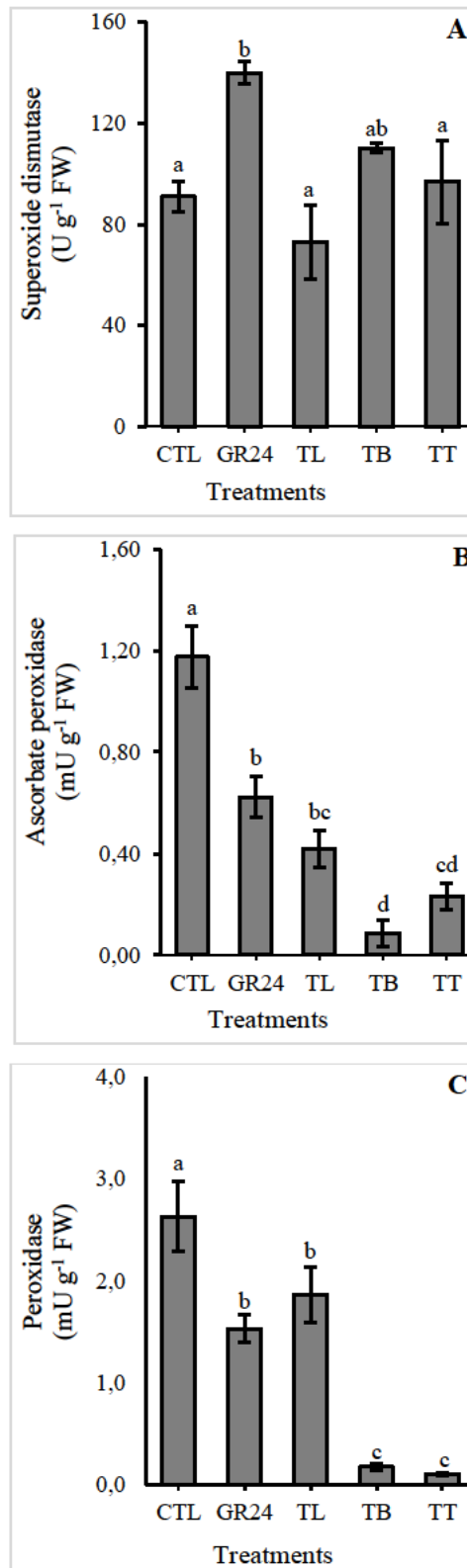


Figure 3.2. Antioxidant enzyme activities, viz. superoxide dismutase (A), ascorbate peroxidase (B), and peroxidase (C) in germinating *Lupinus angustifolius* L. seeds treated with GR24, tolfenamic acid, and tebuconazole germinated under high temperature. Treatments: control, CTL; strigolactone, GR24; tolfenamic acid, TL; tebuconazole, TB; tolfenamic acid + tebuconazole, TT. Different letters indicate statistically significant differences ($p < 0.05$) between the treatment group means. Data represent mean \pm standard error ($n = 4$).

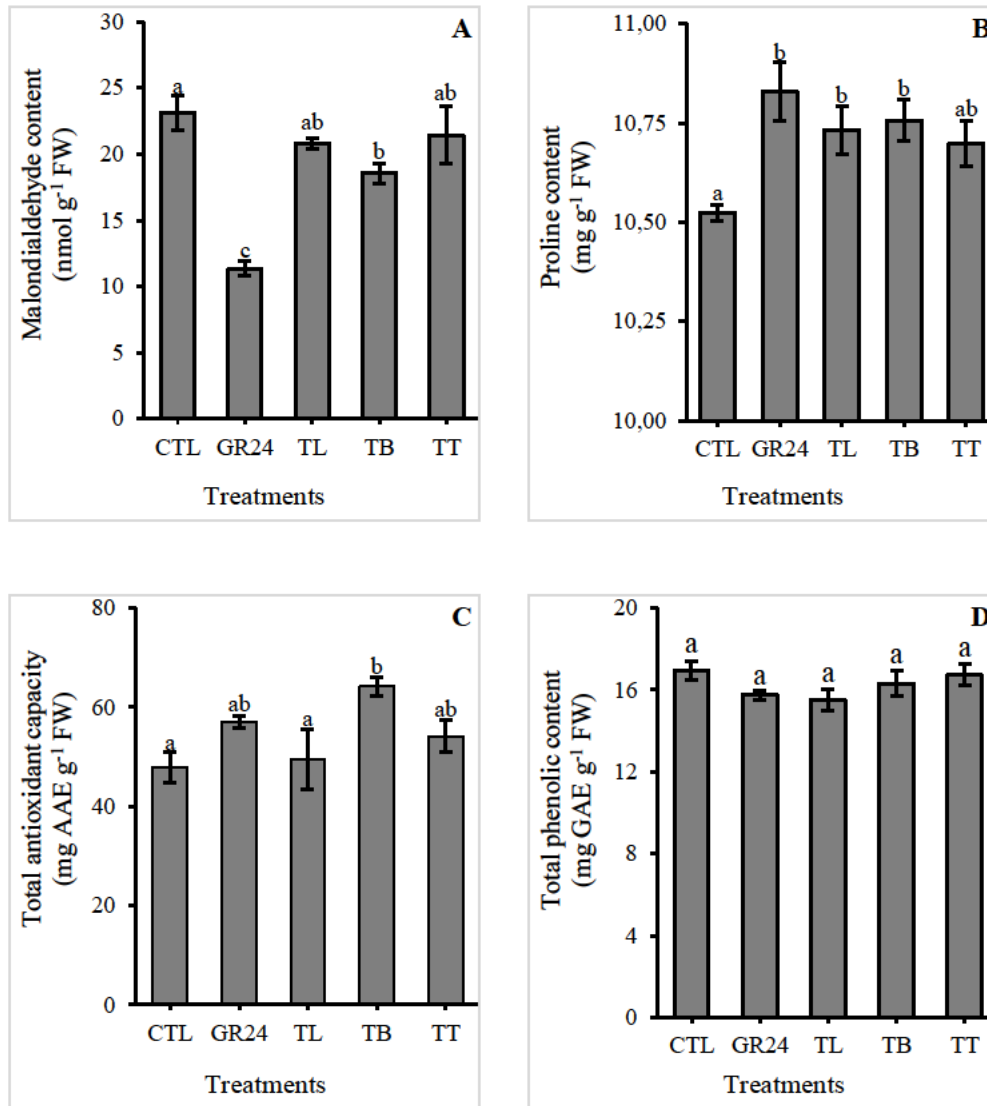


Figure 3.3. Malondialdehyde content (A), proline content (B), total antioxidant capacity (C), and phenolic content (D) of *Lupinus angustifolius* L. seeds treated with GR24, tolfenamic acid, and tebuconazole and germinated under high temperature. Treatments: control, CTL; strigolactone, GR24; tolfenamic acid, TL; tebuconazole, TB; tolfenamic acid + tebuconazole, TT. Different letters indicate statistically significant differences ($p < 0.05$) between the treatment group means. Values represent mean \pm standard error ($n = 4$).

3.3.2. Experiment II: Chlorophyll a fluorescence, biochemical and physiological responses of lupine seedlings under HS

3.3.2.1. *Effects of GR24 and strigolactone inhibitors on PSII and PSI activity in lupine seedlings under HS*

To assess the effects of GR24 and strigolactone inhibitors on PSI and PSII responses to HS in lupine seedlings, biophysical parameters that serve as indicators of photosynthetic behavior were inferred by JIP-test. After three consecutive days of HS treatment, F_o values increased significantly in CTL and TT-treated seedlings but were not significantly affected in GR24, TB, and TL-treated seedlings (Fig. 3.4A). Fluorescence intensity at the K-step was not affected in GR24, TL, and TB-treated seedlings but in CTL and TT-treated seedlings, a significant rise in F_k was observed (Fig. 3.4B). As shown in Fig. 3.4C, a significant increase in F_j was observed in CTL and TT-seedlings but in TL seedlings, F_j decreased though not significant statistically. Fluorescence intensity at the J-step was not significantly affected in GR24 and TB-treated seedlings. Generally, HS induced a rise in F_i as seen in CTL (Fig. 3.4D). Though F_i remained largely unchanged in GR24, TB, and TT after HS, it decreased significantly in TL-treated seedlings. The maximal fluorescence intensity, F_m (Fig. 3.4E), after HS was not significantly different from PreHS values in GR24, TB, and TT-treated seedlings, but significantly increased in CTL and declined in TL-treated seedlings. Finally, M_o (Fig. 3.4F) which is an indicator of the approximated initial slope (in ms^{-1}) of the fluorescence transient was significantly increased in the control seedlings and all treatments except in TL-treated seedlings where it was largely unaffected. In CTL, GR24, TB and TT-treated seedlings, M_o increased significantly by 65%, 22%, 21%, and 57%, respectively, while in TL-treated seedlings, a ~4% increase was observed. Compared to the control, it can be seen that the HS-induced increase in M_o was significantly inhibited by GR24, TB, and TL treatments. The foregoing clearly indicates that GR24, and to some extent, both strigolactone inhibitors exerted some influence on biophysical and functional features of the photosystems of lupine seedlings under HS.

The relative variable fluorescence at the I-step (V_i) was largely unaffected at HS and PstHS (i.e., not significantly different from PreHS) in CTL and all treatments (Fig. 3.5A). In contrast, an HS-induced increase in V_j (Fig. 3.5B) was significantly inhibited by GR24, TL, and TB treatments with 10%, 7%, and 3% increase respectively, which were not significantly different from PreHS while in CTL and TT-treated seedlings, V_j increased significantly by 35% and 32%, respectively. After the recovery period (PstHS), V_j values in GR24, TL, and TB seedlings were lowered back to similar values as in PreHS while in CTL and TT-treated seedlings, V_j were lowered from their HS but remained significantly higher than the PreHS values. Heat stress resulted in a rise in the relative

variable fluorescence at the K-step (V_k), which increased by 60% in CTL and 57% in TT (Fig. 3.5C). This increase was also inhibited in GR24, TL, and TB-treated seedlings with ~21%, 7%, and 23% increase, respectively. These were, however, found to be statistically significant. V_k values at PstHS in CTL and TT seedlings were lower than their corresponding HS values but still significantly higher than the PreHS values while in GR24 and TL-treated seedlings, V_k had returned to a similar level as the PreHS values. Conversely, in TB-treated seedlings, V_k continued to increase at PstHS. The initial slope of the fluorescence transient (M_o) which is dependent on V_k increased significantly under HS (Fig. 3.5D). Treatment with GR24, TB, and TL also limited this heat-induced increase in M_o . At PstHS, M_o values in GR24 and TL-treated seedlings had returned to the PreHS values while it was seen to have reduced in CTL and TT seedlings though still significantly higher than the PreHS values. These observations suggest that GR24, tebuconazole, and tolfenamic acid exerted some thermoprotective influence on the light-harvesting and electron transfer systems of PSII and PSI.

The efficiency with which an absorbed photon is trapped by PSII RCs expressed as the maximum quantum yield of PSII (primary) photochemistry (ϕ_{Po}) and the quantum yield of energy (heat) dissipation (ϕ_{Do}) are shown in Fig. 3.6. Both ϕ_{Po} (Fig. 3.6A) and ϕ_{Do} (Fig. 3.6B) were significantly altered by HS. While ϕ_{Po} decreased, ϕ_{Do} increased in CTL and all treatments. The extent of ϕ_{Po} decrease and ϕ_{Do} increase was largely similar across all treatments and CTL. After recovery (PstHS), both ϕ_{Po} and ϕ_{Do} remained unaltered from their corresponding HS values. On the other hand, an HS-induced significant decrease in ψ_{Eo} , which is a measure of the probability that an electron is moved further than Q_A^- per exciton by the open RCs, was observed in CTL and TT-treated seedlings (Fig. 3.6C). In seedlings treated with GR24, TL, and TB, the slight decrease in ψ_{Eo} observed was not significant ($p > 0.05$). At PstHS, ψ_{Eo} became slightly higher than the PreHS values in GR24 treated seedlings indicating GR24 fostered an amelioration of the diminishing effect of HS on the electron transfer system of PSII. In CTL and TT seedlings, ψ_{Eo} increased from HS values, but it was still significantly lower than the PreHS values while in TB and TL, ψ_{Eo} further decreased. Similarly, the quantum yield of PSII electron transport (ϕ_{Eo}) was significantly ($p < 0.01$) reduced in CTL seedlings and all treatments (Fig. 3.6D). While ϕ_{Eo} decreased by 22% in CTL and TT seedlings, GR24, TL, and TB treatments limited HS-induced decrease in ϕ_{Eo} to 11%, 11% and 7% respectively. At PstHS, ϕ_{Eo} in CTL, GR24 and TT-treated seedlings gradually increased towards the PreHS level but were still lower, while in TB and TL seedlings, ϕ_{Eo} further decreased. The efficiency with which an electron is transferred from the reduced intersystem electron acceptors to PSI end-electron acceptors is given by δ_{Ro} . As shown in Fig. 3.6E, δ_{Ro} increased significantly in CTL seedlings under HS while GR24, TB, TL, and TT

treatments significantly inhibited the HS-induced increase in δ_{Ro} . At recovery, δ_{Ro} in CTL and TB further increased while a decrease in the PreHS values was observed in GR24, TL, and TT seedlings. Conversely, the quantum yield for the reduction of the end-electron acceptors at the PSI acceptor side (ϕ_{Ro}) remained largely unaffected in CTL, and all treatments (Fig. 3.6F) as their values in HS and PstHS were not significantly different from PreHS values.

The parameter ABS/RC is an indicator of specific energy absorption flux, and it depicts, in addition to the effective antenna size per active (Q_A -reducing) RC, the ratio between antenna light-harvesting complex (ABS) and active PSII per RC (Oukarroum *et al.*, 2015). As seen in Fig. 3.7A, HS induced a significant increase in ABS/RC (i.e., a decrease in the fraction of active PSII RC) of CTL, GR24, TB, and TT-treated seedlings except in TL where ABS/RC was largely unaffected. GR24 and TL treatments significantly inhibited this stress-induced increase in ABS/RC compared to the control. After the 3-day recovery period, ABS/RC in TB seedlings remained largely unaffected compared to HS values but significantly higher than PreHS values. In TL seedlings, ABS/RC increased but it was not significantly different from HS and PreHS values. Although ABS/RC in GR24 and TT-treated seedlings declined during recovery, they remained significantly higher than PreHS values. In the control seedlings, ABS/RC increased further during recovery. TR_o/RC , also a specific energy flux parameter, expresses the trapping flux per active RC or initial rate by which an exciton is trapped by the RC resulting in the reduction of Q_A to Q_A^- . As with ABS/RC, a rise in TR_o/RC due to HS was observed in CTL and all treatments (Fig. 3.7B). These increases were significant in CTL and TT seedlings. The values of TR_o/RC under HS, though higher, were not significantly different from the PreHS values in GR24, TL, and TB-treated seedlings. At PstHS, TR_o/RC declined and was not significantly different from the PreHS values in all treatments except the control, where it increased and remained significantly different from the PreHS values. These observations are clear indications that GR24, TL, and TB treatments helped lupine seedlings to resist and ameliorate the deleterious effects of HS on the energy absorption and trapping flux of PSII.

Performance index on absorption basis (PI_{abs}) quantifies the overall photosynthetic activity of PSII, i.e., the energy conservation from photons absorbed by the PSII antenna to the reduction of Q_B . It takes into account the density of RCs, which quadrates with the specific absorption flux, quantum yield of trapping, and probability that a trapped exciton will move an electron into the electron transport chain beyond Q_A^- i.e., to the reduction of intersystem electron acceptors. Heat stress led to a significant reduction in PI_{abs} of control seedlings and all treatments (Fig. 3.8A). While PI_{abs} in CTL and TT seedlings was reduced by 68% and 67% respectively, GR24, TL, and

TB treatments tend to inhibit this decrease as GR24, TL, and TB-treated seedlings showed 49%, 39%, and 43% decrease in PI_{abs} respectively at HS. Though PI_{abs} tend to shift towards the PreHS values in CTL, GR24, and TT after recovery, they remained significantly lower than the PreHS values. At PstHS, PI_{abs} further decreased in TL and TB-treated seedlings. Similarly, the performance index for energy conservation from exciton to the reduction of PSI end electron acceptors (PI_{total}) was significantly reduced in control, and all treated seedlings (Fig. 3.8B). This HS-induced decrease in PI_{total} was resisted in GR24, TL, and TB-treated seedlings (53%, 40%, and 44% reduction respectively) compared to CTL and TT-treated seedlings (71% and 71% decrease respectively). As with PI_{abs} , PI_{total} values were seen to have gradually increased in CTL and GR24-treated seedlings while declining further in TL and TB seedlings after the 3-day recovery period.

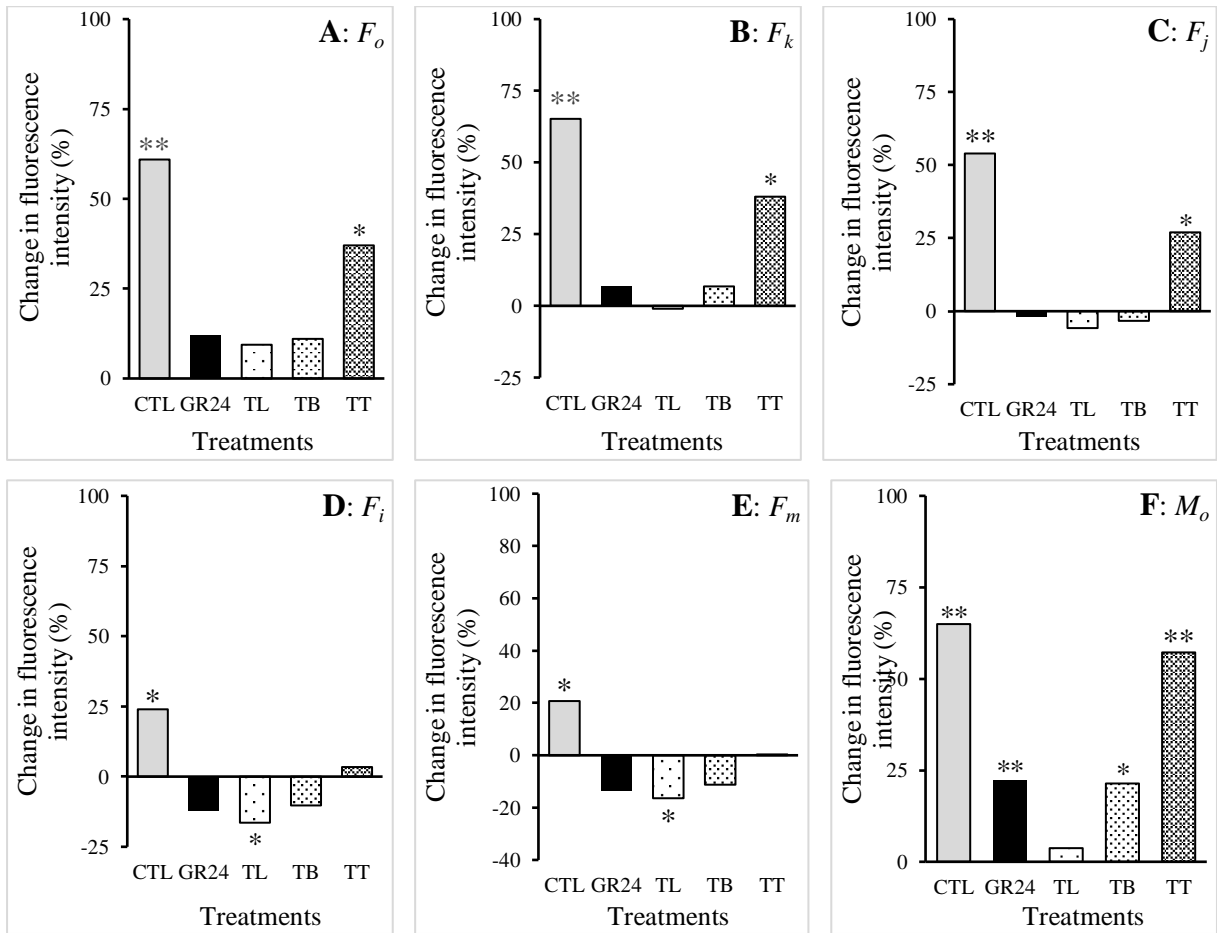


Figure 3.4. The influence of GR24, tolfenamic acid, and tebuconazole treatments on the changes in average foliar fluorescence intensities in *Lupinus angustifolius* L. seedlings after three consecutive days under heat stress (compared to preheat stress values). Percentage change in the minimal fluorescence intensity (F_o) when all PSII reaction centers are open, the O–step (A); the fluorescence intensity at the K–step at $\sim 300 \mu\text{s}$, F_k (B); the fluorescence intensity at the J–step at 2 ms, F_j (C); the fluorescence intensity at the I–step at 30 ms, F_i (D); the maximal fluorescence intensity at the P–step when all PSII reaction centers are closed, F_m (E); and the approximated initial slope (in ms^{-1}) of the fluorescence transient, M_o (F). Positive values indicate a percentage increase, while negative values indicate a percentage decrease. Treatments: control, CTL; strigolactone, GR24; tolfenamic acid, TL; tebuconazole, TB; tolfenamic acid + tebuconazole, TT. Asterisks show significant difference (** at $p < 0.01$ and * for $p < 0.05$) compared to the initial (PreHS) values before heat stress.

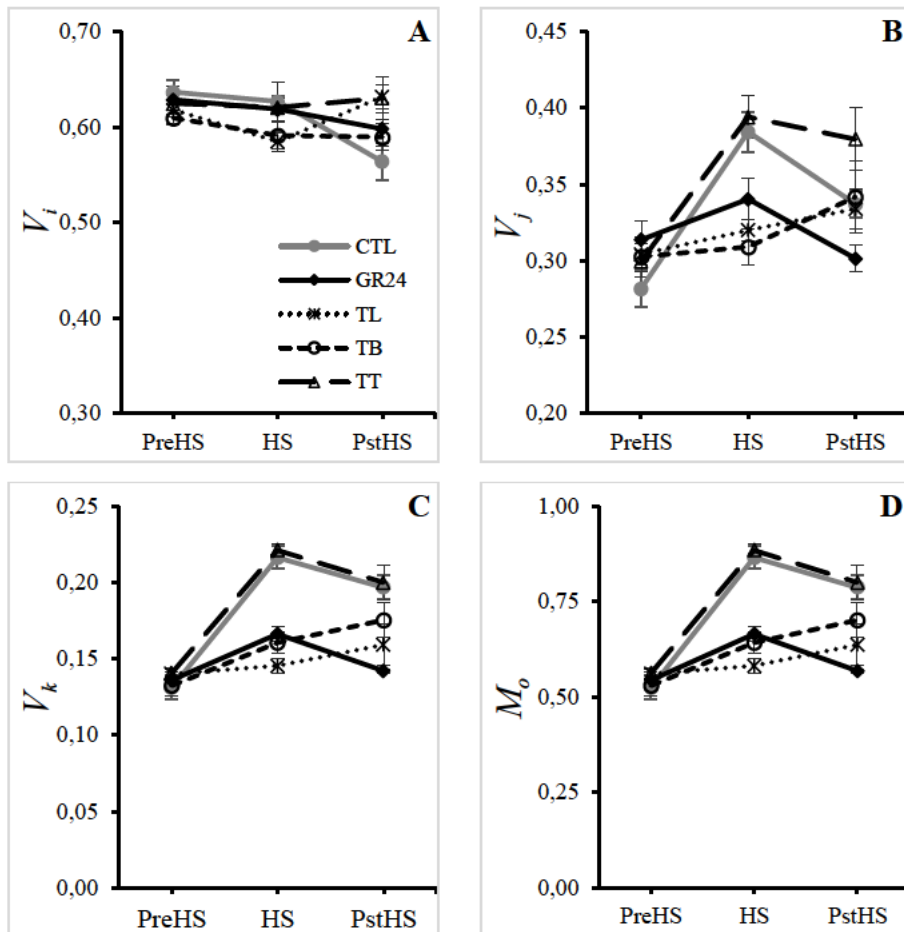


Figure 3.5. The effects of GR24, tolfenamic acid, and tebuconazole on foliar relative variable fluorescence (A–C) and the approximated initial slope of the fluorescence transient (D) of *Lupinus angustifolius* L. seedlings before heat treatment (PreHS), after heat stress (HS), and after 3-day recovery (PstHS). Treatments: control, CTL; strigolactone, GR24; tolfenamic acid, TL; tebuconazole, TB; tolfenamic acid + tebuconazole, TT. Data are means ± standard error ($n = 5$).

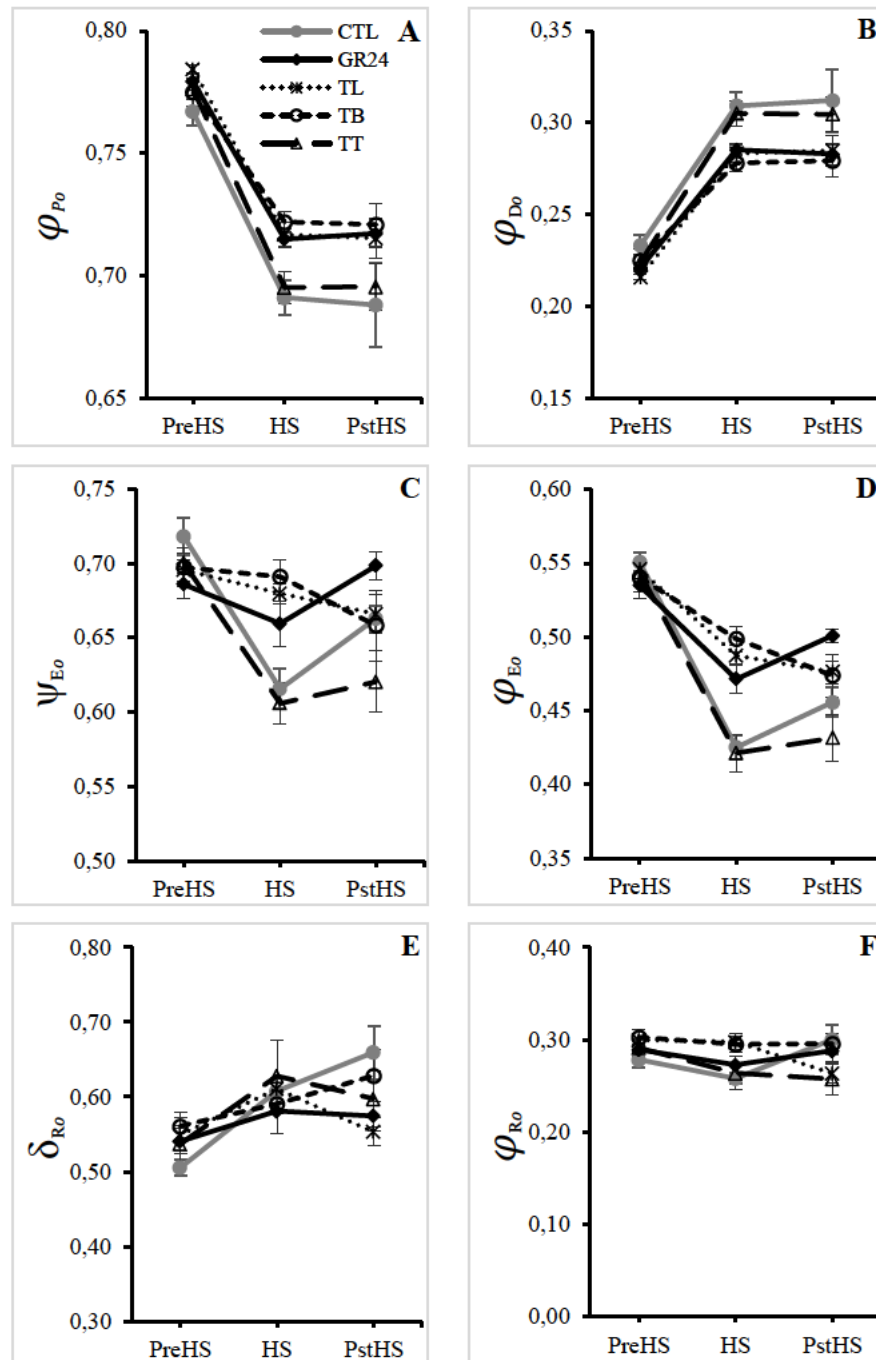


Figure 3.6. Effect of GR24, tolfenamic acid, and tebuconazole treatments on the quantum yields and efficiencies/probabilities of *Lupinus angustifolius* L. seedlings before heat stress (PreHS), after heat stress (HS), and after recovery (PstHS). ϕ_{Po} , the maximum quantum yield of PSII photochemistry (A); ϕ_{Do} , the quantum yield of energy (heat) dissipation (B); ψ_{Eo} , the fraction of electrons transported beyond Q_A^- per exciton trapped by the open reaction centers of PSII (C); ϕ_{Eo} , the quantum yield of electron transport beyond Q_A (D); δ_{Ro} , the efficiency with which an electron can move from the reduced intersystem electron acceptors to the PSI end acceptors (E); and ϕ_{Ro} , the quantum yield of reduction of PSI end acceptors (F). Treatments: control, CTL; strigolactone, GR24; tolfenamic acid, TL; tebuconazole, TB; tolfenamic acid + tebuconazole, TT. Data represent mean \pm standard error ($n = 5$).

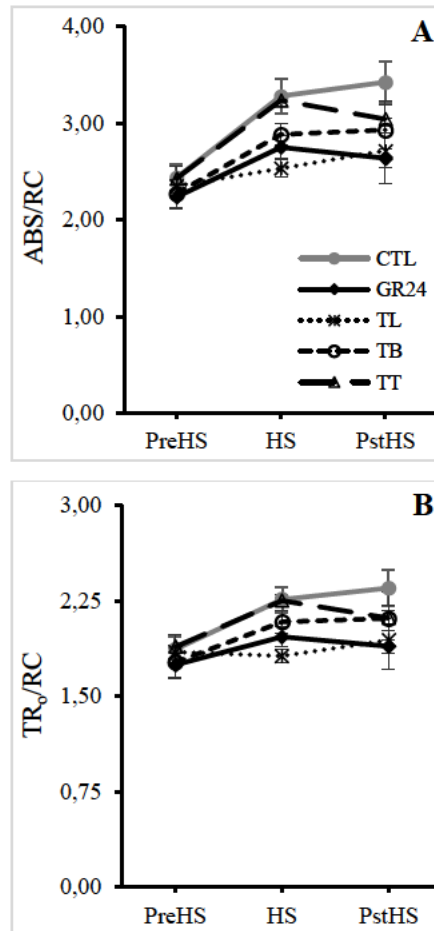


Figure 3.7. Effect of GR24, tolfenamic acid, and tebuconazole treatments on the specific energy fluxes per Q_A reducing PSII reaction center (RC) of *Lupinus angustifolius* L. seedlings before heat stress (PreHS), after heat stress (HS), and after recovery (PstHS). ABS/RC, absorption flux per RC (A); and TR_o/RC, trapped energy flux per RC (B). Treatments: control, CTL; strigolactone, GR24; tolfenamic acid, TL; tebuconazole, TB; tolfenamic acid + tebuconazole, TT. Data represents mean \pm standard error ($n = 5$).

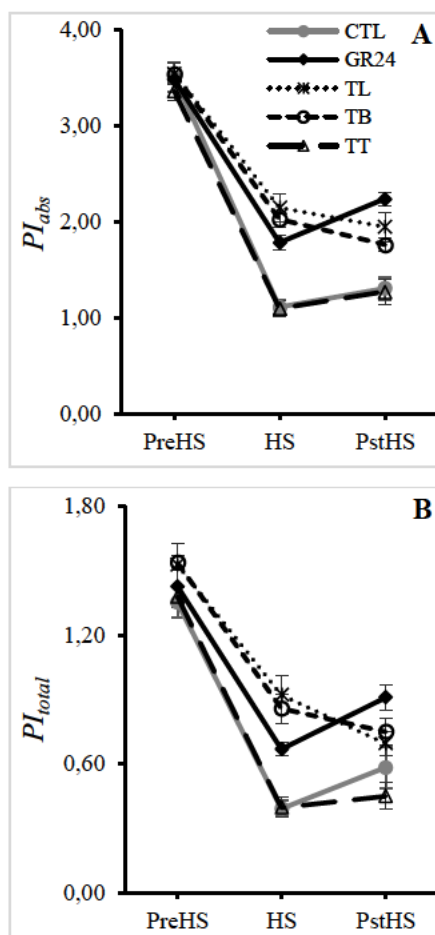


Figure 3.8. The effect of GR24, tolfenamic acid, and tebuconazole treatments on the performance indices of *Lupinus angustifolius* L. seedlings before heat stress (PreHS), after heat stress (HS), and after recovery (PstHS). PI_{abs} , performance index on absorption basis, i.e., energy conservation from photons absorbed by PSII to the reduction of intersystem electron acceptors (A) and PI_{total} , the total performance index for energy conservation from photons absorbed by PSII to the reduction of PSI end acceptors (B). Treatments: control, CTL; strigolactone, GR24; tolfenamic acid, TL; tebuconazole, TB; tolfenamic acid + tebuconazole, TT. Data represents mean \pm standard error ($n = 5$).

3.3.2.2. Antioxidant enzyme activities are enhanced in GR24-treated lupine seedlings under HS

The activities of all three antioxidant enzymes (SOD, APX, and POX) were significantly increased by GR24 (Fig. 3.9). In GR24-treated seedlings, SOD activity was 35% greater than those of control seedlings (Fig. 3.9A). While TL and TB induced a slight increase, TT resulted in a decrease in SOD activity with respect to the control though these differences were not statistically significant. In a similar trend, GR24 induced a ~45% increase in APX activity over the control (Fig. 3.9B). Both strigolactone inhibitors (TB and TL) and the combined treatment (TT) did not significantly affect APX activity. With GR24, POX activity was increased significantly by 31% over the control (Fig. 3.9C). While POX activity was not affected in seedlings treated with TB and TL, the combined treatment (TT) resulted in a decrease (~13%) in POX activity.

3.3.2.3. GR24 stimulates glyoxalase I and II activity in lupine seedlings under HS

As shown in Fig. 3.10A, glyoxalase I activity in heat-stressed lupine seedlings was significantly increased by GR24 (32%) and TB (44%) treatments, while TL resulted in a slight decrease (though not statistically significant) in glyoxalase I activity. Seedlings treated with the combined strigolactone inhibitors (TT) also showed a slight increase in glyoxalase I activity though not statistically significant. In an almost similar trend, GR24, TB, and TT treatments induced a significant increase (39%, 30%, and 32%, respectively) in glyoxalase II activity of seedlings (Fig. 3.10B). Glyoxalase II activity was not significantly affected by TL treatment.

3.3.2.4. Lipid peroxidation and proline accumulation in seedlings

The accumulation of MDA due to HS-induced degradation of lipids was not significantly different in all the treatments (Fig. 3.11A). Though MDA content was slightly higher in TB, TL, and TT-treated seedlings than in the control, these differences were not statistically significant. Proline content in TL and TT-treated seedlings were significantly higher (79% and 146%, respectively) compared to the control. Whereas in GR24 and TB-treated seedlings, proline content was not significantly different from the control (Fig. 3.11B).

3.3.2.5. Total antioxidant capacity and phenolic content

As depicted in Fig. 3.11C, though GR24, TB, and TL induced slight increases in the total antioxidant capacities of treated seedlings, these differences were not statistically significant. In the combined treatment (TT), a slight decrease was observed though also not significant. On the other hand, the amount of total phenols was significantly increased in seedlings treated with GR24, TB, and TL (Fig. 3.11D), while in seedlings that received both inhibitors (TT), total phenol content was not significantly different from that of the control.

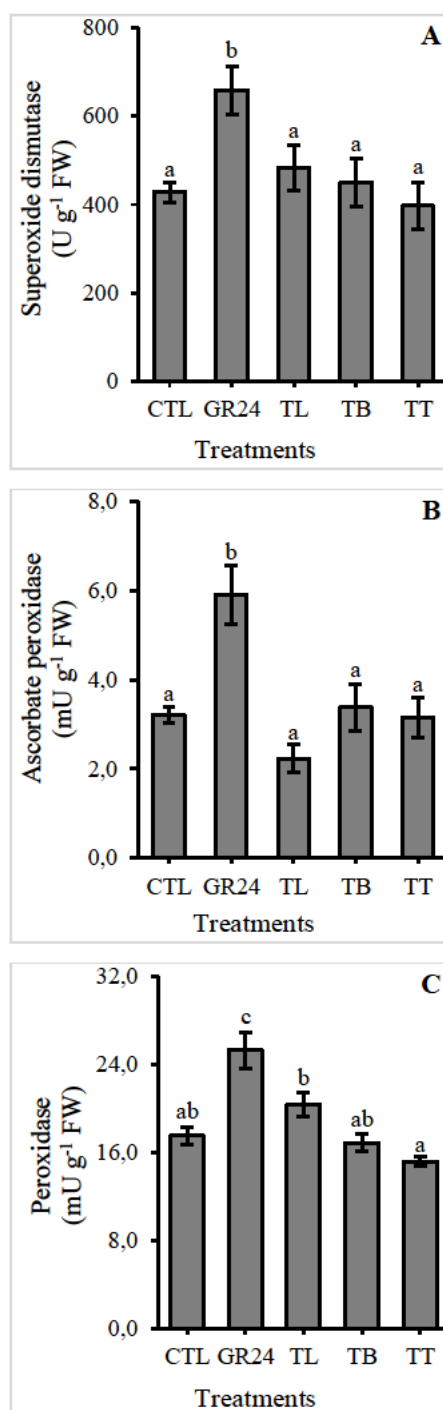


Figure 3.9. The effect of GR24, tolfenamic acid, and tebuconazole on antioxidant enzymes, viz. superoxide dismutase (A), ascorbate peroxidase (B), and peroxidase (C) in *Lupinus angustifolius* L. seedlings under heat stress. Treatments: control, CTL; strigolactone, GR24; tolfenamic acid, TL; tebuconazole, TB; tolfenamic acid + tebuconazole, TT. Different letters indicate statistically significant differences ($p < 0.05$) between the treatment group means. Data represent mean \pm standard error ($n = 4$).

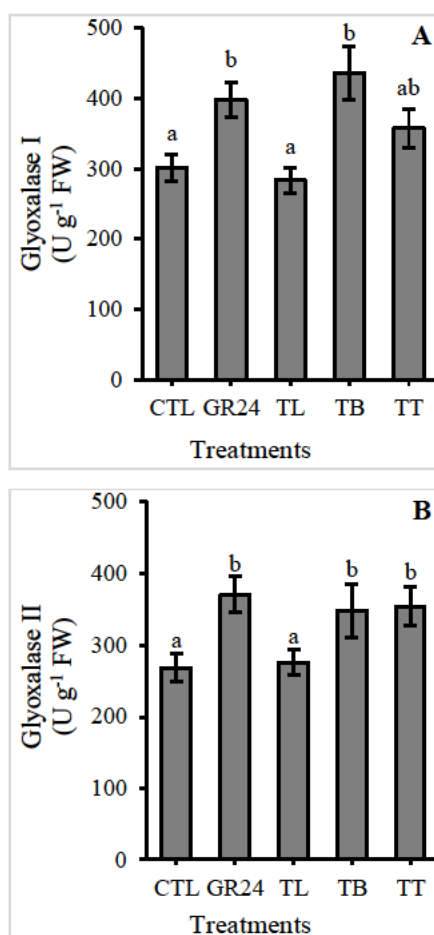


Figure 3.10. Effect of GR24, tolfenamic acid, and tebuconazole treatments on glyoxalase I (**A**) and glyoxalase II (**B**) activities in *Lupinus angustifolius* L. seedlings under heat stress. Treatments: control, CTL; strigolactone, GR24; tolfenamic acid, TL; tebuconazole, TB; tolfenamic acid + tebuconazole, TT. Different letters indicate statistically significant differences ($p < 0.05$) between the treatment group means. Data represent mean \pm standard error ($n = 4$).

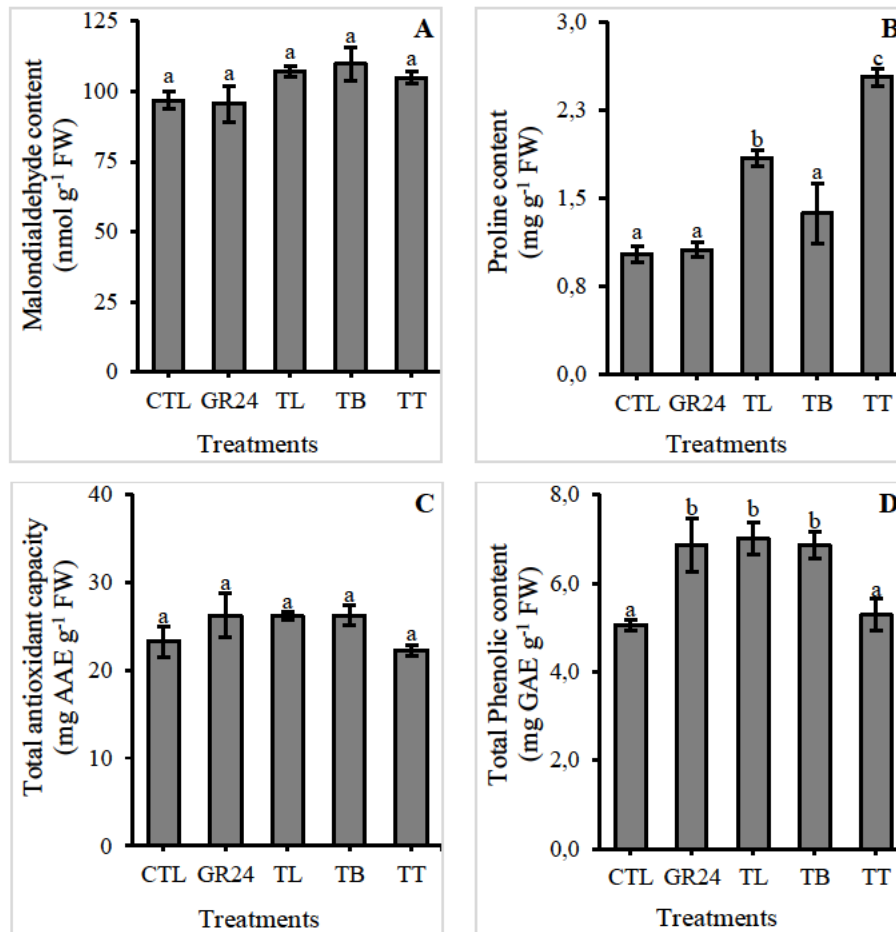


Figure 3.11. Lipid peroxidation levels (A), proline content (B), total antioxidant capacity (C), and phenolic content (D) of heat-stressed *Lupinus angustifolius* L. seedlings treated with GR24, tolfenamic acid, and tebuconazole. Treatments: control, CTL; strigolactone, GR24; tolfenamic acid, TL; tebuconazole, TB; tolfenamic acid + tebuconazole, TT. Different letters indicate statistically significant differences ($p < 0.05$) between the treatment group means. Data represent mean \pm standard error ($n = 4$).

3.4. Discussion

Heat stress is detrimental to seed germination and photosystem function, thus limiting the overall growth and development of plants. Phytohormones play key roles in the mediation of physiological processes that enable plants to combat the limiting effects of HS. Strigolactones have been linked to plant resilience under a number of abiotic stresses (Ha *et al.*, 2014; Ma *et al.*, 2017b; Mostofa *et al.*, 2018). The results presented are indicative of a role for GR24, a synthetic strigolactone analog, in conferring resistance to HS-induced inhibition of seed germination and PSII inactivation.

Our data shows that GR24 induced mitigation of the inhibitory effects of HS on seed germination in lupine. These align with previous reports in which GR24, in addition to breaking primary (Nelson *et al.*, 2009; Waters *et al.*, 2012b) and secondary dormancy, rescued germination in thermoinhibited *Arabidopsis* seeds of a strigolactone biosynthesis mutant (*more axillary growth1; max1-1*) but failed to do so in the signaling mutant (*max2-1*) and another strigolactone biosynthesis mutant (*max3-9*) (Toh *et al.*, 2011). These were, however, attributed to GR24 mediation of germination responses via *KARRIKIN INSENSITIVE2* (KAI2)-dependent signaling (Nelson *et al.*, 2009; Waters *et al.*, 2012b; Scaffidi *et al.*, 2014; Sun *et al.*, 2016b; Brun *et al.*, 2019). *KARRIKIN INSENSITIVE2* is an α/β hydrolase and a paralogue of the strigolactone receptor, D14, which perceives a group of smoke-derived butenolides called karrikins (Nelson *et al.*, 2009; Waters *et al.*, 2012b). Treatment with TB and TT did not significantly affect lupine seed germination under HS. The delay in seed germination by TL treatment [a D14 inhibitor (Hamiaux *et al.*, 2018)] under ambient condition is indicative of a strigolactone/D14-dependent role in seed germination, which if hampered delays, but is not sufficient to terminate germination. These resonate with recent observations that GR24 elicits equal responses with a karrikin, KAR₁ (Brun *et al.*, 2019). In addition, GR24 treatment failed to upregulate CYP707A genes in seeds of *Arabidopsis* mutants (*htl-3*, *max2-1*, and *smax1-2/max2-1*), which are defective in KAI2 signaling, in contrast to the WT (Col-0) where CYP707A genes were significantly upregulated. Conversely, blocking strigolactone biosynthesis (TB treatment) had no effect under normal and HS conditions, thus suggesting strigolactone biosynthesis is not a requirement for lupine seed germination. Taken together, these suggest that D14-dependent signalling plays a limited role in lupine seed germination responses under normal and HS conditions.

With respect to antioxidant activities, GR24 enhanced O₂⁻ scavenging during germination and seedling development under HS, but SOD activities were not significantly affected by TL and TB treatments. APX and POX activities were lowered in GR24, TL, and TT-treated germinating seeds while remaining unaffected in seedlings. In addition to enhanced SOD activity, results indicate that

GR24 fostered glyoxalase enzymes (i.e., both GlyI and GlyII) to enhance MG detoxification and alleviate the detrimental effects of HS in lupine seedlings. Malondialdehyde, an oxidation product of peroxidized polyunsaturated fatty acids, is an indicator of the structural integrity of membranes and a biological marker of oxidative stress (Yamauchi *et al.*, 2008). Oxidative stress elicits an increase in MDA content due to increased oxidation of membrane lipids (Li *et al.*, 2019). Our results demonstrate a GR24 and TB-mediated reduction in the MDA content of germinating seeds. GR24-induced increase in SOD activity might have contributed to the decreased lipid peroxidation levels in GR24-treated seeds. On the other hand, in heat-stressed seedlings, SOD activity was not enough to ameliorate the effect of HS. Furthermore, the amount of proline, an osmolyte accumulated to prevent cellular damage and maintain water balance under abiotic stress (Sharma *et al.*, 2019a), was also increased by all treatments in germinating seeds. In contrast, while neither GR24 nor TB showed any effect on proline contents of seedlings, TL, and TT treatments fostered proline accumulation. Plants accumulate phenolic compounds as a response and coping mechanism for HS (Awasthi *et al.*, 2015). During seed germination, neither GR24 nor the inhibitors had any effect on the phenolic content, which could explain why the total antioxidant capacities, a measure of the redox status of the treated seedlings, were not affected. However, in seedlings, though GR24 elicited a significant phenolic accumulation, this had no bearing on the overall antioxidant capacity of the seedlings.

Photosystem II, especially its closely associated OEC, is the most heat susceptible component of the photosynthetic electron transfer apparatus (Havaux, 1993; Strasser, 1997; Oukarroum *et al.*, 2013; Sun *et al.*, 2017). An HS-induced increase in F_o corresponds to a shift in Q_A/Q_B^- equilibrium toward Q_A (Kouřil *et al.*, 2004); a physical disconnection of PSII light-harvesting pigment antenna from the associated PSII (Yamane *et al.*, 1997); and generally, the loss of PSII structural and functional integrity (Kitajima and Butler, 1975; Čajánek *et al.*, 1998). While a decrease in F_m reflects an increase in non-radiative energy dissipation i.e. the inactivation of RCs making them dissipate the energy of absorbed photons in form of heat instead of QA reduction (Kitajima and Butler, 1975; Brestic *et al.*, 2012). HS generally induced a rise in F_o , and this increase in F_o was significantly inhibited by GR24, TL, and TB treatments. These show that GR24, TL, and TB treatment enabled the seedlings to resist HS-induced injury to OECs and ensured PSII thermostability. With respect to F_m , a significant decrease was only seen in TL-treated seedlings suggesting that while inactivated RCs increased in TL-treated seedlings, RC inactivation was not significant in GR24 and TB-treated seedlings. The increase in F_m observed in CTL and TT-treated seedlings is in contrast to several reports of a reduction of maximal fluorescence under HS (Tóth *et al.*, 2007; Chen *et al.*, 2016; Oukarroum *et al.*, 2016). Whatever may have been the underlying

reason for the rise in F_m , it appeared not to have a positive bearing on the JIP-test parameters of CTL and TT seedlings.

We also observed an HS-induced rise in the fluorescence intensity at the K-step, which indicates the inhibition of electron flow from the OEC to PSII RC (Srivastava *et al.*, 1997; Oukarroum *et al.*, 2016). Under HS, F_k increases (Jedmowski and Brüggemann, 2015; Oukarroum *et al.*, 2016), and consequently V_k and M_o , due to the disruption of OEC functions leading to an imbalance between the electron flow leaving the RC to the acceptor side and the electron flow coming to the RC from the donor side (Strasser, 1997; Tóth *et al.*, 2007; Chen *et al.*, 2008b). Our observations are indications that GR24, TL, and TB treatments mitigated HS-induced disruption of OEC function. The J-step is correlated with the redox state of Q_A and the I-step quadrates with the induction of a kinetic bottleneck of electron transfer between plastoquinol (PQH_2) and cytochrome b_6/f complex. While the I–P phase, on the whole, is related to electron transfer beyond the cytochrome b_6/f complex and the induction of a traffic jam of electrons caused by a transient block at the acceptor side of PSI (inactive ferredoxin-NADP⁺-reductase) (Strasser *et al.*, 2000; Strasser *et al.*, 2004; Schansker *et al.*, 2005). The general increase in F_j , and consequently V_j , is an indication that the acceptor side of PSII became more reduced under HS suggesting an accumulation of Q_A^- due to the inhibition of electron transfer beyond Q_A . A similar increase in V_j of samples under high light and temperature treatments have been reported (Chen *et al.*, 2008b; Yan *et al.*, 2013; Chen *et al.*, 2016). The rise in F_i which suggests an HS-induced inhibition of electron transport beyond PQH_2 (Schansker *et al.*, 2005; Yan *et al.*, 2013) did not translate into a significant change in V_i . This inhibition of electron transport was mitigated in GR24, TL, and TB-treated seedlings.

Damages to the donor sides of PSII by high temperatures results in a decrease in ϕ_{Po} (Chen *et al.*, 2008b; Brestic *et al.*, 2012; Brestic *et al.*, 2013; Haworth *et al.*, 2018). The inhibition of HS-induced decrease in ϕ_{Po} and increase in ϕ_{Do} observed in GR24, TL and TB-treated seedlings is explicable in part by their ability to mediate PSII functional stability. This was evident as resistance to HS-induced increase in F_o while limiting the inactivation of RCs (i.e. non-radiative dissipation of absorbed energy), that is indicated by the inhibition of HS-induced decrease in F_m and increase in ϕ_{Do} . The limiting effects of HS on electron transfer beyond Q_A is evident in the lower ψ_{Eo} and ϕ_{Eo} observed in the control and TT-treated seedlings. A similar decrease in ψ_{Eo} and ϕ_{Eo} was reported in *Vitis amurensis* (Luo *et al.*, 2011), sweet sorghum (Yan *et al.*, 2013), and *Ageratina adenophora* (Chen *et al.*, 2016) under severe HS. Given the limitation of HS on PSII donor side activity and PSII photochemistry efficiency, it is expected that this will reflect on the efficiency and quantum yield of electron transfer beyond Q_A . Interestingly, in addition to resisting the lowering of ψ_{Eo} and

φ_{E0} under HS, GR24 mediated a quick restoration of both parameters during the recovery period. High temperatures increase the probability of electron transfer (δ_{Ro}) and the quantum yield for reduction (φ_{Ro}) of the end-electron acceptors at the PSI acceptor side (Liu *et al.*, 2014a; Chen *et al.*, 2016) and are linked with a boost in PSI activity (Havaux *et al.*, 1991). While we found this to be true for δ_{Ro} , although treatment with GR24 and both strigolactone inhibitors limited the HS-induced δ_{Ro} increase, we observed a contrary response with φ_{Ro} which remained unaffected.

Thus far, the detrimental impact of HS on PSII function and the ameliorative role of GR24, TL, and TB were evident in the efficiencies and quantum yield of PSII components. Further supporting these are the responses of PSII energy flux parameters. Our data on ABS/RC, the size of Q_A -reducing antenna per active RC, reveal GR24 and TL treatments resisted an HS-induced increase in ABS/RC. An upswing in ABS/RC is fostered by increased inactivation of RCs, thus leading to a decrease in active RCs relative to associated antennas. Both PI_{abs} and PI_{total} are multi-parametric expressions which take into consideration: the density of active RCs per chlorophyll, the ratio of the de-excitation rate constants for photochemical and non-photochemical events, and the efficiency of excitation energy conversion to electron transport toward the Q_A pool (Jedrowski and Brüggemann, 2015). And for PI_{total} , in addition to the foregoing, the efficiency of the conversion of excitation energy to electron transport to PSI acceptor side (Strasser *et al.*, 2010). The ability of GR24 to limit HS-induced decrease in PI_{abs} and PI_{total} is a strong indication that strigolactones can enhance plant tolerance to HS by fostering PSII thermotolerance.

We expected TL, a strigolactone perception (D14/DAD2) inhibitor (Hamiaux *et al.*, 2018), and TB, a strigolactone biosynthesis (MAX1: cytochrome P450 monooxygenase) inhibitor (Ito *et al.*, 2013), to elicit opposite actions to that observed with GR24. This was, however, not the case with most parameters, especially in PSII thermotolerance during seedling development, where both inhibitors appeared to mediate similar levels of thermotolerance as GR24. These suggest three possible scenarios: (1) suppressing strigolactone/D14-dependent signaling fosters PSII thermotolerance, (2) D14-dependent signaling plays a limited role in lupine seed, and seedling responses under HS, or (3) both inhibitors influenced other physiological processes that fostered PSII thermotolerance. Since the inhibition of D14 by TL treatment did not limit PSII thermotolerance, the ameliorating effects of GR24 may be attributed to its ability to employ KAI2/MAX2 signal pathway(s) that have been shown to feature in plant tolerance to abiotic stress (Li *et al.*, 2017; Shah *et al.*, 2020). Racemic GR24, used in this study, contains a stereoisomer (GR24^{ent-5DS}) which binds KAI2 and elicits karrikin signaling (Scaffidi *et al.*, 2014; Sun *et al.*, 2016b). With the afore, and as cautioned by Scaffidi *et al.* (2014) that synthetic strigolactone analogs (like GR24) may activate responses that

are not specific to naturally occurring strigolactones, GR24 treatments, and the observed responses cannot be entirely comparable to those of the inhibitors due to its KAI2-dependent bioactivities.

Overall, the data suggests GR24 plays varied and significant roles in the regulation of responses to HS during seed germination and seedling development in narrow-leaved lupine, albeit these effects appeared to be elicited via its KAI2-dependent bioactivity rather than D14-dependent activities. We demonstrate that GR24 is able to elicit plant innate coping and defense mechanisms such as the antioxidant enzyme and glyoxalase systems to mitigate HS during seed germination and seedling growth. Moreover, F_o , F_k , φ_{Po} , φ_{Do} , ψ_{Eo} , ABS/RC, PI_{abs} and PI_{total} values in GR24-treated seedlings are evidence that GR24 mediated PSII thermotolerance by inhibiting HS-induced damages to OECs and the inactivation of PSII RCs. This is in line with a recent report that GR24 enhanced the PSII efficiency of salt-stressed *Sesbania cannabina* seedlings (Ren *et al.*, 2018). The disparities in GR24 actions with respect to proline accumulation, MDA, phenolic content, and total antioxidant capacity during seed germination and seedling growth are indications of a developmental stage specificity in strigolactone actions. Furthermore, the opposite actions observed between GR24 and the inhibitors (especially D14 inhibitor, TL) points towards a KAI2-dependent, rather than a D14-dependent, mechanism of action for GR24 in mediating thermotolerance in lupine. Both inhibitors (TB and TL) may have elicited other physiological responses that could have resulted in these observations since they may not be entirely specific for MAX1 and D14 inhibition, respectively. Studies employing mutants that are defective in karrikin and KAI2 signaling or the stereoisomer GR24^{5DS} would be required to rule out or confirm KAI2-dependent mediation of thermotolerance by GR24.

Chapter 4

Strigolactone in the mediation of tolerance to chilling stress

4.1. Introduction

Ambient temperature is a significant determinant of growth rate and development, phenological responses, and plants' geographical distribution. Temperatures that are considered extreme or suboptimal and fall below or above specific thresholds during critical stages of plant growth and development (such as germination, seedling development, and establishment, flowering, and fruit set) significantly and adversely affect developmental processes in plants. Prolonged exposures to such limiting temperatures may lead to failure of seedling establishment, low yield, and a decrease in overall productivity (Hussain *et al.*, 2018).

Chilling temperatures, defined as temperatures within the range of 0 – 15 °C, elicit cytological, morphological, and physiological changes in chilling sensitive plants. A decrease in growth rate and biomass, tissue dehydration and wilting, disruption of membrane systems and associated organelles, delayed leaf development, and the development of chlorosis and necrotic lesions on leaf tissues occur under chilling conditions (Yadav, 2010; Lukatkin *et al.*, 2012; Chen *et al.*, 2017). Physiological processes that are significantly disrupted by chilling stress include photosynthesis via photoinhibition and photooxidation, gas exchange, nutrient relations, osmotic balance, and water status, as well as redox status via a disruption of reactive oxygen species (ROS) and redox homeostasis [reviewed in Lukatkin *et al.* (2012) and Hussain *et al.* (2018)]. To mitigate the impacts of chilling stress, plants have evolved several mechanisms to cope with chilling conditions. These include both enzymatic and non-enzymatic mechanisms. While chilling-induced oxidative stress is mitigated by antioxidant enzymes and non-enzymatic antioxidants such as ascorbate, carotenoids, and phenolics (Zhou *et al.*, 2005; Hussain *et al.*, 2016; Hussain *et al.*, 2018), chilling-induced water deficit and osmotic imbalance are cushioned by the accumulation of compatible osmolytes such as proline and soluble sugars (Hodges *et al.*, 1997; Hussain *et al.*, 2018).

A diverse array of enzymes feature in plant signaling and responses to chilling to enhance tolerance and enable the plants to cope with chilling-induced stress. Superoxide dismutase (SOD), an antioxidant enzyme, features actively in plant defense against abiotic and biotic stresses by catalyzing the dismutation of the highly reactive O_2^- into O_2 and H_2O_2 , thereby preventing the accumulation of O_2^- to toxic levels and providing H_2O_2 , a ROS necessary for downstream stress

signaling. The role of SOD in the mediating plant tolerance to low temperatures and chilling stress is well documented (Hodges *et al.*, 1997; Shafi *et al.*, 2014; Hussain *et al.*, 2016).

Lipoxygenases (LOXs) form another group of essential enzymes contributing to plant stress signaling and responses (Lee *et al.*, 2005; Lim *et al.*, 2015; Upadhyay and Mattoo, 2018; Upadhyay *et al.*, 2019; Liang *et al.*, 2020). They are a family of widely distributed iron-containing non-heme fatty acid dioxygenases that catalyze the regio- and stereo-specific peroxidation of polyunsaturated fatty acids to produce fatty acid hydroperoxides that are funneled into several biosynthetic pathways that generate stress signal and structural molecules including lignin, jasmonates, and other oxylipins (Shafi *et al.*, 2014; Sharma and Laxmi, 2016; Hayward *et al.*, 2017). Jasmonates, a family of phytohormones with roles in chilling tolerance, are downstream products of (13*S*)-hydroperoxy-(9*Z*,11*E*,15)-octadecatrienoic acid dehydration and oxidation that is derived from 13-LOX-catalysed oxygenation of C₁₃ of α -linoleic acid [Sharma and Laxmi (2016) and references therein]. Increased LOX enzyme activities and/or LOX-encoding gene expression have been reported to mediate tolerance to different forms of environmental stresses, including mechanical injury/wounding, drought, high salinity, heat as well as cold stress (Delaplace *et al.*, 2009; Lim *et al.*, 2015; Upadhyay and Mattoo, 2018; Upadhyay *et al.*, 2019).

Mung bean (*Vigna radiata* (L.) R. Wilczek) is a chilling sensitive legume of tropical and subtropical regions with chilling susceptibility among varieties linked to the differential expression of chilling regulated genes (Chen *et al.*, 2017). Chilling injury in mung bean seedlings include photooxidative degradation of chlorophylls and carotenoids (Guye *et al.*, 1987), ultrastructural damages to photosynthetic apparatus and chlorosis (Yang *et al.*, 2005; Chen *et al.*, 2017), increased peroxidation of lipids and loss of biomembrane integrity (Chang *et al.*, 2001; Saleh, 2007; Chen *et al.*, 2017), decrease in relative growth rate, maximum photochemical efficiency of PSII, and free radical scavenging activity as well as H₂O₂ accumulation and disruption of redox homeostasis (Chen *et al.*, 2017). Osmolyte (soluble carbohydrates and proline) contents were also reported to be lowered in chilling-stressed mung bean seedlings (Saleh, 2007).

Phytohormones are active in plant responses and tolerance against chilling stress. Abscisic acid, cytokinins, ethylene, and jasmonates are crucial phytohormones with active roles in cold acclimation/plant tolerance to chilling (Saleh, 2007; Yadav, 2010; Lukatkin *et al.*, 2012; Sharma and Laxmi, 2016; Upadhyay *et al.*, 2019; Ritonga and Chen, 2020). Strigolactones are increasingly being found to take active roles in the mediation of abiotic stress tolerance in plants (Mostofa *et al.*, 2018). For instance, strigolactone supplementation ameliorated the growth-limiting effects and

drought-sensitive phenotype of strigolactone-deficient mutants while also enhancing drought tolerance in wild-type plants but failed to ameliorate drought sensitivity in strigolactone-signaling mutants (Ha *et al.*, 2014). Strigolactones also mediate a nitric oxide and H₂O₂-dependent, but ABA-independent, regulation of stomatal closure under salinity and water stress with strigolactone biosynthetic genes induced in *Arabidopsis thaliana* under both forms of abiotic stress (Lv *et al.*, 2018). Furthermore, treatment with GR24 improved plant growth, leaf pigment content, SOD and peroxidase activities, gas exchange, and photosystem II quantum yield while significantly decreasing non-photochemical quenching and peroxidation of lipids in rapeseed (*Brassica napus* L.) seedlings subjected to salinity stress (Ma *et al.*, 2017b). With respect to extreme temperatures, strigolactones alleviated heat-induced inhibition of seed germination by modulating endogenous ABA and gibberellin levels (Toh *et al.*, 2011).

Although strigolactone actions have been demonstrated in the amelioration of several forms of abiotic stress in several studies, they are yet to be evaluated in plants under chilling stress. Our objective in this current study was, therefore, to examine how strigolactone (GR24) treatment influence PSII photosynthetic activity, ROS (O₂⁻ and H₂O₂) accumulation and SOD-mediated ROS scavenging, lipoxygenase activity, phenylpropanoid pathway enzyme activities, and osmolyte accumulation in mung bean under chilling stress.

4.2. Materials and methods

4.2.1. Plant material and seedling growth conditions

Healthy mung bean [*Vigna radiata* (L.) R. Wilczek] seeds were selected, rinsed with distilled water three times, and soaked for 6 h in distilled water. After imbibition, the seeds were rinsed again, transferred into three seedling trays with vermiculite as a potting medium, and irrigated with distilled water. The setup was incubated in a growth chamber at ~23 °C to germinate. The resulting seedlings were raised in a growth room with ambient temperature set at 23 ± 2 °C and 75 % humidity, illuminated with white light (LED, PAR ~120 μmol m⁻² s⁻¹) in a 16/8-h light/dark period respectively, and watered every three days.

4.2.2. Strigolactone and chilling treatments

Ten days after germination, the seedling trays were assigned and treated as follows: control seedling tray was irrigated with distilled water with acetone (500 μL in 1 L) while the other two trays were assigned to GR24 treatments of 1 μM and 10 μM each. All GR24 solutions were prepared from a 20 μM stock (6 mg of GR24 dissolved in 500 μL acetone and diluted in 1 L of distilled water). The seedlings were incubated for 24 h after treatment and then transferred to a

Conviron (Controlled Environment Ltd, Winnipeg, Canada) where they were subjected to chilling stress at 7 ± 2 °C under 16/8-h light/dark photoperiod respectively for 3 days.

4.2.3. Chlorophyll fluorescence index

Chlorophyll a fluorescence (ChlF) measurements were carried out 24 h after strigolactone treatments. Data was collected just before chilling treatment (PreCS) and after three consecutive days of chilling treatment (CS). All seedlings were dark-adapted for 1 h, and ChlF measurements were carried out on the adaxial lamina of sampled leaves using a portable chlorophyll fluorometer (OS-30p; Opti-Sciences, Inc., NH, USA) at maximum saturating flash (actinic light intensity; $3500 \mu\text{mol photons m}^{-2} \text{s}^{-1}$) for 1 s in the dark. Fluorescence indexes were computed as described by Strasser *et al.* (2010).

4.2.4. Physiological and biochemical assessment of seedlings

After chilling treatment, sample leaves were harvested and assessed for the following parameters.

4.2.4.1. Estimation of leaf relative water content

Leaf relative water content (RWC) was determined, as described by González and González-Vilar (2001). Whole leaves were used instead of leaf discs. Sampled leaves were immediately weighed to obtain their fresh weight (FW) and incubated in distilled water in pill vials for 4 h in the dark at low temperature (~ 5 °C). After drying surface-adhering water with paper towels, the turgid weights (TW) of the leaves were obtained, and they were dried in an oven at 75 °C for 48 h. Their dry weights (DW) were measured afterward, and the relative water content of the leaves was calculated using the following formula:

$$RWC (\%) = \frac{FW - DW}{TW - DW} \times 100$$

4.2.4.2. Histochemical detection and quantification of reactive oxygen species

4.2.4.2.1. Superoxide radical

Excised leaves were immersed, with their abaxial side up, in a staining solution that contains 0.05% (w/v) nitroblue tetrazolium (NBT), 10 mM sodium azide, and 50 mM potassium phosphate buffer (pH 6.4) in Petri dishes. The leaves were vacuum infiltrated in a vacuum chamber in three cycles of building up a vacuum at 150 mbar for 1 min with a gentle release of the vacuum. After complete infiltration of leaves, they were left in the staining solution for 15 min and then incubated for 20 min under light and ambient temperature to allow for blue formazan development. The stained

leaves were then washed in 95 % (v/v) ethanol with heating to remove chlorophyll and digitally photographed.

Superoxide radical content was determined by extracting and quantifying the formazan formed in NBT-stained leaves from above, as described by Grellet Bournonville and Díaz-Ricci (2011). Each NBT-stained leaf was dried in an oven at 50 °C, and their dry weight was determined. Blue formazan was selectively extracted using 1.2 mL of extraction mixture [2 M KOH: chloroform (1:1, v/v)] by homogenization in a bead beater. The homogenate was mixed with another 2 mL of the extraction mixture in test tubes, vortexed, and centrifuged at 10000 g. Sample extracts were kept away from exposure to light and maintained on ice. A portion of the formazan-containing chloroform phase (800 µL) was collected and then completely dried under a gaseous nitrogen flush. The residue obtained was dissolved in 1.2 mL of DMSO: 2 M KOH (1.167: 1, v/v) by sonication, and the absorbance at 630 nm was immediately read in a spectrophotometer. Pure formazan was obtained from the photochemical reaction of a mixture containing 27 µM riboflavin, 17 mM methionine, and 1 mg/mL of NBT in 50 mM potassium phosphate buffer (pH 7.8) and used as a standard to prepare a calibration curve. Formazan content of NBT-stained leaves was expressed in micrograms per gram dry weight ($\mu\text{g g}^{-1}$ DW).

4.2.4.2.2. *Hydrogen peroxide*

Endogenous H_2O_2 was visualized by 3'3-diaminobenzidine (DAB) staining, as described by Czarnecki *et al.* (2013). Sampled leaves were placed in DAB solution (1 mg/mL at pH 3.8) and incubated for 8 h at room temperature under light. After DAB treatment, the leaves were carefully transferred into boiling 95 % (v/v) ethanol for 10 min to remove chlorophyll pigments and decolorize the leaves, leaving behind the deep brown polymerization product of DAB reaction with H_2O_2 . After cooling, the stained leaves were transferred into ethanol: glycerol solution (4:1 v/v) and preserved at 4 °C until digitally photographed.

The H_2O_2 content of samples was estimated using a potassium iodide based method (Junglee *et al.*, 2014). Briefly, excised leaves were weighed and directly homogenized with 1 mL of assay solution containing 0.5 mL 10 mM potassium phosphate buffer solution [with 0.1 % (w:v) trichloroacetic acid (TCA); pH 5.8] and 0.5 mL KI (1 M) for 10 min. A control was prepared with the KI solution replaced with distilled water for tissue coloration background control, and samples were protected from exposure to light. All homogenates were centrifuged at 10000 g for 20 min and incubated for another 25 min at ambient temperature. The supernatants' absorbance was taken at 350 nm, and the H_2O_2 content determined from a calibration curve prepared using H_2O_2 in 0.1 % TCA as standard.

4.2.4.3. *Quantification of total soluble sugars*

The total soluble sugar (TSS) content of samples was determined using the phenol-sulphuric acid method described by Chow and Landhäusser (2004). Briefly, sampled leaves were weighed, homogenized with 1 mL of 80% ethanol, centrifuged at 12000 g for 10 min, and the supernatants collected in clean tubes. Each sample was extracted a second time as above; the supernatants were collected, pooled, and partitioned for TSS and radical scavenging assay. One mL of the ethanolic extract was dried under a stream of nitrogen; 500 μ L of distilled water was added to the residue and dissolved by sonication. To each dissolved residue, 1 mL of 2% phenol solution and 2.5 mL of 96 % (v/v) sulphuric acid was added and mixed gently. After 30 min of color development in the dark and cooling, the absorbance was measured at 490 nm against a blank (assay mixture with extract replaced with distilled water). The total soluble sugar content was determined from a standard curve prepared using a mixture of glucose:fructose:galactose (GFG) and expressed in milligram soluble sugar per gram fresh weight (mg SS g⁻¹ FW).

4.2.4.4. *Estimation of lipid peroxidation*

The accumulation of malondialdehyde (MDA) due to the peroxidation of lipids was determined, according to Heath and Packer (1968). Weighed leaves were homogenized in 3 mL of 0.1 % TCA and centrifuged at 10000 g for 20 min. One mL of the supernatant was mixed with 2 mL of 20 % TCA and 2 mL of 0.5 % thiobarbituric acid; the mixture was incubated at 95 °C for 30 min and then cooled on ice. Absorbance was taken at 532 nm and 600 nm against a reagent blank, and MDA content was calculated using the extinction coefficient of MDA ($\epsilon = 155 \text{ mM}^{-1} \text{ cm}^{-1}$) and expressed in nanomoles per gram fresh weight (nmol g⁻¹ FW).

4.2.4.5. *Estimation of radical scavenging activity*

The radical scavenging activity of mung bean seedlings was determined by a slightly modified Brand-Williams *et al.* (1995) method using 2,2-diphenyl-1-picrylhydrazyl (DPPH). Ethanolic extract (100 μ L) from above (TSS assay) was added mixed with 1 mL of 120 μ M DPPH solution (prepared in absolute ethanol) and incubated for 30 min. The absorbance at 517 nm was read in a spectrophotometer with a mixture of 1 mL absolute ethanol and 100 μ L 80% ethanol serving as blank. A mixture of 100 μ L extraction solution and 1 mL DPPH solution was used as a control. The DPPH scavenging activity (%) was estimated as follow;

$$\text{DPPH scavenging activity (\%)} = \frac{A_o - A_s}{A_o} \times 100$$

where A_o is the absorption of the control and A_s is the absorption of the extract solution.

4.2.4.6. Total antioxidant capacity and total phenolic content

Freeze-dried samples were weighed (20 mg) and homogenized with 1 mL of distilled water, centrifuged at 15000 g at 4 °C for 30 min. Each supernatant was diluted, i.e., 100 µL to 500 µL, and used for total antioxidant capacity and total phenolic content assays. The total antioxidant capacity of the supernatants was determined, as described by Prieto *et al.* (1999). Briefly, 950 µL of reagent solution (0.6 M H₂SO₄, 28 mM sodium phosphate, 4 mM ammonium molybdate mixture) was mixed with 50 µL diluted aqueous extract in a tube and incubated at 95 °C for 90 min. The absorbance was read at 695 nm after cooling against a blank. An incubated tube containing the reagent solution and 50 µL of distilled water in place of the extract was used as the blank. Total antioxidant capacity was determined from a standard curve prepared using ascorbic acid and expressed as milligram ascorbic acid equivalent per gram dry weight (mg AAE g⁻¹ DW).

Total phenolic content was determined by the Folin–Ciocalteu reagent-based method described by Panuccio *et al.* (2014) with slight modifications. To 2.5 mL of Folin–Ciocalteu reagent (1:10 diluted with distilled water), 100 µL of aqueous extract was added and followed by 2 mL of saturated sodium carbonate solution (~75 gL⁻¹). The tubes were shaken to mix the reaction mixture properly and allowed to stand for 2 h at room temperature before taking the absorbance at 760 nm. Gallic acid was used as a reference standard, and the results expressed as milligram gallic acid equivalents per gram dry weight (mg GAE g⁻¹ DW).

4.2.4.7. Estimation of proline content

Proline content was estimated according to the protocol in Ábrahám *et al.* (2010). Weighed freeze-dried samples (20 mg) were homogenized in 1 mL of 3 % sulfosalicylic acid and centrifuged at 12000 g for 10 min. To 250 µL of the supernatant in a tube, 200 µL of 3 % sulfosalicylic acid, 400 µL glacial acetic acid, and 400 µL acidic ninhydrin were added and incubated at 95 °C for 60 min. The reaction was terminated on ice, and the mixtures were extracted with 2 mL toluene, vortexed, and the organic phase was allowed to separate for 5 min. The absorbance of the chromophore-containing toluene phase was measured at 520 nm using toluene as blank. Proline concentration was determined from a standard concentration curve and expressed in milligram per gram dry weight (mg g⁻¹ DW).

4.2.4.8. Enzyme activity assays

Superoxide dismutase (SOD) activity was estimated by the nitroblue tetrazolium (NBT) method described by Beauchamp and Fridovich (1971), with slight modifications. Briefly, each weighed

leaf was homogenized in 2 mL extraction solution [0.1 M phosphate buffer (pH 7.0) with 0.1 mM EDTA], and the homogenate was centrifuged at 15000 g for 20 min at 4 °C. The 3 mL assay reaction mixture contained 100 µL of 200 mM methionine, 100 µL of 2.25 mM NBT, 100 µL of 3 mM EDTA, 1500 µL of 100 mM potassium phosphate buffer, 1000 µL of distilled water, and 100 µL of enzyme extract. The reaction was initiated by adding 100 µL of 1 mM riboflavin, and the samples were illuminated under white light (LED) for 15 min. Duplicate tubes with the same reaction mixture but without enzyme extract, which developed maximum color, were used as a background control. Absorbance was measured at 560 nm against a blank of a non-irradiated tube with the reaction mixture that did not develop color. One unit of SOD activity was defined as the enzyme quantity that inhibited the photoreduction of NBT by 50 % compared to tubes lacking enzymes and expressed as SOD units per gram fresh weight ($\text{U g}^{-1} \text{FW}$).

Lipoxygenase activity was assayed spectrophotometrically using the method of Gardner (2001). Sampled leaves were weighed, and each homogenized in 990 µL of extraction buffer [50 mM Tris-Cl (pH 7.0) with 1 mM EDTA and 1% PVP] and 10 µL of 1 mM phenylmethylsulfonyl fluoride (prepared in acetone). The homogenate was centrifuged at 30000 g for 30 min at 4 °C. The assay was carried out with an assay buffer [0.1 M Tris-Cl (pH 7.5)] and substrate solution (10 mM linoleic acid solution prepared by emulsifying 28 mg linoleic acid and 28 mg Tween 20 in 3 mL of distilled water, clarified with drops of 1N NaOH, adjusted to pH 9.0 and made up to 10 mL with distilled water). Enzyme extract (20 µL) was mixed with 970 µL of assay buffer in a cuvette, and 10 µL of substrate solution was added to initiate the reaction. The increase in absorbance at 234 nm due to hydroperoxide formation was recorded for 300 s, and the amount of hydroperoxide produced per min was calculated using the molar extinction coefficient of $26800 \text{ cm}^{-1} \text{ mol}^{-1} \text{ L}$. Lipoxygenase activity was expressed as the specific activity of the enzyme in µmoles of hydroperoxide formed per minute per milligram of protein ($\mu\text{mol min}^{-1} \text{ mg}^{-1} \text{ protein}$).

Phenylalanine ammonia-lyase and tyrosine ammonia-lyase activities were quantified by monitoring the production of *trans*-cinnamic (*t*-CA) acid and *p*-coumaric acid (*p*-CA), respectively (Rösler *et al.*, 1997; Cass *et al.*, 2015). Weighed samples were homogenized in 1 mL extraction buffer (100 mM sodium borate pH 8.8 with 2mM EDTA and 5 mM 2-mercaptoethanol) and centrifuged at 12000 g for 30 min. The PAL assay mixture was 1 mL of substrate solution containing 61 mM L-phenylalanine in 30 mM sodium borate buffer (pH 8.8) mixed with 100 µL of extract and incubated at 37 °C in a water bath for 60 min. The reaction was terminated by adding 500 µL of 1 M TCA, and the absorbance at 290 nm read in a spectrophotometer. Plant extract incubated in buffer without substrate was used as the blank. For the TAL assay, the 1 mL substrate

solution contained 1.9 mM L-tyrosine in 30 mM sodium borate buffer (pH 8.8) mixed with 100 μ L of the extract while the incubation temperature and blanking protocol were the same as that of PAL assay but with absorbance read at 310 nm. The molar extinction coefficients of *trans*-cinnamic acid and *p*-coumaric acid ($9000 \text{ M}^{-1} \text{ cm}^{-1}$ and $10000 \text{ M}^{-1} \text{ cm}^{-1}$, respectively) were used to calculate the specific enzyme activities and expressed as nanomoles of product formed per minute per milligram of protein ($\text{nmol min}^{-1} \text{ mg}^{-1}$ protein). The protein concentration of all enzyme extracts was determined by the Bradford method (Bradford, 1976).

4.2.5. Statistical analysis

The data obtained were analyzed by analysis of variance (ANOVA) with treatments (0, 1, and 10 μ M GR24) as the grouping factor, and *post hoc* analysis was executed using Duncan's Multiple Range Test to compare means of each response variable. Confidence levels were set at $p \leq 0.01$ and 0.05 as indicated, and standard error (SE) was calculated for the means. All statistical analyses were performed using SPSS for Windows v26.0 (IBM Corp., Armonk, NY, USA) and Microsoft Excel 2016 (Microsoft Corporation, Redmond, Washington, USA).

4.3. Results

4.3.1. GR24 limits chilling-induced inhibition of PSII function

A consequence of chilling stress in plants is the disruption of absorbed light energy conversion for photochemical reactions due to the inhibition of photosystem functions (Lukatkin *et al.*, 2012). In this study, PSII activity was adversely altered in mung bean seedlings under chilling stress. The maximum photochemical efficiency of PSII (ϕ_{P_o}), the efficiency and the quantum yield of electron transport beyond Q_A^- (ψ_{E_o} and ϕ_{E_o} respectively) decreased from their pre-chilling PreCS) values after chilling treatment (Fig. 4.1A-D). However, chilling-induced decrease in PSII photochemical parameters was limited in GR24-treated seedlings. While control seedlings showed a significant 19 % reduction in ϕ_{P_o} ($p < 0.01$), it was limited to just 9 % in all GR24-treated seedlings (1 and 10 μ M) (Fig. 4.1A). Similarly, ψ_{E_o} was significantly lowered ($p < 0.01$) by 13 % in control seedlings but the 9 % decrease in ψ_{E_o} in seedlings that received 1 μ M GR24 was only statistically significant at $p < 0.05$, while the 4 % decrease in ψ_{E_o} in seedlings treated with 10 μ M GR24 was not significant even at $p \leq 0.05$ (Fig. 4.1B). While a 30 % decrease in ϕ_{E_o} (significant at $p < 0.01$) was observed in control seedlings, a dosage-dependent inhibition of chilling-induced decrease in ϕ_{E_o} (17 % and 12 % decrease in ϕ_{E_o} with 1 and 10 μ M GR24 respectively) were observed in GR24-treated seedlings although these were still significantly different ($p < 0.01$) from their PreCS values (Fig. 4.1C). Contrary to the above, chilling stress increased the quantum yield of energy (heat) dissipation (ϕ_{D_o}) (Fig. 4.1D) with control seedlings showing a significant ($p < 0.01$) 44 %

increase in φ_{Do} while all GR24 treatments limited chilling-induced increase in φ_{Do} to 26 % although these were also significant at $p < 0.01$. Taken together, these show that GR24 treatments diminished the photoinhibition of PSII functions that usually accompany chilling stress in mung bean seedlings.

4.3.2. GR24 inhibits O_2^- and H_2O_2 accumulation in chilling-stressed mung bean seedlings

Histochemical detection of O_2^- by NBT staining and H_2O_2 accumulation by DAB staining revealed a deeper formazan and DAB polymerization product formation in the leaves of control seedlings compared to those of GR24-treated seedlings (Fig. 4.2A). Biochemical quantification of formazan in NBT-stained leaves showed that O_2^- content in seedlings treated with 1 μ M GR24 was not significantly different from that of the control though it was lower (Fig. 4.2B) while the formazan recovered from the NBT-stained leaves of seedlings treated with 10 μ M GR24 was significantly lower ($p < 0.01$) than that of the control. On the other hand, H_2O_2 content in the leaves of all GR24-treated seedlings was substantially lower ($p < 0.01$) than the control (Fig. 4.2C).

4.3.3. Phenolic content and radical scavenging activities are diminished in GR24-treated mung bean seedlings under chilling stress

Since chilling stress induces increased ROS accumulation (Hussain *et al.*, 2018), we investigated the effects of GR24 treatments on phenolic contents and antioxidant capacities of our test plant under chilling conditions. The accumulation of phenolics in response to GR24 treatments (Fig. 4.3A) was significantly diminished ($p < 0.01$) in mung bean seedlings that received 10 μ M GR24 while the phenolic content of seedlings treated with 1 μ M GR24 was not significantly different from the control seedlings. Following an almost similar trend, total antioxidant capacity (Fig. 4.3B), assessed by the ability to reduce Mo(IV) to Mo(V) and subsequently form a phosphomolybdate complex, was lower in seedlings treated with 10 μ M GR24 compared to the control. However, this was not statistically significant even at $p < 0.05$. Radical scavenging activity determined by the ability of sample extracts to scavenge the stable DPPH free radical was significantly diminished ($p < 0.05$) by 10 μ M GR24 treatment compared to the control (Fig. 4.3C). At a lower concentration (1 μ M), GR24 treatment also decreased DPPH scavenging activity but was not significantly different from the control. Surprisingly, despite showing lower radical scavenging activities and similar antioxidant capacities as the control seedlings, all GR24-treated seedlings (1 and 10 μ M) had significantly reduced ($p < 0.01$) peroxidation of lipids as revealed by their lower MDA contents compared to the control (Fig. 4.3D).

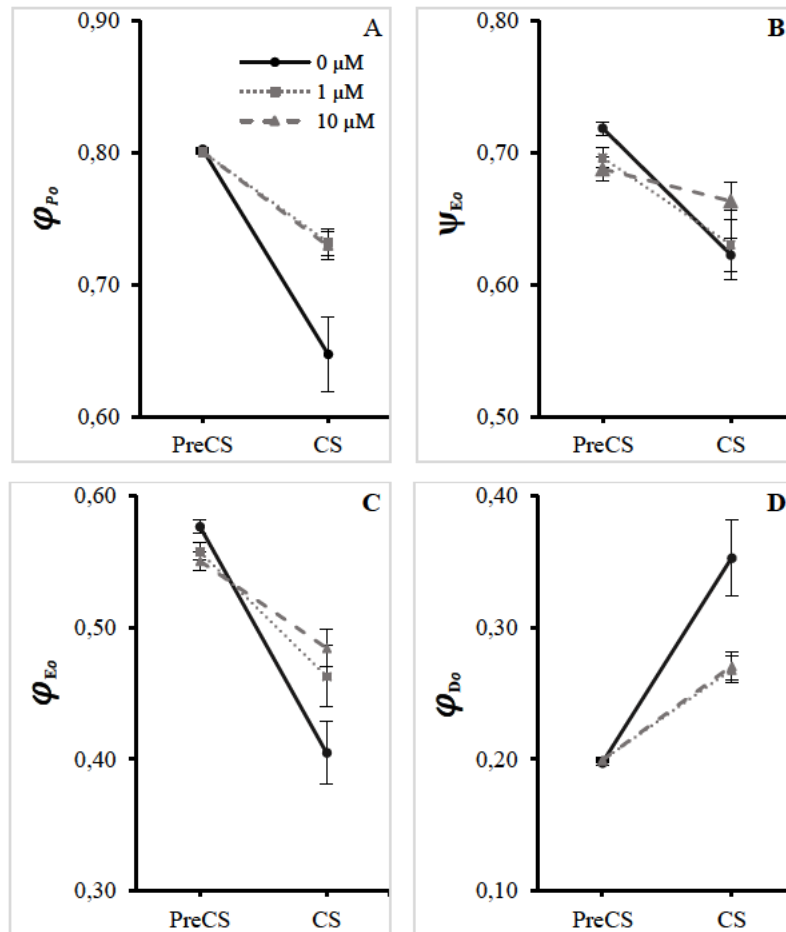


Figure 4.1. Photosystem II quantum yields and efficiencies in GR24-treated mung bean [*Vigna radiata* (L.) R. Wilczek] seedlings before chilling stress (PreCS) and after chilling stress (CS). φ_{Po} , the maximum quantum yield of PSII photochemistry (A); ψ_{Eo} , the efficiency of electron transport beyond Q_A^- per trapped exciton (B); φ_{Eo} , the quantum yield of electron transport beyond Q_A (C); φ_{Do} , the quantum yield of energy (heat) dissipation (D). Data represent means, and the bars depict standard error ($n = 10$) for each treatment.

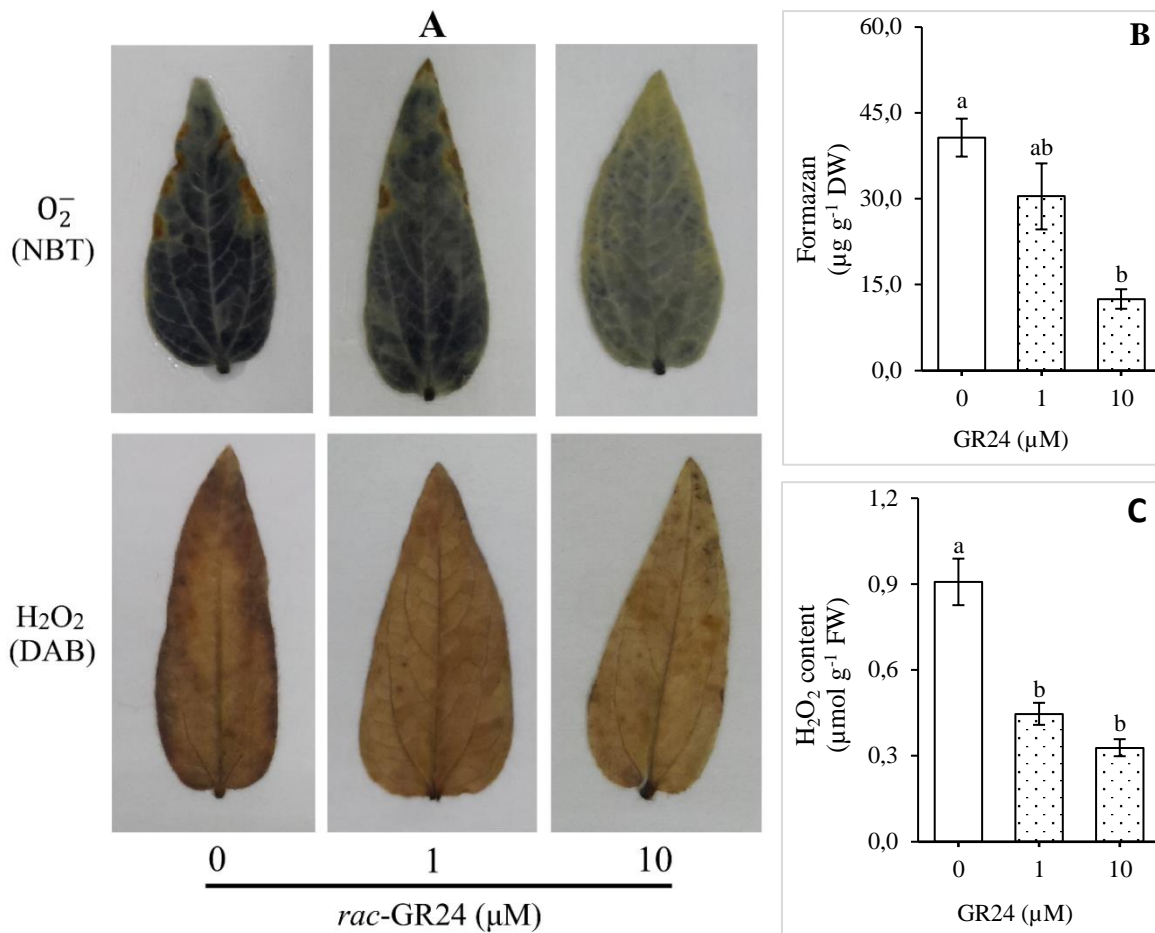


Figure 4.2. Accumulation of superoxide anion (O_2^-) and hydrogen peroxide (H_2O_2) in mung bean [*Vigna radiata* (L.) R. Wilczek] seedlings under chilling conditions and GR24 treatments. (A) Nitroblue tetrazolium (NBT) staining for O_2^- and diaminobenzidine (DAB) staining for H_2O_2 in mung bean leaves. Effect of GR24 treatments on formazan formation in NBT-stained leaves (B) and H_2O_2 content (C) of chilling-stressed mung bean seedlings. Data shown are the means \pm standard error (SE), $n = 4$. Different letters indicate significant differences among treatments according to Duncan's Multiple Range Test with confidence level set at $p < 0.01$.

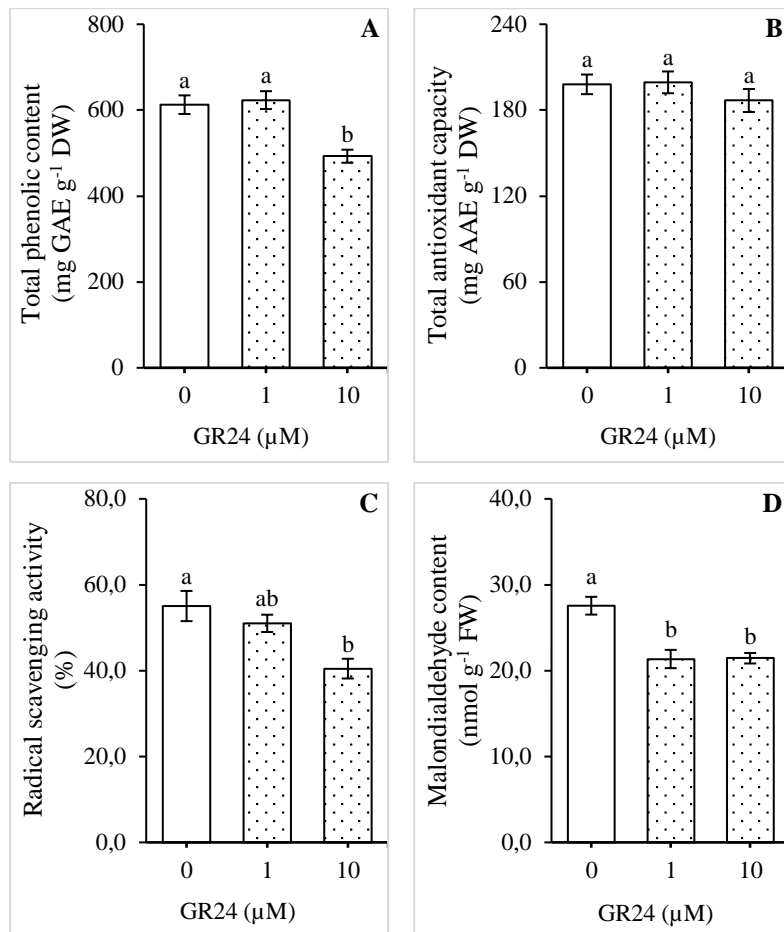


Figure 4.3. The total phenolic contents (**A**), antioxidant capacities (**B**), radical (DPPH) scavenging activities (**C**), and lipid peroxidation levels (**D**) in mung bean [*Vigna radiata* (L.) R. Wilczek] seedlings treated with different doses of GR24 and subjected to chilling stress. Data represent means and standard error of $n = 5$, and significant differences among treatment group means at $p < 0.01$ according to Duncan's Multiple Range Test are indicated by different letters.

4.3.4. GR24 counteracts chilling stress-induced disruption of leaf water status and augment osmolyte accumulation

The relative water content of leaf tissues in seedlings under 1 and 10 μM GR24 treatments was significantly higher ($p < 0.01$) than in the control seedlings (Fig. 4.4A). This was expected since we noticed, by physical observation of seedlings during chilling treatment, severe wilting in the control seedlings compared to mild wilting in GR24-treated seedlings. Osmolyte accumulation (proline and soluble sugars) was significantly improved by GR24 treatment. While proline content was only considerably improved in seedlings that were supplemented with 1 μM GR24 (Fig. 4.4B), seedling soluble sugar content was significantly higher ($p < 0.01$) under 1 and 10 μM GR24 treatments in comparison to the control (Fig. 4.4C).

4.3.5. SOD, LOX, PAL, and TAL activities are stimulated in GR24-treated mung bean seedlings under chilling stress

The maintenance of ROS homeostasis is vital for plant tolerance to chilling-induced oxidative stress, and SOD features actively in this role by detoxifying O_2^- . Mung bean seedlings that received GR24 treatments showed significant ($p < 0.01$) and higher SOD activities than the control seedlings. However, at 10 μM GR24, SOD activity was lower and significantly different ($p < 0.05$) from that of seedlings that received 1 μM GR24 (Fig. 4.5A). Compared to the control, SOD activity in seedlings treated with 10 μM GR24 was significantly higher ($p < 0.01$). With LOX activities, we noted a concentration-dependent increase in enzyme activity from 1 to 10 μM GR24. Although with 1 μM GR24 treatment, LOX activity was higher but not statistically different ($p < 0.05$) from the control, seedlings that received 10 μM GR24 had a 3 fold higher and significantly different ($p < 0.01$) LOX activity compared to the control (Fig. 4.5B). On the other hand, GR24 only significantly induce ($p < 0.01$) the phenylpropanoid pathway enzymes, PAL and TAL, when applied at 10 μM (Fig. 4.5C-D). The activities of PAL and TAL in seedlings supplied with 1 μM GR24 were not significantly different from the controls even at $p \leq 0.05$.

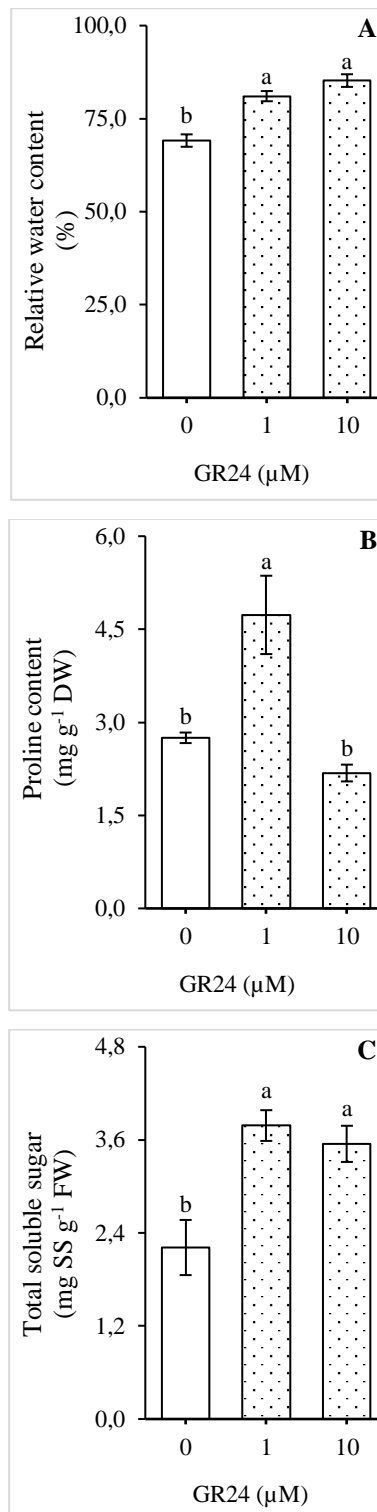


Figure 4.4. Effects of GR24 treatments on relative water content (A), proline (B), and soluble sugar accumulation (C) in mung bean [*Vigna radiata* (L.) R. Wilczek] seedlings exposed to chilling stress. Data are means \pm standard error, $n = 5$. Different letters indicate significant differences among treatments according to Duncan's Multiple Range Test with confidence level set at $p < 0.01$.

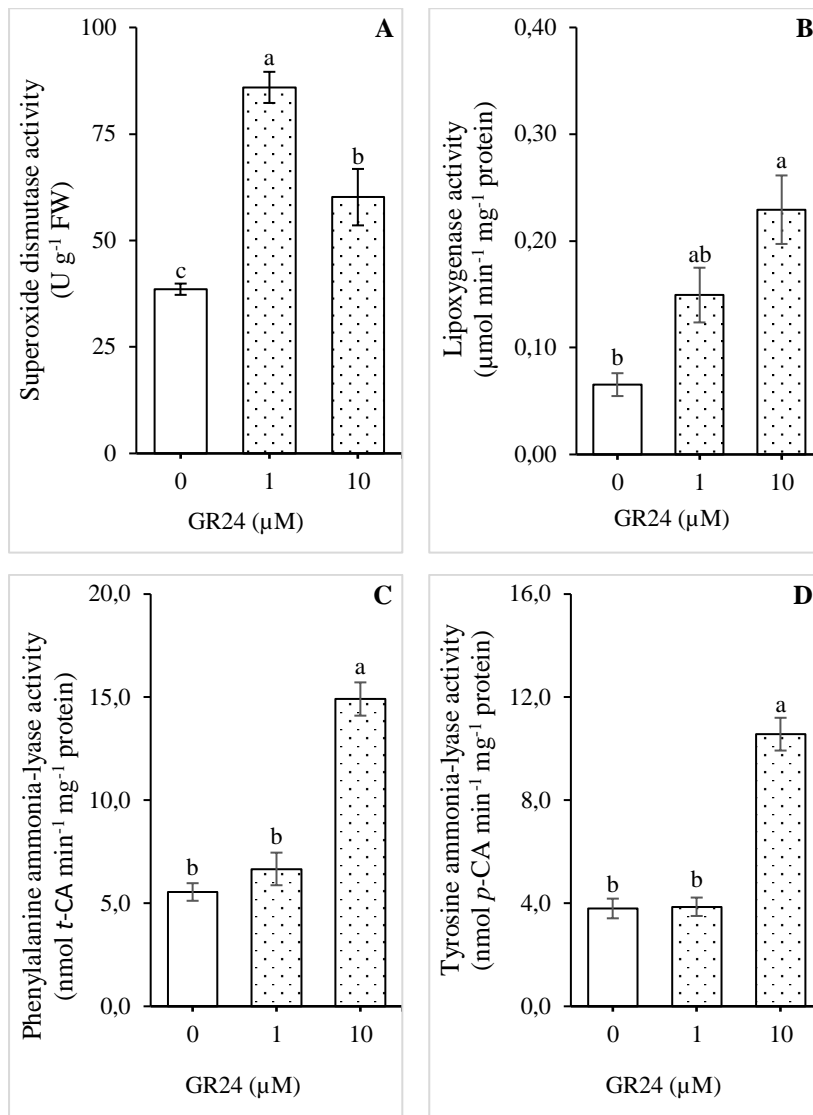


Figure 4.5. The effect of GR24 application on superoxide dismutase (A), lipoxygenase (B), phenylalanine ammonia-lyase (C), and tyrosine ammonia-lyase (D) activities in mung bean [*Vigna radiata* (L.) R. Wilczek] seedlings exposed to chilling stress. Data are presented as means and standard error (n = 4), and significant differences among treatment group mean at $p < 0.01$, according to Duncan's Multiple Range Test, are indicated by different letters.

4.4. Discussion

Chilling stress mediates severe damage to the cell and organelle ultrastructure (Chang *et al.*, 2001; Saleh, 2007; Chen *et al.*, 2017), thus contributing to the disruption of cell ROS balance. The gel-solid state of biomembranes at chilling temperatures negatively affect membrane-bound enzymes and their activities by altering their protein conformation and structure (Liang *et al.*, 2020). Since the photosynthetic and respiratory electron transport proteins are membrane-bound, chilling-induced changes in biomembrane physical properties affect these proteins' activities. Disruptions and the uncoupling of the photosynthetic and respiratory electron transport chain induced by low ambient temperatures trigger ROS production due to the loss of electrons with high-energy state to molecular oxygen (Suzuki and Mittler, 2006), thus triggering photooxidation and photoinhibition, which severely limits PSI and PSII functions. Our results indicate that GR24 brokered a limitation on O_2^- and H_2O_2 accumulation that appeared to be achieved via mechanisms other than phenolics-dependent antioxidant systems since the total antioxidant capacities of GR24-treated seedlings were not different from those of the control seedlings (Fig. 4.3B). Also supporting this view is the reduced phenolic content (Fig. 4.3A) and radical scavenging activities (Fig. 4.3C), and the enhanced soluble sugar contents (Fig. 4.4C) and enzyme (SOD)-mediated O_2^- scavenging activity in GR24-treated seedlings (Fig. 4.5A). A notable implication of the reduced accumulation of O_2^- and H_2O_2 in GR24-treated seedlings is the minimization of the deleterious effects of chilling stress on the photosystems/photosynthetic activities and the reduced peroxidation of lipids. A similar improvement in PSII quantum yield with an attendant decrease in non-photochemical quenching and enhanced SOD activity was mediated by GR24 application in *Brassica napus* under salinity stress (Ma *et al.*, 2017b).

The accumulation of osmolytes such as soluble sugars and proline is a crucial adaptive response in plants under several forms of abiotic stress, including chilling stress (Hodges *et al.*, 1997; Hoque *et al.*, 2008; Lukatkin *et al.*, 2012; Tarkowski and Van den Ende, 2015; Hussain *et al.*, 2018). These compounds, which are known as compatible solutes, enable plants to deal with stress-induced dehydration and the maintenance of water balance by enhancing osmotic adjustment capacities of cells and tissues; mediate the stabilization of biomolecules such as proteins and cellular structures such as biological membranes via their molecular chaperone functions; and also contribute to ROS scavenging as soluble antioxidants (Hoque *et al.*, 2008; Liang *et al.*, 2013; Tarkowski and Van den Ende, 2015). In this study, the higher soluble sugar and proline contents in GR24-treated mung bean seedlings would have contributed to enhancing water retention and maintaining tissue water balance, thus reducing chilling-induced water deficit and wilting. Our observations here with GR24-induced enhancement of leaf water status in seedlings under chilling stress are consistent

with the documented involvement of strigolactones in regulating physiological processes that are closely linked with the maintenance of tissue water status. For instance, strigolactone (*max*) mutants exhibit increased leaf water loss under drought conditions due to altered transpiration rate, and this was rescued by exogenous strigolactone supply (Ha *et al.*, 2014). Furthermore, the report that strigolactones mediate stomatal responses to abiotic stress, thus fostering stress acclimation by limiting water loss (Ha *et al.*, 2014; Lv *et al.*, 2018), supports our observations.

The role of LOX in chilling stress response is quite complicated. Since the proportion of unsaturated fatty acids of biomembranes is closely linked with membrane fluidity and chilling tolerance with increased lipid unsaturation translating to increased membrane fluidity and chilling tolerance (Lee *et al.*, 2005; Liang *et al.*, 2020), there are two implications of the observed GR24-induced increase in LOX activities in seedlings under chilling stress. One, LOX-mediated depletion of polyunsaturated fatty acids from biomembranes would decrease membrane fluidity and increase chilling sensitivity; two, LOX-dependent peroxidation of membrane lipids would increase the fluidity of biomembranes and thus enhance chilling tolerance. Both possibilities are not consistent with the data presented here since GR24-treated seedlings with higher LOX activities (Fig. 4.5B) showed better tolerance to chilling as evident from the limited impacts of chilling stress on PSII photochemical activities (Fig. 4.1) as well as lower levels of membrane lipid peroxidation (Fig. 4.3D). These apparent contradictions could be explained if the higher LOX activities were tailored towards the production of oxylipins, which function in stress (including chilling) signaling and tolerance (Upadhyay *et al.*, 2019). Jasmonates, a class of oxylipin phytohormones that are synthesized from LOX-derived hydroperoxides and with emerging roles in chilling stress, are accumulated under chilling conditions, and they elicit signal cascades that culminate in the activation of cold responses and chilling tolerance (Sharma and Laxmi, 2016; Upadhyay *et al.*, 2019). The GR24-mediated increase in LOX activities noted in this study (Fig. 4.5B) hints at crosstalk between strigolactones and jasmonates in cold tolerance mediation. This is, however, subject to further investigations.

Metabolites synthesized in the phenylpropanoid pathway such as anthocyanins, flavonoids, flavones, and other classes of polyphenols are essential for plant tolerance to chilling stress via their ROS scavenging and osmotic adjustment activities (Yildiztugay *et al.*, 2017; Wang *et al.*, 2019). Furthermore, the expression and activities of many phenylpropanoid pathway enzymes, including PAL and TAL, are stimulated under chilling conditions to promote phenolics accumulation and enhance chilling tolerance (Leyva *et al.*, 1995; Sharma *et al.*, 2019b; Zhou *et al.*, 2019). When supplied at 10 μ M, GR24 elicited about 3-fold higher PAL and TAL activities

compared to control seedlings (Fig. 4.5C-D), but unexpectedly, this did not translate into a higher phenolic content. Instead, seedlings under 10 μ M GR24 treatment showed the least phenolic content (Fig. 4.3A). A plausible explanation for this might be that since many phenylpropanoid pathway enzymes, including PAL and TAL, activities are transcriptionally stimulated under chilling conditions (Zhou *et al.*, 2019), the resulting phenolics accumulated in seedlings supplied with 10 μ M GR24 may have been actively channeled into phenolic sinks such as lignin biosynthesis to maintain phenolics homeostasis. Increased lignin biosynthesis and lignification of cell walls are major cell wall modification processes that are associated with cold acclimation (Le Gall *et al.*, 2015). Furthermore, it is documented that in the presence of an effective ROS scavenging system, which was mediated by the overexpression of antioxidant enzymes that ensured reduced ROS levels, lignin biosynthesis, and vascular bundle lignification were significantly enhanced under cold stress (Shafi *et al.*, 2014). The GR24-induced decrease in ROS accumulation and diminished phenolic contents reported here aligns with these previous reports. While our observations here clearly suggests a role for GR24 in the mediation of chilling tolerance via phenylpropanoid pathway enzyme activities, it also reveals the need for experimental inquiries into the roles of strigolactones in lignification under stress conditions in plants.

In conclusion, the data presented in this chapter demonstrate a role for GR24, and by extension strigolactones, in the mediation of chilling tolerance via enhanced SOD-dependent O_2^- scavenging, reduced H_2O_2 accumulation, maintenance of leaf water status by promoting proline (at low GR24 dose), and soluble sugar accumulation while also inducing lipoxygenase, PAL, and TAL activities. The involvement of lipoxygenase in GR24-induced chilling tolerance suggests an interaction between oxylipins, and possibly jasmonates, in GR24-mediated chilling tolerance, which is open to further investigation. On the other hand, the enhancement and involvement of PAL and TAL actions in GR24-mediated chilling responses bring the phenylpropanoid pathway under strigolactones in their emerging role as regulators of abiotic stress responses in plants.

Chapter 5

Strigolactone targets in the regulation of adventitious root formation

5.1. Introduction

Adventitious roots are post-embryonic roots that are distinguished from primary and lateral roots of the plant's main root system by the fact that they arise from non-root tissues such as leaves, stems, tubers, and corms. Depending on the plant species, they can be formed under normal developmental conditions, e.g., nodal or crown roots in grasses and cereals, or under stress conditions. Nutrient deprivation, heavy metal contamination of soil, drought, flooding, and wounding are some abiotic stress conditions that have been shown to induce adventitious root formation (ARF) [reviewed in Steffens and Rasmussen (2016)]. Under optimal growth ambience, adventitious roots furnish increased root surface area to volume ratio, thus facilitating an efficient exploration of soil and uptake of mineral nutrients and water. They also function in enhancing the anchorage of plants to soil/substrates and serve other root-associated roles such as reserves for food storage. Several external and endogenous factors may induce ARF in plants. In excision-induced ARF formation, exclusion from root-derived resources, wounding, and water stress responses are the major stimulating factors (da Costa *et al.*, 2013; Druege *et al.*, 2019). Excision-induced adventitious rooting is a vital phenomenon with ecological significance since it helps plants to cope with stresses such as flooding, drought, and injuries inflicted by herbivory, diseases, and pests as well as mechanical/physical damage (Steffens and Rasmussen, 2016). Adventitious rooting also furnishes economic advantages because of its applications in agriculture, forestry, and horticulture for mass clonal propagation of plants.

Phytohormones play pivotal roles in the regulation of ARF, an organogenic process that is tightly controlled largely to prevent the diversion and loss of scarce nutritional/metabolic resources for non-essential root formation. For instance, auxin and its attendant polar auxin transport (PAT) signal mechanisms feature prominently in the hormonal networks that control adventitious root initiation and formation (Xu *et al.*, 2005; Druege *et al.*, 2016; Guan *et al.*, 2019; Lin and Sauter, 2019). Other phytohormones with activities and associated regulatory circuits that are implicated in the steering of adventitious root development include ABA (Melo *et al.*, 2016), cytokinins (Druege *et al.*, 2016; Mao *et al.*, 2019), ethylene (da Costa *et al.*, 2013; Druege *et al.*, 2016; Druege *et al.*, 2019), gibberellins (Niu *et al.*, 2013; Kim and Cha, 2015), jasmonates (da Costa *et al.*, 2013; Lischweski *et al.*, 2015; Druege *et al.*, 2016; Druege *et al.*, 2019), salicylic acid (Yang *et al.*, 2013) and strigolactones (Rasmussen *et al.*, 2012a; 2012b). Generally, most existing experimental data

suggests strigolactones are inhibitors/negative regulators of adventitious rooting. Studies that employed exogenous strigolactones (mainly GR24), inhibitors, and strigolactone mutants reported the inhibitory effects of strigolactone treatments on adventitious rooting (Rasmussen *et al.*, 2012a; 2012b), which may be by limiting the stimulatory impact of auxin, and its PAT signaling, on ARF (Rasmussen *et al.*, 2012b).

Signal molecules such as NO and H₂O₂ are among major endogenous factors that feature prominently in the regulation of adventitious rooting (Li *et al.*, 2007; Li and Xue, 2010; Liao *et al.*, 2011; Wei *et al.*, 2018; Zhang *et al.*, 2019). The inductive influence of H₂O₂ in ARF under optimal ambience and in response to cuttings has been established by several experimental reports (Li *et al.*, 2007; Li *et al.*, 2009; Liao *et al.*, 2011) in many of which H₂O₂ acted in concert with phytohormones. In its interactions with phytohormones during signaling for ARF, H₂O₂ serves as an integrator or second messenger for hormonal signals in the tuning of ARF (Liao *et al.*, 2011; Yang *et al.*, 2013; Melo *et al.*, 2016) where inhibition of H₂O₂ activities was reported to have resulted in diminished or even complete loss of hormonal influences on ARF. The participation of H₂O₂ in the induction of ARF is partly attributed to the fact that H₂O₂ production and accumulation is one of the early responses of wounding (da Costa *et al.*, 2013).

Another vital endogenous component of most plant regulatory networks that may be involved in the control of ARF is the plasma membrane (PM) H⁺-ATPase. With its role as an electrogenic pump that actively moves protons out of cells, thus generating a transmembrane electrochemical gradient that powers and drives many proteins, PM H⁺-ATPases drives a plethora of diverse growth and developmental processes in plants [See review by Falhof *et al.* (2016)]. Because auxin gradient formation (and the attendant auxin flux, homeostasis, and PAT signal mechanisms) is central to adventitious root initiation and formation (Druege *et al.*, 2016; Lin and Sauter, 2019), PM H⁺-ATPase which establishes a lateral auxin gradient via its regulation and maintenance of proton gradient across the PM and apoplastic pH (Hohm *et al.*, 2014), may also influence ARF.

Although an array of diverse components participate in the regulation of adventitious root initiation, formation, and development, the molecular and biochemical mechanisms that underpin the signal transductions involved in these processes remain poorly understood. For instance, hormone and signal molecule crosstalk between strigolactones and H₂O₂ during ARF, if any, remains to be determined despite strong shreds of evidence for the role of both in cutting-induced ARF and the fact that strigolactones have been reported to recruit H₂O₂ to mediate other cellular processes like stomatal closure (Lv *et al.*, 2018). Similarly, though a very critical component of

plant physiological regulatory systems, PM H⁺-ATPase actions in ARF and the effects of strigolactones on its activities are yet to be described. This study was therefore carried out using GR24 to test the hypothesis that strigolactones modulates H₂O₂ content, hence H₂O₂ signaling, and PM H⁺-ATPase activity to regulate adventitious rooting in mung bean hypocotyl cuttings.

5.2. Materials and methods

5.2.1. Plant material and explant treatment

Seeds of mung bean [*Vigna radiata* (L.) R. Wilczek] were surface-sterilized for 5 min in 50% v/v NaOCl solution. The seeds were rinsed several times and soaked in distilled water for 6 h in the dark at ambient temperature. After soaking, the seeds were rinsed again and sown in plastic trays using moistened vermiculite as a potting medium. The setup was left to germinate and watered daily for 8 d with the growth room temperature set at 24 ± 1 °C and 16/8-h light/dark photoperiod (LED, PAR: ~120 μmol m⁻² s⁻¹).

5.2.2. Explant treatments

Seedlings with their primary roots excised were used as explants and maintained under the same growth temperature and photoperiod conditions for 24 h in beakers containing 50 mL of the different test solutions. The test solutions were as follows: distilled water (control, CTL); GR24 (1, 5, 10 μM); H₂O₂ (30, 50, 70 mM); fusicoccin (0.5, 1 μM); Na₃VO₄ (100, 300, 500 mM); 30 mM H₂O₂ + GR24 (SL: 1, 5, 10 μM); 100 mM Na₃VO₄ + H₂O₂ (H₂O₂: 30, 50, 70 mM); and 1 μM fusicoccin + 5 μM GR24. The explants were removed from the test solutions afterward, rinsed, and either used for H₂O₂ and plasma membrane H⁺-ATPase assays or placed in distilled water and maintained for another 5 d with the distilled water replaced daily, for the determination of the number of adventitious roots formed. All GR24 solutions were prepared from a 10 μM stock: 3 mg GR24 dissolved in 500 μL acetone and diluted in 1 L of distilled water.

5.2.3. Visualization of H₂O₂ by diaminobenzidine staining

After 24 h in test solutions, hypocotyl sections were cut from rinsed explants and use for the detection of H₂O₂ by 3,3'-diaminobenzidine (DAB) staining as described by Yang *et al.* (2013). In summary, the hypocotyl sections were treated with DAB solution (1 mg/mL at pH 3.8) and incubated for 8 h at 25 °C under light. DAB treatment was immediately followed by transfer of treated hypocotyl sections into boiling 95% ethanol for 10 min to decolorize the hypocotyls, leaving behind the deep brown polymerization product of the reaction between DAB and endogenous H₂O₂. After cooling, the hypocotyl sections were transferred into fresh ethanol solution and

preserved at 4 °C until digitally photographed on a LEICA MZ16 Stereomicroscope (Leica Microsystems, Wetzlar, Germany).

5.2.4. Quantification of endogenous H₂O₂ content

H₂O₂ content of treated samples was determined using a potassium iodide based method as described by Junglee *et al.* (2014). Briefly, excised sections from treated hypocotyls (100 mg) were directly homogenized with 1 mL of a solution containing 0.5 ml 10 mM potassium phosphate buffer solution [with 0.1% (w:v) trichloroacetic acid (TCA); pH 5.8] and 0.5 mL KI (1 M) for 10 min. For each sample, a control was prepared with the KI solution replaced with distilled water for tissue coloration background control, and samples were protected from exposure to light. The homogenized samples were centrifuged at 10000 g for 20 min and allowed to incubate for another 25 min at ambient temperature. The absorbance of the supernatants was read at 350 nm, and H₂O₂ content determined from a calibration curve prepared using H₂O₂ in 0.1% TCA as standard solutions and following the same procedures as used for sample quantification.

5.2.5. Estimation of plasma membrane H⁺-ATPase activity

The activity of PM H⁺-ATPase of hypocotyl sections was determined as the rate of vanadate-sensitive ATP hydrolysis (inorganic phosphate, P_i, released) following the method described by Małgorzata *et al.* (2018) with modifications. The extraction buffer consisted of 25 mM BTP-MES (pH 7.5), 330 mM sorbitol, 5 mM KCl, 5 mM EDTA, 5 mM DTT, 0.5 mM PMSF, 0.2% BSA. For hydrolytic reaction, an incubation buffer with 165 mM TRIS-MES (pH 7.5), 250 mM KCl and 12.5 mM MgSO₄ and a reaction solution containing 1 mM Na₂MoO₄ (acid phosphatase inhibitor), 10mM NaN₃ (mitochondrial ATPase inhibitor), 500 mM NaNO₃ (inhibitor of tonoplast ATPase), 30 mM ATP, 0.2% (v/v) Triton X-100 and with or without 2 mM Na₃VO₄ (PM ATPase inhibitor).

After the incubation in treatment solutions for 24 h, the excised hypocotyl sections were rinsed and 100 mg of each sample homogenized with 1 mL of cold extraction buffer using a bead beater. The homogenates were centrifuged at 10000 g for 15 min. Sample supernatants were stored on ice throughout processing. To initiate ATP hydrolysis, 0.2 mL of incubation buffer was mixed with 0.6 mL reaction solution and 0.4 mL sample supernatant in a tube and incubated in a water bath at 37 °C for 30 mins. For each sample, two reactions were carried out. One with the reaction mix containing Na₃VO₄ and the other in which Na₃VO₄ was excluded from the reaction mix. The reaction was terminated by adding 1 mL 10% TCA to the reaction mixture, centrifuged at 10000 g for 10 min, and the supernatant was used to determine P_i release.

To determine P_i released during enzymatic reactions, 1 mL of the supernatant was added to 2.6 mL of Ames' reagent (mix 10% (w/v) ascorbic acid and 0.42% (w/v) ammonium molybdate in 1 N H_2SO_4 in 1:6 v/v) containing 0.1% (w/v) sodium dodecyl sulfate. This was incubated for 20 min at room temperature, and the absorbance read at 700 nm. The amount of P_i released was determined from a standard curve, and the differences between P_i released in assays without and with Na_3VO_4 , which is due to the activity of vanadate sensitive PM H^+ -ATPase activity, were determined and expressed in nmoles $P_i h^{-1} g^{-1} FW$.

5.2.6. Statistical analyses

All data were subjected to analysis of variance (ANOVA) with treatments as the grouping factor and Duncan's Multiple Range Test to compare means of the variables. The confidence level was set at $p \leq 0.05$, and standard error (SE) was calculated. The statistical analyses were performed using SPSS for Windows v25.0 (IBM Corp., Armonk, NY, USA).

5.3. Results

5.3.1. GR24 inhibits adventitious rooting in mung bean hypocotyls

The results obtained indicated that, in comparison to the controls, treatment of explants with 1, 5, and 10 μM GR24 significantly diminished the average number of adventitious roots per explant ($p < 0.05$, Figs. 5.1a–d, Fig. 5.2A). However, the inhibitory effects of GR24 on ARF was not dosage dependent as there was no significant difference between treatments of different GR24 doses.

5.3.2. GR24 counteracts the stimulatory effects of H_2O_2 on adventitious rooting

H_2O_2 is a signal molecule that is required and fosters adventitious rooting in several plant species. Our results corroborate the stimulatory and dosage-dependent effects of exogenous H_2O_2 on ARF in mung bean hypocotyls ($p < 0.05$, Figs. 5.1e–g, Fig. 5.2B). H_2O_2 concentrations below 70 mM significantly induced ARF while concentrations above that diminished adventitious rooting. To determine if strigolactones exert any influence on H_2O_2 -induced adventitious rooting, we assessed the effects of different concentrations of GR24 in combination with 30 mM H_2O_2 (a concentration with stimulatory effects on ARF). The results showed that GR24 diminished the inductive effect of exogenous H_2O_2 on ARF (Figs. 5.1h–j, Fig. 5.2C). At concentrations of 5 μM or higher, GR24 completely eliminated the stimulatory effect of exogenous H_2O_2 and diminished ARF.

5.3.3. GR24 diminishes H_2O_2 levels in mung bean hypocotyls

The data above suggest that strigolactone may interfere with cutting-induced endogenous H_2O_2 accumulation to achieve its inhibitory effect on ARF. To test this, we measured the H_2O_2 content

of excised hypocotyls treated with different concentrations of GR24 for 24 h. In all hypocotyls treated with GR24, the endogenous H₂O₂ level was significantly lower in comparison to the controls that were incubated in water ($p < 0.05$, Fig. 5.2D). However, GR24 did not act in a concentration-dependent manner as there was no significant difference ($p < 0.05$) in H₂O₂ contents of explants between GR24 treatments. To further check the foregoing, we performed an *in-situ* detection of H₂O₂ by DAB staining. Colour development due to DAB-H₂O₂ reaction product in hypocotyl sections in response to cutting is presented in Fig. 5.3. All GR24 treated hypocotyl sections developed less intense staining compared to the control, thus further corroborating that GR24 mediated a decrease in cutting-induced accumulation of H₂O₂.

5.3.4. Plasma membrane H⁺-ATPase serves as a downstream regulatory component in GR24-mediated control of ARF in mung bean.

A diverse array of plant physiological processes are driven via the electrochemical proton gradient generated by the proton extrusion activity of PM H⁺-ATPase using ATP. To determine if PM H⁺-ATPase features in cutting-induced ARF, we tested and observed adventitious rooting in hypocotyls treated with an activator or an inhibitor of PM H⁺-ATPase activity. The fungal diterpene glucoside phytotoxin, fusicoccin (FC), is a known deregulator and irreversible activator of PM H⁺-ATPase proton pumping while Na₃VO₄ (VA) inhibits PM H⁺-ATPase actions. Our results show that treatment with either FC or VA and in a concentration-dependent manner, adventitious rooting, was strongly inhibited ($p < 0.05$, Figs. 5.1k–o, Fig. 5.4A-B). It can be presumed that while PM H⁺-ATPase action is required for adventitious rooting, since blocking it (VA treatment) strongly inhibits ARF, it also serves as a negative regulator of ARF since altering its activity by overstimulation (FC treatment) also diminishes ARF. To further confirm the requirement of PM H⁺-ATPase proton pumping for adventitious rooting, we treated excised hypocotyls with H₂O₂ (an inducer of ARF) in the presence of 300 mM VA (a concentration which diminished ARF). Adventitious rooting was totally blocked, with no adventitious roots formed after the 5-d observation period, in all H₂O₂ concentrations in the presence of VA (Figs. 5.1p-r).

Having deduced that PM H⁺-ATPase features in the adventitious rooting process, we then proceeded to determine if PM H⁺-ATPase is involved in strigolactone-mediated inhibition of ARF in mung bean. When hypocotyls were treated with GR24 (1, 5 & 10 μM) in the presence of 1 μM FC, adventitious roots formed per explant was as low as that observed with those treated with 1 μM FC alone, i.e., without GR24 ($p < 0.05$, Figs. 5.1s–t, Fig. 5.4C). These findings suggest that an FC-mediated hyperactivation of PM H⁺-ATPase had an overriding influence on GR24 actions during adventitious root formation. However, we noticed by physical observation that GR24 was

able to prevent the characteristic FC-induced wilting in the treated hypocotyls. Since altering PM H⁺-ATPase actions, either activation or inhibition resulted in the downregulation of ARF; we evaluated the effect of GR24 on PM H⁺-ATPase activities. Hypocotyl sections treated with GR24 exhibited a significantly lower PM H⁺-ATPase activity compared to the control and in a concentration-dependent manner ($p < 0.05$, Fig. 5.4D). In contrast, hypocotyls treated with 30 mM H₂O₂ showed a slightly and significantly higher PM H⁺-ATPase activity suggesting H₂O₂ may induce proton pumping during ARF. In hypocotyls treated with a combination of 5 μM GR24 and 30 mM H₂O₂, PM H⁺-ATPase activity was significantly diminished to a similar level as observed in explants, which received 5 μM GR24 alone.

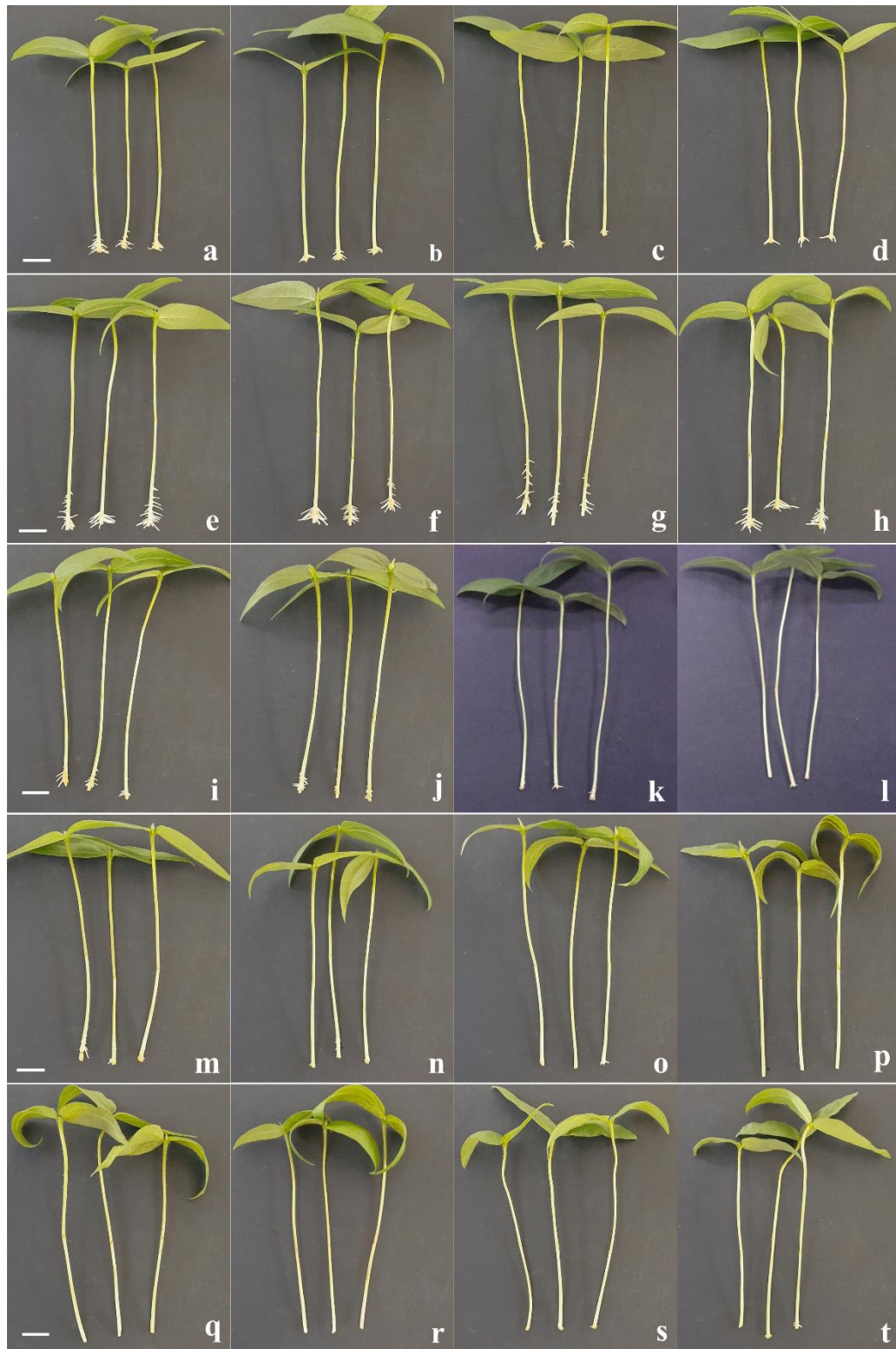


Figure 5.1. Effects of treatments (as outlined below) on adventitious root formation in mung bean hypocotyls. (a) H₂O (control); (b) GR24 1 μM; (c) GR24 5 μM; (d) GR24 10 μM; (e) 30 mM H₂O₂; (f) 50 mM H₂O₂; (g) 70 mM H₂O₂; (h) GR24 1 μM + 30 mM H₂O₂; (i) GR24 5 μM + 30 mM H₂O₂; (j) GR24 10 μM + 30 mM H₂O₂; (k) fusicoccin (FC) 0.5 μM; (l) FC 1 μM; (m) Na₃VO₄ (VA) 100 mM; (n) VA 300 mM; (o) VA 500 mM; (p) 30 mM H₂O₂ + VA 300 mM; (q) 50 mM H₂O₂ + VA 300 mM; (r) 70 mM H₂O₂ + VA 300 mM; (s) GR24 5 μM + FC 1 μM; (t) GR24 10 μM + FC 1 μM. Bar = 1cm.

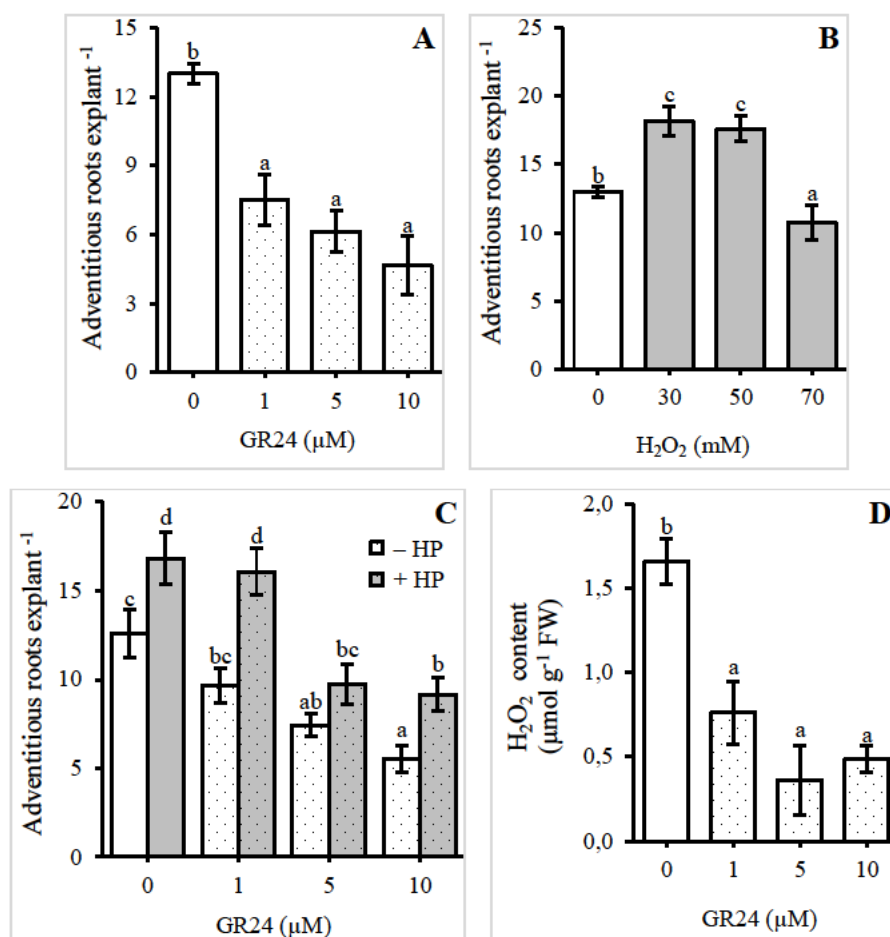


Figure 5.2. Quantitative changes in the number of adventitious roots formed in mung bean hypocotyls in response to (A) GR24; (B) H₂O₂; and (C) combination of GR24 and H₂O₂; and (D) the impact of GR24 on endogenous H₂O₂ during adventitious root formation in mung bean (mean ± SE of $n = 3$). HP, hydrogen peroxide (H₂O₂). Different letters above error bars indicate statistically significant differences among treatments at $p < 0.05$. The expressed number of adventitious roots per explants are means from three independent experiments with 12 explants per treatment.

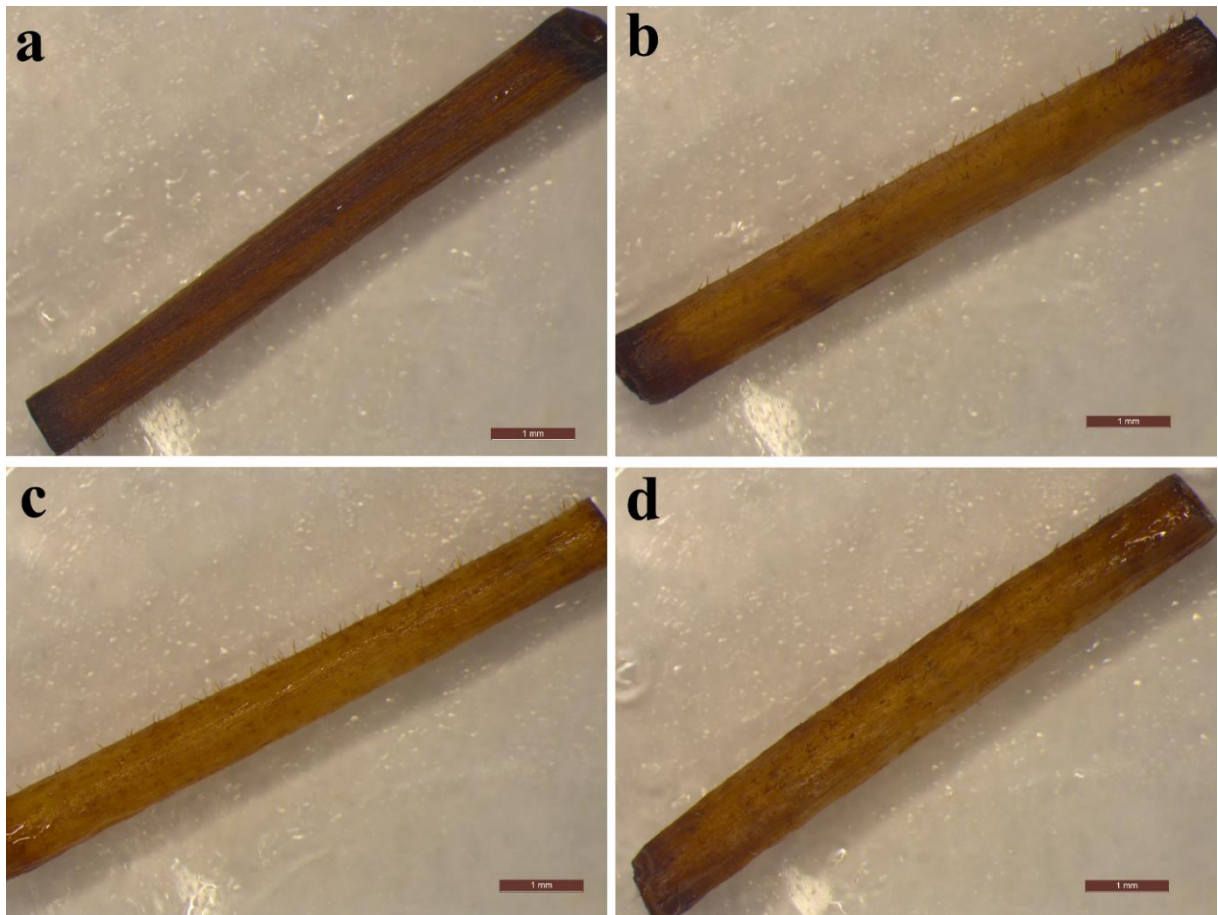


Figure 5.3. *In situ* visualization of H_2O_2 in mung bean hypocotyl sections by 3,3-diaminobenzidine (DAB) staining. The effect of strigolactone (GR24) treatments on the generation of H_2O_2 in explants during cutting-induced adventitious root formation. Treatments: (a) distilled water (control); (b) 1 μ M GR24; (c) 5 μ M GR24; and (d) 10 μ M GR24. Bar = 1 mm.

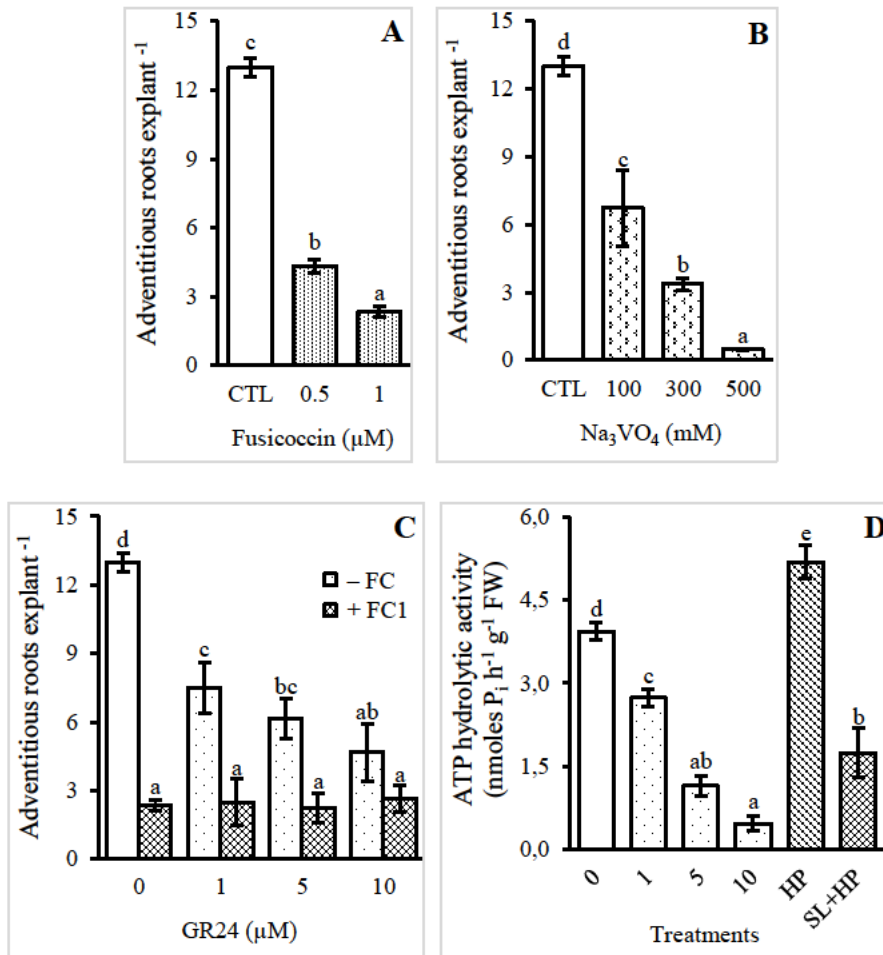


Figure 5.4. The effects of (A) fusicoccin, (B) sodium orthovanadate (Na₃VO₄), and (C) combined GR24-fusicoccin treatments on adventitious root formation; and (D) PM H⁺-ATPase activities in response to GR24 and H₂O₂ treatments (mean ± SE of *n* = 3). GR24 concentrations: 0, 1, 5, 10 μM. HP: 30 mM H₂O₂, SL+HP: 5 μM GR24 + 30 mM H₂O₂. Different letters above the error bars indicate statistically significant differences among treatments at *p* < 0.05. The expressed number of adventitious roots per explants are means from three independent experiments with 12 explants per treatment.

5.4. Discussion

The adaptive and ecological importance of adventitious root formation in plants, as well as the economic value of this process for mass vegetative propagation, cannot be overemphasized. As an organogenic process that enables plants to navigate through a variety of abiotic stresses and one that finds application in agriculture, forestry, and horticulture, it is important to understand the underlying mechanisms behind the intricate hormonal and signalling networks that drive and regulate adventitious rooting. Although a variety of endogenous components, such as H₂O₂ and strigolactones, which induce and feature in the signal transduction pathways that control ARF has been identified, the molecular mechanisms underlying strigolactone-mediated ARF, and the downstream components involved, remain to be identified and defined.

Strigolactones have been implicated in the regulation of a significantly diverse array of morphological processes, including root development. Early findings also point to the role of strigolactones in the control of adventitious rooting (Rasmussen *et al.*, 2012a; 2012b). Our study demonstrates the involvement of strigolactone in the regulation of ARF in mung bean. Consistent with previous studies in which increased ARF was observed in strigolactone deficient mutants and plants treated with strigolactone biosynthesis inhibitor (Rasmussen *et al.*, 2012a; 2012b), we found treatment with different concentrations of GR24 led to a dramatic decrease in the number of adventitious roots formed per explant thus confirming the inhibitory role of strigolactones on ARF in mung bean. From these, and the fact that the root is the major source of endogenous strigolactones, it can be presumed that the excision of seedling roots cuts off strigolactone supply to the hypocotyl, thus lifting the strigolactone-mediated repressive signal on ARF. However, when strigolactone is supplied exogenously, there's a restoration of this signal which attempts to suppress adventitious rooting. On the other hand, H₂O₂ is a well-documented signal transduction molecule and promoter of cutting-induced adventitious rooting (Li *et al.*, 2007; Li *et al.*, 2009; Liao *et al.*, 2011; Yang *et al.*, 2013; Druege *et al.*, 2019; Zhang *et al.*, 2019). Also consistent with these early reports, our study showed that H₂O₂ enhances adventitious rooting in mung bean in a dosage-dependent manner. However, at high H₂O₂ concentration (70 mM), ARF formation was reduced, and this may be attributed to a heightened H₂O₂-induced stress signal that may have elicited an exacerbated oxidative stress response in the treated hypocotyls. Excessive production of H₂O₂ is associated with an oxidative outburst in plants under stress conditions.

Based on the results obtained in this study, we conclude that (1) H₂O₂ is a downstream component of strigolactone hormonal pathways during ARF, and (2) strigolactones may exert their influence on H₂O₂ signaling by modulating H₂O₂ content to downregulate ARF. These correlate with the

already established role of H₂O₂ as a downstream signal component for hormonal actions as seen with ABA (Melo *et al.*, 2016), auxin (Li and Xue, 2010; Wei *et al.*, 2018), and salicylic acid (Yang *et al.*, 2013) in the control of adventitious rooting. In the light of the foregoing, it remains to be determined whether strigolactones control H₂O₂ biosynthesis, catabolism, or both to modulate H₂O₂ content in a bid to inhibit adventitious rooting.

Plasma membrane H⁺-ATPase participates in diverse plant developmental processes and responses to both biotic and abiotic stresses, such as cell growth, mineral and metabolite transport, nutrient uptake, stomatal closure, tolerance to salinity, phosphate deficiency, and metal toxicity (Hohm *et al.*, 2014; Falhof *et al.*, 2016; Zhang *et al.*, 2017). Also, PM H⁺-ATPase activity is under hormonal regulation during these processes (Falhof *et al.*, 2016). From the results obtained in this study, it is evident that PM H⁺-ATPase is involved in ARF, and its activity is a requirement for adventitious rooting. This is demonstrated by the outcome of inhibitor (vanadate) treatments (Fig. 5.4B) even in the presence of H₂O₂ (Figs. 5.1p-r) as well as the fact that both GR24 and H₂O₂ modulated its activity (Fig. 5.4D). Taken together with the preceding, the inhibition of adventitious rooting by FC, in a dosage-dependent manner, suggests PM H⁺-ATPase serves as a channel for the regulation of ARF given that altering its activity, either upwards or downwards, results in decreased adventitious rooting. However, further investigations are required on the influence of FC and PM H⁺-ATPase on adventitious rooting since FC is known to cause deregulation of PM H⁺-ATPase activity leading to membrane hyperpolarisation that may adversely affect some cellular processes (Marre, 1979). This is because FC facilitates an almost irreversible stabilization of PM H⁺-ATPase complex with 14-3-3 (Baunsgaard *et al.*, 1998), a regulatory protein that binds and activates PM H⁺-ATPase catalytic activity. FC-induced sustained PM H⁺-ATPase proton pumping may have inhibited the initiation of other ARF-influencing signals that may require dynamic changes in cell ion gradient and membrane potential.

The reduction of PM H⁺-ATPase activity in GR24-treated hypocotyls, and even in the presence of H₂O₂, is a clear indication that PM H⁺-ATPase is also a downstream component, just like H₂O₂, of strigolactone signal networks for the regulation of adventitious rooting. From our results, it can be inferred that GR24 employs a hormonal pathway that is independent of H₂O₂ to influence PM H⁺-ATPase actions since it was able to diminish PM H⁺-ATPase activity even in the presence of exogenous H₂O₂. These findings are in line with observations from studies on strigolactones and other cellular processes that are known to be regulated by PM H⁺-ATPase activity. For instance, the opening of the stomatal aperture is well known to be actively controlled by PM H⁺-ATPase [See Falhof *et al.* (2016) and references therein]. Recently some studies revealed strigolactone as

potent regulators in the induction of stomatal closure (Zhang *et al.*, 2018c). And interestingly, strigolactone was reported to have required H₂O₂ to exert its influence on stomatal closure (Lv *et al.*, 2018). Furthermore, the regulation of PM H⁺-ATPase by GR24, as suggested by our data, aligns with several reported observations concerning strigolactone-auxin interactions in the inhibition of bud development and shoot branching. Strigolactones are potent modulators of auxin hormonal actions and PAT stream, which features in both bud activation and adventitious rooting (Lin and Sauter, 2019). Given that proton extrusion by PM H⁺-ATPase is required for auxin and PAT establishment (Hohm *et al.*, 2014), strigolactones may dampen PM H⁺-ATPase actions to downregulate auxin hormonal actions, which otherwise fosters ARF (Druege *et al.*, 2016; Druege *et al.*, 2019; Guan *et al.*, 2019), during adventitious rooting as seen with bud inactivation.

In summary, our data contribute to marking out a distinctive role for H₂O₂ and PM H⁺-ATPase in strigolactone-mediated inhibition of adventitious rooting in mung bean hypocotyls. In addition to confirming the inhibitory influence of strigolactones on ARF, the results obtained also indicate that strigolactones may induce a decrease in endogenous H₂O₂ levels and PM H⁺-ATPase activity to diminish adventitious rooting. Based on these observations, we suggest that H₂O₂ and PM H⁺-ATPase are downstream components of the signal transduction pathway(s) required for ARF, which strigolactones may target to exert their inhibitory influence on ARF. However, further investigations are necessary to unravel how strigolactone hormonal actions via H₂O₂ and PM H⁺-ATPase translate into reduced adventitious root formation.

Chapter 6

Strigolactone interactions with ethylene and sucrose in the regulation of pigment accumulation during de-etiolation

6.1. Introduction

De-etiolation and photomorphogenic development are characterized by light-induced or enhanced biosynthesis of biomolecules required for assembling functional thylakoid systems and photosynthetic apparatus with an attendant etioplast-to-chloroplast transition (Pipitone *et al.*, 2020). These include the synthesis of galactolipids such as non-phosphorous mono- and digalactosyldiacylglycerols, thylakoid- and plastid-associated proteins, and protein complexes, the conversion of chlorophyll precursor (protochlorophyllide) into chlorophyll and carotenogenesis (Kobayashi, 2016; Armarego-Marriott *et al.*, 2019; Pipitone *et al.*, 2020). While chlorophylls are basically for the trapping and conversion of light energy into chemical energy, carotenoids are essential for stabilizing the membranes of prolamellar bodies; assembly of light-harvesting complexes where they participate in the optimization of photon energy capture and usage; incorporation into membranes to regulate fluidity and stability; and as antioxidants for protection against the highly oxidative environment within the chloroplast (Havaux, 1998; Pinnola *et al.*, 2013; Pintó-Marijuan and Munné-Bosch, 2014; Kowalewska *et al.*, 2019).

The ability to switch from heterotrophic growth, which is characteristic of early seedling growth in the absence of light in the soil, to photoautotrophic development on exposure to light is essential for seedling survival and establishment. Seedling de-etiolation and photomorphogenic growth are therefore tightly regulated processes with several hormonal and non-hormonal signals contributing to their regulation. Among these hormonal signals, ethylene and its downstream signal components are significant contributors to the regulation of photomorphogenic development. For instance, ethylene and its transcriptional response factors, ETHYLENE INSENSITIVE3/ETHYLENE INSENSITIVE3-LIKE1 (EIN3/EIL1), repress protochlorophyllide accumulation while also inducing the expression of protochlorophyllide oxidoreductase genes in etiolated seedlings [reviewed in Liu *et al.* (2017c)]. EIN3/EIL1 serves to integrate hormonal and light signals via its cooperation with PIFs (Liu *et al.*, 2017c). Ethylene also targets light signaling via the CONSTITUTIVE PHOTOMORPHOGENESIS1 (COP1) and ELONGATED HYPOCOTYL5 (HY5) signal module. The degradation of HY5, a TF that promotes seedling de-etiolation and photomorphogenesis, is enhanced by ethylene via its stabilization of COP1 (Yu *et al.*, 2013; Xu *et*

al., 2016). With regards to pigment accumulation, ethylene was reported to have promoted chlorophyll accumulation in etiolated cucumber cotyledons when applied prior to illumination but diminished chlorophyll content when applied in light (Alscher and Castelfranco, 1972).

As with chlorophyll biosynthesis, ethylene and ethylene signaling components feature actively in the control of carotenoid biosynthesis. Several transcriptional regulators of carotenogenesis act via ethylene signaling with ethylene promoting and/or repressing carotenoid accumulation depending on the growth stage, physiological and ambient conditions (Liu *et al.*, 2012; Liu *et al.*, 2014c; Stanley and Yuan, 2019). A class of phytohormone that also functions in photomorphogenesis is strigolactones. They modulate processes like hypocotyl elongation, adventitious rooting, and seedling establishment by interacting with other key regulators like cryptochromes, phytochromes, and other phytohormones (Shen *et al.*, 2012; Jia *et al.*, 2014; Urquhart *et al.*, 2015; Guo dong *et al.*, 2016; Thussagunpanit *et al.*, 2017).

Reports on the influence of sucrose on pigment accumulation during seedling de-etiolation and establishment are limited. However, some early studies demonstrate some roles of sucrose in the regulation of chlorophyll content in micropropagated test plants [reviewed in Tognetti *et al.* (2013)]. A common conclusion from these findings is that sucrose repressed chlorophyll accumulation. In contrast, carotenoid accumulation was positively regulated by sugar signals. Sucrose has also been recently reported to feature in the regulation of bud development where it represses auxin/strigolactone signals, enhance cytokinin effects, and stimulates bud outgrowth and development (Bertheloot *et al.*, 2020). Furthermore, early seedling development in *Arabidopsis* was also shown to be regulated by sugar signals that acted synergistically with strigolactone to repress seedling establishment (Guo dong *et al.*, 2016). Despite the considerable research progress made so far with strigolactones and their interactions with other regulators of growth and development, there is limited information about how strigolactones influence pigment accumulation during seedling de-etiolation and the interactions between strigolactones, ethylene, and sugar signals (if any) in the regulation of pigment content during seedling transition from development in the dark to growth in light.

6.2. Materials and methods

6.2.1. Plant materials

Mung bean seeds were rinsed several times with distilled water and soaked for 6 h in distilled water. After that, the seeds were rinsed again and sown in seedling trays filled with perlite moistened with distilled water serving as a potting medium. The setup was incubated in a growth room with ambient temperature set at 24 ± 1 °C, and the resulting seedlings were maintained for 7 d in the dark with watering every 2 d.

6.2.2. Chemical treatments

For the chemical treatment of seedlings, one seedling tray was assigned to each treatment and the appropriate test solution was applied to the seedlings. The test solutions were as follows: distilled water (control, CTL); GR24 (1, 10, 20 μ M); sucrose (10, 50, 100 mM); silver thiosulfate (STS; 20 μ M); aminoethoxyvinylglycine (AVG; 20 μ M); 1-aminocyclopropane-1-carboxylic acid (ACC; 50 μ M); tolfenamic acid (TL; 50 μ M); 10 μ M GR24+SUC (SUC: 10, 50, 100 mM); STS+GR24 (20 μ M and 10 μ M respectively); AVG+GR24 (20 μ M and 10 μ M respectively); ACC+GR24 (50 μ M and 10 μ M respectively); STS+SUC (20 μ M and 50 mM respectively); AVG+SUC (20 μ M and 50 mM respectively); ACC+SUC (50 μ M and 50 mM respectively); TL+SUC (50 μ M and 50 mM respectively); TL+GR24 (50 μ M and 10 μ M respectively); GR24+STS+SUC (10 μ M, 20 μ M and 50 mM respectively); GR24+AVG+SUC (10 μ M, 20 μ M and 50 mM respectively); and GR24+ACC+SUC (10 μ M, 50 μ M and 50 mM respectively). The treated seedlings were incubated for 24 h in the dark and then exposed to light (LED, PAR $\sim 120 \mu\text{mol m}^{-2} \text{s}^{-1}$) in a 16/8-h light/dark photoperiod for 1 d.

6.2.3. Chlorophyll and total carotenoid quantification

Sampled leaf from individual seedlings was weighed (~ 25 mg), and pigment extraction was carried out by homogenization with 1.3 mL of 80% acetone (v/v) using a bead beater. After centrifugation at 5,000 g for 10 min, the absorbance of the supernatant at 470 nm, 647 nm, and 663 nm was measured in a spectrophotometer. Chlorophyll and carotenoid concentrations were calculated using the equations below, as described by Lichtenthaler (1987) and expressed in micrograms per gram fresh weight ($\mu\text{g g}^{-1}$ FW).

$$C_a = 12.25A_{663} - 2.79A_{647}$$

$$C_b = 21.50A_{647} - 5.10A_{663}$$

$$C_{a+b} = 7.15A_{663} + 18.71A_{647}$$

$$C_{x+c} = \frac{1000A_{470} - 1.82C_a - 85.02C_b}{198}$$

Where,

C_a represents chlorophyll a,

C_b is chlorophyll b,

C_{a+b} is total chlorophyll,

C_{x+c} is total carotenoid, and

A_{470} , A_{647} , and A_{663} are the extract absorbance at 470, 647, and 663 nm, respectively.

6.2.4. Estimation of total soluble sugar content

The total soluble sugar content of sampled treated and de-etiolating leaves was determined by the phenol-sulphuric acid method (Chow and Landhäusser, 2004). Sampled leaves were weighed, homogenized with 1 mL of 80% ethanol, centrifuged at 10000 g for 10 min, and the resulting supernatant collected in clean tubes. An aliquot (300 μ L) of the ethanolic extract was dried under a nitrogen stream; 500 μ L of distilled water was added to the residue and dissolved by sonication. To each dissolved residue, 2 mL of 2% phenol solution and 2.5 mL of 96 % (v/v) sulphuric acid was added and mixed gently. After 30 min of color development in the dark and cooling, the absorbance was read at 490 nm against a blank (assay mixture with extract replaced with distilled water). The total soluble sugar content was determined from a standard curve prepared using a sugar mixture of glucose:fructose: galactose (GFG) and expressed in milligram soluble sugar per gram fresh weight (mg SS g⁻¹ FW).

6.2.5. Statistical analyses

All data were subjected to analysis of variance (ANOVA) with treatments as the grouping factor and Duncan's Multiple Range Test to compare means of the variables. The confidence level was set at $p \leq 0.05$, and standard error (SE) was calculated. The statistical analyses were performed using SPSS for Windows v25.0 (IBM Corp., Armonk, NY, USA).

6.3. Results

6.3.1. GR24 and ethylene precursor (ACC) repress pigment accumulation in de-etiolating mung bean seedlings

Chlorophyll and carotenoid accumulation were suppressed in GR24-treated seedlings with 1 μM and 10 μM GR24 treatments, significantly reducing the leaf content of both classes of pigment (Fig. 6.1A-B). In contrast, at a high GR24 concentration (20 μM), chlorophyll content was slightly higher than observed in the control seedlings, albeit, this was not statistically significant. In contrast, carotenoid accumulation was significantly ($p \leq 0.05$) induced at a high GR24 concentration (20 μM) compared to the control. Acting in the same manner as 10 μM GR24, ethylene precursor, ACC, applied at 20 μM , also mediated a significant inhibition of both chlorophyll and carotenoid accumulation (Fig. 6.1C-D). In the presence of GR24, ACC's effect on pigment accumulation was not significantly affected (Fig. 6.1C-D). While AVG (an ethylene biosynthesis inhibitor) mediated an increase in both chlorophyll and carotenoid contents (Fig. 6.1C-D), in the presence of GR24, AVG influence was only significantly ($p \leq 0.05$) reversed in chlorophyll accumulation. GR24 treatment did not elicit a statistically significant impact on AVG-mediated increase in carotenoid content (Fig. 6.1D). On the other hand, STS (an ethylene signal blocker) only slightly induced carotenoid accumulation, which was significantly reversed in the presence of GR24 (Fig. 6.1D).

6.3.2. D14 inhibitor (TL) masks the effects of GR24 on pigment accumulation

The inhibitor of the strigolactone signal receptor (D14), TL, elicited a significant ($p \leq 0.05$) increase in chlorophyll content but only slightly increased the carotenoid content of de-etiolating seedlings which was not statistically significant ($p \leq 0.05$) when compared to the control (Fig. 6.2). Supplying GR24 with TL reversed TL-induced chlorophyll accumulation (Fig. 6.2A) but did not do the same for TL-induced increase in carotenoid content (Fig. 6.2B).

6.3.3. Sucrose-induced pigment accumulation is antagonized by GR24

Sucrose involvement, and its interaction with GR24, in pigment accumulation during de-etiolation, was assessed. Sucrose induced a significant ($p \leq 0.05$) increase in both chlorophyll and carotenoid accumulation in a concentration-dependent manner (Fig. 6.3A-B). Application of GR24 with sucrose resulted in a significant ($p \leq 0.05$) reversal of the sucrose-induced increase in chlorophyll content (Fig. 6.3A). In contrast, the sucrose-induced increase in carotenoid content was not significantly affected by GR24 treatment (Fig. 6.3B). To determine if GR24 influenced carotenoid accumulation by regulating endogenous sugar content, we quantified the total soluble sugar content

of de-etiolating leaves of mung bean seedlings. Neither GR24 nor TL exerted any significant effects on endogenous soluble sugar content (Fig. 6.3C).

6.3.4. Sucrose reverses ACC-induced repression of pigment accumulation

The results above show that exogenous sucrose is a positive regulator of pigment accumulation in de-etiolating mung bean seedlings, and GR24 antagonizes this process. With this in mind, the effect of exogenous sucrose supply on ethylene-mediated repression of pigment accumulation in the presence or absence of GR24 was evaluated. Both chlorophyll and carotenoid content were enhanced when 50 μM sucrose was supplied to ACC-treated seedlings (Fig. 6.4). Exogenous sucrose enhanced AVG-induced pigment accumulation though not statistically significant ($p \leq 0.05$) when compared to seedlings treated with AVG alone. Chlorophyll and carotenoid content were not significantly affected in STS-treated seedlings in the presence of sucrose. Supplying 10 μM GR24 to ACC + sucrose-treated seedlings and AVG + sucrose-treated seedlings did not considerably affect chlorophyll and carotenoid content. In contrast, treatment with 10 μM GR24 significantly lowered chlorophyll and carotenoid content in STS + sucrose-treated seedlings

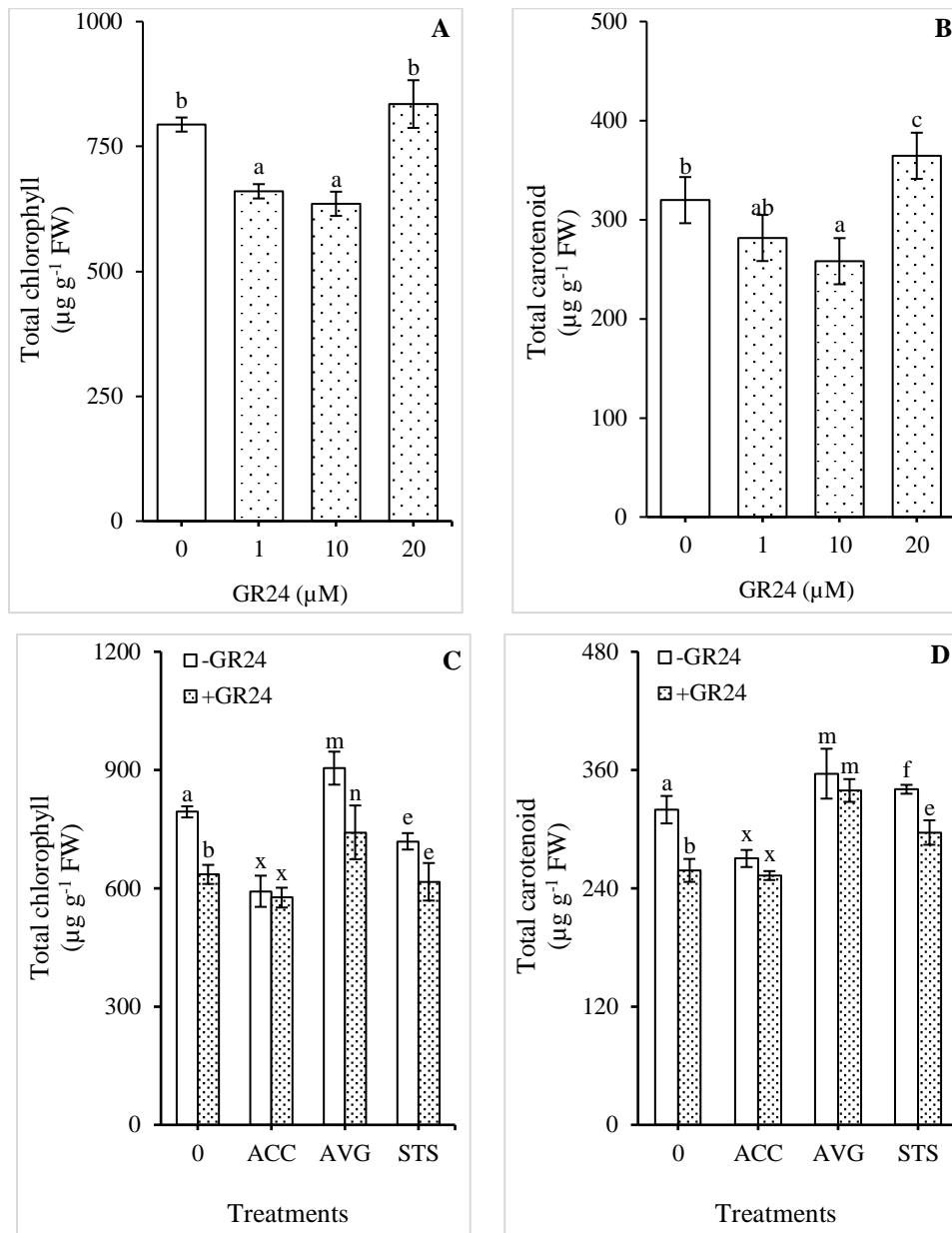


Figure 6.1. The influence of GR24 on pigment accumulation during de-etiolation of dark-grown mung bean seedlings. Total chlorophyll (A) and carotenoid (B) contents in GR24-treated mung bean seedlings after exposure to 16 h of light. Effects of GR24, ethylene precursor (ACC) and inhibitors (AVG & STS) on total chlorophyll (C) and carotenoid (D) contents in de-etiolating mung bean seedlings. Data are presented as means and standard error ($n = 4$), and significant differences among treatment means at $p < 0.05$, according to Duncan's Multiple Range Test, are indicated by different letters.

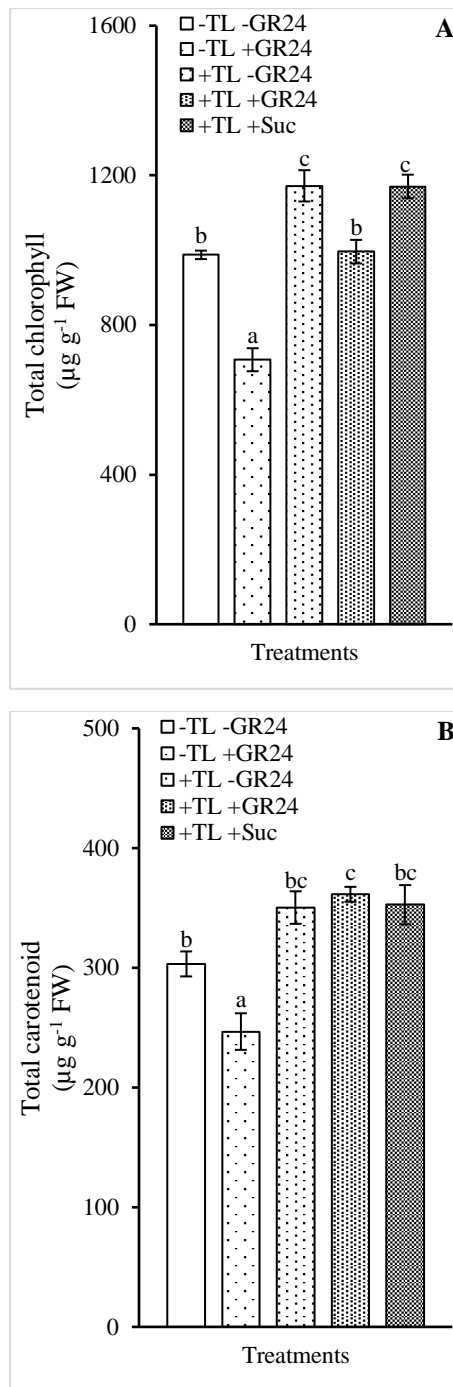


Fig. 6.2. Tolfenamic acid-induced reversal of GR24 influence on pigment accumulation during de-etiolation of dark-grown mung bean seedlings. Total chlorophyll (A) and carotenoid (B) contents of mung bean seedlings treated as indicated and exposed to 16 h of light. TL, tolfenamic acid; GR24, racemic GR24; Suc, sucrose. Data are means \pm standard error ($n = 4$), and significant differences among treatment means at $p < 0.05$ are indicated by different letters.

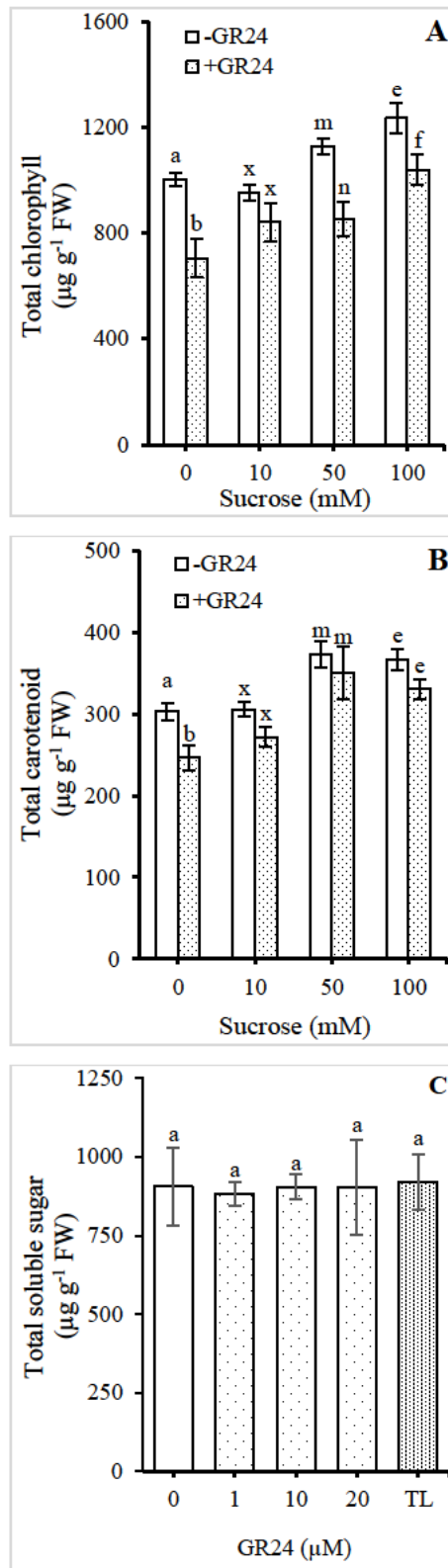


Figure 6.3. Sucrose-GR24 interactions in the regulation of chlorophyll (A) and carotenoid (B) accumulation during the de-etiolation of dark-grown mung bean seedlings. Total soluble sugar (C) content of de-etiolating mung bean seedlings after treatments. TL, tolfenamic acid. Data represent means \pm standard error ($n = 4$), and significant differences among treatment means at $p < 0.05$ are indicated by different letters.

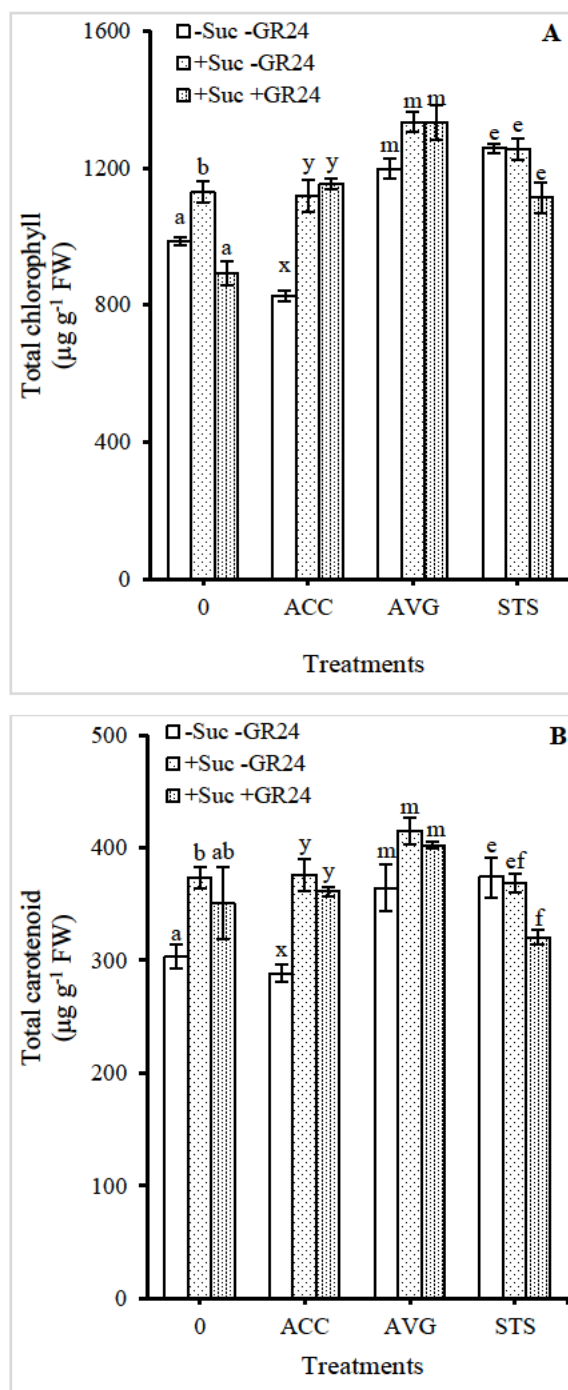


Figure 6.4. Sucrose, ethylene, and GR24 interactions in the regulation of chlorophyll (A) and carotenoid (B) accumulation during the de-etiolation of dark-grown mung bean seedlings. ACC, 1-aminocyclopropane-1-carboxylic acid, AVG, aminoethoxyvinyl glycine; GR24, racemic GR24; Suc, sucrose; STS, silver thiosulfate. Data represent means \pm standard error ($n = 4$), and significant differences among treatment means at $p < 0.05$ are indicated by different letters.

6.4. Discussion

Chlorophyll and carotenoid accumulation were significantly repressed in GR24-treated, dark-grown mung bean seedlings undergoing de-etiolation. The observations with the D14 signal inhibitor, TL, suggest the involvement of the strigolactone-D14 signal pathway in the modulation of pigment accumulation during seedling de-etiolation. Similarly, the observed repression of both chlorophyll and carotenoid accumulation by ACC and the promotion of pigment accumulation by AVG and STS are clear indications that ethylene signals are potent modulators of pigment accumulation and these act to limit pigment content. These observations agree with the ethylene-induced decrease in chlorophyll and carotenoid accumulation in de-etiolating tomato seedlings (Melo *et al.*, 2016). Also consistent with the findings in this study are previous reports of ethylene and its signaling components in the suppression of crucial photomorphogenesis-promoting TFs which promote greening as well as the repression of protochlorophyllide accumulation in dark-grown seedlings (Alscher and Castelfranco, 1972; Yu *et al.*, 2013; Zhong *et al.*, 2014; Shi *et al.*, 2016; Xu *et al.*, 2016). Seedling greening is positively regulated by light via light-sensing cryptochrome and phytochrome as well as phytohormones such as auxin and cytokinins, while ethylene is a known repressor of photomorphogenesis via its downregulation of several TFs such as HY5 (Yu *et al.*, 2013; Melo *et al.*, 2016; Xu *et al.*, 2016; Liu *et al.*, 2017c). The results suggest a connection between ethylene and GR24 in the repression of pigment accumulation, especially carotenoid accumulation, during seedling greening. The inability of GR24 to repress carotenoid accumulation in the presence of AVG suggests a requirement for ethylene signaling in strigolactone-mediated control of carotenogenesis during de-etiolation. Though subject to further validation, GR24 may have elicited its repression of pigment accumulation via its positive influence on ethylene biosynthesis and signaling. Previous reports have demonstrated that strigolactone requires/or interacts with ethylene to elicit other responses like root hair elongation and senescence (Kapulnik *et al.*, 2011b; Ueda and Kusaba, 2015). Furthermore, a recent report demonstrates that GR24 treatment up-regulated ethylene biosynthesis in etiolated *Arabidopsis* seedlings (Lee and Yoon, 2020), thus further lending credence to the idea of strigolactone-mediated control of photomorphogenic growth via ethylene dependent signals.

Sugar signals were previously reported to have acted either synergistically or antagonistically with strigolactones depending on the developmental process under observation (Guo dong *et al.*, 2016; Bertheloot *et al.*, 2020). The results from this study suggest that sucrose acts antagonistically with ethylene and strigolactones in the regulation of chlorophyll and carotenoid accumulation during de-etiolation of mung bean seedlings. These resonate with previous observations in which sucrose suppressed strigolactone inhibition of bud activation and outgrowth (Bertheloot *et al.*, 2020) but

sharply contrasts the synergistic interactions between exogenous glucose and strigolactone in the repression of seedling establishment (Guo dong *et al.*, 2016). However, since GR24 treatment and D14 inhibitor did not significantly affect total soluble sugar content in de-etiolating mung bean seedlings, it can be inferred that strigolactone repression of pigment accumulation is not mediated via the imposition of limitations on sugar content and signaling.

Chapter 7

General conclusions

The hormonal actions of strigolactones in the mediation of tolerance to heat and chilling-induced oxidative stress and limitations on plant growth and development, the regulation of adventitious root formation, and pigment accumulation during seedling de-etiolation were the subject of investigation in this study. As a class of phytohormone which were initially identified as ecological signals for seed germination in root-parasitic plants and the initiation of symbiotic relationships between plants and beneficial microbes, coupled with their emerging roles in abiotic stress responses, it is important to evaluate how strigolactones contribute to the regulation of plant tolerance to extreme temperatures.

Lupine seeds incubated with GR24, strigolactone biosynthesis, or signal inhibitors (TB and TL, respectively) were germinated under supra-optimal temperature. GR24 alleviated thermoinhibition and enhanced seed germination, with GR24-treated seeds attaining 90% final germination and a higher stress tolerance index compared to the control (chapter 3). Enzymatic scavenging of O_2^- was enhanced in GR24-treated seeds with an attendant decreased in the level of lipid peroxidation. Proline content of germinating seeds was also enhanced, thereby improving osmotic balance to enhance seed germination under HS. However, observations with TL-treated seeds suggest that strigolactone-D14 signaling plays a limited role in seed germination, while inhibition of strigolactone biosynthesis (TB treatment) had no effect on germination under normal and HS conditions, thus suggesting that strigolactone biosynthesis is not required for lupine seed germination.

Photosystem tolerance to heat-stressed lupine seedlings was evaluated by OJIP analysis. This showed that GR24-mediated OECs resistance to HS-induced injury and ensured PSII thermostability. The limiting effects of heat stress on the quantum yields and efficiencies of PSII and the performance index on absorption basis and energy conservation were also ameliorated by GR24 treatment. GR24 mediated tolerance to heat stress by mitigating heat-induced disruption of ROS homeostasis. This was achieved by inducing both enzymatic (SOD, APX, and POX) and non-enzymatic (phenolics) ROS scavenging mechanisms to mitigate HS. Glyoxalase enzymes were also involved in GR24-mediated thermotolerance as both glyoxalase I and II activities were significantly enhanced by GR24 treatment. In addition, inhibition of strigolactone signal perception (TL treatment) did not limit PSII thermotolerance. Hence it is possible that the ameliorating effects

of GR24 may be attributed to its ability to elicit the karrikin signal pathway. With respect to developmental stages, GR24 elicited some level of specificity in the biochemical processes it influenced to enhance tolerance to HS.

As observed with HS in lupine, GR24 limited CS-induced inhibition of PSII activities and also regulated ROS (O_2^- and H_2O_2) accumulation, partly by inducing SOD activities, to confer chilling tolerance in mung bean seedlings (chapter 4). The observations with ROS, if taken together with a previous report that strigolactone requires H_2O_2 biosynthesis to trigger stomatal closure (Lv *et al.*, 2018), suggest that recruiting ROS as signal cues and maintaining ROS homeostasis may be a central theme in GR24/strigolactone-mediated tolerance to abiotic stress. The accumulation of soluble sugars and proline, as well as GR24-induced improvement of leaf water content, are indications of the ability of GR24 to mitigate abiotic stress via osmotic adjustment. Furthermore, the induction of PAL, TAL, and LOX by GR24 are indications that the phenylpropanoid pathway and oxylipin-dependent stress coping mechanisms may be under the sphere of influence of strigolactones in abiotic stress mediation. Since a stereoisomer of racemic GR24 has been demonstrated to be capable of eliciting karrikin signals (Scaffidi *et al.*, 2014; Sun *et al.*, 2016b), it is important to carry out further evaluations to determine if indeed these GR24-mediated stress responses were elicited via the strigolactone-D14-MAX2 signal pathway or the KAI2-MAX2 signaling.

In negatively regulating cutting-induced adventitious rooting, GR24 diminished H_2O_2 content of cut hypocotyls and also counteracted H_2O_2 -induced adventitious rooting (chapter 5). This further reiterates a crucial role for ROS signals in strigolactone-mediated adaptive responses in plants. As with H_2O_2 , PM H^+ -ATPase features actively as a regulatory node during ARF and was influenced by GR24. The recruitment of PM H^+ -ATPase by GR24 to control ARF alludes to the modulation of auxin signaling (a requirement for ARF) via proton extrusion. The question of whether strigolactones mediate a PM H^+ -ATPase-dependent down-regulation of auxin and PAT stream during ARF is one that must be answered with further investigations. Only then will a clearer picture of strigolactone, PM H^+ -ATPase, and auxin/PAT signal networks during adventitious rooting be developed.

Based on the findings from the study on seedling de-etiolation (chapter 6), it can be concluded that strigolactones are negative regulators of pigment accumulation during de-etiolation, and they may act via ethylene-dependent signals to elicit their control on pigment accumulation. Conversely, sucrose, and strigolactone signals act antagonistically to regulate pigment accumulation, with

sucrose overriding the effects of GR24. Furthermore, as a downstream product of the oxidative degradation of a carotenoid (β -carotene), the repression of carotenogenesis by GR24 may be an indication of the ability of strigolactones to serve as a feedback regulator of carotenoid metabolism. This is, however, subject to further investigations and validation. Our findings here further contribute to the emerging body of evidence for the existence of strigolactone-sugar signal crosstalk in the regulation of plant development in which sugar signals tend to counteract or mask strigolactone responses.

REFERENCES

- Abe, S., Sado, A., Tanaka, K., Kisugi, T., Asami, K., Ota, S., Kim, H.I., Yoneyama, K., Xie, X., Ohnishi, T., 2014. Carlactone is converted to carlactonoic acid by MAX1 in *Arabidopsis* and its methyl ester can directly interact with AtD14 in vitro. *Proceedings of the National Academy of Sciences* 111, 18084-18089.
- Ábrahám, E., Hourton-Cabassa, C., Erdei, L., Szabados, L. 2010. Methods for determination of proline in plants, In: Sunkar, R. (Ed.) *Plant Stress Tolerance (methods and protocols)*. Springer, New York, 317-331.
- Aguilar-Martínez, J.A., Poza-Carrión, C., Cubas, P., 2007. *Arabidopsis* BRANCHED1 acts as an integrator of branching signals within axillary buds. *The Plant Cell* 19, 458-472.
- Agusti, J., Herold, S., Schwarz, M., Sanchez, P., Ljung, K., Dun, E.A., Brewer, P.B., Beveridge, C.A., Sieberer, T., Sehr, E.M., 2011. Strigolactone signaling is required for auxin-dependent stimulation of secondary growth in plants. *Proceedings of the National Academy of Sciences* 108, 20242-20247.
- Ahammed, G.J., Li, X., Zhou, J., Zhou, Y.-H., Yu, J.-Q. 2016. Role of hormones in plant adaptation to heat stress, In: Ahammed, G.J., Yu, J.-Q. (Eds.) *Plant hormones under challenging environmental factors*. Springer, Dordrecht, 1-21.
- Akiyama, K., Matsuzaki, K.-i., Hayashi, H., 2005. Plant sesquiterpenes induce hyphal branching in arbuscular mycorrhizal fungi. *Nature* 435, 824-827.
- Akiyama, K., Ogasawara, S., Ito, S., Hayashi, H., 2010. Structural requirements of strigolactones for hyphal branching in AM fungi. *Plant and Cell Physiology* 51, 1104-1117.
- Alder, A., Jamil, M., Marzorati, M., Bruno, M., Vermathen, M., Bigler, P., Ghisla, S., Bouwmeester, H., Beyer, P., Al-Babili, S., 2012. The path from β -carotene to carlactone, a strigolactone-like plant hormone. *Science* 335, 1348-1351.
- Alscher, R.G., Castelfranco, P.A., 1972. Stimulation by ethylene of chlorophyll biosynthesis in dark-grown cucumber cotyledons. *Plant Physiology* 50, 400-403.
- Arite, T., Iwata, H., Ohshima, K., Maekawa, M., Nakajima, M., Kojima, M., Sakakibara, H., Kyojuka, J., 2007. DWARF10, an RMS1/MAX4/DAD1 ortholog, controls lateral bud outgrowth in rice. *The Plant Journal* 51, 1019-1029.
- Arite, T., Kameoka, H., Kyojuka, J., 2012. Strigolactone positively controls crown root elongation in rice. *Journal of Plant Growth Regulation* 31, 165-172.
- Armarego-Marriott, T., Sandoval-Ibañez, O., Kowalewska, Ł., 2019. Beyond the darkness: recent lessons from etiolation and de-etiolation studies. *Journal of Experimental Botany* 71, 1215-1225.

- Askari, E., Ehsanzadeh, P., 2015. Effectiveness of exogenous salicylic acid on root and shoot growth attributes, productivity, and water use efficiency of water-deprived fennel genotypes. *Horticulture, Environment, and Biotechnology* 56, 687-696.
- Asseng, S., Ewert, F., Martre, P., Rötter, R.P., Lobell, D.B., Cammarano, D., Kimball, B.A., Ottman, M.J., Wall, G., White, J.W., 2015. Rising temperatures reduce global wheat production. *Nature Climate Change* 5, 143-147.
- Awasthi, R., Bhandari, K., Nayyar, H., 2015. Temperature stress and redox homeostasis in agricultural crops. *Frontiers in Environmental Science* 3, 11.
- Balla, J., Kalousek, P., Reinöhl, V., Friml, J., Procházka, S., 2011. Competitive canalization of PIN-dependent auxin flow from axillary buds controls pea bud outgrowth. *The Plant Journal* 65, 571-577.
- Balla, J., Medved'ová, Z., Kalousek, P., Matiješuková, N., Friml, J., Reinöhl, V., Procházka, S., 2016. Auxin flow-mediated competition between axillary buds to restore apical dominance. *Scientific Reports* 6, 35955.
- Baunsgaard, L., Fuglsang, A.T., Jahn, T., Korthout, H., Palmgren, M., 1998. The 14-3-3 proteins associate with the plant plasma membrane H (+)-ATPase to generate a fusicoccin binding complex and a fusicoccin responsive system. *The Plant Journal* 13, 661-671.
- Baz, L., Mori, N., Mi, J., Jamil, M., Kountche, B.A., Guo, X., Balakrishna, A., Jia, K.-P., Vermathen, M., Akiyama, K., 2018. 3-Hydroxycaractone, a novel product of the strigolactone biosynthesis core pathway. *Molecular Plant* 11, 1312-1314.
- Beauchamp, C., Fridovich, I., 1971. Superoxide dismutase: improved assays and an assay applicable to acrylamide gels. *Analytical Biochemistry* 44, 276-287.
- Bennett, T., Liang, Y., Seale, M., Ward, S., Müller, D., Leyser, O., 2016. Strigolactone regulates shoot development through a core signalling pathway. *Biology Open* 5, 1806-1820.
- Bennett, T., Sieberer, T., Willett, B., Booker, J., Luschnig, C., Leyser, O., 2006. The *Arabidopsis* MAX pathway controls shoot branching by regulating auxin transport. *Current Biology* 16, 553-563.
- Bergkamp, B., Impa, S., Asebedo, A., Fritz, A., Jagadish, S.K., 2018. Prominent winter wheat varieties response to post-flowering heat stress under controlled chambers and field based heat tents. *Field Crops Research* 222, 143-152.
- Berry, J., Bjorkman, O., 1980. Photosynthetic response and adaptation to temperature in higher plants. *Annual Review of Plant Physiology* 31, 491-543.
- Bertheloot, J., Barbier, F., Boudon, F., Perez-García, M.D., Péron, T., Citerne, S., Dun, E., Beveridge, C., Godin, C., Sakr, S., 2020. Sugar availability suppresses the auxin-induced strigolactone pathway to promote bud outgrowth. *New Phytologist* 225, 866-879.

- Beveridge, C.A., 2000. Long-distance signalling and a mutational analysis of branching in pea. *Plant Growth Regulation* 32, 193-203.
- Booker, J., Auldridge, M., Wills, S., McCarty, D., Klee, H., Leyser, O., 2004. MAX3/CCD7 is a carotenoid cleavage dioxygenase required for the synthesis of a novel plant signaling molecule. *Current Biology* 14, 1232-1238.
- Bradford, M.M., 1976. A rapid and sensitive method for the quantitation of microgram quantities of protein utilizing the principle of protein-dye binding. *Analytical Biochemistry* 72, 248-254.
- Brand-Williams, W., Cuvelier, M.-E., Berset, C., 1995. Use of a free radical method to evaluate antioxidant activity. *LWT-Food Science and Technology* 28, 25-30.
- Braun, N., de Saint Germain, A., Pillot, J.-P., Boutet-Mercey, S., Dalmais, M., Antoniadi, I., Li, X., Maia-Grondard, A., Le Signor, C., Bouteiller, N., 2012. The pea TCP transcription factor PsBRC1 acts downstream of strigolactones to control shoot branching. *Plant Physiology* 158, 225-238.
- Brestic, M., Zivcak, M., Kalaji, H.M., Carpentier, R., Allakhverdiev, S.I., 2012. Photosystem II thermostability in situ: environmentally induced acclimation and genotype-specific reactions in *Triticum aestivum* L. *Plant Physiology and Biochemistry* 57, 93-105.
- Brestic, M., Zivcak, M., Olsovska, K., Repkova, J. 2013. Involvement of chlorophyll a fluorescence analyses for identification of sensitiveness of the photosynthetic apparatus to high temperature in selected wheat genotypes. In: *Photosynthesis Research for Food, Fuel and the Future*, Berlin, Heidelberg, 2013//, 510-513.
- Brewer, P.B., Dun, E.A., Gui, R., Mason, M.G., Beveridge, C.A., 2015. Strigolactone inhibition of branching independent of polar auxin transport. *Plant Physiology* 168, 1820-1829.
- Brewer, P.B., Yoneyama, K., Filardo, F., Meyers, E., Scaffidi, A., Frickey, T., Akiyama, K., Seto, Y., Dun, E.A., Cremer, J.E., 2016. *LATERAL BRANCHING OXIDOREDUCTASE* acts in the final stages of strigolactone biosynthesis in *Arabidopsis*. *Proceedings of the National Academy of Sciences* 113, 6301-6306.
- Brun, G., Braem, L., Thoiron, S., Gevaert, K., Goormachtig, S., Delavault, P., 2018. Seed germination in parasitic plants: what insights can we expect from strigolactone research? *Journal of Experimental Botany* 69, 2265-2280.
- Brun, G., Thoiron, S., Braem, L., Pouvreau, J.B., Montiel, G., Lechat, M.M., Simier, P., Gevaert, K., Goormachtig, S., Delavault, P., 2019. CYP707As are effectors of karrikin and strigolactone signalling pathways in *Arabidopsis thaliana* and parasitic plants. *Plant, Cell & Environment* 42, 2612-2626.
- Bruno, M., Al-Babili, S., 2016. On the substrate specificity of the rice strigolactone biosynthesis enzyme DWARF27. *Planta* 243, 1429-1440.

- Bruno, M., Hofmann, M., Vermathen, M., Alder, A., Beyer, P., Al-Babili, S., 2014. On the substrate-and stereospecificity of the plant carotenoid cleavage dioxygenase 7. *FEBS Letters* 588, 1802-1807.
- Bu, Q., Lv, T., Shen, H., Luong, P., Wang, J., Wang, Z., Huang, Z., Xiao, L., Engineer, C., Kim, T.H., 2014. Regulation of drought tolerance by the F-box protein MAX2 in *Arabidopsis*. *Plant Physiology* 164, 424-439.
- Čajánek, M., Štroch, M., Lachetová, I., Kalina, J., Spunda, V., 1998. Characterization of the photosystem II inactivation of heat-stressed barley leaves as monitored by the various parameters of chlorophyll a fluorescence and delayed fluorescence. *Journal of Photochemistry and Photobiology B: Biology* 47, 39-45.
- Cardoso, C., Zhang, Y., Jamil, M., Hepworth, J., Charnikhova, T., Dimkpa, S.O., Meharg, C., Wright, M.H., Liu, J., Meng, X., 2014. Natural variation of rice strigolactone biosynthesis is associated with the deletion of two MAX1 orthologs. *Proceedings of the National Academy of Sciences* 111, 2379-2384.
- Carlsson, G.H., Hasse, D., Cardinale, F., Prandi, C., Andersson, I., 2018. The elusive ligand complexes of the DWARF14 strigolactone receptor. *Journal of Experimental Botany* 69, 2345-2354.
- Cass, C.L., Peraldi, A., Dowd, P.F., Mottiar, Y., Santoro, N., Karlen, S.D., Bukhman, Y.V., Foster, C.E., Thrower, N., Bruno, L.C., Moskvina, O.V., Johnson, E.T., Willhoit, M.E., Phutane, M., Ralph, J., Mansfield, S.D., Nicholson, P., Sedbrook, J.C., 2015. Effects of *PHENYLALANINE AMMONIA LYASE (PAL)* knockdown on cell wall composition, biomass digestibility, and biotic and abiotic stress responses in *Brachypodium*. *Journal of Experimental Botany* 66, 4317-4335.
- Caverzan, A., Casassola, A., Brammer, S.P., 2016. Antioxidant responses of wheat plants under stress. *Genetics and Molecular Biology* 39, 1-6.
- Chang, M.-Y., Chen, S.-L., Lee, C.-F., Chen, Y.-M., 2001. Cold-acclimation and root temperature protection from chilling injury in chilling-sensitive mungbean (*Vigna radiata* L.) seedlings. *Botanical Bulletin of Academia Sinica* 42, 53-60.
- Charnikhova, T.V., Gaus, K., Lumbroso, A., Sanders, M., Vincken, J.-P., De Mesmaeker, A., Ruyter-Spira, C.P., Screpanti, C., Bouwmeester, H.J., 2017. Zealactones. Novel natural strigolactones from maize. *Phytochemistry* 137, 123-131.
- Charnikhova, T.V., Gaus, K., Lumbroso, A., Sanders, M., Vincken, J.-P., De Mesmaeker, A., Ruyter-Spira, C.P., Screpanti, C., Bouwmeester, H.J., 2018. Zeapyranolactone— A novel strigolactone from maize. *Phytochemistry Letters* 24, 172-178.
- Cheminant, S., Wild, M., Bouvier, F., Pelletier, S., Renou, J.-P., Erhardt, M., Hayes, S., Terry, M.J., Genschik, P., Achard, P., 2011. DELLAs regulate chlorophyll and carotenoid biosynthesis

- to prevent photooxidative damage during seedling deetiolation in *Arabidopsis*. *The Plant Cell* 23, 1849-1860.
- Chen, H., Zhang, J., Neff, M.M., Hong, S.-W., Zhang, H., Deng, X.-W., Xiong, L., 2008a. Integration of light and abscisic acid signaling during seed germination and early seedling development. *Proceedings of the National Academy of Sciences* 105, 4495-4500.
- Chen, L.-R., Ko, C.-Y., Folk, W.R., Lin, T.-Y., 2017. Chilling susceptibility in mungbean varieties is associated with their differentially expressed genes. *Botanical Studies* 58, 7-7.
- Chen, L.-S., Li, P., Cheng, L., 2008b. Effects of high temperature coupled with high light on the balance between photooxidation and photoprotection in the sun-exposed peel of apple. *Planta* 228, 745.
- Chen, S., Yang, J., Zhang, M., Strasser, R.J., Qiang, S., 2016. Classification and characteristics of heat tolerance in *Ageratina adenophora* populations using fast chlorophyll a fluorescence rise OJIP. *Environmental and Experimental Botany* 122, 126-140.
- Cheng, X., Floková, K., Bouwmeester, H., Ruyter-Spira, C., 2017. The role of endogenous strigolactones and their interaction with ABA during the infection process of the parasitic weed *Phelipanche ramosa* in tomato plants. *Frontiers in Plant Science* 8, 392.
- Chow, P.S., Landhäusser, S.M., 2004. A method for routine measurements of total sugar and starch content in woody plant tissues. *Tree Physiology* 24, 1129-1136.
- Cook, C., Whichard, L.P., Wall, M., Egley, G.H., Coggon, P., Luhan, P.A., McPhail, A., 1972. Germination stimulants. II. Structure of strigol, a potent seed germination stimulant for witchweed (*Striga lutea*). *Journal of the American Chemical Society* 94, 6198-6199.
- Cortleven, A., Schmülling, T., 2015. Regulation of chloroplast development and function by cytokinin. *Journal of Experimental Botany* 66, 4999-5013.
- Crawford, S., Shinohara, N., Sieberer, T., Williamson, L., George, G., Hepworth, J., Müller, D., Domagalska, M.A., Leyser, O., 2010. Strigolactones enhance competition between shoot branches by dampening auxin transport. *Development* 137, 2905-2913.
- Czarnecki, O., Yang, J., Weston, D.J., Tuskan, G.A., Chen, J.-G., 2013. A dual role of strigolactones in phosphate acquisition and utilization in plants. *International Journal of Molecular Sciences* 14, 7681-7701.
- da Costa, C.T., de Almeida, M.R., Ruedell, C.M., Schwambach, J., Maraschin, F.S., Fett-Neto, A.G., 2013. When stress and development go hand in hand: main hormonal controls of adventitious rooting in cuttings. *Frontiers in Plant Science* 4.
- Datta, S., Prescott, H., Dolan, L., 2015. Intensity of a pulse of RSL4 transcription factor synthesis determines *Arabidopsis* root hair cell size. *Nature Plants* 1, 1-6.

- Daws, M.I., Davies, J., Pritchard, H.W., Brown, N.A., Van Staden, J., 2007. Butenolide from plant-derived smoke enhances germination and seedling growth of arable weed species. *Plant Growth Regulation* 51, 73-82.
- De Cuyper, C., Fromentin, J., Yocgo, R.E., De Keyser, A., Guillotin, B., Kunert, K., Boyer, F.-D., Goormachtig, S., 2015. From lateral root density to nodule number, the strigolactone analogue GR24 shapes the root architecture of *Medicago truncatula*. *Journal of Experimental Botany* 66, 137-146.
- de Saint Germain, A., Clavé, G., Badet-Denisot, M.A., Pillot, J.P., Cornu, D., Le Caer, J.P., Burger, M., Pelissier, F., Retailleau, P., Turnbull, C., Bonhomme, S., Chory, J., Rameau, C., Boyer, F.D., 2016. An histidine covalent receptor and butenolide complex mediates strigolactone perception. *Nature Chemical Biology* 12, 787-794.
- de Saint Germain, A., Ligerot, Y., Dun, E.A., Pillot, J.-P., Ross, J.J., Beveridge, C.A., Rameau, C., 2013. Strigolactones stimulate internode elongation independently of gibberellins. *Plant Physiology* 163, 1012.
- Delaplace, P., Frettinger, P., Ghanem, M., Blondiaux, A., Bauwens, J., Cotton, S., de Clerck, C., Dewalque, A., Guy, J., Heuze, F., Massoz, A., Tassignon, T., Van Aubel, G., du Jardin, P., Fauconnier, M.-L., 2009. Lipoxygenase pathway and antioxidant system in salt stressed tomato seedlings (*Lycopersicon esculentum* Mill.). *Biotechnologie, Agronomie, Société et Environnement* 13, 529-536.
- Domagalska, M.A., Leyser, O., 2011. Signal integration in the control of shoot branching. *Nature Reviews Molecular Cell Biology* 12, 211-221.
- Druege, U., Franken, P., Hajirezaei, M.R., 2016. Plant hormone homeostasis, signaling, and function during adventitious root formation in cuttings. *Frontiers in Plant Science* 7.
- Druege, U., Hilo, A., Pérez-Pérez, J.M., Klopotek, Y., Acosta, M., Shahinnia, F., Zerche, S., Franken, P., Hajirezaei, M.R., 2019. Molecular and physiological control of adventitious rooting in cuttings: phytohormone action meets resource allocation. *Annals of Botany* 123, 929-949.
- Dun, E.A., de Saint Germain, A., Rameau, C., Beveridge, C.A., 2012. Antagonistic action of strigolactone and cytokinin in bud outgrowth control. *Plant Physiology* 158, 487.
- Dun, E.A., de Saint Germain, A., Rameau, C., Beveridge, C.A., 2013. Dynamics of strigolactone function and shoot branching responses in *Pisum sativum*. *Molecular Plant* 6, 128-140.
- Egli, D., TeKrony, D., Spears, J., 2005. Effect of high temperature stress during different stages of seed development in soybean [*Glycine max* (L.) Merrill]. *Seed Technology*, 177-189.
- Ergin, S., Gülen, H., Kesici, M., Turhan, E., Ipek, A., Köksal, N., 2016. Effects of high temperature stress on enzymatic and nonenzymatic antioxidants and proteins in strawberry plants. *Turkish Journal of Agriculture and Forestry* 40, 908-917.

- Essemine, J., Ammar, S., Jbir, N., Bouzid, S., 2007. Sensitivity of two wheat species's seeds (*Triticum durum*, Variety Karim and *Triticum aestivum*, Variety Salambo) to heat constraint during germination. *Pakistan Journal of Biological Sciences* 10, 3762-3768.
- Essemine, J., Govindachary, S., Ammar, S., Bouzid, S., Carpentier, R., 2011. Abolition of photosystem I cyclic electron flow in *Arabidopsis thaliana* following thermal-stress. *Plant Physiology and Biochemistry* 49, 235-243.
- Falhof, J., Pedersen, J.T., Fuglsang, A.T., Palmgren, M., 2016. Plasma membrane H⁺-ATPase regulation in the center of plant physiology. *Molecular Plant* 9, 323-337.
- Feng, Y., Xu, P., Li, B., Li, P., Wen, X., An, F., Gong, Y., Xin, Y., Zhu, Z., Wang, Y., Guo, H., 2017. Ethylene promotes root hair growth through coordinated EIN3/EIL1 and RHD6/RSL1 activity in *Arabidopsis*. *Proceedings of the National Academy of Sciences* 114, 13834.
- Ferrero, M., Pagliarani, C., Novák, O., Ferrandino, A., Cardinale, F., Visentin, I., Schubert, A., 2018. Exogenous strigolactone interacts with abscisic acid-mediated accumulation of anthocyanins in grapevine berries. *Journal of Experimental Botany* 69, 2391-2401.
- Flematti, G.R., Ghisalberti, E.L., Dixon, K.W., Trengove, R.D., 2004. A compound from smoke that promotes seed germination. *Science* 305, 977.
- Flematti, G.R., Waters, M.T., Scaffidi, A., Merritt, D.J., Ghisalberti, E.L., Dixon, K.W., Smith, S.M., 2013. Karrikin and cyanohydrin smoke signals provide clues to new endogenous plant signaling compounds. *Molecular Plant* 6, 29-37.
- Foo, E., 2013. Auxin influences strigolactones in pea mycorrhizal symbiosis. *Journal of Plant Physiology* 170, 523-528.
- Foo, E., Davies, N.W., 2011. Strigolactones promote nodulation in pea. *Planta* 234, 1073.
- Foo, E., Yoneyama, K., Hugill, C.J., Quittenden, L.J., Reid, J.B., 2013. Strigolactones and the regulation of pea symbioses in response to nitrate and phosphate deficiency. *Molecular Plant* 6, 76-87.
- Gao, Z., Qian, Q., Liu, X., Yan, M., Feng, Q., Dong, G., Liu, J., Han, B., 2009. Dwarf 88, a novel putative esterase gene affecting architecture of rice plant. *Plant Molecular Biology* 71, 265-276.
- Gardner, H.W., 2001. Analysis of lipoxygenase activity and products. *Current Protocols in Food Analytical Chemistry* 00, C4.2.1-C4.2.16.
- Genre, A., Chabaud, M., Balzergue, C., Puech-Pagès, V., Novero, M., Rey, T., Fournier, J., Rochange, S., Bécard, G., Bonfante, P., Barker, D.G., 2013. Short-chain chitin oligomers from arbuscular mycorrhizal fungi trigger nuclear Ca²⁺ spiking in *Medicago truncatula* roots and their production is enhanced by strigolactone. *New Phytologist* 198, 190-202.
- Goh, T., Kasahara, H., Mimura, T., Kamiya, Y., Fukaki, H., 2012. Multiple AUX/IAA-ARF modules regulate lateral root formation: the role of *Arabidopsis* SHY2/IAA3-mediated auxin

- signalling. *Philosophical Transactions of the Royal Society of London. Series B, Biological Sciences* 367, 1461-1468.
- González, L., González-Vilar, M. 2001. Determination of relative water content, In: Reigosa Roger, M.J. (Ed.) *Handbook of plant ecophysiology techniques*. Springer Netherlands, Dordrecht, 207-212.
- Grellet Bournonville, C.F., Díaz-Ricci, J.C., 2011. Quantitative determination of superoxide in plant leaves using a modified NBT staining method. *Phytochemical Analysis* 22, 268-271.
- Guan, J.C., Koch, K.E., Suzuki, M., Wu, S., Latshaw, S., Petruff, T., Goulet, C., Klee, H.J., McCarty, D.R., 2012. Diverse roles of strigolactone signaling in maize architecture and the uncoupling of a branching-specific subnetwork. *Plant Physiology* 160, 1303.
- Guan, L., Tayengwa, R., Cheng, Z., Peer, W.A., Murphy, A.S., Zhao, M., 2019. Auxin regulates adventitious root formation in tomato cuttings. *BMC Plant Biology* 19, 435.
- Guillotín, B., Etemadi, M., Audran, C., Bouzayen, M., Bécard, G., Combier, J.-P., 2017. SI-IAA27 regulates strigolactone biosynthesis and mycorrhization in tomato (var. MicroTom). *The New Phytologist* 213, 1124-1132.
- Guo dong, L., Pan, L., Jiang, K., Takahashi, I., Nakamura, H., Xu, Y., Asami, T., Shen, R.F., 2016. Strigolactones are involved in sugar signaling to modulate early seedling development in *Arabidopsis*. *Plant Biotechnology* 33, 1–11.
- Guo, M., Liu, J.-H., Ma, X., Luo, D.-X., Gong, Z.-H., Lu, M.-H., 2016. The plant heat stress transcription factors (HSFs): structure, regulation, and function in response to abiotic stresses. *Frontiers in Plant Science* 7, 114.
- Guo, S., Xu, Y., Liu, H., Mao, Z., Zhang, C., Ma, Y., Zhang, Q., Meng, Z., Chong, K., 2013. The interaction between OsMADS57 and OsTB1 modulates rice tillering via *DWARF14*. *Nature Communications* 4, 1566.
- Guye, M.G., Vigh, L., Wilson, J.M., 1987. Choline induced chill-tolerance in mung bean (*Vigna radiata* L. Wilcz.). *Plant Science* 53, 223-228.
- Ha, C.V., Leyva-González, M.A., Osakabe, Y., Tran, U.T., Nishiyama, R., Watanabe, Y., Tanaka, M., Seki, M., Yamaguchi, S., Dong, N.V., Yamaguchi-Shinozaki, K., Shinozaki, K., Herrera-Estrella, L., Tran, L.-S.P., 2014. Positive regulatory role of strigolactone in plant responses to drought and salt stress. *Proceedings of the National Academy of Sciences of the United States of America* 111, 851-856.
- Haider, I., Andreo-Jimenez, B., Bruno, M., Bimbo, A., Floková, K., Abuauf, H., Ntui, V.O., Guo, X., Charnikhova, T., Al-Babili, S., Bouwmeester, H.J., Ruyter-Spira, C., 2018. The interaction of strigolactones with abscisic acid during the drought response in rice. *Journal of Experimental Botany* 69, 2403-2414.

- Hamiaux, C., Drummond, R.S., Luo, Z., Lee, H.W., Sharma, P., Janssen, B.J., Perry, N.B., Denny, W.A., Snowden, K.C., 2018. Inhibition of strigolactone receptors by N-phenylanthranilic acid derivatives: structural and functional insights. *Journal of Biological Chemistry* 293, 6530-6543.
- Hamiaux, C., Drummond, R.S.M., Janssen, B.J., Ledger, S.E., Cooney, J.M., Newcomb, R.D., Snowden, K.C., 2012. DAD2 is an α/β hydrolase likely to be involved in the perception of the plant branching hormone, strigolactone. *Current Biology* 22, 2032-2036.
- Hauck, C., Müller, S., Schildknecht, H., 1992. A germination stimulant for parasitic flowering plants from *Sorghum bicolor*, a genuine host plant. *Journal of Plant Physiology* 139, 474-478.
- Havaux, M., 1993. Characterization of thermal damage to the photosynthetic electron transport system in potato leaves. *Plant Science* 94, 19-33.
- Havaux, M., 1998. Carotenoids as membrane stabilizers in chloroplasts. *Trends in Plant Science* 3, 147-151.
- Havaux, M., Greppin, H., Strasser, R.J., 1991. Functioning of photosystems I and II in pea leaves exposed to heat stress in the presence or absence of light. *Planta* 186, 88-98.
- Haworth, M., Marino, G., Brunetti, C., Killi, D., De Carlo, A., Centritto, M., 2018. The impact of heat stress and water deficit on the photosynthetic and stomatal physiology of olive (*Olea europaea* L.)—A case study of the 2017 heat wave. *Plants* 7, 76.
- Hayward, A., Stirnberg, P., Beveridge, C., Leyser, O., 2009. Interactions between auxin and strigolactone in shoot branching control. *Plant Physiology* 151, 400.
- Hayward, S., Cilliers, T., Swart, P., 2017. Lipoxygenases: from isolation to application. *Comprehensive Reviews in Food Science and Food Safety* 16, 199-211.
- Heath, R.L., Packer, L., 1968. Photoperoxidation in isolated chloroplasts: I. Kinetics and stoichiometry of fatty acid peroxidation. *Archives of Biochemistry and Biophysics* 125, 189-198.
- Herrera-Vásquez, A., Salinas, P., Holuigue, L., 2015. Salicylic acid and reactive oxygen species interplay in the transcriptional control of defense genes expression. *Frontiers in Plant Science* 6.
- Hodges, D.M., Andrews, C.J., Johnson, D.A., Hamilton, R.I., 1997. Antioxidant enzyme responses to chilling stress in differentially sensitive inbred maize lines. *Journal of Experimental Botany* 48, 1105-1113.
- Hohm, T., Demarsy, E., Quan, C., Allenbach Petrolati, L., Preuten, T., Vernoux, T., Bergmann, S., Fankhauser, C., 2014. Plasma membrane H⁺-ATPase regulation is required for auxin gradient formation preceding phototropic growth. *Molecular Systems Biology* 10, 751-751.
- Hoque, M.A., Banu, M.N.A., Nakamura, Y., Shimoishi, Y., Murata, Y., 2008. Proline and glycinebetaine enhance antioxidant defense and methylglyoxal detoxification systems and

- reduce NaCl-induced damage in cultured tobacco cells. *Journal of Plant Physiology* 165, 813-824.
- Hu, Q., Zhang, S., Huang, B., 2018. Strigolactones and interaction with auxin regulating root elongation in tall fescue under different temperature regimes. *Plant Science* 271, 34-39.
- Hussain, H.A., Hussain, S., Khaliq, A., Ashraf, U., Anjum, S.A., Men, S., Wang, L., 2018. Chilling and drought stresses in crop plants: Implications, cross talk, and potential management opportunities. *Frontiers in Plant Science* 9, 393.
- Hussain, S., Khan, F., Cao, W., Wu, L., Geng, M., 2016. Seed priming alters the production and detoxification of reactive oxygen intermediates in rice seedlings grown under sub-optimal temperature and nutrient supply. *Frontiers in Plant Science* 7, 439.
- Iloh, A., Omatta, G., Ogbadu, G., Onyenekwe, P., 2014. Effects of elevated temperature on seed germination and seedling growth on three cereal crops in Nigeria. *Scientific Research and Essays* 9, 806-813.
- Ioio, R.D., Linhares, F.S., Scacchi, E., Casamitjana-Martinez, E., Heidstra, R., Costantino, P., Sabatini, S., 2007. Cytokinins determine *Arabidopsis* root-meristem size by controlling cell differentiation. *Current Biology* 17, 678-682.
- Ioio, R.D., Nakamura, K., Moubayidin, L., Perilli, S., Taniguchi, M., Morita, M.T., Aoyama, T., Costantino, P., Sabatini, S., 2008. A genetic framework for the control of cell division and differentiation in the root meristem. *Science* 322, 1380-1384.
- Iseki, M., Shida, K., Kuwabara, K., Wakabayashi, T., Mizutani, M., Takikawa, H., Sugimoto, Y., 2018. Evidence for species-dependent biosynthetic pathways for converting carlactone to strigolactones in plants. *Journal of Experimental Botany* 69, 2305-2318.
- Ito, S., Ito, K., Abeta, N., Takahashi, R., Sasaki, Y., Yajima, S., 2016. Effects of strigolactone signaling on *Arabidopsis* growth under nitrogen deficient stress condition. *Plant Signaling & Behavior* 11, e1126031-e1126031.
- Ito, S., Umehara, M., Hanada, A., Yamaguchi, S., Asami, T., 2013. Tebuconazole derivatives are potent inhibitors of strigolactone biosynthesis. *Journal of Pesticide Science* 38, 147-151.
- Ito, S., Yamagami, D., Umehara, M., Hanada, A., Yoshida, S., Sasaki, Y., Yajima, S., Kyojuka, J., Ueguchi-Tanaka, M., Matsuoka, M., Shirasu, K., Yamaguchi, S., Asami, T., 2017. Regulation of strigolactone biosynthesis by gibberellin signaling. *Plant Physiology* 174, 1250-1259.
- Jedrowski, C., Brüggemann, W., 2015. Imaging of fast chlorophyll fluorescence induction curve (OJIP) parameters, applied in a screening study with wild barley (*Hordeum spontaneum*) genotypes under heat stress. *Journal of Photochemistry and Photobiology B: Biology* 151, 153-160.

- Ji, Y., Liu, J., Xing, D., 2016. Low concentrations of salicylic acid delay methyl jasmonate-induced leaf senescence by up-regulating nitric oxide synthase activity. *Journal of Experimental Botany* 67, 5233-5245.
- Jia, K.-P., Luo, Q., He, S., Lu, X.-D., Yang, H.-Q., 2014. Strigolactone-regulated hypocotyl elongation is dependent on cryptochrome and phytochrome signaling pathways in *Arabidopsis*. *Molecular Plant* 7, 528-540.
- Jiang, L., Liu, X., Xiong, G., Liu, H., Chen, F., Wang, L., Meng, X., Liu, G., Yu, H., Yuan, Y., Yi, W., Zhao, L., Ma, H., He, Y., Wu, Z., Melcher, K., Qian, Q., Xu, H.E., Wang, Y., Li, J., 2013. DWARF 53 acts as a repressor of strigolactone signalling in rice. *Nature* 504, 401-405.
- Jiang, L., Matthys, C., Marquez-Garcia, B., De Cuyper, C., Smet, L., De Keyser, A., Boyer, F.-D., Beeckman, T., Depuydt, S., Goormachtig, S., 2016. Strigolactones spatially influence lateral root development through the cytokinin signaling network. *Journal of Experimental Botany* 67, 379-389.
- Josse, E.-M., Halliday, K.J., 2008. Skotomorphogenesis: The dark side of light signalling. *Current Biology* 18, R1144-R1146.
- Junglee, S., Urban, L., Huguette, S., Lopez, F., 2014. Optimized assay for hydrogen peroxide determination in plant tissue using potassium iodide. *American Journal of Analytical Chemistry* 5, 730-736.
- Kader, M., 2005. A comparison of seed germination calculation formulae and the associated interpretation of resulting data. *Journal and Proceeding of the Royal Society of New South Wales* 138, 65-75.
- Kalaji, H.M., Bąba, W., Gediga, K., Goltsev, V., Samborska, I.A., Cetner, M.D., Dimitrova, S., Piszcz, U., Bielecki, K., Karmowska, K., 2018. Chlorophyll fluorescence as a tool for nutrient status identification in rapeseed plants. *Photosynthesis Research* 136, 329-343.
- Kalaji, H.M., Jajoo, A., Oukarroum, A., Brestic, M., Zivcak, M., Samborska, I.A., Cetner, M.D., Łukasik, I., Goltsev, V., Ladle, R.J., 2016. Chlorophyll a fluorescence as a tool to monitor physiological status of plants under abiotic stress conditions. *Acta Physiologiae Plantarum* 38, 102.
- Kalaji, H.M., Oukarroum, A., Alexandrov, V., Kouzmanova, M., Brestic, M., Zivcak, M., Samborska, I.A., Cetner, M.D., Allakhverdiev, S.I., Goltsev, V., 2014. Identification of nutrient deficiency in maize and tomato plants by in vivo chlorophyll a fluorescence measurements. *Plant Physiology and Biochemistry* 81, 16-25.
- Kapulnik, Y., Delaux, P.-M., Resnick, N., Mayzlish-Gati, E., Wininger, S., Bhattacharya, C., Séjalon-Delmas, N., Combiér, J.-P., Bécárd, G., Belausov, E., Beeckman, T., Dor, E.,

- Hershenhorn, J., Koltai, H., 2011a. Strigolactones affect lateral root formation and root-hair elongation in *Arabidopsis*. *Planta* 233, 209-216.
- Kapulnik, Y., Resnick, N., Mayzlish-Gati, E., Kaplan, Y., Wininger, S., Hershenhorn, J., Koltai, H., 2011b. Strigolactones interact with ethylene and auxin in regulating root-hair elongation in *Arabidopsis*. *Journal of Experimental Botany* 62, 2915-2924.
- Khan, M.I.R., Fatma, M., Per, T.S., Anjum, N.A., Khan, N.A., 2015. Salicylic acid-induced abiotic stress tolerance and underlying mechanisms in plants. *Frontiers in Plant Science* 6.
- Kim, H., Cha, H.-C., 2015. Effect of gibberellin on the adventitious root formation from the leaves-derived calli in *Persicaria perfoliata*. *Journal of Life Science* 25, 390-396.
- Kim, H.I., Kisugi, T., Khetkam, P., Xie, X., Yoneyama, K., Uchida, K., Yokota, T., Nomura, T., McErlean, C.S.P., Yoneyama, K., 2014. Avenaol, a germination stimulant for root parasitic plants from *Avena strigosa*. *Phytochemistry* 103, 85-88.
- Kim, H.I., Xie, X., Kim, H.S., Chun, J.C., Yoneyama, K., Nomura, T., Takeuchi, Y., Yoneyama, K., 2010. Structure-activity relationship of naturally occurring strigolactones in *Orobancha minor* seed germination stimulation. *Journal of Pesticide Science* 35, 344-347.
- Kitajima, M., Butler, W., 1975. Quenching of chlorophyll fluorescence and primary photochemistry in chloroplasts by dibromothymoquinone. *Biochimica et Biophysica Acta (BBA)-Bioenergetics* 376, 105-115.
- Kobayashi, K., 2016. Role of membrane glycerolipids in photosynthesis, thylakoid biogenesis and chloroplast development. *Journal of Plant Research* 129, 565-580.
- Kohlen, W., Ng, J.L.P., Deinum, E.E., Mathesius, U., 2017. Auxin transport, metabolism, and signalling during nodule initiation: indeterminate and determinate nodules. *Journal of Experimental Botany* 69, 229-244.
- Koltai, H., 2013. Strigolactones activate different hormonal pathways for regulation of root development in response to phosphate growth conditions. *Annals of Botany* 112, 409-415.
- Koltai, H., 2015. Cellular events of strigolactone signalling and their crosstalk with auxin in roots. *Journal of Experimental Botany* 66, 4855-4861.
- Koltai, H., Dor, E., Hershenhorn, J., Joel, D.M., Weininger, S., Lekalla, S., Shealtiel, H., Bhattacharya, C., Eliahu, E., Resnick, N., Barg, R., Kapulnik, Y., 2010. Strigolactones' effect on root growth and root-hair elongation may be mediated by auxin-efflux carriers. *Journal of Plant Growth Regulation* 29, 129-136.
- Koren, D., Resnick, N., Gati, E.M., Belausov, E., Weininger, S., Kapulnik, Y., Koltai, H., 2013. Strigolactone signaling in the endodermis is sufficient to restore root responses and involves SHORT HYPOCOTYL 2 (SHY2) activity. *New Phytologist* 198, 866-874.

- Kouřil, R., Lazár, D., Ilík, P., Skotnica, J., Krchňák, P., Nauš, J., 2004. High-temperature induced chlorophyll fluorescence rise in plants at 40–50 C: experimental and theoretical approach. *Photosynthesis Research* 81, 49-66.
- Kowalewska, Ł., Bykowski, M., Mostowska, A., 2019. Spatial organization of thylakoid network in higher plants. *Botany Letters* 166, 326-343.
- Kretschmar, T., Kohlen, W., Sasse, J., Borghi, L., Schlegel, M., Bachelier, J.B., Reinhardt, D., Bours, R., Bouwmeester, H.J., Martinoia, E., 2012. A petunia ABC protein controls strigolactone-dependent symbiotic signalling and branching. *Nature* 483, 341-344.
- Kulkarni, M.G., Ascough, G.D., Verschaeve, L., Baeten, K., Arruda, M.P., Van Staden, J., 2010. Effect of smoke-water and a smoke-isolated butenolide on the growth and genotoxicity of commercial onion. *Scientia Horticulturae* 124, 434-439.
- Kumar, M., Pandya-Kumar, N., Dam, A., Haor, H., Mayzlish-Gati, E., Belausov, E., Winer, S., Abu-Abied, M., McErlean, C.S.P., Bromhead, L.J., Prandi, C., Kapulnik, Y., Koltai, H., 2015. Arabidopsis response to low-phosphate conditions includes active changes in actin filaments and PIN2 polarization and is dependent on strigolactone signalling. *Journal of Experimental Botany* 66, 1499-1510.
- Lanfranco, L., Fiorilli, V., Venice, F., Bonfante, P., 2017. Strigolactones cross the kingdoms: plants, fungi, and bacteria in the arbuscular mycorrhizal symbiosis. *Journal of Experimental Botany* 69, 2175-2188.
- Lantzouni, O., Klermund, C., Schwechheimer, C., 2017. Largely additive effects of gibberellin and strigolactone on gene expression in *Arabidopsis thaliana* seedlings. *The Plant Journal* 92, 924-938.
- Lauresergues, D., André, O., Peng, J., Wen, J., Chen, R., Ratet, P., Tadege, M., Mysore, K.S., Rochange, S.F., 2015. Strigolactones contribute to shoot elongation and to the formation of leaf margin serrations in *Medicago truncatula* R108. *Journal of Experimental Botany* 66, 1237-1244.
- Le Gall, H., Philippe, F., Domon, J.-M., Gillet, F., Pelloux, J., Rayon, C., 2015. Cell wall metabolism in response to abiotic stress. *Plants (Basel, Switzerland)* 4, 112-166.
- Lee, H.Y., Yoon, G.M., 2020. Strigolactone elevates ethylene biosynthesis in etiolated *Arabidopsis* seedlings. *Plant Signaling & Behavior* 15, 1805232.
- Lee, S.H., Ahn, S.J., Im, Y.J., Cho, K., Chung, G.-C., Cho, B.-H., Han, O., 2005. Differential impact of low temperature on fatty acid unsaturation and lipoxygenase activity in figleaf gourd and cucumber roots. *Biochemical and Biophysical Research Communications* 330, 1194-1198.
- Lewis, D.R., Negi, S., Sukumar, P., Muday, G.K., 2011. Ethylene inhibits lateral root development, increases IAA transport and expression of PIN3 and PIN7 auxin efflux carriers. *Development* 138, 3485.

- Leyser, O., 2018. Auxin Signaling. *Plant Physiology* 176, 465.
- Leyva, A., Jarillo, J.A., Salinas, J., Martinez-Zapater, J.M., 1995. Low temperature induces the accumulation of phenylalanine ammonia-lyase and chalcone synthase mRNAs of *Arabidopsis thaliana* in a light-dependent manner. *Plant Physiology* 108, 39-46.
- Li, J., Yang, Y., Sun, K., Chen, Y., Chen, X., Li, X., 2019. Exogenous melatonin enhances cold, salt and drought stress tolerance by improving antioxidant defense in tea plant (*Camellia sinensis* (L.) O. Kuntze). *Molecules* 24, 1826.
- Li, S.-W., Xue, L., 2010. The interaction between H₂O₂ and NO, Ca²⁺, cGMP, and MAPKs during adventitious rooting in mung bean seedlings. *In Vitro Cellular & Developmental Biology - Plant* 46, 142-148.
- Li, S.-W., Xue, L., Xu, S., Feng, H., An, L., 2009. Hydrogen peroxide acts as a signal molecule in the adventitious root formation of mung bean seedlings. *Environmental and Experimental Botany* 65, 63-71.
- Li, S., Xue, L., Xu, S., Feng, H., An, L., 2007. Hydrogen peroxide involvement in formation and development of adventitious roots in cucumber. *Plant Growth Regulation* 52, 173-180.
- Li, W., Nguyen, K.H., Chu, H.D., Ha, C.V., Watanabe, Y., Osakabe, Y., Leyva-González, M.A., Sato, M., Toyooka, K., Voges, L., Tanaka, M., Mostofa, M.G., Seki, M., Seo, M., Yamaguchi, S., Nelson, D.C., Tian, C., Herrera-Estrella, L., Tran, L.-S.P., 2017. The karrikin receptor KAI2 promotes drought resistance in *Arabidopsis thaliana*. *PLOS Genetics* 13, e1007076.
- Li, W., Nguyen, K.H., Watanabe, Y., Yamaguchi, S., Tran, L.-S.P., 2016. OaMAX2 of *Orobanchae aegyptiaca* and *Arabidopsis* AtMAX2 share conserved functions in both development and drought responses. *Biochemical and Biophysical Research Communications* 478, 521-526.
- Liang, S.-m., Kuang, J.-f., Ji, S.-j., Chen, Q.-f., Deng, W., Min, T., Shan, W., Chen, J.-y., Lu, W.-j., 2020. The membrane lipid metabolism in horticultural products suffering chilling injury. *Food Quality and Safety* 4, 9-14.
- Liang, X., Zhang, L., Natarajan, S.K., Becker, D.F., 2013. Proline mechanisms of stress survival. *Antioxidants & Redox Signaling* 19, 998-1011.
- Liao, W., Huang, G., Yu, J., Zhang, M., Shi, X., 2011. Nitric oxide and hydrogen peroxide are involved in indole-3-butyric acid-induced adventitious root development in marigold. *The Journal of Horticultural Science and Biotechnology* 86, 159-165.
- Lichtenthaler, H.K. 1987. Chlorophylls and carotenoids: Pigments of photosynthetic biomembranes, In: Packer, L., Douce, R. (Eds.) *Methods in Enzymology*. Academic Press, 350-382.

- Light, M.E., Burger, B.V., Staerk, D., Kohout, L., Van Staden, J., 2010. Butenolides from plant-derived smoke: Natural plant-growth regulators with antagonistic actions on seed germination. *Journal of Natural Products* 73, 267-269.
- Lim, C.W., Han, S.-W., Hwang, I.S., Kim, D.S., Hwang, B.K., Lee, S.C., 2015. The pepper lipoxygenase *CaLOX1* plays a role in osmotic, drought and high salinity stress response. *Plant and Cell Physiology* 56, 930-942.
- Lin, C., Sauter, M., 2019. Polar auxin transport determines adventitious root emergence and growth in rice. *Frontiers in Plant Science* 10, 444-444.
- Lischweski, S., Muchow, A., Guthörl, D., Hause, B., 2015. Jasmonates act positively in adventitious root formation in petunia cuttings. *BMC Plant Biology* 15, 229-229.
- Liu, G.-T., Ma, L., Duan, W., Wang, B.-C., Li, J.-H., Xu, H.-G., Yan, X.-Q., Yan, B.-F., Li, S.-H., Wang, L.-J., 2014a. Differential proteomic analysis of grapevine leaves by iTRAQ reveals responses to heat stress and subsequent recovery. *BMC Plant Biology* 14, 110.
- Liu, G., Pfeifer, J., de Brito Francisco, R., Emonet, A., Stirnemann, M., Gübeli, C., Hutter, O., Sasse, J., Mattheyer, C., Stelzer, E., Walter, A., Martinoia, E., Borghi, L., 2018. Changes in the allocation of endogenous strigolactone improve plant biomass production on phosphate-poor soils. *New Phytologist* 217, 784-798.
- Liu, H., Wang, S., Yu, X., Yu, J., He, X., Zhang, S., Shou, H., Wu, P., 2005. ARL1, a LOB-domain protein required for adventitious root formation in rice. *The Plant Journal* 43, 47-56.
- Liu, J., Cheng, X., Liu, P., Sun, J., 2017a. miR156-Targeted SBP-Box transcription factors interact with DWARF53 to regulate *TEOSINTE BRANCHED1* and *BARREN STALK1* expression in bread wheat. *Plant Physiology* 174, 1931.
- Liu, J., He, H., Vitali, M., Visentin, I., Charnikhova, T., Haider, I., Schubert, A., Ruyter-Spira, C., Bouwmeester, H.J., Lovisolo, C., Cardinale, F., 2015. Osmotic stress represses strigolactone biosynthesis in *Lotus japonicus* roots: exploring the interaction between strigolactones and ABA under abiotic stress. *Planta* 241, 1435-1451.
- Liu, J., Moore, S., Chen, C., Lindsey, K., 2017b. Crosstalk complexities between auxin, cytokinin, and ethylene in arabidopsis root development: From experiments to systems modeling, and back again. *Molecular Plant* 10, 1480-1496.
- Liu, L., Jia, C., Zhang, M., Chen, D., Chen, S., Guo, R., Guo, D., Wang, Q., 2014b. Ectopic expression of a *BZR1-ID* transcription factor in brassinosteroid signalling enhances carotenoid accumulation and fruit quality attributes in tomato. *Plant Biotechnology Journal* 12, 105-115.
- Liu, L., Shao, Z., Zhang, M., Wang, Q., 2014c. Regulation of carotenoid metabolism in tomato. *Molecular Plant* 8, 28-39.

- Liu, L., Wei, J., Zhang, M., Zhang, L., Li, C., Wang, Q., 2012. Ethylene independent induction of lycopene biosynthesis in tomato fruits by jasmonates. *Journal of Experimental Botany* 63, 5751-5761.
- Liu, W., Kohlen, W., Lillo, A., Op den Camp, R., Ivanov, S., Hartog, M., Limpens, E., Jamil, M., Smaczniak, C., Kaufmann, K., Yang, W.-C., Hooiveld, G.J.E.J., Charnikhova, T., Bouwmeester, H.J., Bisseling, T., Geurts, R., 2011. Strigolactone biosynthesis in *Medicago truncatula* and rice requires the symbiotic GRAS-type transcription factors NSP1 and NSP2. *The Plant Cell* 23, 3853-3865.
- Liu, X., Li, Y., Zhong, S., 2017c. Interplay between light and plant hormones in the control of *Arabidopsis* seedling chlorophyll biosynthesis. *Frontiers in Plant Science* 8, 1433.
- Lo, S.-F., Yang, S.-Y., Chen, K.-T., Hsing, Y.-I., Zeevaart, J.A.D., Chen, L.-J., Yu, S.-M., 2008. A novel class of gibberellin 2-oxidases control semidwarfism, tillering, and root development in rice. *The Plant Cell* 20, 2603.
- López-Ráez, J.A., Kohlen, W., Charnikhova, T., Mulder, P., Undas, A.K., Sergeant, M.J., Verstappen, F., Bugg, T.D.H., Thompson, A.J., Ruyter-Spira, C., Bouwmeester, H., 2010. Does abscisic acid affect strigolactone biosynthesis? *New Phytologist* 187, 343-354.
- Lukatkin, A., Brazaitytė, A., Bobinas, C., Duchovskis, P., 2012. Chilling injury in chilling-sensitive plants: A review. *Žemdirbystė* 99, 111-124.
- Luo, H.-B., Ma, L., Xi, H.-F., Duan, W., Li, S.-H., Loescher, W., Wang, J.-F., Wang, L.-J., 2011. Photosynthetic responses to heat treatments at different temperatures and following recovery in grapevine (*Vitis amurensis* L.) leaves. *PLoS One* 6, e23033.
- Lv, S., Zhang, Y., Li, C., Liu, Z., Yang, N., Pan, L., Wu, J., Wang, J., Yang, J., Lv, Y., Zhang, Y., Jiang, W., She, X., Wang, G., 2018. Strigolactone-triggered stomatal closure requires hydrogen peroxide synthesis and nitric oxide production in an abscisic acid-independent manner. *New Phytologist* 217, 290-304.
- Ma, H., Duan, J., Ke, J., He, Y., Gu, X., Xu, T.-H., Yu, H., Wang, Y., Brunzelle, J.S., Jiang, Y., Rothbart, S.B., Xu, H.E., Li, J., Melcher, K., 2017a. A D53 repression motif induces oligomerization of TOPLESS corepressors and promotes assembly of a corepressor-nucleosome complex. *Science Advances* 3, e1601217-e1601217.
- Ma, N., Hu, C., Wan, L., Hu, Q., Xiong, J., Zhang, C., 2017b. Strigolactones improve plant growth, photosynthesis, and alleviate oxidative stress under salinity in rapeseed (*Brassica napus* L.) by regulating gene expression. *Frontiers in Plant Science* 8, 1671.
- Małgorzata, J., Wdowikowska, A., Klobus, G. 2018. Assay of plasma membrane H⁺-ATPase in plant tissues under abiotic stresses, In: Mock, H.-P., Matros, A., Witzel, K. (Eds.) *Plant membrane proteomics: Methods and protocols*. Humana Press, New York, 205-215.

- Manandhar, S., Funnell, K., Woolley, D., Cooney, J., 2018. Interaction between strigolactone and cytokinin on axillary and adventitious bud development in *Zantedeschia*. . Journal of Plant Physiology & Pathology 6, 2.
- Mao, J., Zhang, D., Meng, Y., Li, K., Wang, H., Han, M., 2019. Inhibition of adventitious root development in apple rootstocks by cytokinin is based on its suppression of adventitious root primordia formation. Physiologia Plantarum 166, 663-676.
- Marre, E., 1979. Fusicoccin: a tool in plant physiology. Annual Review of Plant Physiology 30, 273-288.
- Marzec, M., Gruszka, D., Tylec, P., Szarejko, I., 2016. Identification and functional analysis of the *HvD14* gene involved in strigolactone signaling in *Hordeum vulgare*. Physiologia Plantarum 158, 341-355.
- Marzec, M., Melzer, M., 2018. Regulation of root development and architecture by strigolactones under optimal and nutrient deficiency conditions. International Journal of Molecular Sciences 19, 1887.
- Marzec, M., Muszynska, A., 2015. *In silico* analysis of the genes encoding proteins that are involved in the biosynthesis of the RMS/MAX/D pathway revealed new roles of strigolactones in plants. International Journal of Molecular Sciences 16, 6757-6782.
- Mayzlish-Gati, E., De-Cuyper, C., Goormachtig, S., Beeckman, T., Vuylsteke, M., Brewer, P.B., Beveridge, C.A., Yermiyahu, U., Kaplan, Y., Enzer, Y., Wininger, S., Resnick, N., Cohen, M., Kapulnik, Y., Koltai, H., 2012. Strigolactones are involved in root response to low phosphate conditions in *Arabidopsis*. Plant Physiology 160, 1329-1341.
- McAdam, E.L., Hugill, C., Fort, S., Samain, E., Cottaz, S., Davies, N.W., Reid, J.B., Foo, E., 2017. Determining the site of action of strigolactones during nodulation. Plant Physiology 175, 529-542.
- Melo, N.K.G., Bianchetti, R.E., Lira, B.S., Oliveira, P.M.R., Zuccarelli, R., Dias, D.L.O., Demarco, D., Peres, L.E.P., Rossi, M., Freschi, L., 2016. Nitric oxide, ethylene, and auxin cross talk mediates greening and plastid development in deetioliating tomato seedlings. Plant Physiology 170, 2278-2294.
- Minakuchi, K., Kameoka, H., Yasuno, N., Umehara, M., Luo, L., Kobayashi, K., Hanada, A., Ueno, K., Asami, T., Yamaguchi, S., Kyojuka, J., 2010. *FINE CULM1 (FC1)* works downstream of strigolactones to inhibit the outgrowth of axillary buds in rice. Plant and Cell Physiology 51, 1127-1135.
- Mori, N., Nishiuma, K., Sugiyama, T., Hayashi, H., Akiyama, K., 2016. Carlactone-type strigolactones and their synthetic analogues as inducers of hyphal branching in arbuscular mycorrhizal fungi. Phytochemistry 130, 90-98.

- Mostofa, M.G., Li, W., Nguyen, K.H., Fujita, M., Tran, L.-S.P., 2018. Strigolactones in plant adaptation to abiotic stresses: An emerging avenue of plant research. *Plant, Cell & Environment* 41, 2227-2243.
- Moubayidin, L., Perilli, S., Dello Ioio, R., Di Mambro, R., Costantino, P., Sabatini, S., 2010. The rate of cell differentiation controls the *Arabidopsis* root meristem growth phase. *Current Biology* 20, 1138-1143.
- Müller, S., Hauck, C., Schildknecht, H., 1992. Germination stimulants produced by *Vigna unguiculata* Walp cv Saunders Upright. *Journal of Plant Growth Regulation* 11, 77.
- Mustafiz, A., Sahoo, K.K., Singla-Pareek, S.L., Sopory, S.K. 2010. Metabolic engineering of glyoxalase pathway for enhancing stress tolerance in plants, In: Sunkar, R. (Ed.) *Plant stress tolerance: Methods and protocols*. Humana Press, Totowa, NJ, 95-118.
- Nakamura, H., Xue, Y.-L., Miyakawa, T., Hou, F., Qin, H.-M., Fukui, K., Shi, X., Ito, E., Ito, S., Park, S.-H., Miyauchi, Y., Asano, A., Totsuka, N., Ueda, T., Tanokura, M., Asami, T., 2013. Molecular mechanism of strigolactone perception by DWARF14. *Nature Communications* 4, 2613.
- Nakano, Y., Asada, K., 1981. Hydrogen peroxide is scavenged by ascorbate-specific peroxidase in spinach chloroplasts. *Plant and Cell Physiology* 22, 867-880.
- Narayanan, S., Prasad, P.V.V., Fritz, A.K., Boyle, D.L., Gill, B.S., 2015. Impact of high night-time and high daytime temperature stress on winter wheat. *Journal of Agronomy and Crop Science* 201, 206-218.
- Naseem, M., Mugdha, S., Muhammad, T., Nazeer, A., 2015. Auxin crosstalk to plant immune networks: A plant-pathogen interaction perspective. *Current Protein & Peptide Science* 16, 389-394.
- Nelson, D.C., Riseborough, J.-A., Flematti, G.R., Stevens, J., Ghisalberti, E.L., Dixon, K.W., Smith, S.M., 2009. Karrikins discovered in smoke trigger *Arabidopsis* seed germination by a mechanism requiring gibberellic acid synthesis and light. *Plant Physiology* 149, 863.
- Nelson, D.C., Scaffidi, A., Dun, E.A., Waters, M.T., Flematti, G.R., Dixon, K.W., Beveridge, C.A., Ghisalberti, E.L., Smith, S.M., 2011. F-box protein MAX2 has dual roles in karrikin and strigolactone signaling in *Arabidopsis thaliana*. *Proceedings of the National Academy of Sciences* 108, 8897.
- Nelson, S.K., Steber, C.M. 2016. Gibberellin hormone signal perception: down-regulating DELLA repressors of plant growth and development, In: Hedden, P., Thomas, S. (Eds.) *Annual Plant Reviews*, Volume 49. John Wiley & Sons, Chichester, 153-188.
- Nisar, N., Li, L., Lu, S., Khin, Nay C., Pogson, Barry J., 2015. Carotenoid metabolism in plants. *Molecular Plant* 8, 68-82.

- Niu, S., Li, Z., Yuan, H., Fang, P., Chen, X., Li, W., 2013. Proper gibberellin localization in vascular tissue is required to regulate adventitious root development in tobacco. *Journal of Experimental Botany* 64, 3411-3424.
- Nomura, S., Nakashima, H., Mizutani, M., Takikawa, H., Sugimoto, Y., 2013. Structural requirements of strigolactones for germination induction and inhibition of *Striga gesnerioides* seeds. *Plant Cell Reports* 32, 829-838.
- Olatunji, D., Geelen, D., Verstraeten, I., 2017. Control of endogenous auxin levels in plant root development. *International Journal of Molecular Sciences* 18, 2587.
- Oukarroum, A., Bussotti, F., Goltsev, V., Kalaji, H.M., 2015. Correlation between reactive oxygen species production and photochemistry of photosystems I and II in *Lemna gibba* L. plants under salt stress. *Environmental and Experimental Botany* 109, 80-88.
- Oukarroum, A., El Madidi, S., Strasser, R.J., 2016. Differential heat sensitivity index in barley cultivars (*Hordeum vulgare* L.) monitored by chlorophyll a fluorescence OKJIP. *Plant Physiology and Biochemistry* 105, 102-108.
- Oukarroum, A., Goltsev, V., Strasser, R.J., 2013. Temperature effects on pea plants probed by simultaneous measurements of the kinetics of prompt fluorescence, delayed fluorescence and modulated 820 nm reflection. *PLoS One* 8, e59433.
- Pachauri, R.K., Allen, M.R., Barros, V.R., Broome, J., Cramer, W., Christ, R., Church, J.A., Clarke, L., Dahe, Q., Dasgupta, P., 2014. Climate change 2014: synthesis report. Contribution of Working Groups I, II and III to the fifth assessment report of the Intergovernmental Panel on Climate Change. IPCC, Geneva.
- Pandya-Kumar, N., Shema, R., Kumar, M., Mayzlish-Gati, E., Levy, D., Zemach, H., Belausov, E., Wininger, S., Abu-Abied, M., Kapulnik, Y., Koltai, H., 2014. Strigolactone analog GR24 triggers changes in PIN2 polarity, vesicle trafficking and actin filament architecture. *New Phytologist* 202, 1184-1196.
- Panuccio, M.R., Jacobsen, S.E., Akhtar, S.S., Muscolo, A., 2014. Effect of saline water on seed germination and early seedling growth of the halophyte quinoa. *AoB PLANTS* 6.
- Park, C.-J., Seo, Y.-S., 2015. Heat shock proteins: A review of the molecular chaperones for plant immunity. *The Plant Pathology Journal* 31, 323-333.
- Partheeban, C., Chandrasekhar, C.N., Jeyakumar, P., R, R., Ramasamy, G., 2017. Effect of PEG induced drought stress on seed germination and seedling characters of maize (*Zea mays* L.) genotypes. *International Journal of Current Microbiology and Applied Sciences* 6, 1095-1104.
- Pinnola, A., Dall'Osto, L., Gerotto, C., Morosinotto, T., Bassi, R., Alboresi, A., 2013. Zeaxanthin binds to light-harvesting complex stress-related protein to enhance nonphotochemical quenching in *Physcomitrella patens*. *The Plant Cell* 25, 3519.

- Pintó-Marijuan, M., Munné-Bosch, S., 2014. Photo-oxidative stress markers as a measure of abiotic stress-induced leaf senescence: advantages and limitations. *Journal of Experimental Botany* 65, 3845-3857.
- Pipitone, R., Eicke, S., Pfister, B., Glauser, G., Falconet, D., Uwizeye, C., Pralon, T., Zeeman, S., Kessler, F., Demarsy, E., 2020. Two distinct phases of chloroplast biogenesis during de-etiolation in *Arabidopsis thaliana*. *bioRxiv*, 2020.2008.2030.274043.
- Prieto, P., Pineda, M., Aguilar, M., 1999. Spectrophotometric quantitation of antioxidant capacity through the formation of a phosphomolybdenum complex: Specific application to the determination of vitamin E. *Analytical Biochemistry* 269, 337-341.
- Prodhan, M.Y., Munemasa, S., Nahar, M.N.-E.N., Nakamura, Y., Murata, Y., 2018. Guard cell salicylic acid signaling is integrated into abscisic acid signaling via the Ca²⁺/CPK-dependent pathway. *Plant Physiology* 178, 441.
- Prusinkiewicz, P., Crawford, S., Smith, R.S., Ljung, K., Bennett, T., Ongaro, V., Leyser, O., 2009. Control of bud activation by an auxin transport switch. *Proceedings of the National Academy of Sciences* 106, 17431.
- Ranieri, A., Petacco, F., Castagna, A., Soldatini, G.F., 2000. Redox state and peroxidase system in sunflower plants exposed to ozone. *Plant Science* 159, 159-167.
- Rashid, M.A., Andersen, M.N., Wollenweber, B., Kørup, K., Zhang, X., Olesen, J.E., 2018. Impact of heat-wave at high and low VPD on photosynthetic components of wheat and their recovery. *Environmental and Experimental Botany* 147, 138-146.
- Rasmussen, A., Beveridge, C.A., Geelen, D., 2012a. Inhibition of strigolactones promotes adventitious root formation. *Plant Signaling & Behavior* 7, 694-697.
- Rasmussen, A., Hu, Y., Depaepe, T., Vandenbussche, F., Boyer, F.-D., Van Der Straeten, D., Geelen, D., 2017. Ethylene controls adventitious root initiation sites in *Arabidopsis* hypocotyls independently of strigolactones. *Journal of Plant Growth Regulation* 36, 897-911.
- Rasmussen, A., Mason, M.G., De Cuyper, C., Brewer, P.B., Herold, S., Agusti, J., Geelen, D., Greb, T., Goormachtig, S., Beeckman, T., Beveridge, C.A., 2012b. Strigolactones suppress adventitious rooting in *Arabidopsis* and pea. *Plant Physiology* 158, 1976.
- Ren, C.-G., Kong, C.-C., Xie, Z.-H., 2018. Role of abscisic acid in strigolactone-induced salt stress tolerance in arbuscular mycorrhizal *Sesbania cannabina* seedlings. *BMC Plant Biology* 18, 74-74.
- Ritonga, F.N., Chen, S., 2020. Physiological and molecular mechanism involved in cold stress tolerance in plants. *Plants* 9, 560.
- Rösler, J., Krekel, F., Amrhein, N., Schmid, J., 1997. Maize phenylalanine ammonia-lyase has tyrosine ammonia-lyase activity. *Plant Physiology* 113, 175-179.

- Rozpądek, P., Domka, A.M., Nosek, M., Ważny, R., Jędrzejczyk, R.J., Wiciarz, M., Turnau, K., 2018. The role of strigolactone in the cross-talk between *Arabidopsis thaliana* and the endophytic fungus *Mucor* sp. *Frontiers in Microbiology* 9, 441-441.
- Ruyter-Spira, C., Kohlen, W., Charnikhova, T., van Zeijl, A., van Bezouwen, L., de Ruijter, N., Cardoso, C., Lopez-Raez, J.A., Matusova, R., Bours, R., Verstappen, F., Bouwmeester, H., 2011. Physiological effects of the synthetic strigolactone analog GR24 on root system architecture in arabidopsis: Another belowground role for strigolactones? *Plant Physiology* 155, 721.
- Saeed, W., Naseem, S., Ali, Z., 2017. Strigolactones biosynthesis and their role in abiotic stress resilience in plants: A critical review. *Frontiers in Plant Science* 8, 1487-1487.
- Saleh, A.A., 2007. Amelioration of chilling injuries in mung bean (*Vigna radiata* L.) seedlings by paclobutrazol, abscisic acid and hydrogen peroxide. *American Journal of Plant Physiology* 2, 318-332.
- Salvucci, M.E., Osteryoung, K.W., Crafts-Brandner, S.J., Vierling, E., 2001. Exceptional sensitivity of rubisco activase to thermal denaturation *in vitro* and *in vivo*. *Plant Physiology* 127, 1053.
- Sasse, J., Simon, S., Gübeli, C., Liu, G.W., Cheng, X., Friml, J., Bouwmeester, H., Martinoia, E., Borghi, L., 2015. Asymmetric localizations of the ABC transporter *PaPDR1* trace paths of directional strigolactone transport. *Current Biology* 25, 647-655.
- Scaffidi, A., Waters, M.T., Sun, Y.K., Skelton, B.W., Dixon, K.W., Ghisalberti, E.L., Flematti, G.R., Smith, S.M., 2014. Strigolactone hormones and their stereoisomers signal through two related receptor proteins to induce different physiological responses in *Arabidopsis*1[W]. *Plant Physiology* 165, 1221 - 1232.
- Schansker, G., Tóth, S.Z., Strasser, R.J., 2005. Methylviologen and dibromothymoquinone treatments of pea leaves reveal the role of photosystem I in the Chl *a* fluorescence rise OJIP. *Biochimica et Biophysica Acta (BBA) - Bioenergetics* 1706, 250-261.
- Seale, M., Bennett, T., Leyser, O., 2017. BRC1 expression regulates bud activation potential but is not necessary or sufficient for bud growth inhibition in *Arabidopsis*. *Development* 144, 1661-1673.
- Seto, Y., Sado, A., Asami, K., Hanada, A., Umehara, M., Akiyama, K., Yamaguchi, S., 2014. Carlactone is an endogenous biosynthetic precursor for strigolactones. *Proceedings of the National Academy of Sciences* 111, 1640.
- Seto, Y., Yasui, R., Kameoka, H., Tamiru, M., Cao, M., Terauchi, R., Sakurada, A., Hirano, R., Kisugi, T., Hanada, A., Umehara, M., Seo, E., Akiyama, K., Burke, J., Takeda-Kamiya, N., Li, W., Hirano, Y., Hakoshima, T., Mashiguchi, K., Noel, J.P., Kyojuka, J., Yamaguchi, S., 2019.

- Strigolactone perception and deactivation by a hydrolase receptor DWARF14. *Nature Communications* 10, 191.
- Shabek, N., Ticchiarelli, F., Mao, H., Hinds, T.R., Leyser, O., Zheng, N., 2018. Structural plasticity of D3–D14 ubiquitin ligase in strigolactone signalling. *Nature* 563, 652-656.
- Shafi, A., Dogra, V., Gill, T., Ahuja, P., Sreenivasulu, Y., 2014. Simultaneous over-expression of *PaSOD* and *RaAPX* in transgenic *Arabidopsis thaliana* confers cold stress tolerance through increase in vascular lignifications. *PLoS ONE* 9, e110302.
- Shah, F.A., Wei, X., Wang, Q., Liu, W., Wang, D., Yao, Y., Hu, H., Chen, X., Huang, S., Hou, J., Lu, R., Liu, C., Ni, J., Wu, L., 2020. Karrikin improves osmotic and salt stress tolerance via the regulation of the redox homeostasis in the oil plant *Sapium sebiferum*. *Frontiers in Plant Science* 11, 216.
- Sharma, A., Shahzad, B., Kumar, V., Kohli, S.K., Sidhu, G.P.S., Bali, A.S., Handa, N., Kapoor, D., Bhardwaj, R., Zheng, B., 2019a. Phytohormones regulate accumulation of osmolytes under abiotic stress. *Biomolecules* 9, 285.
- Sharma, A., Shahzad, B., Rehman, A., Bhardwaj, R., Landi, M., Zheng, B., 2019b. Response of phenylpropanoid pathway and the role of polyphenols in plants under abiotic stress. *Molecules* 24, 2452.
- Sharma, M., Laxmi, A., 2016. Jasmonates: Emerging players in controlling temperature stress tolerance. *Frontiers in Plant Science* 6, 1129.
- Shen, H., Zhu, L., Bu, Q.-Y., Huq, E., 2012. MAX2 affects multiple hormones to promote photomorphogenesis. *Molecular Plant* 5, 750-762.
- Shi, H., Shen, X., Liu, R., Xue, C., Wei, N., Deng, X.W., Zhong, S., 2016. The red light receptor phytochrome B directly enhances substrate-E3 ligase interactions to attenuate ethylene responses. *Developmental Cell* 39, 597-610.
- Shinohara, N., Taylor, C., Leyser, O., 2013. Strigolactone can promote or inhibit shoot branching by triggering rapid depletion of the auxin efflux protein PIN1 from the plasma membrane. *PLOS Biology* 11, e1001474.
- Singla-Pareek, S.L., Reddy, M.K., Sopory, S.K., 2003. Genetic engineering of the glyoxalase pathway in tobacco leads to enhanced salinity tolerance. *Proceedings of the National Academy of Sciences of the United States of America* 100, 14672-14677.
- Song, X., Lu, Z., Yu, H., Shao, G., Xiong, J., Meng, X., Jing, Y., Liu, G., Xiong, G., Duan, J., Yao, X.-F., Liu, C.-M., Li, H., Wang, Y., Li, J., 2017. IPA1 functions as a downstream transcription factor repressed by D53 in strigolactone signaling in rice. *Cell Research* 27, 1128-1141.

- Soós, V., Sebestyén, E., Juhász, A., Pintér, J., Light, M.E., Van Staden, J., Balázs, E., 2009. Stress-related genes define essential steps in the response of maize seedlings to smoke-water. *Functional & Integrative Genomics* 9, 231-242.
- Soós, V., Sebestyén, E., Posta, M., Kohout, L., Light, M.E., Van Staden, J., Balázs, E., 2012. Molecular aspects of the antagonistic interaction of smoke-derived butenolides on the germination process of Grand Rapids lettuce (*Lactuca sativa*) achenes. *New Phytologist* 196, 1060-1073.
- Soundappan, I., Bennett, T., Morffy, N., Liang, Y., Stanga, J.P., Abbas, A., Leyser, O., Nelson, D.C., 2015. SMAX1-LIKE/D53 family members enable distinct MAX2-dependent responses to strigolactones and karrikins in *Arabidopsis*. *The Plant Cell* 27, 3143.
- Srivastava, A., Guissé, B., Greppin, H., Strasser, R.J., 1997. Regulation of antenna structure and electron transport in Photosystem II of *Pisum sativum* under elevated temperature probed by the fast polyphasic chlorophyll a fluorescence transient: OKJIP. *Biochimica et Biophysica Acta (BBA) - Bioenergetics* 1320, 95-106.
- Stanga, J.P., Smith, S.M., Briggs, W.R., Nelson, D.C., 2013. SUPPRESSOR OF MORE AXILLARY GROWTH2 1 controls seed germination and seedling development in *Arabidopsis*. *Plant Physiology* 163, 318.
- Stanley, L., Yuan, Y.-W., 2019. Transcriptional regulation of carotenoid biosynthesis in plants: So many regulators, so little consensus. *Frontiers in Plant Science* 10, 1017.
- Steffens, B., Rasmussen, A., 2016. The physiology of adventitious roots. *Plant Physiology* 170, 603.
- Stirnberg, P., Furner, I.J., Ottoline Leyser, H.M., 2007. MAX2 participates in an SCF complex which acts locally at the node to suppress shoot branching. *The Plant Journal* 50, 80-94.
- Strasser, B.J., 1997. Donor side capacity of Photosystem II probed by chlorophyll a fluorescence transients. *Photosynthesis Research* 52, 147-155.
- Strasser, R., Srivastava, A., Tsimilli-Michael, M. 2000. The fluorescence transient as a tool to characterize and screen photosynthetic samples, In: Yunus, M., Pathre, U., Mohanty, P. (Eds.) *Probing photosynthesis: Mechanism, regulation and adaptation*. Taylor and Francis, London, 443–480.
- Strasser, R.J., Tsimilli-Michael, M., Qiang, S., Goltsev, V., 2010. Simultaneous *in vivo* recording of prompt and delayed fluorescence and 820-nm reflection changes during drying and after rehydration of the resurrection plant *Haberlea rhodopensis*. *Biochimica et Biophysica Acta (BBA) - Bioenergetics* 1797, 1313-1326.

- Strasser, R.J., Tsimilli-Michael, M., Srivastava, A. 2004. Analysis of the chlorophyll a fluorescence transient, In: Papageorgiou, G.C., Govindjee (Eds.) Chlorophyll a fluorescence: A signature of photosynthesis. Springer Netherlands, Dordrecht, 321-362.
- Strasser, R.J., Srivastava, A., Govindjee, 1995. Polyphasic chlorophyll a fluorescence transient in plants and cyanobacteria. *Photochemistry and Photobiology* 61, 32-42.
- Su, L., Diretto, G., Purgatto, E., Danoun, S., Zouine, M., Li, Z., Roustan, J.-P., Bouzayen, M., Giuliano, G., Chervin, C., 2015. Carotenoid accumulation during tomato fruit ripening is modulated by the auxin-ethylene balance. *BMC Plant Biology* 15, 114.
- Sugimoto, Y., Ali, A.M., Yabuta, S., Kinoshita, H., Inanaga, S., Itai, A., 2003. Germination strategy of *Striga hermonthica* involves regulation of ethylene biosynthesis. *Physiologia Plantarum* 119, 137-145.
- Sun, H., Tao, J., Gu, P., Xu, G., Zhang, Y., 2016a. The role of strigolactones in root development. *Plant Signaling & Behavior* 11, e1110662-e1110662.
- Sun, H., Tao, J., Hou, M., Huang, S., Chen, S., Liang, Z., Xie, T., Wei, Y., Xie, X., Yoneyama, K., Xu, G., Zhang, Y., 2015. A strigolactone signal is required for adventitious root formation in rice. *Annals of Botany* 115, 1155-1162.
- Sun, H., Tao, J., Liu, S., Huang, S., Chen, S., Xie, X., Yoneyama, K., Zhang, Y., Xu, G., 2014. Strigolactones are involved in phosphate- and nitrate-deficiency-induced root development and auxin transport in rice. *Journal of Experimental Botany* 65, 6735-6746.
- Sun, Y., Geng, Q., Du, Y., Yang, X., Zhai, H., 2017. Induction of cyclic electron flow around photosystem I during heat stress in grape leaves. *Plant Science* 256, 65-71.
- Sun, Y.K., Flematti, G.R., Smith, S.M., Waters, M.T., 2016b. Reporter gene-facilitated detection of compounds in *Arabidopsis* leaf extracts that activate the karrikin signaling pathway. *Frontiers in Plant Science* 7, 1799-1799.
- Suzuki, N., Mittler, R., 2006. Reactive oxygen species and temperature stresses: A delicate balance between signaling and destruction. *Physiologia Plantarum* 126, 45-51.
- Tarkowski, Ł.P., Van den Ende, W., 2015. Cold tolerance triggered by soluble sugars: a multifaceted countermeasure. *Frontiers in Plant Science* 6.
- Thussagunpanit, J., Nagai, Y., Nagae, M., Mashiguchi, K., Mitsuda, N., Ohme-Takagi, M., Nakano, T., Nakamura, H., Asami, T., 2017. Involvement of STH7 in light-adapted development in *Arabidopsis thaliana* promoted by both strigolactone and karrikin. *Bioscience, Biotechnology, and Biochemistry* 81, 292-301.
- Tian, M.-Q., Jiang, K., Takahashi, I., Li, G.-D., 2018. Strigolactone-induced senescence of a bamboo leaf in the dark is alleviated by exogenous sugar. *Journal of Pesticide Science* 43, 173-179.

- Tognetti, J.A., Pontis, H.G., Martínez-Noël, G.M.A., 2013. Sucrose signaling in plants: a world yet to be explored. *Plant Signaling & Behavior* 8, e23316-e23316.
- Toh, S., Kamiya, Y., Kawakami, N., Nambara, E., McCourt, P., Tsuchiya, Y., 2011. Thermoinhibition uncovers a role for strigolactones in *Arabidopsis* seed germination. *Plant and Cell Physiology* 53, 107-117.
- Torres-Vera, R., García, J.M., Pozo, M.J., López-Ráez, J.A., 2014. Do strigolactones contribute to plant defence? *Molecular Plant Pathology* 15, 211-216.
- Tóth, S.Z., Schansker, G., Garab, G., Strasser, R.J., 2007. Photosynthetic electron transport activity in heat-treated barley leaves: The role of internal alternative electron donors to photosystem II. *Biochimica et Biophysica Acta (BBA) - Bioenergetics* 1767, 295-305.
- Tsuchiya, Y., Yoshimura, M., Sato, Y., Kuwata, K., Toh, S., Holbrook-Smith, D., Zhang, H., McCourt, P., Itami, K., Kinoshita, T., Hagihara, S., 2015. PARASITIC PLANTS. Probing strigolactone receptors in *Striga hermonthica* with fluorescence. *Science* 349, 864-868.
- Ueda, H., Kusaba, M., 2015. Strigolactone regulates leaf senescence in concert with ethylene in *Arabidopsis*. *Plant Physiology* 169, 138.
- Ueno, K., Furumoto, T., Umeda, S., Mizutani, M., Takikawa, H., Batchvarova, R., Sugimoto, Y., 2014. Heliolactone, a non-sesquiterpene lactone germination stimulant for root parasitic weeds from sunflower. *Phytochemistry* 108, 122-128.
- Upadhyay, R.K., Handa, A.K., Mattoo, A.K., 2019. Transcript abundance patterns of 9- and 13-lipoxygenase subfamily gene members in response to abiotic stresses (heat, cold, drought or salt) in tomato (*Solanum lycopersicum* L.) highlights member-specific dynamics relevant to each stress. *Genes* 10, 683.
- Upadhyay, R.K., Mattoo, A.K., 2018. Genome-wide identification of tomato (*Solanum lycopersicum* L.) lipoxygenases coupled with expression profiles during plant development and in response to methyl-jasmonate and wounding. *Journal of Plant Physiology* 231, 318-328.
- Urban, L., Aarouf, J., Bidel, L.P.R., 2017. Assessing the effects of water deficit on photosynthesis using parameters derived from measurements of leaf gas exchange and of chlorophyll a fluorescence. *Frontiers in Plant Science* 8, 2068-2068.
- Urquhart, S., Foo, E., Reid, J.B., 2015. The role of strigolactones in photomorphogenesis of pea is limited to adventitious rooting. *Physiologia Plantarum* 153, 392-402.
- van Staden, J., Drewes, F.E., Jäger, A.K., 1995. The search for germination stimulants in plant-derived smoke extracts. *South African Journal of Botany* 61, 260-263.
- van Staden, J., Jäger, A.K., Light, M.E., Burger, B.V., Brown, N.A.C., Thomas, T.H., 2004. Isolation of the major germination cue from plant-derived smoke. *South African Journal of Botany* 70, 654-659.

- van Zeijl, A., Liu, W., Xiao, T.T., Kohlen, W., Yang, W.-C., Bisseling, T., Geurts, R., 2015. The strigolactone biosynthesis gene DWARF27 is co-opted in rhizobium symbiosis. *BMC Plant Biology* 15, 260.
- Visentin, I., Vitali, M., Ferrero, M., Zhang, Y., Ruyter-Spira, C., Novák, O., Strnad, M., Lovisolo, C., Schubert, A., Cardinale, F., 2016. Low levels of strigolactones in roots as a component of the systemic signal of drought stress in tomato. *New Phytologist* 212, 954-963.
- Wang, H., Chen, W., Eggert, K., Charnikhova, T., Bouwmeester, H., Schweizer, P., Hajirezaei, M.R., Seiler, C., Sreenivasulu, N., von Wirén, N., Kuhlmann, M., 2018. Abscisic acid influences tillering by modulation of strigolactones in barley. *Journal of Experimental Botany* 69, 3883-3898.
- Wang, L., Shan, T., Xie, B., Ling, C., Shao, S., Jin, P., Zheng, Y., 2019. Glycine betaine reduces chilling injury in peach fruit by enhancing phenolic and sugar metabolisms. *Food Chemistry* 272, 530-538.
- Wang, L., Wang, B., Jiang, L., Liu, X., Li, X., Lu, Z., Meng, X., Wang, Y., Smith, S.M., Li, J., 2015. Strigolactone signaling in *Arabidopsis* regulates shoot development by targeting D53-Like SMXL repressor proteins for ubiquitination and degradation. *The Plant Cell* 27, 3128.
- Wang, Y., Sun, S., Zhu, W., Jia, K., Yang, H., Wang, X., 2013. Strigolactone/MAX2-induced degradation of brassinosteroid transcriptional effector BES1 regulates shoot branching. *Developmental Cell* 27, 681-688.
- Waters, M.T., Brewer, P.B., Bussell, J.D., Smith, S.M., Beveridge, C.A., 2012a. The *Arabidopsis* ortholog of rice DWARF27 acts upstream of MAX1 in the control of plant development by strigolactones. *Plant Physiology* 159, 1073.
- Waters, M.T., Gutjahr, C., Bennett, T., Nelson, D.C., 2017. Strigolactone Signaling and Evolution. *Annual Review of Plant Biology* 68, 291-322.
- Waters, M.T., Nelson, D.C., Scaffidi, A., Flematti, G.R., Sun, Y.K., Dixon, K.W., Smith, S.M., 2012b. Specialisation within the DWARF14 protein family confers distinct responses to karrikins and strigolactones in *Arabidopsis*. *Development* 139, 1285-1295.
- Waters, M.T., Scaffidi, A., Flematti, G.R., Smith, S.M., 2012c. Karrikins force a rethink of strigolactone mode of action. *Plant Signaling & Behavior* 7, 969-972.
- Wei, K., Wang, L.-y., Ruan, L., Zhang, C.-c., Wu, L.-y., Li, H.-l., Cheng, H., 2018. Endogenous nitric oxide and hydrogen peroxide detection in indole-3-butyric acid-induced adventitious root formation in *Camellia sinensis*. *Journal of Integrative Agriculture* 17, 2273-2280.
- Woo, H.R., Chung, K.M., Park, J.H., Oh, S.A., Ahn, T., Hong, S.H., Jang, S.K., Nam, H.G., 2001. ORE9, an F-box protein that regulates leaf senescence in *Arabidopsis*. *The Plant Cell* 13, 1779-1790.

- Xie, X., Kisugi, T., Yoneyama, K., Nomura, T., Akiyama, K., Uchida, K., Yokota, T., McErlean, C.S.P., Yoneyama, K., 2017. Methyl zealactonoate, a novel germination stimulant for root parasitic weeds produced by maize. *Journal of Pesticide Science* 42, 58-61.
- Xie, X., Mori, N., Yoneyama, K., Nomura, T., Uchida, K., Yoneyama, K., Akiyama, K., 2019. Lotuslactone, a non-canonical strigolactone from *Lotus japonicus*. *Phytochemistry* 157, 200-205.
- Xie, X., Wang, G., Yang, L., Cheng, T., Gao, J., Wu, Y., Xia, Q., 2015a. Cloning and characterization of a novel *Nicotiana tabacum* ABC transporter involved in shoot branching. *Physiologia Plantarum* 153, 299-306.
- Xie, X., Yoneyama, K., Kisugi, T., Nomura, T., Akiyama, K., Asami, T., Yoneyama, K., 2015b. Strigolactones are transported from roots to shoots, although not through the xylem. *Journal of Pesticide Science* 40, 214-216.
- Xie, X., Yoneyama, K., Kisugi, T., Nomura, T., Akiyama, K., Asami, T., Yoneyama, K., 2016. Structure- and stereospecific transport of strigolactones from roots to shoots. *Journal of Pesticide Science* 41, 55-58.
- Xie, X., Yoneyama, K., Kisugi, T., Uchida, K., Ito, S., Akiyama, K., Hayashi, H., Yokota, T., Nomura, T., Yoneyama, K., 2013. Confirming stereochemical structures of strigolactones produced by rice and tobacco. *Molecular Plant* 6, 153-163.
- Xu, J., Zha, M., Li, Y., Ding, Y., Chen, L., Ding, C., Wang, S., 2015. The interaction between nitrogen availability and auxin, cytokinin, and strigolactone in the control of shoot branching in rice (*Oryza sativa* L.). *Plant Cell Reports* 34, 1647-1662.
- Xu, M., Zhu, L., Shou, H., Wu, P., 2005. A PIN1 family gene, OsPIN1, involved in auxin-dependent adventitious root emergence and tillering in rice. *Plant and Cell Physiology* 46, 1674-1681.
- Xu, X., Chi, W., Sun, X., Feng, P., Guo, H., Li, J., Lin, R., Lu, C., Wang, H., Leister, D., Zhang, L., 2016. Convergence of light and chloroplast signals for de-etiolation through ABI4–HY5 and COP1. *Nature Plants* 2, 16066.
- Yadav, S.K., 2010. Cold stress tolerance mechanisms in plants. A review. *Agronomy for Sustainable Development* 30, 515-527.
- Yadav, S.K., Singla-Pareek, S.L., Reddy, M.K., Sopory, S.K., 2005. Transgenic tobacco plants overexpressing glyoxalase enzymes resist an increase in methylglyoxal and maintain higher reduced glutathione levels under salinity stress. *FEBS Letters* 579, 6265-6271.
- Yamada, Y., Furusawa, S., Nagasaka, S., Shimomura, K., Yamaguchi, S., Umehara, M., 2014. Strigolactone signaling regulates rice leaf senescence in response to a phosphate deficiency. *Planta* 240, 399-408.

- Yamane, Y., Kashino, Y., Koike, H., Satoh, K., 1997. Increases in the fluorescence F_0 level and reversible inhibition of Photosystem II reaction center by high-temperature treatments in higher plants. *Photosynthesis Research* 52, 57-64.
- Yamauchi, Y., Furutera, A., Seki, K., Toyoda, Y., Tanaka, K., Sugimoto, Y., 2008. Malondialdehyde generated from peroxidized linolenic acid causes protein modification in heat-stressed plants. *Plant Physiology and Biochemistry* 46, 786-793.
- Yan, K., Chen, P., Shao, H., Shao, C., Zhao, S., Brestic, M., 2013. Dissection of photosynthetic electron transport process in sweet sorghum under heat stress. *PLoS One* 8, e62100-e62100.
- Yang, M.-T., Chen, S.-L., Lin, C.-Y., Chen, Y.-M., 2005. Chilling stress suppresses chloroplast development and nuclear gene expression in leaves of mung bean seedlings. *Planta* 221, 374-385.
- Yang, W., Zhu, C., Ma, X., Li, G., Gan, L., Ng, D., Xia, K., 2013. Hydrogen peroxide is a second messenger in the salicylic acid-triggered adventitious rooting process in mung bean seedlings. *PLOS ONE* 8, e84580.
- Yao, J., Waters, M.T., 2019. Perception of karrikins by plants: a continuing enigma. *Journal of Experimental Botany* 71, 1774-1781.
- Yao, R., Ming, Z., Yan, L., Li, S., Wang, F., Ma, S., Yu, C., Yang, M., Chen, L., Chen, L., Li, Y., Yan, C., Miao, D., Sun, Z., Yan, J., Sun, Y., Wang, L., Chu, J., Fan, S., He, W., Deng, H., Nan, F., Li, J., Rao, Z., Lou, Z., Xie, D., 2016. DWARF14 is a non-canonical hormone receptor for strigolactone. *Nature* 536, 469-473.
- Yao, R., Wang, L., Li, Y., Chen, L., Li, S., Du, X., Wang, B., Yan, J., Li, J., Xie, D., 2018. Rice DWARF14 acts as an unconventional hormone receptor for strigolactone. *Journal of Experimental Botany* 69, 2355-2365.
- Yi, K., Menand, B., Bell, E., Dolan, L., 2010. A basic helix-loop-helix transcription factor controls cell growth and size in root hairs. *Nature Genetics* 42, 264-267.
- Yildiztugay, E., Ozfidan-Konakci, C., Kucukoduk, M., 2017. Improvement of cold stress resistance via free radical scavenging ability and promoted water status and photosynthetic capacity of gallic acid in soybean leaves. *Journal of Soil Science and Plant Nutrition* 17, 366-384.
- Yokota, T., Sakai, H., Okuno, K., Yoneyama, K., Takeuchi, Y., 1998. Alectrol and orobanchol, germination stimulants for *Orobanche minor*, from its host red clover. *Phytochemistry* 49, 1967-1973.
- Yoneyama, K., Mori, N., Sato, T., Yoda, A., Xie, X., Okamoto, M., Iwanaga, M., Ohnishi, T., Nishiwaki, H., Asami, T., Yokota, T., Akiyama, K., Yoneyama, K., Nomura, T., 2018. Conversion of carlactone to carlactonoic acid is a conserved function of MAX1 homologs in strigolactone biosynthesis. *New Phytologist* 218, 1522-1533.

- Yoneyama, K., Xie, X., Kim, H.I., Kisugi, T., Nomura, T., Sekimoto, H., Yokota, T., Yoneyama, K., 2012. How do nitrogen and phosphorus deficiencies affect strigolactone production and exudation? *Planta* 235, 1197-1207.
- Yoneyama, K., Yoneyama, K., Takeuchi, Y., Sekimoto, H., 2007. Phosphorus deficiency in red clover promotes exudation of orobanchol, the signal for mycorrhizal symbionts and germination stimulant for root parasites. *Planta* 225, 1031-1038.
- Yoshida, S., Kameoka, H., Tempo, M., Akiyama, K., Umehara, M., Yamaguchi, S., Hayashi, H., Kyojuka, J., Shirasu, K., 2012. The D3 F-box protein is a key component in host strigolactone responses essential for arbuscular mycorrhizal symbiosis. *New Phytologist* 196, 1208-1216.
- Yu, Y., Wang, J., Zhang, Z., Quan, R., Zhang, H., Deng, X.W., Ma, L., Huang, R., 2013. Ethylene promotes hypocotyl growth and hy5 degradation by enhancing the movement of COP1 to the nucleus in the light. *PLOS Genetics* 9, e1004025.
- Yuan, H., Zhang, J., Nageswaran, D., Li, L., 2015. Carotenoid metabolism and regulation in horticultural crops. *Horticulture Research* 2, 15036-15036.
- Zdarska, M., Dobisová, T., Gelová, Z., Pernisová, M., Dabravolski, S., Hejátko, J., 2015. Illuminating light, cytokinin, and ethylene signalling crosstalk in plant development. *Journal of Experimental Botany* 66, 4913-4931.
- Zhang, J., Wei, J., Li, D., Kong, X., Rengel, Z., Chen, L., Yang, Y., Cui, X., Chen, Q., 2017. The role of the plasma membrane H⁺-ATPase in plant responses to aluminum toxicity. *Frontiers in Plant Science* 8, 1757.
- Zhang, S., Li, G., Fang, J., Chen, W., Jiang, H., Zou, J., Liu, X., Zhao, X., Li, X., Chu, C., Xie, Q., Jiang, X., Zhu, L., 2010. The interactions among DWARF10, auxin and cytokinin underlie lateral bud outgrowth in rice. *Journal of Integrative Plant Biology* 52, 626-638.
- Zhang, Y., Li, Z., Tu, Y., Cheng, W., Yang, Y., 2018a. Tomato (*Solanum lycopersicum*) SIIPT4, encoding an isopentenyltransferase, is involved in leaf senescence and lycopene biosynthesis during fruit ripening. *BMC Plant Biology* 18, 107.
- Zhang, Y., Lv, S., Wang, G., 2018b. Strigolactones are common regulators in induction of stomatal closure *in planta*. *Plant Signaling & Behavior* 13, e1444322-e1444322.
- Zhang, Y., Lv, S., Wang, G., 2018c. Strigolactones are common regulators in induction of stomatal closure in planta. *Plant Signaling & Behavior* 13, e1444322.
- Zhang, Y., van Dijk, A.D.J., Scaffidi, A., Flematti, G.R., Hofmann, M., Charnikhova, T., Verstappen, F., Hepworth, J., van der Krol, S., Leyser, O., Smith, S.M., Zwanenburg, B., Al-Babili, S., Ruyter-Spira, C., Bouwmeester, H.J., 2014. Rice cytochrome P450 MAX1 homologs catalyze distinct steps in strigolactone biosynthesis. *Nature Chemical Biology* 10, 1028-1033.

- Zhang, Y., Xiao, Z.a., Zhan, C., Liu, M., Xia, W., Wang, N., 2019. Comprehensive analysis of dynamic gene expression and investigation of the roles of hydrogen peroxide during adventitious rooting in poplar. *BMC Plant Biology* 19, 99.
- Zhao, L.-H., Zhou, X.E., Wu, Z.-S., Yi, W., Xu, Y., Li, S., Xu, T.-H., Liu, Y., Chen, R.-Z., Kovach, A., Kang, Y., Hou, L., He, Y., Xie, C., Song, W., Zhong, D., Xu, Y., Wang, Y., Li, J., Zhang, C., Melcher, K., Xu, H.E., 2013. Crystal structures of two phytohormone signal-transducing α/β hydrolases: karrikin-signaling KAI2 and strigolactone-signaling DWARF14. *Cell Research* 23, 436-439.
- Zhao, L.-H., Zhou, X.E., Yi, W., Wu, Z., Liu, Y., Kang, Y., Hou, L., de Waal, P.W., Li, S., Jiang, Y., Scaffidi, A., Flematti, G.R., Smith, S.M., Lam, V.Q., Griffin, P.R., Wang, Y., Li, J., Melcher, K., Xu, H.E., 2015. Destabilization of strigolactone receptor DWARF14 by binding of ligand and E3-ligase signaling effector DWARF3. *Cell Research* 25, 1219-1236.
- Zhong, S., Shi, H., Xue, C., Wei, N., Guo, H., Deng, X.W., 2014. Ethylene-orchestrated circuitry coordinates a seedling's response to soil cover and etiolated growth. *Proceedings of the National Academy of Sciences of the United States of America* 111, 3913-3920.
- Zhou, B., Guo, Z., Xing, J., Huang, B., 2005. Nitric oxide is involved in abscisic acid-induced antioxidant activities in *Stylosanthes guianensis*. *Journal of Experimental Botany* 56, 3223-3228.
- Zhou, F., Lin, Q., Zhu, L., Ren, Y., Zhou, K., Shabek, N., Wu, F., Mao, H., Dong, W., Gan, L., Ma, W., Gao, H., Chen, J., Yang, C., Wang, D., Tan, J., Zhang, X., Guo, X., Wang, J., Jiang, L., Liu, X., Chen, W., Chu, J., Yan, C., Ueno, K., Ito, S., Asami, T., Cheng, Z., Wang, J., Lei, C., Zhai, H., Wu, C., Wang, H., Zheng, N., Wan, J., 2013. D14-SCF^{D3}-dependent degradation of D53 regulates strigolactone signalling. *Nature* 504, 406-410.
- Zhou, P., Li, Q., Liu, G., Xu, N., Yang, Y., Zeng, W., Chen, A., Wang, S., 2019. Integrated analysis of transcriptomic and metabolomic data reveals critical metabolic pathways involved in polyphenol biosynthesis in *Nicotiana tabacum* under chilling stress. *Functional Plant Biology* 46, 30-43.
- Zivcak, M., Brestic, M., Omaovská, K., Slamka, P., 2008. Performance index as a sensitive indicator of water stress in *Triticum aestivum* L. *Plant Soil and Environment* 54, 133-139.
- Zou, J., Zhang, S., Zhang, W., Li, G., Chen, Z., Zhai, W., Zhao, X., Pan, X., Xie, Q., Zhu, L., 2006. The rice HIGH-TILLERING DWARF1 encoding an ortholog of *Arabidopsis* MAX3 is required for negative regulation of the outgrowth of axillary buds. *The Plant Journal* 48, 687-698.
- Zushi, K., Matsuzoe, N., 2017. Using of chlorophyll a fluorescence OJIP transients for sensing salt stress in the leaves and fruits of tomato. *Scientia Horticulturae* 219, 216-221.

Zwanenburg, B., Pospíšil, T., 2013. Structure and activity of strigolactones: New plant hormones with a rich future. *Molecular Plant* 6, 38-62.